Modeling Climate Change Impacts on the Effectiveness of Stormwater Control Measures in Urban Watersheds

Nasrin Alamdari

Dissertation submitted to the faculty of Virginia Polytechnic Institute and State University in partial fulfillment of the requirements for the degree of

Doctor of Philosophy
in
Biological Systems Engineering

David J Sample
Zachary Easton
Jennifer L Irish
Venkataramana Rao Sridhar

July 20, 2018
Blacksburg, Virginia

Keywords: climate change, cost-optimization, retention pond, rainwater harvesting systems, cost effectiveness, load reduction

Modeling Climate Change Impacts on the Effectiveness of Stormwater Control Measures in Urban Watersheds

Nasrin Alamdari

Abstract

Climate change (CC) science has made significant progress in development of predictive models. Despite these recent advances, the assessment of CC impacts in urban watersheds remains an area of active research, in part due to the small temporal and spatial scales needed to adequately characterize urban systems. Urban watersheds have been the focus of considerable efforts to restore hydrology and water quality, and the aquatic habitat of receiving waters, yet CC impacts threaten to reduce the effectiveness of these efforts. Thus, assessing the impacts of CC in urban watershed assessment are essential for assuring the success of water quality improvement programs and is an important research need. Simulations of CC for the 2041-2068 period were developed using downscaled Global Climate Models (GCMs) from the North American Regional CC Assessment Program (NARCCAP) and Coupled Model Intercomparison Project Phase 5 (CMIP5) to forecast precipitation and temperature time series. This data were then used to force a Storm Water Management Model (SWMM) of the Difficult Run watershed of Fairfax County, Virginia, a tributary of Potomac River, which flows into Chesapeake Bay. NARCCAP uses a scenario represents a medium-high greenhouse gas emissions assumption, A2; the latter, uses five GCMs, and two Representative Concentration Pathways (RCP 4.5 and 8.5) scenarios in an ensemble approach to better assess variability of model predictions in presenting precipitation, temperature, runoff quantity and quality. Then, the effects of CC on runoff peak, volume, and nutrient and sediment loads delivered to the Chesapeake Bay and on the treatment performance of a very common stormwater control measure (SCM), retention ponds, was assessed.

Rainwater Harvesting (RWH) systems are an unusual SCM in that they recycle and reuse stormwater, normally from rooftops, and increase water supply and reduce runoff. The efficiency of RWH systems for projected CC for these dual purposes was assessed. NARCAAP data for selected locations across the U.S. were statistically downscaled using a modified version of the equiratio cumulative distribution function matching method to create a time series of projected

precipitation and temperature. These data were used to force a simulation model, the Rainwater Analysis and Simulation Program (RASP) to assess the impacts of CC on RWH with respect to the reliability of water supply and runoff capture. .

To support CC modeling, an easy-to-use software tool, RSWMM-Cost, was developed. RSWMM-Cost automates the execution of SWMM, which is commonly used for simulating urban watersheds. Several features were incorporated into the RSWMM-Cost tool, including automated calibration, sensitivity analysis, and cost optimization modules; the latter can assist in identifying the most cost-effective combination of SCMs in an urban watershed. As an example, RSWMM-Cost was applied to a headwater subcatchment the Difficult Run watershed

Modeling Climate Change Impacts on the Effectiveness of Stormwater Control Measures in Urban Watersheds

Nasrin Alamdari

General Audience Abstract

Urban watersheds have been the focus of considerable efforts to restore water quantity and quality, and the aquatic habitat of receiving waters, yet climate change impacts threaten to reduce the effectiveness of these efforts. The assessment of climate change impacts in urban watersheds remains an area of active research, in part due to the small temporal and spatial scales needed to adequately characterize urban systems. Thus, assessing the impacts of climate change in urban watershed assessment are essential for assuring the success of water quality improvement programs and is an important research need. In this study, simulations of climate change for the 2041-2068 period were developed to forecast precipitation and temperature data. These data were then used to force a hydrologic model for the Difficult Run watershed of Fairfax County, Virginia, a tributary of Potomac River, which flows into Chesapeake Bay. Then, the effects of climate change on runoff, nutrient and sediment loads delivered to the Chesapeake Bay and on the treatment efficiency of a very common management practice called retention ponds, was assessed. Rainwater harvesting systems are an unusual management practice that recycle and reuse stormwater, normally from rooftops, and increase water supply and reduce runoff. The efficiency of rainwater harvesting systems for projected climate change with respect to the reliability of water supply and runoff capture was assessed for the 2041-2068 period.

To support climate change modeling, an easy-to-use tool, was also developed to select the most cost-optimized combination of best management practices in urban watersheds considering site constraints, limitations, and size. As an example, the tool was applied to a headwater subcatchment of the Difficult Run watershed.

The ability to assess the impact of climate change on both hydrologic and water quality treatment could assist in the selection of the most appropriate management practices to address water management goals and conserve limited financial resources.

Acknowledgments

I would like to thank my major advisor **Dr. David J Sample** for his continued support and guidance throughout my PhD program. Dr. Sample gave me great latitude in pursuing the research area of my interest. He had been extremely patient during my learning phase, my rough times, and has been very instrumental in shaping my career.

I would also like to thank my committee members, **Dr. Zach Easton, Dr. Jen Irish and Dr. Venkat Sridhar** for accepting to serve on my committee and providing valued input and feedback. I would like to thank lab members for having our shared of learning experiences, **Dr. Emily Bock, Dr. Heather Governor, Rachael Johnson, Dr. Tyler Keys, Mohammad Nayeb Yazdi and Dr. Moges Wagena**. They are great colleagues who made the lab so interactive and fun to work in, involved me in many opportunities to learn more, and provided me with helping hands to make this work possible. I also thank all my friends in Tennessee and Virginia, who made our life in the U.S. more comfortable and happy, especially **Houman Babazadeh**, **Dr. Arash Baghaei Lakeh, Fereshte Firouzi, Negin Forouzesh, Faranak Mahmoudi, Elham Nikoo, Hadi Parsian, Elahe Raisi, and Dr. Sina Zarrabian.**

Support for a portion of this research was provided by the National Science Foundation, Water Sustainability and Climate WSC-Category 1 Collaborative Project: Coupled Multi-Scale Economic, Hydrologic and Estuarine Modeling to assess Impacts of Climate Change on Water Quality Management, Grant #23032. I would like to thank the Principal Investigator of the NSF Project, **Dr. Zach Easton**, of Virginia Tech, who provided constructive review and support on our papers. I also would like to thank National Oceanographic and Atmospheric Administration (NOAA)/Virginia Institute of Marine Sciences (VIMS) for awarding me the Mid-Atlantic Coastal Storms Fellowship and **Greg Johnson** in City of Virginia Beach for providing funding during my study.

A special thank you to **Dr. Mary Leigh Wolfe**, our department head, who supported me during my PhD. This work would not have happened without her support.

Finally, and most importantly, I would like to thank my husband, **Dr. Ebrahim Ahmadisharaf**. His support, encouragement, quiet patience and unwavering love were undeniably have been built my life. I thank my parents for their support and prays for me, and my lovely and supportive siblings, **Dr. Shahram, Hamidreza, Alireza, Shahnaz, Dr. Azam, and Dr. Aliakbar Alamdari.**

Table of Contents

List of Figures

List of Tables

List of Acronyms

ANN	Artificial Neural Network
BCSD	Bias-Correction and Spatial Disaggregation
BMP	Best Management Practices
BMPDSS	BMP Decision Support System
CB	Chesapeake Bay
CC	Climate Change
CMIP5	Coupled Model Intercomparison Project Phase 5
CSO	Combined Sewer Overflow
CDF	Cumulative Distribution Function
NSGA-II	Elitist Non-dominated Sorting Genetic algorithm
EMC	Event Mean Concentration
ET	Evapotranspiration
GA	Genetic Algorithm
GCM	Global Climate Models
GHG	Greenhouse Gas
GSI	green stormwater infrastructure
HEC-HMS	Hydrologic Engineering Center Hydrologic Modeling System
HRT	Hydraulic Retention Time
IDF	Intensity-Duration-Frequency
IPCC	Intergovernmental Panel on Climate Change
LID	Low Impact Development
LI	Linear Interpolation
L-THIA-LID	Long-Term Hydrologic Impact Assessment-Low Impact Development
MUSIC	Model for Urban Stormwater Improvement Conceptualization
MOSEBEND	Multi-Objective, Socio-Economic, Boundary-Emanating, Nearest Distance
NARCAAP	North American Regional CC Assessment Program
NSE	Nash Sutcliffe Efficiency
NCDC	National Climate Data Center
NOAA	National Oceanic and Atmospheric Administration
NLDAS	North American Land Data Assimilation System
NPDES	National Pollutant Discharge Elimination System
NURP	National Urban Runoff Program
PBIAS	Percent Bias
USEPA	United States Environmental Protection Agency
RAP	Rainwater Accumulation Potential
RASP	Rainwater Analysis and Simulation Program
RCM	Regional Climate Models
RWH	Rainwater Harvesting
SARET	Storage and Reliability Estimation Tool
SCMs	Stormwater Control Measures
SD	Spatial Disaggregation
SUSTAIN	System for Urban Stormwater Treatment and Analysis Integration
SWMM	Stormwater Management Model

TMDL	Total Maximum Daily Load
TN	Total Nitrogen
TOPMODEL	Topography-Based Hydrological Model
TP	Total Phosphorus
TSS	Total Suspended Solids
λ_{WS}	Water Supply Reliability
λ_{RC}	Runoff Capture Reliability
TankV	Tank Volume
RoofA	Roof Area
IrArea	Irrigated Area
Pop	Indoor Population

Chapter 1. Introduction

Stormwater Control Measures (SCMs) are used in urban areas to mitigate the negative effects of urbanization (Hathaway et al., 2014). SCMs are typically designed based on the assumption of hydrologic stationarity (Simonovic and Peck, 2009). However, due to climate change (CC), this fundamental guiding principle has been found by some to now no longer be universally assumed (Milly et al., 2008). The efficiency of stormwater management systems in runoff reduction and pollutant removal will likely decrease due to the CC (Milly et al., 2008; Shongwe et al., 2011; Trenberth, 2011), with changes in precipitation duration, frequency, and intensity (Hathaway et al., 2014).

CC may increase the effects of urbanization by increasing runoff, transport of sediment, nitrogen (N), phosphorus (P), and other pollutants (Imteaz et al., 2012; Lee et al., 2005). SCMs have water quality treatment and runoff or mass reduction capabilities and thus can reduce downstream loadings of sediment, N and P. A variety of SCMs are available, with different capabilities, costs, and limitations; once selected, each SCM must then be appropriately sized. Increased rainfall intensities and longer dry weather periods from CC may reduce the efficiency of SCMs by increasing buildup and wash off of pollutants from land surfaces, thereby increasing pollutant loading (Sharma et al., 2016). Bypasses of untreated flows increase because the design capacity of the SCM has been exceeded. These effects must be considered so that the most resilient SCMs (with respect to projected CC conditions) can be identified. There is a need for methods to evaluate the impacts of CC on water quantity and quality in urban watersheds. Furthermore, there is a lack of understanding on the degree of resiliency these SCMs may provide and how CC may affect their function. Resiliency is the ability of a stormwater system and its associated SCMs to accommodate or recover from the effects of climate change in a timely and efficient manner through restoration or improvement of its essential functions (Field et al., 2012). Advances in downscaling methods coupled with continuous simulation hydrologic and water quality models make it feasible to assess the performance of SCMs affected by CC at appropriate spatial and temporal scales.

The Chesapeake Bay estuary is experiencing eutrophication due to excessive loading of sediment and nutrients (nitrogen, N, and phosphorus, P) (National Research Council, 2000). The U.S. Environmental Protection Agency (USEPA) established a Total Maximum Daily Load (TMDL) for the Chesapeake Bay, limiting N, P, and sediment discharges to its tributaries

(USEPA, 2010). Significant efforts are being made by local governments to comply with the TMDL. Reductions in the effectiveness of SCMs will likely need to be offset, adding cost and, diverting resources from other urban needs. Robust methods to predict the effects of CC on water quantity and quality and for assessing the cost-effectiveness of watershed restoration projects are needed to develop resilient strategies that meet water quality goals and minimize costs.

Significant investments are being made to implement SCMs in urban watersheds to meet local and downstream water quality improvement goals. Funding for water quality programs is limited and often must compete with other urban priorities. It is essential that the selection of SCM for a watershed, consider site constraints, limitations, size, and cost-effectiveness. Tools that combine simulation with cost estimation and optimization to form a simulation-optimization framework could greatly assist in the evaluation of watershed restoration strategies. This would enable more robust watershed restoration planning.

1.1 Goals and Objectives

The goal of this research is to advance the ability to predict CC impacts on the performance of the SCMs, in managing quantity and quality. To advance this goal, the following objectives will be addressed:

To assess the effects of CC on runoff peak, volume, and nutrient and sediment loads delivered to the Chesapeake Bay for a selected watershed in the Difficult Run watershed, Fairfax, VA (Chapter 3).

To assess the function and performance of a common SCM, retention ponds, in the Difficult Run watershed with respect to CC impacts. (Chapter 4).

To assess the effects of CC on water supply and runoff capture functions of hypothetical RWH systems (an SCM) across the U.S., and identify how RWH designs can be modified to offset the effect of CC (Chapter 5).

To develop an easy-to-use tool to calibrate urban watershed models, perform sensitivity analysis, and to identify the most cost-effective SCMs in a headwater portion of the Difficult Run watershed (Chapter 6).

1.2 Dissertation Organization

Chapter 1 of this dissertation introduces the general concepts of SCMs and CC impacts. Chapter 2 provides a detailed literature review of watershed modeling, cost optimization and CC

impacts on SCMs. Chapters 3-6 are specific to each of the previously mentioned four main objectives of this research. As each is a self-supporting journal article, there is some unavoidable repetition between chapters. Chapter 7 contains the overall conclusion of this research.

References for Chapter 1:

Field, C.B., Barros, V., Stocker, T.F., Qin, D., Dokken, D.J., Ebi, K.L., Mastrandrea, M.D., Mach, K.J., Plattner, G.-K., Allen, S.K., M. Tignor, P.M.M., 2012. Glossary of Terms. In: Managing the Risks of Extreme Events and Disasters to Advance Climate Change Adaptation, . A Special Report of Working Groups I and Ii of the Intergovernmental Panel on Climate Change (Ipcc). Cambridge University Press, Cambridge, Uk, and New York, Ny, USA, Pp. 555-564.

Hathaway, J., Brown, R., Fu, J., Hunt, W., 2014. Bioretention Function under Climate Change Scenarios in North Carolina, USA. Journal of Hydrology 519, 503-511.

Imteaz, M.A., Rahman, A., Ahsan, A., 2012. Reliability Analysis of Rainwater Tanks: A Comparison between South-East and Central Melbourne. Resources, Conservation and Recycling 66, 1-7.

Lee, J.G., Heaney, J.P., Lai, F.-h., 2005. Optimization of Integrated Urban Wet-Weather Control Strategies. Journal of Water Resources Planning and Management 131(4), 307-315.

Milly, P.C.D., Betancourt, J., Falkenmark, M., Hirsch, R.M., Kundzewicz, Z.W., Lettenmaier, D.P., Stouffer, R.J., 2008. Stationarity Is Dead: Whither Water Management? Science 319(5863), 573-574.

National Research Council, 2000. Clean Coastal Waters: Understanding and Reducing the Effects of Nutrient Pollution. National Academies Press.

Sharma, A.K., Vezzaro, L., Birch, H., Arnbjerg-Nielsen, K., Mikkelsen, P.S., 2016. Effect of Climate Change on Stormwater Runoff Characteristics and Treatment Efficiencies of Stormwater Retention Ponds: A Case Study from Denmark Using Tss and Cu as Indicator Pollutants. Springerplus 5(1), 1984.

Shongwe, M.E., van Oldenborgh, G.J., van den Hurk, B., van Aalst, M., 2011. Projected Changes in Mean and Extreme Precipitation in Africa under Global Warming. Part Ii: East Africa. Journal of Climate 24(14), 3718-3733.

Simonovic, S.P., Peck, A., 2009. Updated Rainfall Intensity Duration Frequency Curves for the City of London under the Changing Climate. Department of Civil and Environmental Engineering, The University of Western Ontario.

Trenberth, K.E., 2011. Changes in Precipitation with Climate Change. Climate Research 47(1-2), 123-138.

USEPA, 2010. Chesapeake Bay Total Maximum Daily Load for Nitrogen, Phosphorus, and Sediment. Annapolis, MD: US Environmental Protection Agency, Chesapeake Bay Program Office. Also Available at http://www. epa. gov/reg3wapd/tmdl/ChesapeakeBay/tmdlexec. html.

Chapter 2. Literature Review

The following sections review the literature pertinent to urbanization and its impacts on runoff quantity and quality, and methods for their potential mitigation. Watershed modeling, the impacts of CC on water quality and quantity in urban watersheds, and the impacts of CC on stormwater control measures (SCMs) are reviewed in the next sections. Cost estimation and optimization of SCMs are reviewed in the last section.

2.1 Urban Runoff Impacts

Urban development creates large amounts of impervious surfaces for the creation of roads, parking, building roofs, and sidewalks, resulting in large increases in runoff peaks and volume which have been extensively studied (Arnold Jr and Gibbons, 1996; Dietz and Clausen, 2005; Jennings and Jarnagin, 2002; Leopold, 1968; Pyke et al., 2011; Walsh et al., 2012). Impervious surfaces limit infiltration and thus results in decreased groundwater recharge and baseflow contributions to streams. Larger runoff rates increase pollutant washoff from the land, and stormwater conveyance systems accelerate the transport of pollutants to surface waters (Hatt et al., 2004). Increased runoff from urban development facilitates erosion from landscapes and streambanks, as well as channel scour and degradation; these effect are often collectively known as “urban stream syndrome” (Kaushal and Belt, 2012; Nelson and Booth, 2002).

Urban stormwater can contain numerous pollutants including suspended solids, nutrients, heavy metals, bacteria and toxic pesticides (Akan, 1993). Pollutants like phosphorus may be highly variable because of the dynamic nature of the P partitioning and also a portion of that is distributed across hetero-disperse particulate matter (Sample et al., 2012). Pollutants accumulation on impervious urban surfaces during dry weather periods is referred to as build-up (Egodawatta et al., 2007). Mobilization of accumulated pollutants during storm events is referred to pollutant washoff (Egodawatta et al., 2007; Vaze and Chiew, 2003). Buildup and washoff processes depend on factors such as land-use, traffic volume and climate variables (Wijesiri et al., 2015a, b). However, estimating these parameters remains a challenge; several findings indicate that the performance of these models and simulated concentrations are subject to very large uncertainties (Dotto et al., 2010; Freni et al., 2009; Sage et al., 2015; Vezzaro et al., 2012).

Event mean concentration (EMC) is a method used to estimate washoff load (Sansalone and Buchberger, 1997); it is defined as the flow proportional concentration of a given pollutant

during the storm event. EMC is an effective method for estimation of pollutant concentrations as shown by Charbeneau and Barrett (1998). Authors investigated several methods including EMC to generate constituent concentrations for use in stormwater modeling and found that a single EMC for all urban land uses provided a reasonable estimate of solids loads. Sage et al. (2015) used conceptual and empirical models to estimate the process of buildup and washoff as a function of EMC and demonstrated that the model accurately replicates load estimates. Authors found that EMC methods provided sufficient accuracy for estimating washoff loads. Even though the concentration of a pollutant may vary during a rainfall event, a single EMC can be used to characterize runoff constituents (Butcher, 2003).

The National Urban Runoff Database under the USEPA's National Pollutant Discharge Elimination System (NPDES) Stormwater MS4 Phase I Program is created to identify the range of EMC values for different pollutants (Pitt et al., 2004). A summary of P concentrations from urban runoff is illustrated in the study by Sample et al. (2012). These data represent concentrations of TP in urban stormwater from the 29 prototype National Urban Runoff Program (NURP) USEPA (1983). In order to estimate washoff pollutant parameters for TSS, TN, and TP in this study, initial values were chosen as mean values from the NURP report (USEPA, 1983) and other studies in the Virginia and Chesapeake Bay (Hirschman et al., 2008; Schueler, 2011; USEPA, 2010b).The selected EMCs for TSS, TN, and TP were 40 mg/L, 2.9 mg/L, and 0.27 mg/L, respectively.

Runoff from urban and agricultural areas, in addition to discharges from wastewater treatment facilities have resulted in elevated nutrients such as nitrogen (N) and phosphorus (P) and sediment levels in downstream receiving waters. Excessive loading of sediment and nutrients have caused some downstream estuaries such as the Chesapeake Bay (CB) have become degraded. Excess nutrients cause algae to grow, which, reduces water clarity. Increased sediment loading also reduces water clarity. When the algae die, they deplete available oxygen, creating aquatic "dead zones" in the CB (National Research Council, 2000). To address the deteriorating aquatic health of the CB, the USEPA established a Total Maximum Daily Load (TMDL) which restricts the levels of N, P, and sediment in discharges to tributaries of the Chesapeake Bay (USEPA, 2010a) through a variety of voluntary and involuntary (i.e., through permits) means. The CB TMDL goals are being met in urban areas by implementing SCMs, which reduce or treat runoff prior to discharge.

2.2 Mitigation Methods

Remediating degraded surface waters resulting from urban development is often accomplished through implementation of watershed-based management strategies. Stormwater control measures (SCMs) (also known as best management practices, or BMPs) are one method used to restore urban watersheds and achieve downstream water quality goals.

Historically, SCMs were used to simply attenuate peak runoff; however, SCM functions were subsequently expanded to include limited water quality treatment. New methods for mitigating urban impacts have emerged; in the U.S. these are known collectively as green infrastructure (GI), green stormwater infrastructure (GSI) or low impact development (LID) (NRC, 2009). Dietz and Clausen (2008) examined the capability of LID in peak and runoff volume reduction and found that LID design, rainfall, and soil characteristics play important roles in the hydrologic performance of them in urban areas. The objective of LID is to create an equivalent hydrologic landscape to pre-developed, natural conditions (Prince George's County, 2000) and to enhance runoff reduction, increase infiltration, groundwater recharge, and stream protection; and treat pollutants such as nutrients and sediment. Implementing LID improves the infiltrative, storage, and treatment capacity of an urban catchment (Askarizadeh et al., 2015). LID practices such as green roofs, bioretention systems, grass swales, porous pavements, and infiltration trenches are commonly used in many urban areas; these have been demonstrated to be effective in reducing runoff volume and pollutant loading (Bedan and Clausen, 2009; Davis et al., 2009; Elliott and Trowsdale, 2007; Hathaway et al., 2008; Hunt et al., 2006; Myers et al., 2011).Peak flows may also be reduced, particularly for storms with recurrence intervals less than 20 years, if the particular practice has sufficient capacity. Dietz and Clausen (2008); Hood et al. (2007) found that design practices, rainfall, and soil characteristics play important roles on the effectiveness of LID practices.

2.3 Watershed Modeling

A variety of models are available for simulation of urban stormwater quantity and quality, including Win TR-55 (Natural Resources Conservation Service, 2016), Hydrologic Engineering Center Hydrologic Modeling System (HEC-HMS) (U.S. Army Corps of Engineers, 2016), HYDRUS model (Šimůnek et al., 2006), System for Urban Stormwater Treatment and Analysis Integration (SUSTAIN) (Lee et al., 2012), Model for Urban Stormwater Improvement

Conceptualization (MUSIC) (Wong et al., 2002), Mike-Urban (Danish Hydrauic Institute, 2016), and the Storm Water Management Model (SWMM) (Huber et al., 1988; Rossman, 2004). HEC-HMS, Mike-Urban, and SWMM can be used for event-based and continuous simulation modes (Elliott and Trowsdale, 2007; Zoppou, 2001). SWMM is able to simulate the hydrologic performance of infiltrative SCMs (Gironás et al., 2009). SWMM has been widely applied in urban areas. Hydrologic and physical processes modeled within SWMM include rainfall-runoff, infiltration, evapotranspiration (ET), snowmelt, surface water routing, surface water storage, groundwater, water quality, and treatment. SWMM is also able to simulate the production of pollutant loads associated with runoff through modeling buildup during dry weather and washoff during storm events from specific land uses (James et al., 2010). SWMM allows treatment functions which express the removal of pollutants to be applied to any water quality constituent at any node of the conveyance system (Rossman, 2015); retention ponds are storage nodes. LID practices in SWMM are modeled as a collection of physical processes unique to each, and are simulate using a combination of vertical layers representing the surface, pavement, and soil, storage, and underdrain portions of each LID practice. Infiltration, drainage, and overflow, control the storage in each of the layers dynamically (Niazi et al., 2017). SWMM can model the hydrology of bioretention cells, infiltration trenches, porous pavement, rain barrels, vegetated swales, green roofs, and street planters (James et al., 2010; Rossman, 2015), however, it cannot model water quality treatment within LID SCMs. SWMM has been successfully applied to evaluate the hydrologic impacts of urbanization in multiple studies (Bhaduri and Minner, 2001; Karamouz et al., 2011; Karamouz and Nazif, 2013; Kovács and Clement, 2009; Warwick and Tadepalli, 1991; Zahmatkesh et al., 2014) and to assess potential benefits of implementing LID (Kong et al., 2017; Lucas and Sample, 2015; Palla and Gnecco, 2015; Rossman, 2010).

2.4 Sensitivity Analysis

Sensitivity analysis (SA) is a simple way to find the relative influence of each input parameter on model results. Research suggests that use of SA reduces variance in model results (Hameed, 2015). SA can identify the parameters that provide the most effect on selected results during calibration (Song et al., 2015). The hydrologic performance of SCMs varies with design configurations (Ahiablame et al., 2012; Li and Babcock, 2014). SA was conducted using System for Urban Stormwater Treatment and Analysis Integration (SUSTAIN) by Lee et al. (2012). The authors found that flow volume was reduced and pollutant removal efficiency increased when

the SCM footprint, vertical storage, and interception of upstream drainage area increased. Jia et al. (2015) varied 12 key parameters of two impervious land covers (roof and pavement) within SUSTAIN. Results indicated that the most sensitive parameters were land washoff coefficient, and the exponent to the peak flow reduction rate, followed by the maximum buildup and washoff exponent to different pollutant loadings. Chui et al. (2016) assessed the sensitivity of the hydrological performance of green roofs, bioretention and permeable pavements to varying design parameters, including initial saturation, hydraulic conductivity, and berm height. Results indicated that green roofs were sensitive to initial saturation and hydraulic conductivity, while bioretention was sensitive to hydraulic conductivity and berm height. Permeable pavement was sensitive only to hydraulic conductivity. These limited studies indicate that more research focused upon the sensitivity of SCM performance to design parameters is needed; few tools exist that can facilitate this task.

2.5 Calibration of Watershed Models

Hydrologic models are characterized by complex relationships between rainfall, runoff and other physical processes, and a relatively large number of variables and parameters. These parameters and variables often cannot be measured directly due to measurement error and spatial variability. Calibration is often performed to assist in assigning values to some inputs, and assures the model is accurately representing the actual system (Eckhardt and Arnold, 2001; Gupta et al., 1998; Yapo et al., 1998). Proper calibration of hydrologic models for urban watersheds is necessary to ensure reliable assessment of SCMs. Manual calibration and verification can be tedious and time consuming. Thus, efficient methods to calibrate hydrologic models are needed. Calibration of hydrologic models can be performed over individual storm events or over a particular period of time. Hydrologic models have been calibrated successfully using neuro-fuzzy systems (Talei et al., 2010) and evolutionary computation (Fang and Ball, 2007), Gradient-based approaches (Gallagher and Doherty, 2007; Tan et al., 2008) are primarily used for continuous event calibration of urban watershed models and they are well known for finding local optima. The gradient based Elitist Non-dominated Sorting Genetic algorithm (NSGA-II) has been widely applied in different studies for multi-objective optimization (Niksokhan et al., 2009). NSGA-II has been applied to groundwater monitoring design (Reed and Minsker, 2004), water distribution network design (Atiquzzaman et al., 2006), hydraulic structure design (Rasekh et al., 2010), and optimal sizing of detention ponds (Yu et al., 2015).

A calibration procedure of SWMM was suggested by Maalel and Huber (1984). Delleur and Baffaut (1990) used an expert system approach to assist in the automatic calibration and estimation of parameters in a SWMM model. Another auto calibration method, knowledge-based systems, was adapted to SWMM by Liong et al. (1991); a similar method using a multiple search driver. The model-independent parameter estimation system (PEST) was adapted to SWMM by Balascio et al. (1998); Liong et al. (1995); Mancipe-Munoz et al. (2014) applied genetic algorithm (GA) to find the optimal values calibration parameters. An artificial neural network (ANN) solution of inverse parameters was used by Zaghloul and Abu Kiefa (2001) for calibration of SWMM.

Single-objective calibration optimization methods have inherent limitations as they tend to lump multiple objectives into a single objective. It may not account for various objectives of calibration such as minimizing the errors and maximizing correlation between model predictions and observations (Yapo et al., 1998). In a single objective calibration optimization for maximizing correlation, generally we may have unrealistic over- or underestimates of the predicted time series. Multi-objective optimization applications to calibration provides parameters that collectively broadly meet a variety of calibration performance criteria (Savic, 2002). The interaction among different objectives gives rise to sets of alternative solutions known as the trade-off, non-dominated, or Pareto-optimal solutions (Gupta et al., 1998; Madsen, 2000; Reed et al., 2013; Savic, 2002; Yapo et al., 1998). While the advantages of multi-objective calibration optimization may be obvious based on previous studies, to date, there have been few applications of it with SWMM.

2.6 Climate Change Impacts

Projected greenhouse gas emission scenarios have been developed based on the expected changes in the global economy, environment, and population (Moss et al., 2010; Pachauri et al., 2014) and are used as critical assumptions in global climate models (GCMs). As reported by the Intergovernmental Panel on Climate Change (IPCC), global mean temperatures are expected to increase 1.1 to 6.4 °C by 2100 (IPCC, 2014). Historical evaluations of the U.S. climate (1950-2009) revealed significant temperature increases for nearly all U.S. cities, which was attributed to climate change (CC) rather than urbanization (Mishra and Lettenmaier (2011), and nearly 30% of the urban areas exhibited a significant increase in extreme precipitation. Changes in heating degree days in about 50% of U.S. urban areas from 1950-2009 declined by a median of -1.7%

per decade (Mishra and Lettenmaier, 2011). In addition, the number of warm nights with the minimum temperature of 32 °C increased by 6.5% per decade for all urban areas (Mishra and Lettenmaier, 2011). In the Northeast U.S., Hayhoe et al. (2008) predicted precipitation increases during winter and spring for both higher (A1F1) and lower (B1) greenhouse gas emission scenarios by 2100. Najjar et al. (2010) found that in the mid-Atlantic region of the U.S., CO_2 concentrations are expected to increase by 50-160% by 2100. During this same period, seal level is expected to rise about 0.7-1.6 m, and water temperatures are expected to rise by 2 to 6 °C (Najjar et al., 2010). CC may have significant impacts on stream discharge frequency, peak discharge, runoff volume, base flows, stream systems, channel morphology, aquatic habitats, water supplies, and pollutant loads (Bhaduri et al., 2000; Burns et al., 2005; Olang and Fürst, 2011; Tang et al., 2005). Rainfall patterns will change with projected CC which may aggravate the effects of urbanization by influencing urban runoff volume, timing, and peak, overwhelming stormwater systems designed for smaller events (Semadeni-Davies et al., 2008).

2.6.1 Climate Change in Urbanized Watersheds

Design of urban stormwater systems are based on the assumption of stationarity in precipitation records and extreme statistics (Zahmatkesh et al., 2014). However, CC projection indicate changes in rainfall magnitude, frequency, and intensity (IPCC, 2014; Shongwe et al., 2011; Trenberth, 2011).

Continuous simulation methods usually incorporate altered climate predictions, often produced by a global climate model (GCM) and/or a regional climate model (RCM). Unfortunately, GCMs often lack the requisite spatial and temporal resolution for application to urban watersheds, and while the spatial resolution of RCMs (50 km^2) is acceptable, they typically do not accurately resolve the sub-hourly temporal scales necessary to simulate the flashy urban runoff response (Schoof, 2012). Downscaling methods are used to bridge the mismatch between the spatial and temporal resolution of GCMs and RCMs and the required resolution for assessment of the CC impacts (Fowler and Wilby, 2007).

Two widely used downscaling methods are dynamical and statistical downscaling. Systematic errors are inevitable in RCM outputs; therefore, bias correction is often necessary after downscaling to a higher spatial resolution. Biases may occur in the climate model outputs due to a coarse spatial resolution, simplified processes, or numerical diffusion inherent in any model. Such errors can affect the projected results and should be corrected before using any

climate model (Chen et al., 2013). Wood et al. (2004) reviewed linear interpolation (LI), spatial disaggregation (SD), and bias-correction and spatial disaggregation (BCSD) bias correction methods. The authors found that the BCSD was able to reproduce observed weather and provided the most accurate results. Teutschbein and Seibert (2012) compared linear scaling, local intensity scaling, power transformation, variance scaling, distribution transfer, and the delta-change bias correction methods, and found each was suitable for bias corrections, however there were significant differences in ease of use. Gudmundsson et al. (2012) compared derived distribution, parametric, and nonparametric bias correction methods. Results indicated the nonparametric transformation method was better at reducing bias. Chen et al. (2013) compared linear scaling, local intensity scaling, daily translation, daily bias correction, quantile mapping based on an empirical distribution, and quantile mapping based on a gamma distribution. Results revealed that all methods performed reasonably well, however, the authors suggest that the performance of a hydrological model may be dependent on the bias correction method selected. Rosenberg et al. (2010) used a dynamically downscaled dataset from Washington State from 2020-2050 to estimate streamflow. While a few areas showed statistically significant differences in streamflow, the authors recommended that downscaling methods for RCM outputs be used with caution for drainage design. Recently, Wang and Chen (2014) developed a bias correction method using a modified version of an equiratio cumulative distribution function matching method, which corrects model data using multiplicative scaling factors and improves the equidistant approach in bias correction of precipitation.

The impacts of CC on water quantity in urban watersheds have been investigated. Cameron (2006) assessed the effects of CC on flood magnitude and frequency in the Lossie watershed in Northeast Scotland, UK using a dynamically downscaled GCM and the topography-based hydrological model (TOPMODEL). Results showed the change in projected flood magnitudes ranging from -10% to 56% depending on the choice of CC scenario. Zahmatkesh et al. (2014) evaluated the impact of CC on runoff using Intergovernmental Panel on Climate Change Coupled Model Intercomparison Project Phase 5 (IPCC CMIP5) in a New York City watershed. The authors found that urban runoff peak would increase up to 80% with projected CC. Semadeni-Davies et al. (2008) evaluated the combined effects of CC and urbanization on a stream in south Sweden. Results indicated larger increase in peak flow volume and flood risks due to CC than from urban development. Collectively, these studies provide a

first cut assessment of what could be a major impact of CC, increased flooding of urban areas, which will require major investments to mitigate (Wright et al., 2012). Few studies to date have focused on the impact of CC on water quality in urban watersheds. Improving the ability to predict CC impacts on water quality in urban watershed is needed to evaluate conditions and select the best treatment options.

2.6.2 Impacts of Climate Change on Stormwater Control Measures

SCMs are typically designed based on the assumption of stationarity of historical climate data (Simonovic and Peck, 2009). However, performance of SCMs for runoff reduction or pollutant removal may decrease in the future due to CC as design are exceeded (Milly et al., 2008; Shongwe et al., 2011; Trenberth, 2011). Since SCMs are typically the lowest feature in a given drainage area to intercept runoff, they may be the most susceptible component of stormwater infrastructure to CC-induced changes in rainfall. Paradoxically, SCMs can be used as climate adaptation strategies to mitigate potential projected CC impacts (Gill et al., 2007; Pyke et al., 2011). SCMs such as bioretention can reduce the adverse hydrologic and water quality effects of urbanization through infiltration and evaporation (Elliott and Trowsdale, 2007; Jia et al., 2012; Semadeni-Davies et al., 2008; Van Liew et al., 2012; Woznicki et al., 2011). The performance of bioretention systems subjected to CC scenarios was evaluated by Hathaway et al. (2014) for several locations in North Carolina, U.S. The authors found that CC would likely cause a significant increase in the frequency and magnitude of untreated overflows and between 9 and 31 cm of additional storage would be required to compensate. Wang et al. (2016) modeled the potential impacts of CC and urbanization on bioretention function in a catchment located in Singapore and found that the performance of bioretention was more sensitive to urbanization than that for CC in an urban catchment.

Retention ponds are a ubiquitous SCM in most urban watersheds in the U.S. (Balascio and Lucas, 2009; Semadeni-Davies, 2006). Removal of TSS, TN, and TP in retention ponds depends on the hydraulic retention time (HRT) (Sharma et al., 2016; Vollertsen et al., 2007). Increased rainfall intensities and longer dry weather periods may affect the efficiency of retention ponds by increasing buildup and washoff of pollutants from land surfaces, increasing pollutant loading (Sharma et al., 2016). Furthermore, high flows may shorten the HRTs of retention ponds during extreme events. These effects should be considered to achieve resilient SCMs and urban drainage systems for projected CC conditions. Resiliency can be defined as the

ability of a stormwater system and/or SCM to accommodate or recover from CC impacts in a timely and efficient manner either through restoration or improvement of its essential functions (Field et al., 2012)

Rainwater Harvesting (RWH) systems are unusual SCMs in that they recycle and reuse stormwater, normally from rooftops, and can help increasing water supply and reducing runoff. RWH has been used for millennia to meet water supply needs; they have recently been repurposed as an SCM for managing runoff (Alam et al., 2012; Kahinda et al., 2010; Lassaux et al., 2007; Steffen et al., 2013; Tam et al., 2010). RWH systems store runoff from rooftops or other impervious areas for later use for outdoor irrigation or indoor nonpotable uses such as flushing toilets (Silva et al., 2015). A recent, comprehensive review of RWH is provided by Campisano et al. (2017). By reusing stored rainfall instead of discharging it, RWH systems may reduce runoff in addition to providing an alternative nonpotable water supply. RWH was found to be an effective water supply adaptation strategy for mitigating CC effects, particularly in areas with high water demand (Aladenola and Adeboye, 2010; Boelee et al., 2013; Kahinda et al., 2010; Mukheibir, 2008; Pandey et al., 2003; Rozos et al., 2009). The effective storage capacity of RWH will likely be reduced with CC as shown in the studies by Youn et al. (2012) in South Korea and Lash et al. (2014) for the U.K. Lo and Koralegedara (2015)evaluated the effects of CC on urban RWH in Colombo City, Sri Lanka, and found that residential RWH systems would likely be more affected by CC than non-residential systems. Palla et al. (2012) assessed the performance of domestic RWH systems across Europe with respect to optimal design with CC. Results indicated that the duration of antecedent dry conditions was strongly correlated with RWH system behavior, while event rainfall depth, intensity and duration were weakly correlated. These studies demonstrate the need for improved analysis of CC conditions to improve the resilience of RWH systems. SWMM was used in combination with downscaled Coupled Model Intercomparison Project Phase 5 (CMIP5) projections by Tavakol-Davani et al. (2016). The authors found that RWH increased resilience of urban stormwater infrastructure to CC by limiting CSOs. Downscaling is a method used to bridge the mismatch between the spatial and temporal resolution of GCMs and RCMs and the resolution needed for urban hydrologic models of at least 50-100 km^2 and time steps of less than an hour, respectively (Fowler and Wilby, 2007). RWH systems typically need a sub-daily temporal scale to accurately address water supply and runoff capture benefits (Burian and Jones, 2010; Coombes and Barry, 2007;

Coombes et al., 2002; Fewkes and Butler, 2000; Herrmann and Schmida, 2000; Sample and Heaney, 2006).While there have been a few studies that assessed the effects of CC on RWH systems, nearly all of these addressed only water supply benefits. No studies were found that assessed the effects of CC on RWH systems with respect to the dual objectives of water supply and runoff reduction.

2.7 Cost Optimization

A key challenge in urban watershed management is identifying cost-effective stormwater management strategies that will meet water quality objectives. Liu et al. (2016) applied nonlinear spatial optimization techniques for selection and placement of GI SCMs using the Long-Term Hydrologic Impact Assessment-Low Impact Development (L-THIA-LID) model to reduce the impacts of urban development and climate change on runoff and water quality. Chang et al. (2011) determined optimal design strategies for green roofs and cisterns for a residential home using a cost-benefit-risk trade-off method. Jia et al. (2015); Lee et al. (2012); Sun et al. (2016) applied SUSTAIN to urban watersheds to determine the optimal location, type, and cost of SCMs and generated a cost-effectiveness curve for meeting water quality and quantity goals. SUSTAIN is a simulation-optimization tool for optimizing the selection and sizing of SCMs in a watershed, using computation algorithms similar to SWMM but within an ArcGIS interface (version 9.3.31). SUSTAIN is able to analyze SCMs applications using an optimization algorithm to find sets of cost-effective solutions and generate a cost-effectiveness curve. SUSTAIN, like SWMM, incorporates LID simulation. While SUSTAIN is similar to SWMM, it is a completely separate model that must be developed independently, within ArcGIS 9.3.1 and an associated extension, Spatial Analyst. The use of ArcGIS 9.3.1 limits the utility of SUSTAIN, because this version of ArcGIS is dated (ArcGIS 10.6 was available during the drafting of this thesis). In the authors' opinion, this effort might be better spent refining and/or calibrating existing urban watershed models. Model software such as SWMM that is relatively easy to use and has a wide user base may be a better platform for an optimization tool. Several studies have coupled existing hydrological models, including the Soil and Water Assessment Tool (SWAT) and the Model for Urban Stormwater Improvement Conceptualization (MUSIC) with a genetic algorithm (GA) to achieve water quantity goals (e.g., peak flow reduction) (Kaini et al., 2008; Montaseri et al., 2015). Tools such as the BMP Decision Support System (BMPDSS) and the Multi-Objective, Socio-Economic, Boundary-Emanating, Nearest Distance (MOSEBEND), have

been developed to optimize location, and selection of SCMs to meet runoff reduction goals (Cano and Barkdoll, 2016; Jia et al., 2012). BMPDSS is unable to simulate infiltrative SCMs such as permeable pavement, and no automated calibration capability is available. MOSEBEND focuses solely on runoff reduction goals and does not consider pollutant removal efficiency.

Zhang and Chui (2018) commented that coupling SWMM with optimization is straightforward because SWMM has a simple link-node structure, open source features, and an LID module. Optimization tools such as SWMM-GA, SWMM-TOPSIS, SWMM-PSO, and GreenPlan-IT use SWMM as a basis (Sebti et al., 2016; Song and Chung, 2017) and have been demonstrated to be effective for urban drainage planning and design. Baek et al. (2015); Duan et al. (2016); Jung et al. (2016); Li et al. (2015) coupled optimization methods with SWMM to find the optimal size of SCMs such as retention ponds and permeable pavement with the goal of minimizing local flooding. These studies used a single rather than multiple objectives, such as maximizing runoff reduction, and/or maximizing reduction in multiple pollutant loads (i.e. TSS, total nitrogen, or TN, and total phosphorous, or TP). The ability to optimize selection and size of SCMs using an existing SWMM model of a realistic, medium-sized catchment (200-400 ha) remains a research need. This scale is large enough to be realistic, but not so large that it could become unwieldy in terms of combinations and choices of SCMs.

2.8 Summary

Significant investments are being made to implement SCMs in urban watersheds to meet local and downstream water quality improvement goals. The cost of SCMs and budget limitation of cities increase the complexity of identifying the cost-effective practices in urban watersheds. Public domain tools that combine simulation modeling with cost optimization to help identify optimal strategies that meet water quality goals is needed. This could lower the costs of watershed restoration, speed up the restoration process, and allowing more load reductions for the same investment. While tools are available for simulating urban hydrology and water quality, in general, they are difficult to calibrate, perform sensitivity analysis, and cost optimization must be performed separately. Developing an easy to use tool that performs these tasks and wraps around the current version of the dominant urban simulation model, SWMM, without altering its source code would be extremely beneficial. This type of tool would thus help develop robust assessments of CC to water quantity and quality in urban watersheds. On the other hand, the investments and water quality progress are imperiled by CC, which, in the Mid-Atlantic, is

projected to result in increased precipitation which will lead to increased runoff, sediment and nutrient fluxes (Najjar et al., 2010). There is a need for methods to integrate CC into watershed models so the impacts of CC on water quantity and quality can be assessed. Furthermore, there is a lack of understanding the degree of resiliency SCMs can provide and how CC might affect their function and water quality performance. Advances in downscaling methods coupled with continuous simulation hydrologic and water quality models make it feasible to assess the treatment performance of SCMs impacted by CC at appropriate spatial and temporal scales.

References for Chapter 2:

Ahiablame, L.M., Engel, B.A., Chaubey, I., 2012. Effectiveness of Low Impact Development Practices: Literature Review and Suggestions for Future Research. Water, Air, & Soil Pollution 223(7), 4253-4273.

Akan, O.A., 1993. Urban Stormwater Hydrology: A Guide to Engineering Calculations. Crc Press.

Aladenola, O.O., Adeboye, O.B., 2010. Assessing the Potential for Rainwater Harvesting. Water Resources Management 24(10), 2129-2137.

Alam, R., Munna, G., Chowdhury, M., Sarkar, M., Ahmed, M., Rahman, M., Jesmin, F., Toimoor, M., 2012. Feasibility Study of Rainwater Harvesting System in Sylhet City. Environmental Monitoring and Assessment 184(1), 573-580.

Arnold Jr, C.L., Gibbons, C.J., 1996. Impervious Surface Coverage: The Emergence of a Key Environmental Indicator. Journal of the American Planning Association 62(2), 243-258.

Askarizadeh, A., Rippy, M.A., Fletcher, T.D., Feldman, D.L., Peng, J., Bowler, P., Mehring, A.S., Winfrey, B.K., Vrugt, J.A., AghaKouchak, A., Jiang, S.C., Sanders, B.F., Levin, L.A., Taylor, S., Grant, S.B., 2015. From Rain Tanks to Catchments: Use of Low-Impact Development to Address Hydrologic Symptoms of the Urban Stream Syndrome. Environmental Science & Technology 49(19), 11264-11280.

Atiquzzaman, M., Liong, S.-Y., Yu, X., 2006. Alternative Decision Making in Water Distribution Network with Nsga-Ii. Journal of Water Resources Planning and Management 132(2), 122-126.

Baek, S.-S., Choi, D.-H., Jung, J.-W., Lee, H.-J., Lee, H., Yoon, K.-S., Cho, K.H., 2015. Optimizing low impact development (LID) for stormwater runoff treatment in urban area, Korea: Experimental and modeling approach. Water research 86, 122-131.

Balascio, C., Palmeri, D., Gao, H., 1998. Use of a Genetic Algorithm and Multi-Objective Programming for Calibration of a Hydrologic Model. Transactions of the Asae 41(3), 615-619.

Balascio, C.C., Lucas, W.C., 2009. A Survey of Storm-Water Management Water Quality Regulations in Four Mid-Atlantic States. Journal of Environmental Management 90(1), 1-7.

Bedan, E.S., Clausen, J.C., 2009. Stormwater Runoff Quality and Quantity from Traditional and Low Impact Development Watersheds1. Wiley Online Library.

Bhaduri, Minner, 2001. Long-Term Hydrologic Impact of Urbanization: A Tale of Two Models. Journal of Water Resources Planning and Management 127(1), 13-19.

Bhaduri, B., Harbor, J., Engel, B., Grove, M., 2000. Assessing Watershed-Scale, Long-Term Hydrologic Impacts of Land-Use Change Using a Gis-Nps Model. Environmental Management 26(6), 643-658.

Boelee, E., Yohannes, M., Poda, J.-N., McCartney, M., Cecchi, P., Kibret, S., Hagos, F., Laamrani, H., 2013. Options for Water Storage and Rainwater Harvesting to Improve Health and Resilience against Climate Change in Africa. Regional Environmental Change 13(3), 509-519.
Burian, S.J., Jones, D., 2010. National Assessment of Rainwater Harvesting as a Stormwater Best Management Practice: Challenges, Needs, and Recommendations, Low Impact Development 2010: Redefining Water in the City. pp. 842-852.
Burns, D., Vitvar, T., McDonnell, J., Hassett, J., Duncan, J., Kendall, C., 2005. Effects of Suburban Development on Runoff Generation in the Croton River Basin, New York, USA. Journal of Hydrology 311(1), 266-281.
Butcher, J.B., 2003. Buildup, Washoff, and Event Mean Concentrations. JAWRA Journal of the American Water Resources Association 39(6), 1521-1528.
Cameron, D., 2006. An Application of the Ukcip02 Climate Change Scenarios to Flood Estimation by Continuous Simulation for a Gauged Catchment in the Northeast of Scotland, Uk (with Uncertainty). Journal of Hydrology 328(1), 212-226.
Campisano, A., Butler, D., Ward, S., Burns, M.J., Friedler, E., DeBusk, K., Fisher-Jeffes, L.N., Ghisi, E., Rahman, A., Furumai, H., Han, M., 2017. Urban Rainwater Harvesting Systems: Research, Implementation and Future Perspectives. Water Research 115, 195-209.
Cano, O.M., Barkdoll, B.D., 2016. Multiobjective, Socioeconomic, Boundary-Emanating, Nearest Distance Algorithm for Stormwater Low-Impact Bmp Selection and Placement. Journal of Water Resources Planning and Management 143(1), 05016013.
Chang, N.-B., Rivera, B.J., Wanielista, M.P., 2011. Optimal Design for Water Conservation and Energy Savings Using Green Roofs in a Green Building under Mixed Uncertainties. Journal of Cleaner Production 19(11), 1180-1188.
Charbeneau, R.J., Barrett, M.E., 1998. Evaluation of methods for estimating stormwater pollutant loads. Water Environment Research 70(7), 1295-1302.
Chen, J., Brissette, F.P., Chaumont, D., Braun, M., 2013. Finding Appropriate Bias Correction Methods in Downscaling Precipitation for Hydrologic Impact Studies over North America. Water Resources Research 49(7), 4187-4205.
Chui, T.F.M., Liu, X., Zhan, W., 2016. Assessing Cost-Effectiveness of Specific Lid Practice Designs in Response to Large Storm Events. Journal of Hydrology 533, 353-364.
Coombes, P.J., Barry, M.E., 2007. The Effect of Selection of Time Steps and Average Assumptions on the Continuous Simulation of Rainwater Harvesting Strategies. Water Science & Technology 55(4), 125-133.
Coombes, P.J., Kuczera, G., Kalma, J.D., Argue, J.R., 2002. An Evaluation of the Benefits of Source Control Measures at the Regional Scale. Urban Water 4(4), 307-320.
Danish Hydrauic Institute, 2016. Mike Urban.
Davis, A.P., Hunt, W.F., Traver, R.G., Clar, M., 2009. Bioretention Technology: Overview of Current Practice and Future Needs. Journal of Environmental Engineering 135(3), 109-117.
Delleur, J.W., Baffaut, C., 1990. Calibration of Swmm Runoff Quality Model with Expert System. Journal of Water Resources Planning and Management 116(2), 247-261.
Dietz, M.E., Clausen, J.C., 2005. A Field Evaluation of Rain Garden Flow and Pollutant Treatment. Water, Air, and Soil Pollution 167(1), 123-138.
Dietz, M.E., Clausen, J.C., 2008. Stormwater Runoff and Export Changes with Development in a Traditional and Low Impact Subdivision. Journal of Environmental Management 87(4), 560-566.

Dotto, C., Kleidorfer, M., Deletic, A., Fletcher, T., McCarthy, D., Rauch, W., 2010. Stormwater Quality Models: Performance and Sensitivity Analysis. Water Science and Technology 62(4), 837-843.
Duan, H.-F., Li, F., Yan, H., 2016. Multi-Objective Optimal Design of Detention Tanks in the Urban Stormwater Drainage System: Lid Implementation and Analysis. Water Resources Management 30(13), 4635-4648.
Eckhardt, K., Arnold, J., 2001. Automatic Calibration of a Distributed Catchment Model. Journal of Hydrology 251(1), 103-109.
Egodawatta, P., Thomas, E., Goonetilleke, A., 2007. Mathematical interpretation of pollutant wash-off from urban road surfaces using simulated rainfall. Water Research 41(13), 3025-3031.
Elliott, A., Trowsdale, S., 2007. A Review of Models for Low Impact Urban Stormwater Drainage. Environmental Modelling & Software 22(3), 394-405.
Fang, T., Ball, J.E., 2007. Evaluation of Spatially Variable Control Parameters in a Complex Catchment Modelling System: A Genetic Algorithm Application. Journal of Hydroinformatics 9(3), 163-173.
Fewkes, A., Butler, D., 2000. Simulating the Performance of Rainwater Collection and Reuse Systems Using Behavioural Models. Building Services Engineering Research and Technology 21(2), 99-106.
Field, C.B., Barros, V., Stocker, T.F., Qin, D., Dokken, D.J., Ebi, K.L., Mastrandrea, M.D., Mach, K.J., Plattner, G.-K., Allen, S.K., M. Tignor, P.M.M., 2012. Glossary of Terms. In: Managing the Risks of Extreme Events and Disasters to Advance Climate Change Adaptation, . A Special Report of Working Groups I and Ii of the Intergovernmental Panel on Climate Change (Ipcc). Cambridge University Press, Cambridge, Uk, and New York, Ny, USA, Pp. 555-564.
Fowler, H.J., Wilby, R.L., 2007. Beyond the Downscaling Comparison Study. International Journal of Climatology 27(12), 1543-1545.
Freni, G., Mannina, G., Viviani, G., 2009. Identifiability Analysis for Receiving Water Body Quality Modelling. Environmental Modelling & Software 24(1), 54-62.
Gallagher, M., Doherty, J., 2007. Parameter Estimation and Uncertainty Analysis for a Watershed Model. Environmental Modelling & Software 22(7), 1000-1020.
Gill, S.E., Handley, J.F., Ennos, A.R., Pauleit, S., 2007. Adapting Cities for Climate Change: The Role of the Green Infrastructure. Built Environment 33(1), 115-133.
Gironás, J., Roesner, L.A., Davis, J., Rossman, L.A., Supply, W., 2009. Storm Water Management Model Applications Manual. National Risk Management Research Laboratory, Office of Research and Development, US Environmental Protection Agency Cincinnati, OH.
Gudmundsson, L., Bremnes, J., Haugen, J., Engen-Skaugen, T., 2012. Technical Note: Downscaling Rcm Precipitation to the Station Scale Using Statistical Transformations–a Comparison of Methods. Hydrology and Earth System Sciences 16(9), 3383-3390.
Gupta, H.V., Sorooshian, S., Yapo, P.O., 1998. Toward Improved Calibration of Hydrologic Models: Multiple and Noncommensurable Measures of Information. Water Resources Research 34(4), 751-763.
Hameed, M.A., 2015. Evaluating Global Sensitivity Analysis Methods for Hydrologic Modeling over the Columbia River Basin. Portland State University.
Hathaway, A.M., Hunt, W.F., Jennings, G.D., 2008. A Field Study of Green Roof Hydrologic and Water Quality Performance. Transactions of the Asabe 51(1), 37-44.
Hathaway, J., Brown, R., Fu, J., Hunt, W., 2014. Bioretention Function under Climate Change Scenarios in North Carolina, USA. Journal of Hydrology 519, 503-511.

Hatt, B.E., Fletcher, T.D., Walsh, C.J., Taylor, S.L., 2004. The Influence of Urban Density and Drainage Infrastructure on the Concentrations and Loads of Pollutants in Small Streams. Environmental Management 34(1), 112-124.
Hayhoe, K., Wake, C., Anderson, B., Liang, X.-Z., Maurer, E., Zhu, J., Bradbury, J., DeGaetano, A., Stoner, A., Wuebbles, D., 2008. Regional Climate Change Projections for the Northeast USA. Mitig Adapt Strateg Glob Change 13(5-6), 425-436.
Herrmann, T., Schmida, U., 2000. Rainwater Utilisation in Germany: Efficiency, Dimensioning, Hydraulic and Environmental Aspects. Urban Water 1(4), 307-316.
Hirschman, D., Collins, K., Schueler, T., 2008. Technical Memorandum: The Runoff Reduction Method. Center for Watershed Protection & Chesapeake Stormwater Network.
Hood, M.J., Clausen, J.C., Warner, G.S., 2007. Comparison of Stormwater Lag Times for Low Impact and Traditional Residential Development. Jawra Journal of the American Water Resources Association 43(4), 1036-1046.
Huber, W.C., Dickinson, R.E., Rosener, L.A., Aldrich, J.A., 1988. Stormwater Management Model User's Manual, Version 4. U.S. Environmental Protection Agency, Athens, GA.
Hunt, W.F., Jarrett, A.R., Smith, J.T., Sharkey, L.J., 2006. Evaluating Bioretention Hydrology and Nutrient Removal at Three Field Sites in North Carolina. Journal of Irrigation and Drainage Engineering 132(6), 600-608.
IPCC, 2014. Climate Change 2014–Impacts, Adaptation and Vulnerability: Regional Aspects. Cambridge University Press.
James, W., Rossman, L.A., James, W.R.C., 2010. User's Guide to Swmm 5 Computational Hydraulics International, Guelph, Ontario, Canada.
Jennings, D.B., Jarnagin, S.T., 2002. Changes in Anthropogenic Impervious Surfaces, Precipitation and Daily Streamflow Discharge: A Historical Perspective in a Mid-Atlantic Subwatershed. Landscape Ecology 17(5), 471.
Jia, H., Lu, Y., Shaw, L.Y., Chen, Y., 2012. Planning of Lid–Bmps for Urban Runoff Control: The Case of Beijing Olympic Village. Separation and Purification Technology 84, 112-119.
Jia, H., Yao, H., Tang, Y., Shaw, L.Y., Field, R., Tafuri, A.N., 2015. Lid-Bmps Planning for Urban Runoff Control and the Case Study in China. Journal of Environmental Management 149, 65-76.
Jung, Y.-w., Han, S.-i., Jo, D., 2016. Optimal Design of Permeable Pavement Using Harmony Search Algorithm with Swmm, Harmony Search Algorithm. Springer, pp. 385-394.
Kahinda, J.M., Taigbenu, A., Boroto, R., 2010. Domestic Rainwater Harvesting as an Adaptation Measure to Climate Change in South Africa. Physics and Chemistry of the Earth, Parts a/B/C 35(13), 742-751.
Kaini, P., Artita, K., Nicklow, J., 2008. Designing Bmps at a Watershed-Scale Using Swat and a Genetic Algorithm, World Environmental and Water Resources Congress 2008: Ahupua'a. pp. 1-10.
Karamouz, M., Hosseinpour, A., Nazif, S., 2011. Improvement of Urban Drainage System Performance under Climate Change Impact: Case Study. Journal of Hydrologic Engineering 16(5), 395-412.
Karamouz, M., Nazif, S., 2013. Reliability-Based Flood Management in Urban Watersheds Considering Climate Change Impacts. Journal of Water Resources Planning and Management 139(5), 520-533.
Kaushal, S.S., Belt, K.T., 2012. The Urban Watershed Continuum: Evolving Spatial and Temporal Dimensions. Urban Ecosystems 15(2), 409-435.

Kong, F., Ban, Y., Yin, H., James, P., Dronova, I., 2017. Modeling Stormwater Management at the City District Level in Response to Changes in Land Use and Low Impact Development. Environmental Modelling & Software 95, 132-142.
Kovács, A., Clement, A., 2009. Impacts of the Climate Change on Runoff and Diffuse Phosphorus Load to Lake Balaton (Hungary). Water Science & Technology 59(3), 417-423.
Lash, D., Ward, S., Kershaw, T., Butler, D., Eames, M., 2014. Robust Rainwater Harvesting: Probabilistic Tank Sizing for Climate Change Adaptation. Journal of Water and Climate Change 5(4), 526.
Lassaux, S., Renzoni, R., Germain, A., 2007. Life Cycle Assessment of Water from the Pumping Station to the Wastewater Treatment Plant. International Journal of Life Cycle Assessment 12(2), 118.
Lee, J.G., Selvakumar, A., Alvi, K., Riverson, J., Zhen, J.X., Shoemaker, L., Lai, F.-h., 2012. A Watershed-Scale Design Optimization Model for Stormwater Best Management Practices. Environmental Modelling & Software 37, 6-18.
Leopold, L.B., 1968. Hydrology for Urban Land Planning: A Guidebook on the Hydrologic Effects of Urban Land Use.
Li, F., Duan, H.-F., Yan, H., Tao, T., 2015. Multi-Objective Optimal Design of Detention Tanks in the Urban Stormwater Drainage System: Framework Development and Case Study. Water Resources Management 29(7), 2125-2137.
Li, Y., Babcock, R.W., 2014. Green Roof Hydrologic Performance and Modeling: A Review. Water Science & Technology 69(4), 727-738.
Liong, S., Chan, W., Lum, L., 1991. Knowledge-Based System for Swmm Runoff Component Calibration. Journal of Water Resources Planning and Management 117(5), 507-524.
Liong, S., Chan, W., ShreeRam, J., 1995. Peak-Flow Forecasting with Genetic Algorithm and Swmm. Journal of Hydraulic Engineering 121(8), 613-617.
Liu, Y., Theller, L.O., Pijanowski, B.C., Engel, B.A., 2016. Optimal Selection and Placement of Green Infrastructure to Reduce Impacts of Land Use Change and Climate Change on Hydrology and Water Quality: An Application to the Trail Creek Watershed, Indiana. Science of the Total Environment 553(Supplement C), 149-163.
Lo, K.F.A., Koralegedara, S.B., 2015. Effects of Climate Change on Urban Rainwater Harvesting in Colombo City, Sri Lanka. Environments 2(1), 105-124.
Lucas, W.C., Sample, D.J., 2015. Reducing combined sewer overflows by using outlet controls for Green Stormwater Infrastructure: Case study in Richmond, Virginia. Journal of Hydrology 520(Supplement C), 473-488.
Maalel, K., Huber, W., 1984. Swmm Calibration Using Continuous and Multiple Event Simulation, 3rd International Conference on Urban Storm Drainage. Chalmers University, Goteborg, Sweden, pp. 595-604.
Madsen, H., 2000. Automatic Calibration of a Conceptual Rainfall–Runoff Model Using Multiple Objectives. Journal of Hydrology 235(3), 276-288.
Mancipe-Munoz, N., Buchberger, S., Suidan, M., Lu, T., 2014. Calibration of Rainfall-Runoff Model in Urban Watersheds for Stormwater Management Assessment. Journal of Water Resources Planning and Management 140(6), 05014001.
Milly, P.C.D., Betancourt, J., Falkenmark, M., Hirsch, R.M., Kundzewicz, Z.W., Lettenmaier, D.P., Stouffer, R.J., 2008. Stationarity Is Dead: Whither Water Management? Science 319(5863), 573-574.

Mishra, V., Lettenmaier, D.P., 2011. Climatic Trends in Major U.S. Urban Areas, 1950–2009. Geophysical Research Letters 38(16), L16401.
Montaseri, M., Afshar, M.H., Bozorg-Haddad, O., 2015. Development of Simulation-Optimization Model (Music-Ga) for Urban Stormwater Management. Water Resources Management 29(13), 4649-4665.
Moss, R.H., Edmonds, J.A., Hibbard, K.A., Manning, M.R., Rose, S.K., Van Vuuren, D.P., Carter, T.R., Emori, S., Kainuma, M., Kram, T., 2010. The Next Generation of Scenarios for Climate Change Research and Assessment. Nature 463(7282), 747.
Mukheibir, P., 2008. Water Resources Management Strategies for Adaptation to Climate-Induced Impacts in South Africa. Water Resources Management 22(9), 1259-1276.
Myers, B., Beecham, S., van Leeuwen, J.A., 2011. Water Quality with Storage in Permeable Pavement Basecourse. Proceedings of the Institution of Civil Engineers. Water Management 164(7), 361-361.
Najjar, R.G., Pyke, C.R., Adams, M.B., Breitburg, D., Hershner, C., Kemp, M., Howarth, R., Mulholland, M.R., Paolisso, M., Secor, D., Sellner, K., Wardrop, D., Wood, R., 2010. Potential Climate-Change Impacts on the Chesapeake Bay. Estuarine, Coastal and Shelf Science 86(1), 1-20.
National Research Council, 2000. Clean Coastal Waters: Understanding and Reducing the Effects of Nutrient Pollution. National Academies Press.
Natural Resources Conservation Service, 2016. Win Tr-55. USDA Natural Resource Conservation Service, Washington, DC.
Nelson, E.J., Booth, D.B., 2002. Sediment Sources in an Urbanizing, Mixed Land-Use Watershed. Journal of Hydrology 264(1–4), 51-68.
Niazi, M., Nietch, C., Maghrebi, M., Jackson, N., Bennett, B.R., Tryby, M., Massoudieh, A., 2017. Storm Water Management Model: Performance Review and Gap Analysis. Journal of Sustainable Water in the Built Environment 3(2), 04017002.
Niksokhan, M.H., Kerachian, R., Karamouz, M., 2009. A Game Theoretic Approach for Trading Discharge Permits in Rivers. Water Science and Technology 60(3), 793-804.
NRC, 2009. Urban Stormwater Management in the United States. National Academies Press.
Olang, L., Fürst, J., 2011. Effects of Land Cover Change on Flood Peak Discharges and Runoff Volumes: Model Estimates for the Nyando River Basin, Kenya. Hydrological Processes 25(1), 80-89.
Pachauri, R.K., Allen, M.R., Barros, V.R., Broome, J., Cramer, W., Christ, R., Church, J.A., Clarke, L., Dahe, Q., Dasgupta, P., 2014. Climate Change 2014: Synthesis Report. Contribution of Working Groups I, Ii and Iii to the Fifth Assessment Report of the Intergovernmental Panel on Climate Change. IPCC.
Palla, A., Gnecco, I., 2015. Hydrologic Modeling of Low Impact Development Systems at the Urban Catchment Scale. Journal of Hydrology 528, 361-368.
Palla, A., Gnecco, I., Lanza, L., La Barbera, P., 2012. Performance Analysis of Domestic Rainwater Harvesting Systems under Various European Climate Zones. Resources, Conservation and Recycling 62, 71-80.
Pandey, D.N., Gupta, A.K., Anderson, D.M., 2003. Rainwater Harvesting as an Adaptation to Climate Change. Current Science 85(1), 46-59.
Pitt, R., Maestre, A., Morquecho, R., 2004. The National Stormwater Quality Database (Nsqd, Version 1.1), 1st Annual Stormwater Management Research Symposium Proceedings. pp. 13-51.

Prince George's County, 2000. Low-Impact Development Design Strategies, an Integrated Design Approach. Department of Environmental Resources, Programs and Planning Division,, Largo, MD.
Pyke, C., Warren, M.P., Johnson, T., LaGro, J., Scharfenberg, J., Groth, P., Freed, R., Schroeer, W., Main, E., 2011. Assessment of Low Impact Development for Managing Stormwater with Changing Precipitation Due to Climate Change. Landscape and Urban Planning 103(2), 166-173.
Rasekh, A., Afshar, A., Afshar, M.H., 2010. Risk-Cost Optimization of Hydraulic Structures: Methodology and Case Study. Water Resources Management 24(11), 2833-2851.
Reed, P.M., Hadka, D., Herman, J.D., Kasprzyk, J.R., Kollat, J.B., 2013. Evolutionary Multiobjective Optimization in Water Resources: The Past, Present, and Future. Advances in Water Resources 51, 438-456.
Reed, P.M., Minsker, B.S., 2004. Striking the Balance: Long-Term Groundwater Monitoring Design for Conflicting Objectives. Journal of Water Resources Planning and Management 130(2), 140-149.
Rosenberg, E.A., Keys, P.W., Booth, D.B., Hartley, D., Burkey, J., Steinemann, A.C., Lettenmaier, D.P., 2010. Precipitation Extremes and the Impacts of Climate Change on Stormwater Infrastructure in Washington State. Climatic Change 102(1), 319-349.
Rossman, L., 2015. Storm Water Management Model Reference Manual: Volume I–Hydrology. Us Envrionmental Protection Agency, Office of Research and Developement, National Risk Management Laboratory, Cincinnati, Oh 45268.
Rossman, L.A., 2004. Storm Water Management Model User's Manual, Version 5.0, in: U.S. Environmental Protection Agency (Ed.). Cincinatti, OH.
Rossman, L.A., 2010. Modeling Low Impact Development Alternatives with Swmm. Journal of Water Management Modeling.
Rozos, E., Makropoulos, C., Butler, D., 2009. Design Robustness of Local Water-Recycling Schemes. Journal of Water Resources Planning and Management 136(5), 531-538.
Sage, J., Bonhomme, C., Al Ali, S., Gromaire, M.-C., 2015. Performance Assessment of a Commonly Used “Accumulation and Wash-Off” Model from Long-Term Continuous Road Runoff Turbidity Measurements. Water Research 78, 47-59.
Sample, D.J., Grizzard, T.J., Sansalone, J., Davis, A.P., Roseen, R.M., Walker, J., 2012. Assessing Performance of Manufactured Treatment Devices for the Removal of Phosphorus from Urban Stormwater. Journal of Environmental Management 113, 279-291.
Sample, D.J., Heaney, J.P., 2006. Integrated Management of Irrigation and Urban Storm-Water Infiltration. Journal of Water Resources Planning and Management 132(5), 362-373.
Sansalone, J.J., Buchberger, S.G., 1997. Partitioning and First Flush of Metals in Urban Roadway Storm Water. Journal of Environmental Engineering 123(2), 134-143.
Savic, D., 2002. Single-Objective Vs. Multiobjective Optimisation for Integrated Decision Support.
Schoof, J.T., 2012. Scale Issues in the Development of Future Precipitation Scenarios. Journal of Contemporary Water Research & Education 147(1), 8-16.
Schueler, T., 2011. Nutrient Accounting Methods to Document Local Stormwater Load Reductions in the Chesapeake Bay Watershed. Technical Bulletin 9.
Sebti, A., Carvallo Aceves, M., Bennis, S., Fuamba, M., 2016. Improving Nonlinear Optimization Algorithms for Bmp Implementation in a Combined Sewer System. Journal of Water Resources Planning and Management 142(9), 04016030.

Semadeni-Davies, A., Hernebring, C., Svensson, G., Gustafsson, L.-G., 2008. The Impacts of Climate Change and Urbanisation on Drainage in Helsingborg, Sweden: Combined Sewer System. Journal of Hydrology 350(1), 100-113.
Semadeni-Davies, A., 2006. Winter Performance of an Urban Stormwater Pond in Southern Sweden. Hydrological Processes 20(1), 165-182.
Sharma, A.K., Vezzaro, L., Birch, H., Arnbjerg-Nielsen, K., Mikkelsen, P.S., 2016. Effect of Climate Change on Stormwater Runoff Characteristics and Treatment Efficiencies of Stormwater Retention Ponds: A Case Study from Denmark Using Tss and Cu as Indicator Pollutants. Springerplus 5(1), 1984.
Shongwe, M.E., van Oldenborgh, G.J., van den Hurk, B., van Aalst, M., 2011. Projected Changes in Mean and Extreme Precipitation in Africa under Global Warming. Part Ii: East Africa. Journal of Climate 24(14), 3718-3733.
Silva, C.M., Sousa, V., Carvalho, N.V., 2015. Evaluation of Rainwater Harvesting in Portugal: Application to Single-Family Residences. Resources, Conservation and Recycling 94, 21-34.
Simonovic, S.P., Peck, A., 2009. Updated Rainfall Intensity Duration Frequency Curves for the City of London under the Changing Climate. Department of Civil and Environmental Engineering, The University of Western Ontario.
Šimůnek, J., Van Genuchten, M.T., Šejna, M., 2006. The Hydrus Software Package for Simulating Two-and Three-Dimensional Movement of Water, Heat, and Multiple Solutes in Variably-Saturated Media. Technical Manual, Version 1, 241.
Song, J.Y., Chung, E.-S., 2017. A Multi-Criteria Decision Analysis System for Prioritizing Sites and Types of Low Impact Development Practices: Case of Korea. Water 9(4), 291.
Song, X., Zhang, J., Zhan, C., Xuan, Y., Ye, M., Xu, C., 2015. Global Sensitivity Analysis in Hydrological Modeling: Review of Concepts, Methods, Theoretical Framework, and Applications. Journal of Hydrology 523, 739-757.
Steffen, J., Jensen, M., Pomeroy, C.A., Burian, S.J., 2013. Water Supply and Stormwater Management Benefits of Residential Rainwater Harvesting in Us Cities. Jawra Journal of the American Water Resources Association 49(4), 810-824.
Sun, Y., Tong, S., Yang, Y.J., 2016. Modeling the Cost-Effectiveness of Stormwater Best Management Practices in an Urban Watershed in Las Vegas Valley. Applied Geography 76, 49-61.
Talei, A., Chua, L.H.C., Quek, C., 2010. A Novel Application of a Neuro-Fuzzy Computational Technique in Event-Based Rainfall–Runoff Modeling. Expert Systems with Applications 37(12), 7456-7468.
Tam, V.W., Tam, L., Zeng, S., 2010. Cost Effectiveness and Tradeoff on the Use of Rainwater Tank: An Empirical Study in Australian Residential Decision-Making. Resources, Conservation and Recycling 54(3), 178-186.
Tan, S.B., Chua, L.H., Shuy, E.B., Lo, E.Y.-M., Lim, L.W., 2008. Performances of Rainfall-Runoff Models Calibrated over Single and Continuous Storm Flow Events. Journal of Hydrologic Engineering 13(7), 597-607.
Tang, Z., Engel, B., Pijanowski, B., Lim, K., 2005. Forecasting Land Use Change and Its Environmental Impact at a Watershed Scale. Journal of Environmental Management 76(1), 35-45.
Tavakol-Davani, H., Goharian, E., Hansen, C.H., Tavakol-Davani, H., Apul, D., Burian, S.J., 2016. How Does Climate Change Affect Combined Sewer Overflow in a System Benefiting from Rainwater Harvesting Systems? Sustainable Cities and Society 27, 430-438.

Teutschbein, C., Seibert, J., 2012. Bias Correction of Regional Climate Model Simulations for Hydrological Climate-Change Impact Studies: Review and Evaluation of Different Methods. Journal of Hydrology 456, 12-29.
Trenberth, K.E., 2011. Changes in Precipitation with Climate Change. Climate Research 47(1-2), 123-138.
U.S. Army Corps of Engineers, 2016. Hydrologic Modeling System, Version 4.1.
USEPA, 1983. Results of the Nationwide Urban Runoff Program. Water Planning Division Washington, DC.
USEPA, 2010a. Chesapeake Bay Total Maximum Daily Load for Nitrogen, Phosphorus, and Sediment. Annapolis, MD: US Environmental Protection Agency, Chesapeake Bay Program Office. Also Available at http://www. epa. gov/reg3wapd/tmdl/ChesapeakeBay/tmdlexec. html.
USEPA, 2010b. Guidance for Federal Land Management in the Chesapeake Bay Watershed. Chapter 3. Urban and Suburban
Van Liew, M.W., Feng, S., Pathak, T.B., 2012. Climate Change Impacts on Streamflow, Water Quality, and Best Management Practices for the Shell and Logan Creek Watersheds in Nebraska.
Vaze, J., Chiew, F.H., 2003. Study of Pollutant Washoff from Small Impervious Experimental Plots. Water Resources Research 39(6).
Vezzaro, L., Eriksson, E., Ledin, A., Mikkelsen, P.S., 2012. Quantification of Uncertainty in Modelled Partitioning and Removal of Heavy Metals (Cu, Zn) in a Stormwater Retention Pond and a Biofilter. Water Research 46(20), 6891-6903.
Vollertsen, J., Åstebøl, S.O., Coward, J.E., Fageraas, T., Madsen, H.I., Hvitved-Jacobsen, T., Nielsen, A., 2007. Monitoring and Modelling the Performance of a Wet Pond for Treatment of Highway Runoff in Cold Climates, Highway and Urban Environment. Springer, pp. 499-509.
Walsh, C.J., Fletcher, T.D., Burns, M.J., 2012. Urban Stormwater Runoff: A New Class of Environmental Flow Problem. Plos One 7(9), e45814.
Wang, L., Chen, W., 2014. Equiratio Cumulative Distribution Function Matching as an Improvement to the Equidistant Approach in Bias Correction of Precipitation. Atmospheric Science Letters 15(1), 1-6.
Wang, M., Zhang, D., Adhityan, A., Ng, W.J., Dong, J., Tan, S.K., 2016. Assessing Cost-Effectiveness of Bioretention on Stormwater in Response to Climate Change and Urbanization for Future Scenarios. Journal of Hydrology 543, 423-432.
Warwick, J., Tadepalli, P., 1991. Efficacy of Swmm Application. Journal of Water Resources Planning and Management 117(3), 352-366.
Wijesiri, B., Egodawatta, P., McGree, J., Goonetilleke, A., 2015a. Incorporating process variability into stormwater quality modelling. Science of the Total Environment 533, 454-461.
Wijesiri, B., Egodawatta, P., McGree, J., Goonetilleke, A., 2015b. Influence of pollutant build-up on variability in wash-off from urban road surfaces. Science of the Total Environment 527, 344-350.
Wong, T.H., Fletcher, T.D., Duncan, H.P., Coleman, J.R., Jenkins, G.A., 2002. A Model for Urban Stormwater Improvement: Conceptualization, Global Solutions for Urban Drainage. pp. 1-14.
Wood, A.W., Leung, L.R., Sridhar, V., Lettenmaier, D.P., 2004. Hydrologic Implications of Dynamical and Statistical Approaches to Downscaling Climate Model Outputs. Climatic Change 62(1-3), 189-216.

Woznicki, S., Nejadhashemi, A., Smith, C., 2011. Assessing Best Management Practice Implementation Strategies under Climate Change Scenarios. Transactions of the Asabe 54(1), 171-190.
Wright, L., Chinowsky, P., Strzepek, K., Jones, R., Streeter, R., Smith, J., Mayotte, J.-M., Powell, A., Jantarasami, L., Perkins, W., 2012. Estimated Effects of Climate Change on Flood Vulnerability of U.S. Bridges. Mitig Adapt Strateg Glob Change 17(8), 939-955.
Yapo, P.O., Gupta, H.V., Sorooshian, S., 1998. Multi-Objective Global Optimization for Hydrologic Models. Journal of Hydrology 204(1-4), 83-97.
Youn, S.-g., Chung, E.-S., Kang, W.G., Sung, J.H., 2012. Probabilistic Estimation of the Storage Capacity of a Rainwater Harvesting System Considering Climate Change. Resources, Conservation and Recycling 65, 136-144.
Yu, P.-S., Yang, T.-C., Kuo, C.-M., Tai, C.-W., 2015. Integration of Physiographic Drainage-Inundation Model and Nondominated Sorting Genetic Algorithm for Detention-Pond Optimization. Journal of Water Resources Planning and Management 141(11), 04015028.
Zaghloul, N.A., Abu Kiefa, M.A., 2001. Neural Network Solution of Inverse Parameters Used in the Sensitivity-Calibration Analyses of the Swmm Model Simulations. Advances in Engineering Software 32(7), 587-595.
Zahmatkesh, Z., Karamouz, M., Goharian, E., Burian, S., 2014. Analysis of the Effects of Climate Change on Urban Storm Water Runoff Using Statistically Downscaled Precipitation Data and a Change Factor Approach. Journal of Hydrologic Engineering 20(7), 05014022.
Zhang, K., Chui, T.F.M., 2018. A Comprehensive Review of Spatial Allocation of Lid-Bmp-Gi Practices: Strategies and Optimization Tools. Science of the Total Environment 621, 915-929.
Zoppou, C., 2001. Review of Urban Storm Water Models. Environmental Modelling & Software 16(3), 195-231.

Chapter 3. Assessing the Effects of Climate Change on Water Quantity and Quality in an Urban Watershed Using a Calibrated Stormwater Model.

Taken from:
Alamdari, N., Sample, D. J., Steinberg, P., Ross, A. C., & Easton, Z. M. (2017). Assessing the Effects of Climate Change on Water Quantity and Quality in an Urban Watershed Using a Calibrated Stormwater Model. Water, 9(7), 464.

Abstract

Assessing climate change (CC) impacts on urban watersheds is difficult due to differences in model spatial and temporal scales, making prediction of hydrologic restoration a challenge. A methodology was developed using an autocalibration tool to calibrate a previously developed Storm Water Management Model (SWMM) of Difficult Run in Fairfax, Virginia. Calibration was assisted by use of multi-objective optimization. Results showed a good agreement between simulated and observed data. Simulations of CC for the 2041–2068 period were developed using dynamically downscaled North American Regional CC Assessment Program models. Washoff loads were used to simulate water quality, and a method was developed to estimate treatment performed in stormwater control measures (SCMs) to assess water quality impacts from CC. CC simulations indicated that annual runoff volume would increase by 6.5%, while total suspended solids, total nitrogen, and total phosphorus would increase by 7.6%, 7.1%, and 8.1%, respectively. The simulations also indicated that within season variability would increase by a larger percentage. Treatment practices (e.g., bioswale) that were intended to mitigate the negative effects of urban development will need to deal with additional runoff volumes and nutrient loads from CC to achieve the required water quality goals.

Keywords. global climate models; regional climate models; dynamic downscaling; TMDL.

3.1 Introduction

Historical evaluations of the U.S. climate (1950-2009) revealed significant temperature increases for nearly all US cities, which was attributed to climate change (CC) as opposed to "heat island" effects caused by urban development (Mishra and Lettenmaier (2011). Nearly 30% of the urban areas exhibited a significant increase in extreme precipitation. Hayhoe et al. (2008) predicted an increase in precipitation during winter and spring for higher and lower emissions by

the end of 21st century. Najjar et al. (2010) found that, in the mid-Atlantic region, precipitation magnitude and intensity, CO_2 concentrations, sea level, and water temperatures are likely to increase by the end of the 21st century. These predicted increases in rainfall magnitude and intensity could cause infrastructure failures due to increased runoff volumes and rates (Ahmadisharaf and Kalyanapu, 2015; Pavlovic et al.; Semadeni-Davies et al., 2008; Zahmatkesh et al., 2014a), overwhelming systems designed for much less. Limited studies using design storms and intensity-duration-frequency (IDF) curves have been conducted on the relative impact of CC on stormwater infrastructure. For example, Madsen and Figdor (2007) found that CC in the mid-Atlantic region would increase the frequency of a 1-year return period storm to 7.7 months. Moglen and Rios Vidal (2014) used intensity-duration-frequency (IDF) curves generated from regional climate models (RCMs) to assess impacts from urban development and CC and concluded that the impact on infrastructure from each was roughly equivalent. Peck et al. (2012) used a non-parametric weather generator to develop IDF curves for CC scenarios and found significant increases in anticipated precipitation intensities. Collectively, these studies provide a first cut assessment of what could be a major impact of CC, increased flooding of urban areas, which will require major investments to address (Wright et al., 2012).

More complex methods have been conducted using continuous simulation modeling incorporating altered climate predictions produced by a global climate model (GCM) and/or RCMs. Unfortunately, GCMs lack the spatial and temporal resolution for application to urban watersheds, and while the spatial resolution of RCMs (50 km^2) is acceptable, they cannot achieve the sub-hourly temporal scales necessary to simulate the flashy urban runoff response (Schoof, 2012). Downscaling is a method used to bridge the mismatch between the spatial resolution of GCMs and RCMs and the required resolution for assessment of the CC impacts (Fowler and Wilby, 2007). Two widely used downscaling methods are dynamical and statistical downscaling. Systematic errors are inevitable in RCM outputs; therefore, bias correction is often necessary after downscaling to a higher spatial resolution. Biases may occur in the climate model outputs due to a coarse spatial resolution, simplified processes, or numerical diffusion inherent in any model. Such errors can affect the projected results and should be corrected before using any climate model (Chen et al., 2013). Wood et al. (2004) reviewed six methods for generating future precipitation data for use in runoff modeling, consisting of three statistical downscaling methods: linear interpolation (LI), spatial disaggregation (SD), and bias-correction and spatial

disaggregation (BCSD) applied to either the Parallel Climate Model GCM (PCM) or to the output after using a RCM to downscale the PCM. The authors found that the BCSD applied to the dynamically downscaled RCM was able to reproduce observed weather and provided the most plausible results compared to historical data. Teutschbein and Seibert (2012) compared linear scaling, local intensity scaling, power transformation, variance scaling, distribution transfer, and the delta-change approach, and found that all methods were capable of correcting bias, however, significant differences were apparent between them in actual use. Gudmundsson et al. (2012) compared distribution derived, parametric, and nonparametric transformation methods for correcting bias of RCM outputs. The results indicated that nonparametric transformations were best at reducing bias in RCM outputs. Lafon et al. (2013) compared linear, nonlinear, γ-based quantile mapping, and empirical quantile mapping for reducing bias in RCM precipitation output. The results revealed that the third and fourth moments were sensitive to the choice of bias correction method, and the γ-based quantile-mapping technique performed significantly better than others. Linear scaling, local intensity scaling, daily translation, daily bias correction, quantile mapping based on an empirical distribution, and quantile mapping based on a gamma distribution were compared by Chen et al. (2013) to reduce bias from RCM outputs driven by NARCCAP data. The results indicated all methods improved RCM output. Chen et al found the calibration performance of a hydrological model was influenced by bias correction method and watershed location. Rosenberg et al. (2010) compared historical hourly precipitation datasets from Washington State from 1970-2000 to a generated dynamically downscaled dataset from 2020-2050 and output from a weather generator from several GCMs, and used these data to estimate streamflow. While few areas showed statistically significant differences in streamflow, the authors caution that improvements in downscaling methods for RCM outputs need to be made before results could be generalized sufficient for drainage design. Recently, Wang and Chen (2014) developed and tested a bias correction method using a modified version of equiratio cumulative distribution function matching. This method corrects model data using multiplicative scaling factors and improves the equidistant approach in bias correction of precipitation and enhances its performance. A modified version of this method was used for downscaling RCMs in this paper.

A variety of models are available for simulation of runoff, including Win TR-55 (Natural Resources Conservation Service, 2016), Hydrologic Engineering Center Hydrologic Modeling

System (HEC-HMS) (U.S. Army Corps of Engineers, 2016), Mike-Urban (Danish Hydrauic Institute, 2016), and the U.S. Environmental Protection Agency's (USEPA) Storm Water Management Model (SWMM) (Huber et al., 1988; Rossman, 2004). HEC-HMS, Mike-Urban, and SWMM have the capability of being used in both event-based and continuous simulation modes (Elliott and Trowsdale, 2007; Zoppou, 2001). Of these three, HEC-HMS and SWMM are in the public domain. SWMM is widely applied for continuous rainfall-runoff simulation in urban areas (Campbell and Sullivan, 2002; Selvalingam et al., 1987; Warwick and Tadepalli, 1991). SWMM simulates surface runoff, infiltration, evapotranspiration (ET), snowmelt, surface water routing, surface water storage, groundwater, water quality, and treatment processes. SWMM is able to simulate the production of pollutant loads associated with runoff through modeling buildup and washoff processes from specific land uses during dry weather and storm events respectively (James et al., 2010).

Urban development creates large amounts of impervious surfaces for roads, parking, buildings, and sidewalks. As impervious surfaces are created, large increases in runoff volume and rates occur. SWMM has been applied to evaluate the combined hydrologic impacts of urbanization and CC (Barco et al., 2008; Bhaduri and Minner, 2001; Warwick and Tadepalli, 1991; Zahmatkesh et al., 2014b). Few studies were found addressing water quality impacts from CC in urban areas at the watershed scale. Hydrologic changes from urban development cause erosion from landscapes and streambanks, and channel scour and degradation (Kaushal and Belt, 2012; Nelson and Booth, 2002). Runoff mobilizes pollutants such as metals, nutrients, and toxicants (Hatt et al., 2004), affecting streams, lakes, rivers, and estuaries as runoff is transported downstream. Elevated nutrient levels contribute to aquatic "dead zones" affecting many estuaries worldwide, perhaps the most notable example being the Chesapeake Bay (National Research Council, 2000). To address deterioration of the aquatic health of the Bay, the USEPA established a Total Maximum Daily Load (TMDL), restricting nitrogen (N), phosphorus (P), and sediment in discharges to each tributary of the Chesapeake Bay (USEPA, 2010a). The objective of the TMDL is to reduce N, P, and sediment loadings by implementing stormwater control measures better known as stormwater control measures (SCMs) to reduce runoff or N, or P, and/or sediment loading. CC impacts temperature, precipitation, and other climatic variables (Lee et al., 2013; Scully, 2010), leading to changes, often reductions in SCM effectiveness (Hathaway et al., 2014). N, P, and sediment export from the landscape to surface waters are controlled by the

combination of key biogeochemical processes driven by hydrologic transport. When the potential impact of CC variability is added to the system, critical biogeochemical processes will be altered across the Chesapeake Bay watershed (Schaefer and Alber, 2007). A better understanding of these coupled processes is critical to managing N, P and sediment exports from the Bay watershed to the estuary from urban and agricultural systems; this paper focuses on the urban contribution to watershed loading for N, P, and sediment. Improving the ability to predict CC impacts on water quality in urban watershed is needed to evaluate conditions and select the best treatment options.

The objective of this study is to evaluate the impacts of CC on an urban watershed including the impact on runoff volume, peak flow, and water quality (Total Suspended Solids, TSS; Total Nitrogen, TN; and Total Phosphorous, TP), using a SWMM model calibrated with a robust autocalibration tool, RSWMM, developed within the R environment. RSWMM is used to calibrate water quantity and quality. Water quality calibration which has not been performed in previous studies is of an interest. Hourly precipitation data from one emissions scenario and one regional climate model are used to force the SWMM model. A multi-objective optimization package, the NSGA-II was incorporated into RSWMM, providing functions for box-constrained multi-objective optimization using a genetic algorithm. A postprocessor for classifying output into events and plotting probability of exceedance curves of user selected outputs was incorporated for ease of comparing scenarios. As a case study, the tool is applied to the calibration of a previously developed SWMM model of the Difficult Run watershed in Fairfax County, Virginia, which is tributary to the Chesapeake Bay, using historical and downscaled projected precipitation and temperature data.

3.2 Materials and Methods

3.2.1 Description of Study Area

The Difficult Run watershed, the largest watershed in Fairfax County VA, is 150 km^2 in size, and consists of 18 named tributary sub-watersheds (**Figure 3.1**). The Difficult Run mainstem is approximately 63 km in length, the length of its tributaries is approximately 233 km. Ground slope is low to moderate. The watershed is within Piedmont physiographic province of Virginia and is part of the greater Washington, D.C., metropolitan region.

Soils are classified by NRCS into four different soil hydrologic groups ranging from A to D where A has the least runoff potential and D has the greatest runoff potential. The majority of the soils in the watershed (40.5%) are Glenelg, soil hydrologic group B, which signifies a moderate infiltration capacity, but is also highly susceptible to erosion (Fairfax County, 2007). A small proportion (5%) of the soils adjacent to streambeds are subject to inundation during high flows. Current land uses in the Difficult Run watershed range from forest to urban; of the latter, the most predominant subtype is urban residential development at approximately 57% (Fairfax County, 2007); shown in **Table 3-1**. The percentage of impervious surfaces in the watershed is approximately 18.4% which is about 1/3 of the urban area (Fairfax County, 2007).

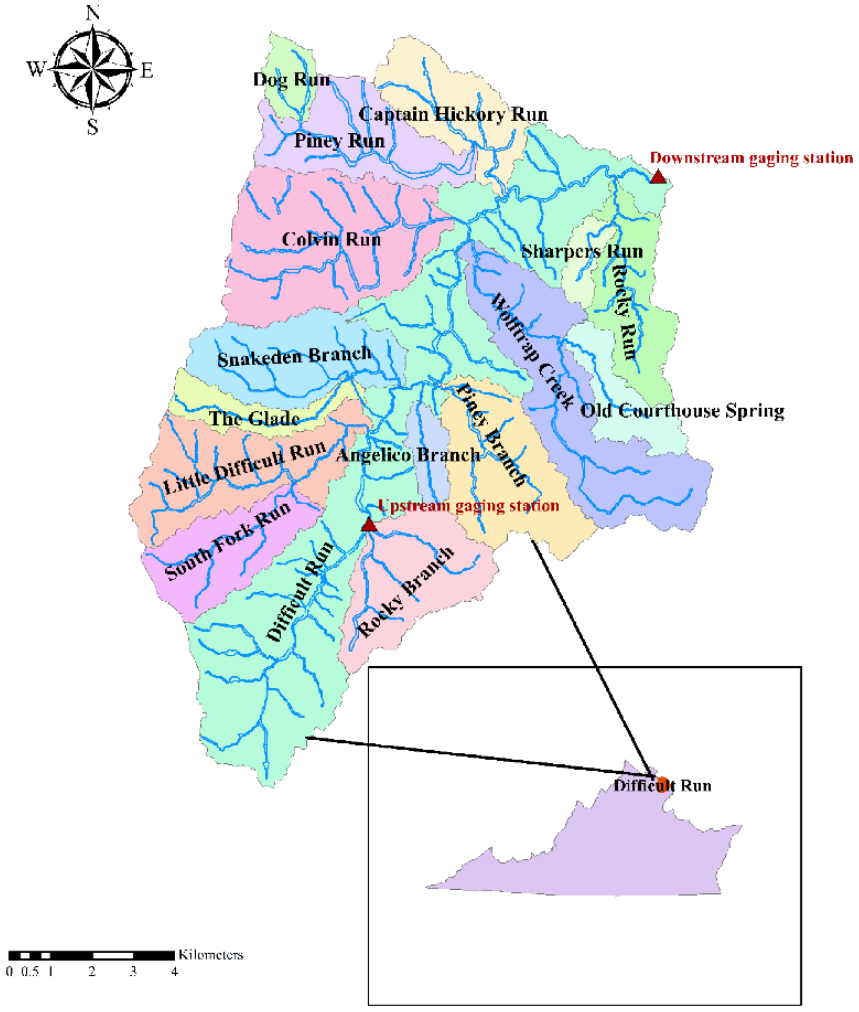

Figure 3.1. Subwatershed location map.

Like much of Fairfax County and metropolitan DC, the Difficult Run watershed has experienced significant urban development, which has degraded water quality, reduced aquatic

habitat, and increased flooding not unlike other streams draining rapidly urbanized watersheds (Liu et al., 2014). After conducting a detailed hydrologic and water quality study of the Difficult Run watershed, a comprehensive watershed management plan (WMP) was adopted by Fairfax County (2007) to address water quality and quantity issues. In the development of the WMP, over 900 existing SCMs were assessed. These SCMs provide peak flow storage and varying degrees of treatment for urban runoff. The WMP assessed stream conditions for the mainstem and 18 main tributaries. Using geographic information system (GIS) data provided by the county, hydraulic/hydrologic (H/H) and water quality models were developed for the Difficult Run watershed (Fairfax County, 2007). These models were used to assess current conditions, and to guide future management planning to meet water quantity and quality goals for anticipated projected conditions.

After the study was complete, the U.S. Geological Survey (USGS), in partnership with Fairfax County, conducted a comprehensive, seven-year monitoring program of Difficult Run (Jastram, 2014). This study provided the hydrologic and water quality data used for calibration and verification. Difficult Run TSS loads ranged from 289-10,275 tons and sediment yields ranged from 378.3-9,939.2 kg per ha (kg/ha) annually; with higher loads associated with the degree of urbanization. Total N loads ranged from 4.1-18.2 metric tons and corresponding yields ranged from 5.9-14.7 kg per ha (kg/ha), annually. Total P loads ranged from 0.190-3.79 metric tons and corresponding yields ranged from 0.24-2.8 kg per ha (kg/ha), annually. Monitoring stations in Difficult Run showed higher TSS loading in 2008, and 2011 associated with Tropical Storms Hanna and Lee, respectively. Dissolved N composed 60 to 85 percent of the total annual N load, and the annual dissolved N load was correlated with runoff volume (Jastram, 2014). Total P loads were composed of about 74% sediment-associated P, resulting in a strong correlation between total and dissolved P and annual peak runoff. Dissolved TN and TP sources in Difficult Run were attributed to application of fertilizer to residential lawns, and human and animal waste from inefficient septic systems (Jastram, 2014).

<THIS SPACE LEFT INTENTIONALLY BLANK>

Table 3-1. Existing Land use/Land cover (LULC) in Difficult Run Watershed.

LULC Type	Existing (%)
Open Water	0.4
Developed, Open Space	32.2
Developed, Low Intensity	12.5
Developed, Medium Intensity	6.6
Developed, High Intensity	1.47
Barren Land (Rock/Sand/Clay)	0.02
Deciduous Forest	35.9
Evergreen Forest	2.11
Mixed Forest	1.39
Shrub/Scrub	0.9
Grassland/Herbaceous	0.06
Pasture/Hay	1
Cultivated Crops	0.8
Woody Wetlands	4.3
Emergent Herbaceous Wetlands	0.01

3.2.2 Hydraulic/Hydrology (H/H) Modeling

Urban H/H models use climatological data (precipitation, temperature), land use data, and hydraulic system data to estimate water and pollutant flux across the landscape by simulating hydrologic and water quality processes. Key hydrologic processes include rainfall-runoff, infiltration, evapotranspiration, and flow routing. In this study, the U.S. Environmental Protection Agency's (USEPA) Storm Water Management Model (SWMM) version 5.1.010 was employed for H/H modeling. SWMM can perform both single event and continuous simulation and has been widely used in urban areas (Ahmadisharaf et al., 2016; Huber et al., 1988; James et al., 2010; Rossman, 2004). Outputs of the model include runoff and/or streamflow and water quality constituent loads and/or concentrations. SWMM simulates groundwater flow for each subcatchment through a single aquifer, which is defined by the depth of its unsaturated upper zone and lower saturated zone, bottom of aquifer, groundwater flow parameters, porosity, wilting point, field capacity and saturated hydraulic conductivity. This data was obtained from the geologic map (Dicken et al., 2007; Drake, 1986) and SSURGO database (Natural Resources Conservation Service, 2015). These parameters were taken from raster grids or attributes associates with a specific area. GIS spatial operations were conducted to create a weighted area average for each subwatershed.

Evaporation from subcatchment surfaces, from subsurface water in aquifers, and from streams was modeled using methods outlined in (Rossman, 2015). SWMM uses the Hargreaves equation for evaporation simulation (James et al., 2010). Evaporation in the SWMM models used in this study was computed from daily temperatures, including historical or projected. The Green-Ampt infiltration method was used to estimate infiltration and excess rainfall. This method was selected due to the physical basis of its parameters (suction head, hydraulic conductivity, and initial moisture deficit), and their availability in the Natural Resources Conservation Service (NRCS) (2015, http://websoilsurvey.nrcs.usda.gov/) database. Flow routing used SWMM's dynamic wave option was selected due to its accuracy and ability to simulate non-uniform, unsteady state flow conditions. Land use and soil data for the watershed were obtained from the WMP (Fairfax County, 2007). Two U.S. Geological Survey (USGS) stream gages draining areas of 7 km^2 and 150 km^2, respectively, are located within the watershed. Data from these stations were used to calibrate and verify the model. Then, projections for precipitation, and temperature across the watershed from the North American Regional CC assessment program (NARCCAP) (Mearns et al., 2009) for historical and projected conditions was used in the calibrated and verified model to predict streamflow; and TSS, TN and TP concentrations for historical and projected CC conditions.

3.2.3 Water Quality Modeling

Water quality was modeled using an estimated event mean concentration (EMC) washoff loading during runoff events and simple treatment functions similar to $C_{i+1} = C_0(1 - e^{-kt})$ common to many urban models. Water quality characteristics were developed based upon EMCs, which were set to 40 mg/L for TSS, 2.9 mg/L for TN, and 0.27 mg/L for TP, based upon average values for Virginia (Hirschman et al., 2008).

In SWMM, water quality treatment expressions have the form of:

$$R = \{P, R_P, V\} \tag{3-1}$$

$$C = \{P, R_P, V\} \tag{3-2}$$

Where: R is fractional removal, C is concentration of pollutant in mg/l, P, R_P is the pollutant removal for pollutant, P, and V is a process variable such as: Q = inflow rate in m^3/s, D

= water depth in m, *HRT* = hydraulic residence time in seconds, *DT* = time step in seconds, *A* = surface area in m^2.

Treatment expressions in SWMM were developed by assuming irreducible concentrations (USEPA, 2010b). This concept holds that treatment effectiveness is reduced once a low level of pollutant concentration has been reached, i.e. it gets more difficult to remove the last fraction of pollutant. The irreducible concentrations assumption is commonly observed in runoff quality data (Park and Roesner, 2012)). TSS and TN were estimated by:

$$C_{TSS,i+1} = 20 + \left(C_{TSS,i} - 20\right)e^{-10^{-4}\left(\frac{DT}{D}\right)} \quad (3\text{-}3)$$

$$C_{TN,i+1} = 1.9 + \left(C_{TN,i} - 1.9\right)e^{-0.5\cdot10^{-9}\left(\frac{DT}{D}\right)} \quad (3\text{-}4)$$

TP was split into two fractions, soluble phosphorus (SP) and particulate phosphorus (PP):

$$C_{TP,i+1} = C_{SP,i+1} + C_{PP,i+1} \quad (3\text{-}5)$$

The SP reduction was estimated by:

$$C_{SP,i+1} = 0.23 + \left(C_{SP,i} - 0.23\right)e^{-5.2\cdot10^{-5}\left(\frac{DT}{D}\right)} \quad (3\text{-}6)$$

The PP reduction was computed as a function of removal of TSS:

$$RR_{PP} = R_{TSS} \quad (3\text{-}7)$$

3.2.4 RSWMM

To efficiently calibrate the model without altering the SWMM source code, an external, freely available control program was needed. SWMM is constantly being updated; so, use of a non-altered SWMM source code and ensures compatibility with future updates. R (RCD Team, 2015) is an open source, freely available system that can be used for statistical analysis and programming. R has been successfully used in hydrological modeling and its capabilities are well recognized (Fuka et al., 2014). R is compatible with most operating systems. Because of these capabilities, R was chosen for use in this study for development of a control module that could execute SWMM simulations repetitively, changing key parameters according to user needs. An existing R code known as RSWMM (Steinberg, 2014) was identified and was used for this study. Several enhancements were developed as part of this project, including separation of events, incorporating an autocalibration tool described in a later section, and a post-processor to

view exceedance curves of the output. The reader is referred to Table A-1 in the appendix for further information on the RSWMM code.

3.2.4.1 **Calibration Procedure**

A typical SWMM model application contains many input parameters. As mentioned previously, SWMM model outputs are sensitive to hydraulic width, imperviousness and depression storage depth (Barco et al., 2008; Temprano et al., 2006), the first two parameters being positively correlated to peak flow, the latter, negatively correlated. Calibration of the Difficult Run watershed model was conducted by varying hydraulic width (the sub-catchment area divided by the maximum overland flow length), imperviousness and depression storage depth (a depth that must be filled prior to the runoff occurs) for 2010 data. Hourly rainfall data were disaggregated to 15-min time step for the proposed H/H simulations using NETSTORM (CDM Smith Inc., 2015). Then, the simulation results were aggregated to an hourly time series and SWMM was calibrated with respect to peak flows and runoff volume during all events in upstream and downstream catchments. A 6-hr minimum inter-event period was used to classify data into events. Two gaging stations located in upstream and downstream sub-watersheds (location shown in **Figure 3.1**) were used for calibration and verification.

3.2.4.2 **Autocalibration methods**

The autocalibration tool within RSWMM utilizes a multi-objective optimization package called the Elitist Non-dominated Sorting Genetic algorithm (NSGA-II). NSGA-II provides functions for box-constrained multi-objective optimization. Three objective functions were used. These included: coefficient of determination (R^2), Nash Sutcliffe Efficiency (NSE), and Percent Bias (PBIAS). R^2 describe the degree of collinearity between simulated and observed data and ranges from 0 to 1. R^2 close to 1 indicate less error variance and is desirable. The values greater than 0.5 is considered satisfactory in the study by Santhi et al. (2001) and Van Liew et al. (2003).

NSE is a normalized statistic which indicates how well the plot of observed versus simulated data fits and ranges from $-\infty$ and 1.0 (Nash and Sutcliffe, 1970). A value of NSE close to 1 is considered as an excellent level of performance. NSE was calculated as:

$$NSE = \left[\frac{\sum_{i=1}^{i=n}(Y_i^{obs} - Y_i^{sim})^2}{\sum_{i=1}^{i=n}(Y_i^{obs} - Y^{mean})^2}\right] \quad (3\text{-}8)$$

Where Y_i^{obs} is observed data values, Y_i^{sim} is simulated data values, and Y^{mean} is the mean of observed data.

Percent bias (PBIAS) shows the deviation of data and expressed as a percentage. It measures the average tendency of the simulated data to be different from observed data (Gupta et al., 1999). PBIAS close to 0 is considered to be an excellent level of performance. PBIAS was calculated as:

$$PBIAS = \left[\frac{\sum_{i=1}^{i=n}\left(Y_i^{obs} - Y_i^{sim}\right) * 100}{\sum_{i=1}^{i=n}(Y_i^{obs})^2}\right] \quad (3\text{-}9)$$

Where Y_i^{obs} is observed data values, and Y_i^{sim} is simulated data values.

SWMM was calibrated using an autocalibration procedure, adjusting specific model parameters described within a defined range. Observed and simulated outputs were compared at upstream and downstream gaging stations to determine the parameter set that provide the best model simulated runoff peak and volume. With the completion of a given optimization, sets of calibrated parameters were obtained through optimization. Default values that were used from the previously developed model as initial model parameters. Based on the study by Santhi et al. (2001) and Van Liew et al. (2003) R^2 and NSE $\geq$ 0.75 and PBIAS $\leq \pm$10%, which are considered to be very good calibration performance. R^2 and NSE $\geq$ 0.65 and $\pm$10% $\leq$ PBIAS $\leq \pm$15%, which are considered to be good calibration performance. R^2 and NSE $\geq$ 0. 5 and $\pm$15% $\leq$ PBIAS $\leq$ $\pm$20% are considered as satisfactory calibration performance. The autocalibration approach aims to minimize the difference between measured and simulated values. Initial parameter values were allowed to vary by ± 20% to create parameter sets to initialize the autocalibration procedure. Calibration and verification were performed on the 2010 and 2013 data, respectively, with a maximum number of iterations set at 500. Because the SWMM model was based on subhourly rainfall data, the run time for each iteration was large. Therefore, calibration and verification were done for events in 2010 and 2013, to calibrate and verify the model performance, respectively.

3.2.5 Climate Modeling

To predict future CC impacts on runoff quantity and quality, projections are required for precipitation and temperature across the watershed. In this study, simulations from the North American Regional CC assessment program (NARCCAP) (Mearns et al., 2009) were used.

Projections were based upon dynamical downscaling; embedding a regional climate model (RCM) with 50 km^2 spatial resolution into a global climate model (GCM). Two time periods, 1971-1998 and 2041-2068 were used for historical and projected CC conditions, respectively. The latter scenario represents a medium-high greenhouse gas emissions assumption, A2 (Nakićenović and Swart, 2000).

Data were obtained from one GCM-RCM combination, the MM5I-CCSM, which was selected based on its ability to accurately simulate historical temperature and precipitation. Annual mean historical temperature and precipitation were averaged over the region for 9 of the NARCCAP models, and compared the means to the mean obtained from an observation-based dataset. **Figure 3.2** show the annual mean temperature and precipitation of 9 different models.

<THIS SPACE LEFT INTENTIONALLY BLANK>

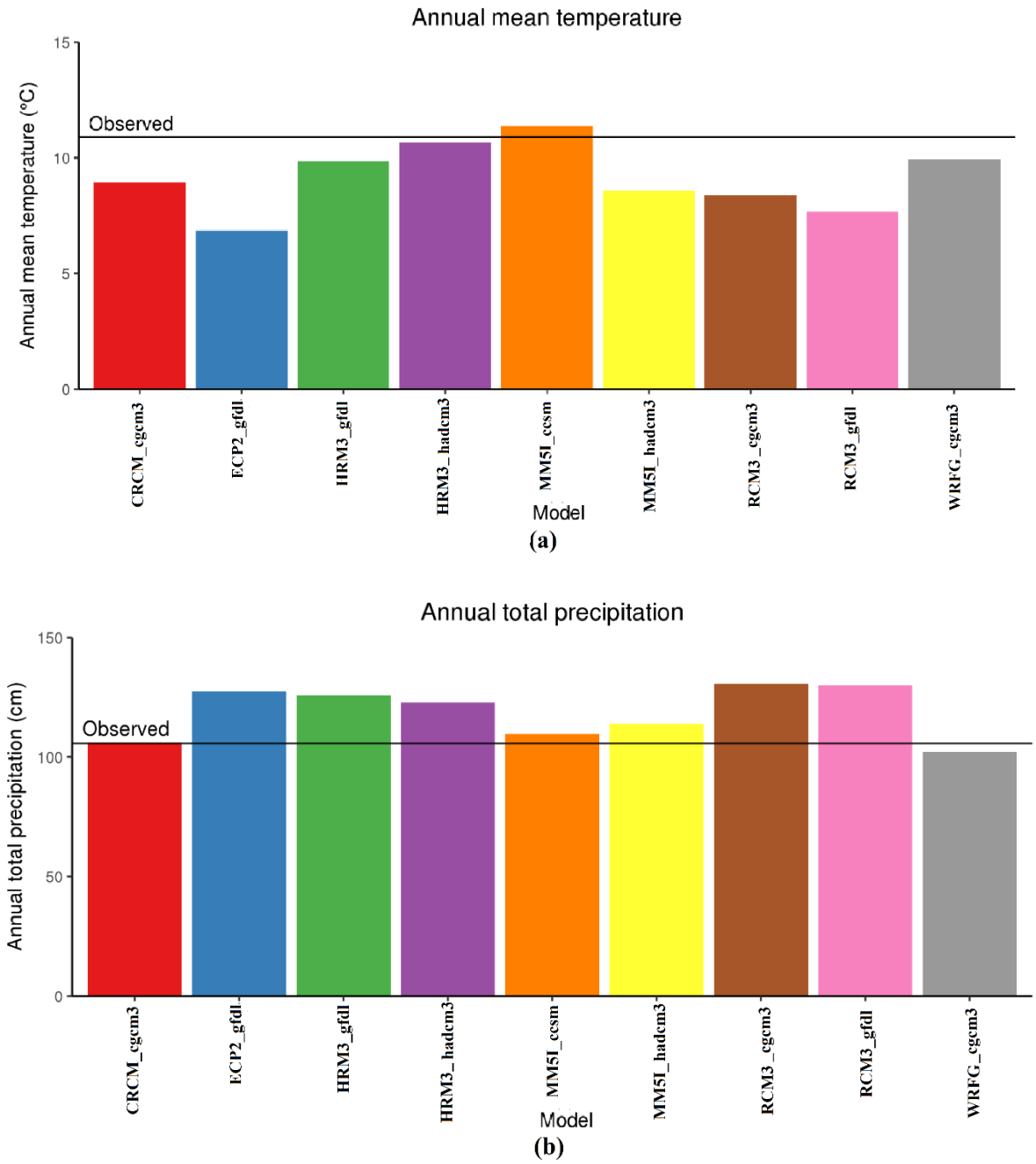

Figure 3.2. (a) Annual mean temperature for nine global climate models / regional climate models (GCM-RCM). (b) Annual mean precipitation for nine GCM-RCM.

Although the historical performance of the model was reasonable, bias was still evident, so, bias-correction was conducted. Bias correction was applied using a modified version of the equiratio cumulative distribution function matching method (Wang and Chen, 2014). This method corrects model data using multiplicative scaling factors. The scaling factor applied to

each model data point is the ratio of the observed value at the data point's quantile to the historical-period model value at the data point's quantile. Using the notation of Wang and Chen (2014), this is expressed mathematically as:

$$\tilde{x}_{m-p,adjust} = x_{m-p} \times \frac{F_{o-c}^{-1}(F_{m-p}(x_{m-p}))}{F_{m-c}^{-1}(F_{m-p}(x_{m-p}))} \quad (3\text{-}10)$$

where x_{m-p} is a value from the model during the prediction period (which may be either the historical or projected period), F_{m-p} is the empirical cumulative distribution function (CDF) of the model prediction data, F_{o-c}^{-1} is the inverse CDF of the observed data, and F_{m-c}^{-1} is the inverse CDF of the model data during the historical (or current) period. This correction method was applied to the model-simulated precipitation and temperature data for both time periods. The observed CDFs in the numerator of equation 10 were determined using forcing data from Phase 2 of the North American Land Data Assimilation System (NLDAS-2) (Xia et al., 2012). This dataset was selected since it has matching variables for all climate model data, it has a relatively high spatial (1/8 degree) and temporal (hourly) resolution, and did not have missing data.

Several modifications were applied to the correction algorithm. For precipitation, use of equation 10 would set the frequency of zero precipitation to be equal to the observed frequency in the historical and projected periods. To relax this restriction, model data with a CDF value less than the frequency of no precipitation in the observed dataset were set to zero. For the historical period, this results in the frequency of corrected model dry values equaling the frequency of observed dry values. However, for the projected period the frequency of dry values in the corrected data may change. The correction in equation 10 was then applied using only values greater than zero in each dataset. For downwelling shortwave radiation, the bias correction was only applied using modelled and observed values greater than zero. Model air temperature predictions were corrected using an additive shift rather than a multiplicative ratio. Unlike precipitation and other variables, an additive correction applied to temperature is unlikely to produce values that are below zero. The bias correction and temporal disaggregation were applied separately for each calendar month.

NARCCAP provides model output at three-hour intervals. This temporal resolution was deemed sufficient for all variables except precipitation. Temporal disaggregation was applied to convert precipitation data to hourly frequency using a method developed to create input data for the Variable Infiltration Capacity model (Gao et al., 2010). This method starts with daily

precipitation totals (produced from upscaled and subsequently bias-corrected 3-hour NARCCAP precipitation) and uses a CDF mapping approach to assign the daily amounts to fall during hours such that the disaggregated model CDFs of precipitation duration and hour of occurrence match the observed CDFs, using hourly precipitation totals at the Ronald Reagan National Airport in Washington, D.C. Separate CDFs and corrections were applied for each calendar month and for five daily-total precipitation bins: 0-5, 5-10, 10-15, 15-20, and 20+ mm. Unlike the bias correction method, this temporal disaggregation method does not allow the distributions of duration and time of occurrence to change from the historical to the future period. However, because the disaggregation step preserves the daily total amounts, which it receives from the bias correction step, the daily total precipitation amounts may still change from the historical to the future CC projection.

3.2.6 Statistical Analysis

Changes in precipitation, runoff, TSS, TN, and TP in the watershed were investigated using the student's t-test to find whether there was a significant difference between the historical and projected conditions. The two-sample t-test was used to test the null hypothesis that the population means of two groups are the same. The t-test assumes the underlying distribution is normal, therefore the normality of the datasets was tested using Shapiro-Wilk test (Shapiro and Wilk, 1965). In addition, flow statistics, i.e., Q95, Q50 and Q10, which represent low, median, and high flows, respectively, were computed and compared to historical and predicted conditions using exceedance probability plots.

3.3 Results and Discussion

3.3.1 Calibration and Verification

Calibration and verification were performed using the data from upstream and downstream gauging stations. Performance metrics of the model with respect to peak flow and runoff volume after calibration and verification for upstream and downstream gauges are provided in **Table 3-2** and **Table 3-3**, respectively. According to the criteria of Moriasi et al. (2007); Santhi et al. (2001); Van Liew et al. (2003), simulated and observed runoff volume showed a good level of agreement on an event basis.

Table 3-2. Summary of model performance for calibration and verification periods at the Difficult Run upstream gauging station with respect to hourly peak flow.

Period	Model Performance		
	R^2	NSE	PBIAS
Calibration	0.77	0.72	14.9%
Verification	0.83	0.79	13.8%

Table 3-3. Summary of model performance for calibration and verification periods at the Difficult Run downstream gauging station with respect to hourly peak flow.

Period	Model Performance		
	R^2	NSE	PBIAS
Calibration	0.84	0.76	14.5%
Verification	0.78	0.73	12.1%

The most sensitive parameters identified in previous studies were hydraulic width, imperviousness, and depression storage for impervious and previous areas. During calibration, each parameter was adjusted to improve agreement between observed and predicted peak flows and runoff volume. However, adjusting the hydraulic width of some of the smaller catchments in the watershed did not have much impact on runoff. Depression storage for impervious and pervious did not have significant effects on the results. Calibration and verification results based on the peak flows are shown in **Figure 3.3** and **Figure 3.4**.

<THIS SPACE LEFT INTENTIONALLY BLANK>

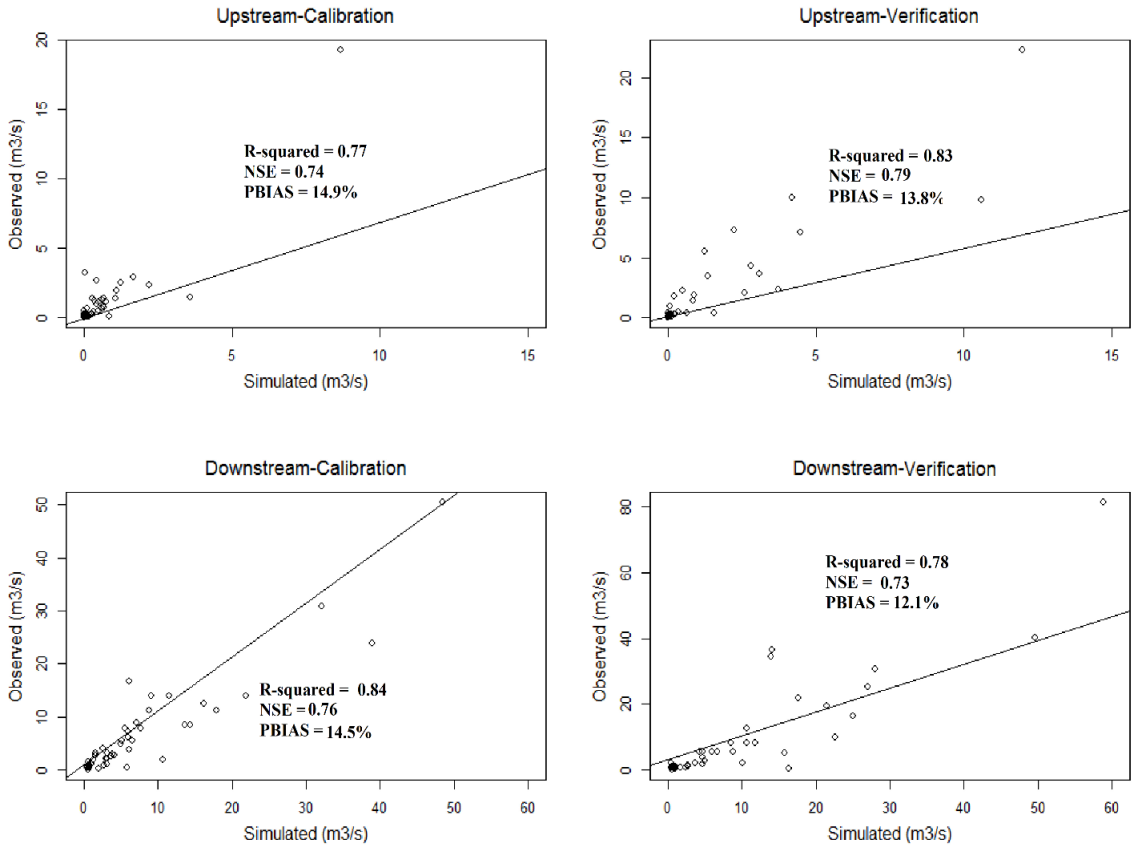

Figure 3.3. (a) Calibration and validation results at the Difficult Run upstream and downstream gauging stations.

<THIS SPACE LEFT INTENTIONALLY BLANK>

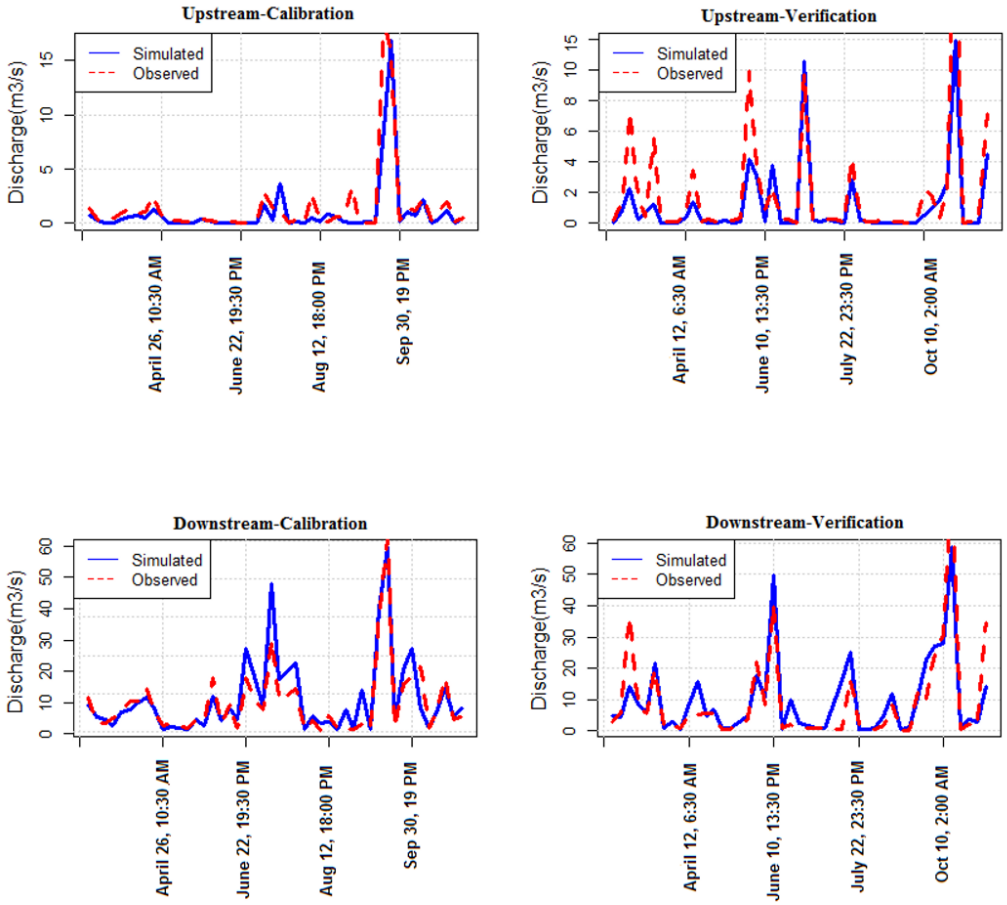

Figure 3.4. Comparison of observed and simulated data at the Difficult Run upstream and downstream gauging stations for hourly calibration (2010) and verification (2013) periods.

The results indicate an underestimation of peak flow in the verification period, especially in wet events that may be due to missing of some processes in the SWMM model such as groundwater recharge. While SWMM has a groundwater flow component, it is primarily a surface runoff model, and some subsurface processes are neglected. Flows that are produced via infiltration loss and routed through subsurface may not be fully captured and simulated by the model.

Performance metrics of the model with respect to runoff volume for upstream and downstream gauges are provided in

Table 3-4 and **Table 3-5**, respectively. The results revealed that simulated and observed runoff volume showed a good level of agreement on an event basis.

Table 3-4. Summary of model performance for calibration and verification periods at the Difficult Run upstream gauging station with respect to hourly runoff volume.

Period	Model Performance		
	R^2	NSE	PBIAS
Calibration	0.74	0.71	-17.8%
Verification	0.75	0.65	6.1%

Table 3-5. Summary of model performance for calibration and verification periods at the Difficult Run downstream gauging station with respect to hourly runoff volume.

Period	Model Performance		
	R^2	NSE	PBIAS
Calibration	0.78	0.73	13.3%
Verification	0.72	0.69	15.4%

Simulated and observed hydrographs for some selective events including dry and wet events are shown in **Figure 3.5**.

<THIS SPACE LEFT INTENTIONALLY BLANK>

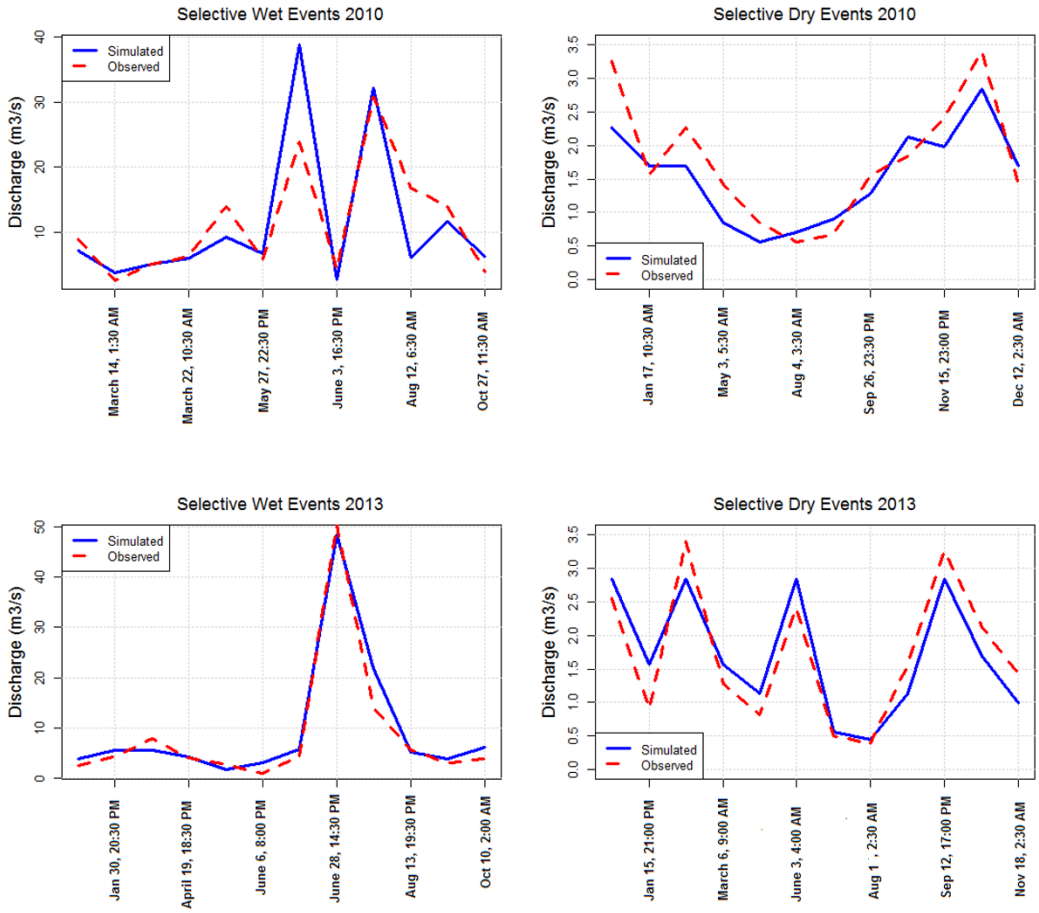

Figure 3.5. Comparison of observed and simulated data at the Difficult Run downstream gaging station for hourly selective events.

Average annual flow in the calibration and verification period at upstream and downstream gauging stations are provided in **Table 3-6** and **Table 3-7**, respectively. The results indicate good performance of the calibration in simulating mean annual flow during calibration and verification periods.

Table 3-6. Annual mean flow of simulated and observed data at the Difficult Run upstream gauging station.

Period	**Annual flow (m^3/s)**	
	Simulated	**Observed**
Calibration	0.34	0.26
Verification	0.29	0.23

Table 3-7. Annual mean flow of simulated and observed data at the Difficult Run downstream gauging station.

Period	Annual flow (m^3/s)	
	Simulated	**Observed**
Calibration	1.81	2.01
Verification	1.76	1.67

The final model parameters for each sub-catchment are provided in **Table 3-8**.

Table 3-8. Model calibrated parameters for sub-catchments in Difficult Run watershed.

Sub catchments	Model Parameters			
	Hydraulic Width (m)	**Imperviousness (%)**	**Depression Storage (Previous) (cm)**	**Depression Storage (Impervious) (cm)**
Angelico Branch	667.8	7.4	0.51	0.3
Captain Hickory	674.1	7.7	0.58	0.31
Colvin Run	645.6	16.3	0.68	0.38
Difficult (Lower)	779.1	6.5	0.67	0.29
Difficult (Middle)	200.7	10.1	0.54	0.37
Difficult (Upper)	850.3	24.8	0.56	0.43
Dog Run	667.8	11.1	0.53	0.41
The Glade	699.6	11.3	0.61	0.33
Little Difficult Run	683.7	7.4	0.64	0.31
Old Courthouse	745.7	29.5	0.53	0.35
Piney Branch	689.1	16	0.56	0.32
Piney Run	604.2	11.4	0.56	0.27
Rocky Branch	689.1	12.2	0.61	0.38
Rocky Run	705.9	8.4	0.66	0.3
Sharpers Run	665.6	6.8	0.63	0.3
Snakeden Branch	711.7	19	0.69	0.27
South Fork Run	715.5	8.6	0.55	0.43
Wolftrap Creek	685.3	16.2	0.53	0.36

A map of the model calibrated parameters by sub-catchments in the watershed are provided in **Figure 3.6**.

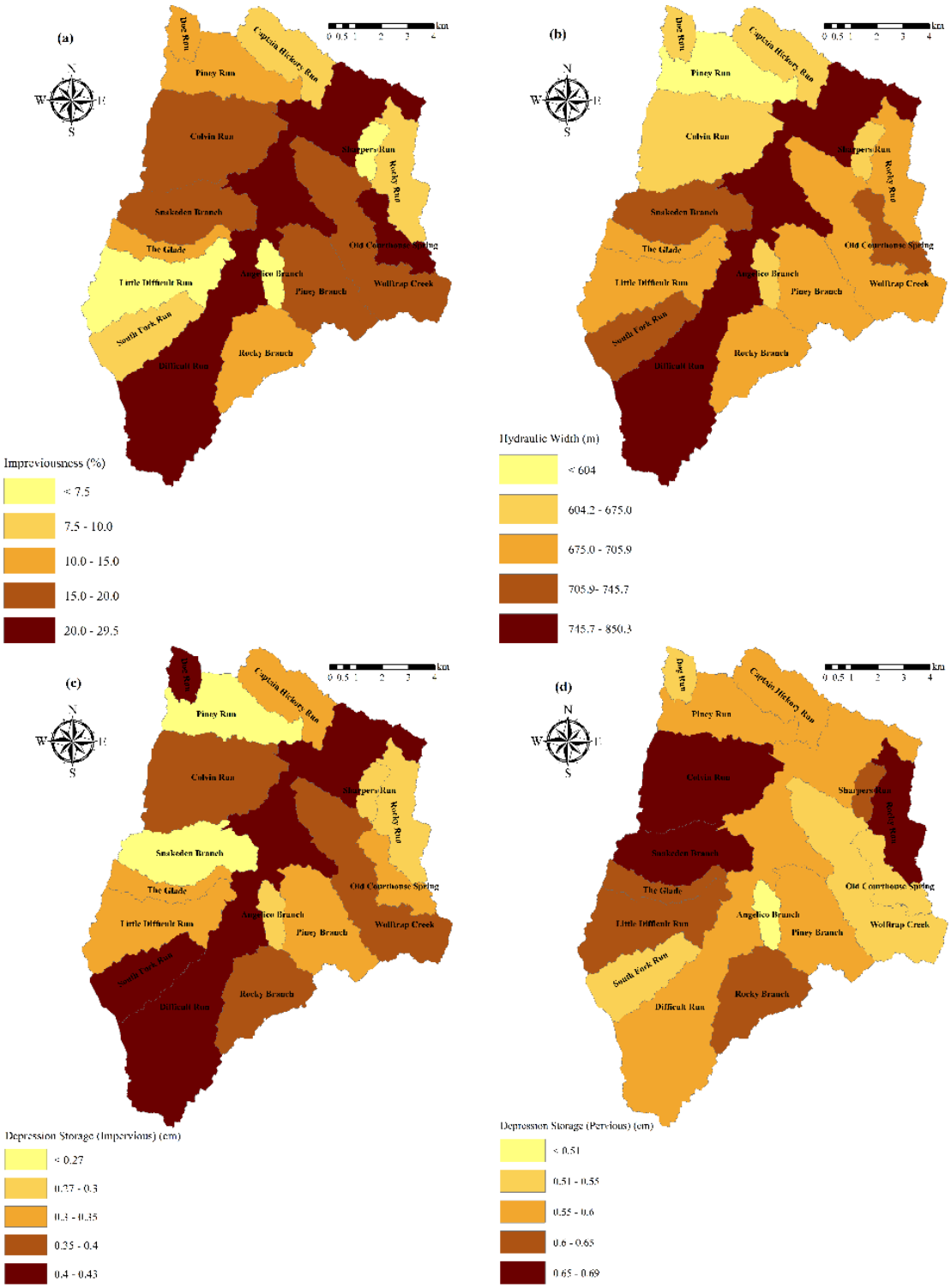

Figure 3.6. Model calibrated parameters for sub-catchments in Difficult Run watershed, (a) imperviousness (percentage), (b) hydraulic width (m), (c) depression storage (of impervious portion) (cm), and (d) depression storage (of pervious portion) (cm).

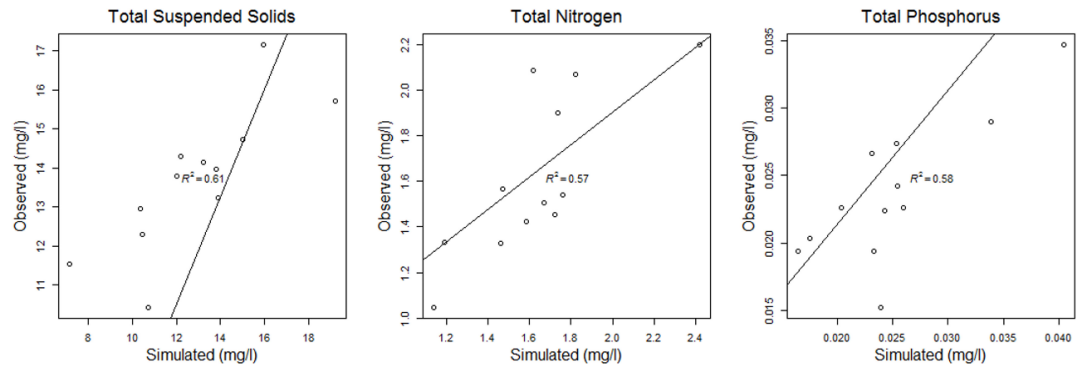

(a)

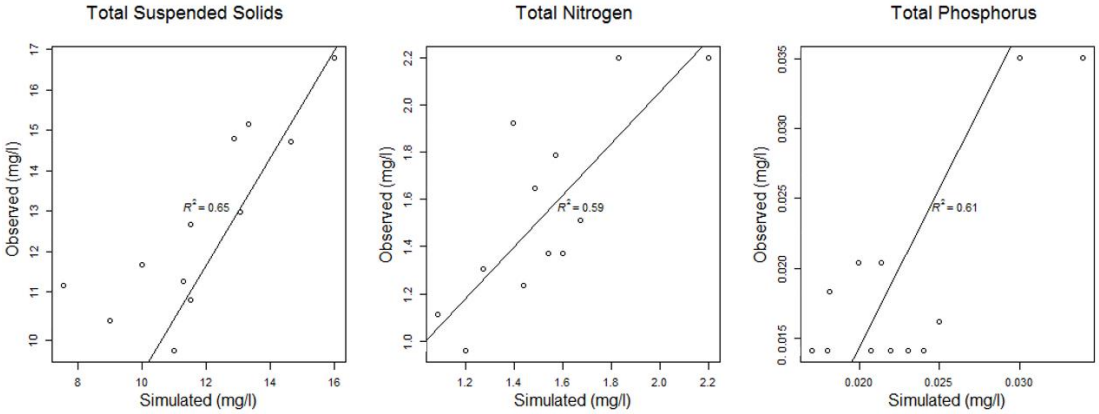

(b)

Figure 3.7. Water quality calibration results at the Difficult Run upstream gauging station; (b) Water quality calibration results at the Difficult Run downstream gauging station.

A simplified assessment of performance was conducted by comparing predicted values with station annual loads. Model results at the upstream gauging station for TSS, TN, and TP showed an R^2 of 0.61, 0.57, and 0.58, respectively, during the calibration; and an R^2 of 0.65, 0.59, and 0.61, during the calibration at the downstream gauging station. The performance of the model through calibration for TSS, TN, and TP is illustrated in **Figure 3.7** for upstream and downstream gauge locations, respectively.

3.3.2 Climate Change Impacts

After calibration and verification, the flow and water quality in the watershed was simulated for the 2041–2068 period. The annual average flow and water quality during historical and projected periods were calculated and compared. The simulation results indicate that the mean annual runoff is predicted to increase by 6.5% with CC. The mean annual TSS, TN, and TP were predicted to increase by 7.7%, 7.0%, and 8.1%, for upstream and downstream locations, respectively.

Seasonal changes in runoff, TSS, TN, and TP are shown in **Figure 3.8**.

Annual precipitation for 2041–2068 increased by 6.1%, while temperature rose by 1.6 °C relative to 1971–1998. Seasonal changes in runoff during 2041–2068 ranged from −22.3% to 32.3%, with the highest increase occurring from October to December. Analysis of seasonal runoff variations indicates increasing runoff in fall and summer and decreasing in winter and spring. Smaller increases in runoff were predicted during the summer, which could be due to increased evapotranspiration and less groundwater recharge. In the CC projections, summer and fall are associated with more precipitation and higher temperatures, with more frequent occurrences of heavy precipitation. Higher temperatures will lead to higher evapotranspiration rates and lower soil moisture. Lower rainfall and higher temperatures in the winter and spring will result in less runoff volume because the water can be absorbed by the soil, whereas higher rainfall and temperature in summer and fall will lead to increased runoff volume due to more precipitation.

Precipitation during the CC projection was characterized by more frequent occurrences of heavy precipitation. Annual mean temperature during the CC projection was 1.6 °C warmer than during the historical period; the warming is relatively uniform throughout the seasons. During September–December, the model predicted runoff, TSS, TN, and TP to increase by 22.5%, 13.2%, 12.8%, and 14.1%, respectively, relative to the historic time period. On a monthly basis, the greatest expected increase was December, with runoff volume, TSS, TN, and TP projected to increase by 32.3%, 29.7%, 24.8%, and 37.7%, respectively. April shows the greatest decrease, with runoff volume, TSS, TN, and TP projected to decrease by 22.3%, 25.7%, 24.7%, and 27.3%, respectively. Imperviousness in highly urbanized watersheds like Difficult Run has been identified as one of the main drivers of runoff pollution and stream degradation (Jastram, 2014)

from this watershed. Increased precipitation resulting from CC would result in increased streamflow which will likely lead to further stream instability and erosion, resulting in further water quality degradation from anticipated higher level of imperviousness, temperature, and precipitation.

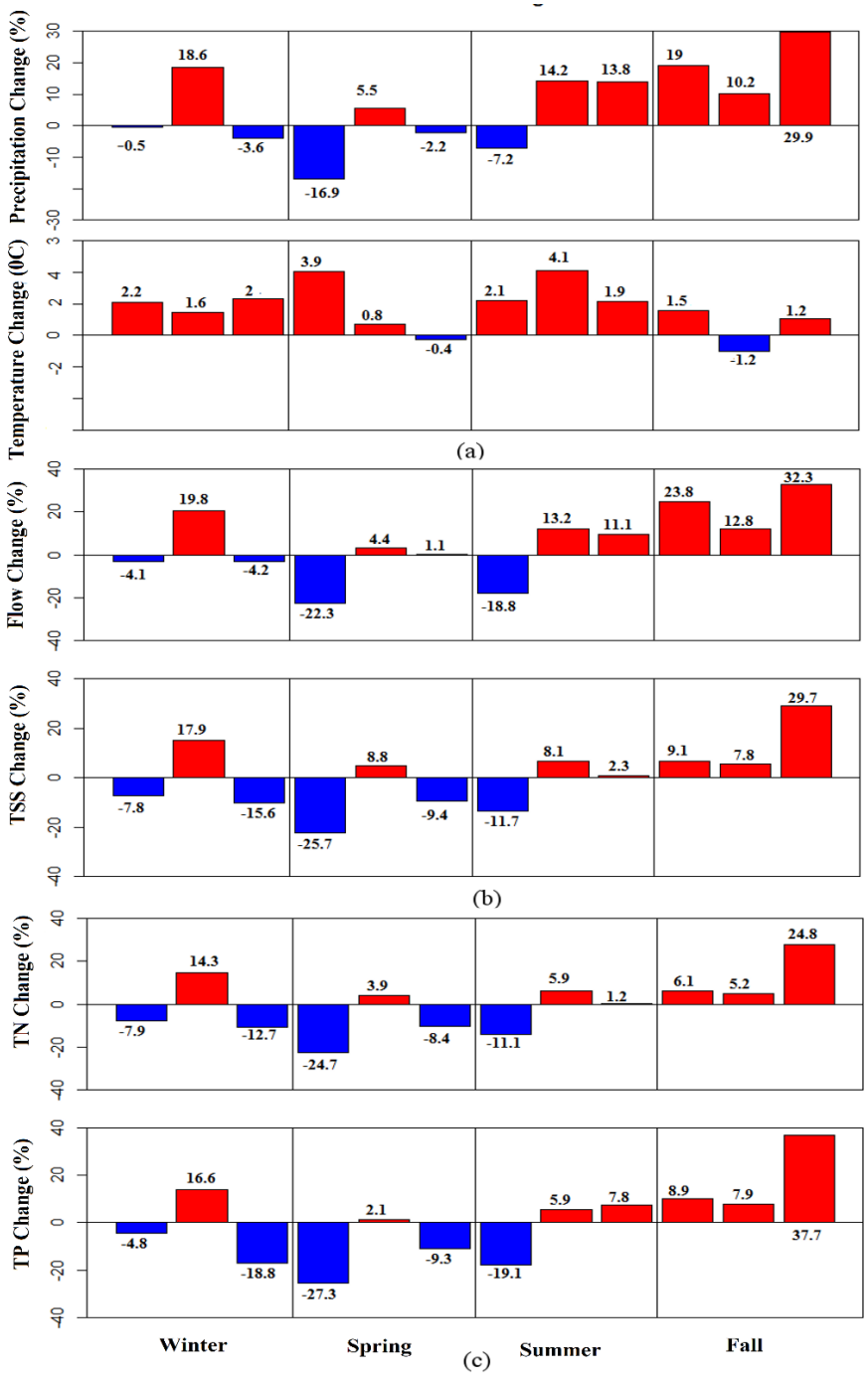

Figure 3.8. Seasonal changes. (a) Precipitation (top) and temperature (bottom); (b) flow (top) and Total Suspended Solids (TSS) (bottom); (c) Total Nitrogen (TN) (top) and Total Phosphorus (TP) (bottom).

Pair-wise comparison to determine if there was a significant difference between the mean monthly historical and CC projections was conducted using a *t*-test for runoff volume, TSS, TN, and TP. A Shapiro-Wilk test (Shapiro and Wilk, 1965) indicated that, at *p*-value > 0.05, the dataset follows a normal distribution. The results of *t*-test are shown in **Table 3-9**.

Table 3-9. t-test pairwise comparison.

Simulation Results	**Statistical Parameters**		
	t-calculated	**t-critical**	**P-value**
Runoff Volume	0.27	2.2	0.78
TSS	1.64	2.2	0.12
TN	1.35	2.2	0.2
TP	3.63	2.2	0.003

The results of the *t*-test indicated that the differences between the mean monthly values of historical and predicted CC runoff volume, TSS, and TN were not significant at the 95% confidence level. TP values were significantly different at 95% confidence interval, which implies that TP may be more sensitive to CC. In general, TP loads are composed of soluble phosphorus (SP) and particulate phosphorus (PP), both of which are strongly correlated with TSS and peak runoff. As a result, increases in peak runoff and TSS may lead to higher levels of TP compared to runoff, TSS, and TN in the watershed for anticipated CC.

The mean, median, and maximum values, and the range between the 10th and 95th percentiles (Q10 and Q95) for the projected period, were compared with statistical parameters for the historical period (**Table 3-10**). Compared with the historical period, the mean, median, maximum runoff volume, TSS, TN, and TP loads during the events increase for CC.

<THIS SPACE LEFT INTENTIONALLY BLANK>

Table 3-10. Statistical parameters during events for the historical and projected periods.

Simulation Results	Statistical Parameters			
	Mean	**Median**	**Max**	**Range (90^{th}-10^{th})**
Historical Period				
Runoff Volume (m^3)	4.5	0.8	100.3	26.91
TSS (mg/l)	186.4	154.2	859.4	510.4
TN (mg/l)	18	14.9	79.4	48.7
TP (mg/l)	0.29	0.0008	3.49	1.5
Projected Period				
Runoff Volume (m^3)	10.4	1.32	166.2	53.9
TSS (mg/l)	221.7	167.1	1010	553.1
TN (mg/l)	21.2	15.89	93.8	53
TP (mg/l)	0.45	0.06	4.2	1.8

In addition to the increase in the mean, median, maximum, runoff, TSS, TN, and TP, the interannual variability increased in most months. Interannual variability of precipitation, temperature, streamflow, TSS, TN, and TP are shown in **Figure 3.9**, respectively.

To analyze the effect of CC on runoff volume and water quality parameters, exceedance probability curves were developed, as shown in **Figure 3.10**, for runoff volume, TSS, TN, and TP, respectively. The curves were created by plotting the simulated results by event for the historical and projected periods. Values of runoff volume, TSS, TN, and TP for the 10th, the 50th, and 95th percentiles are provided in **Table 3-11**.

<THIS SPACE LEFT INTENTIONALLY BLANK>

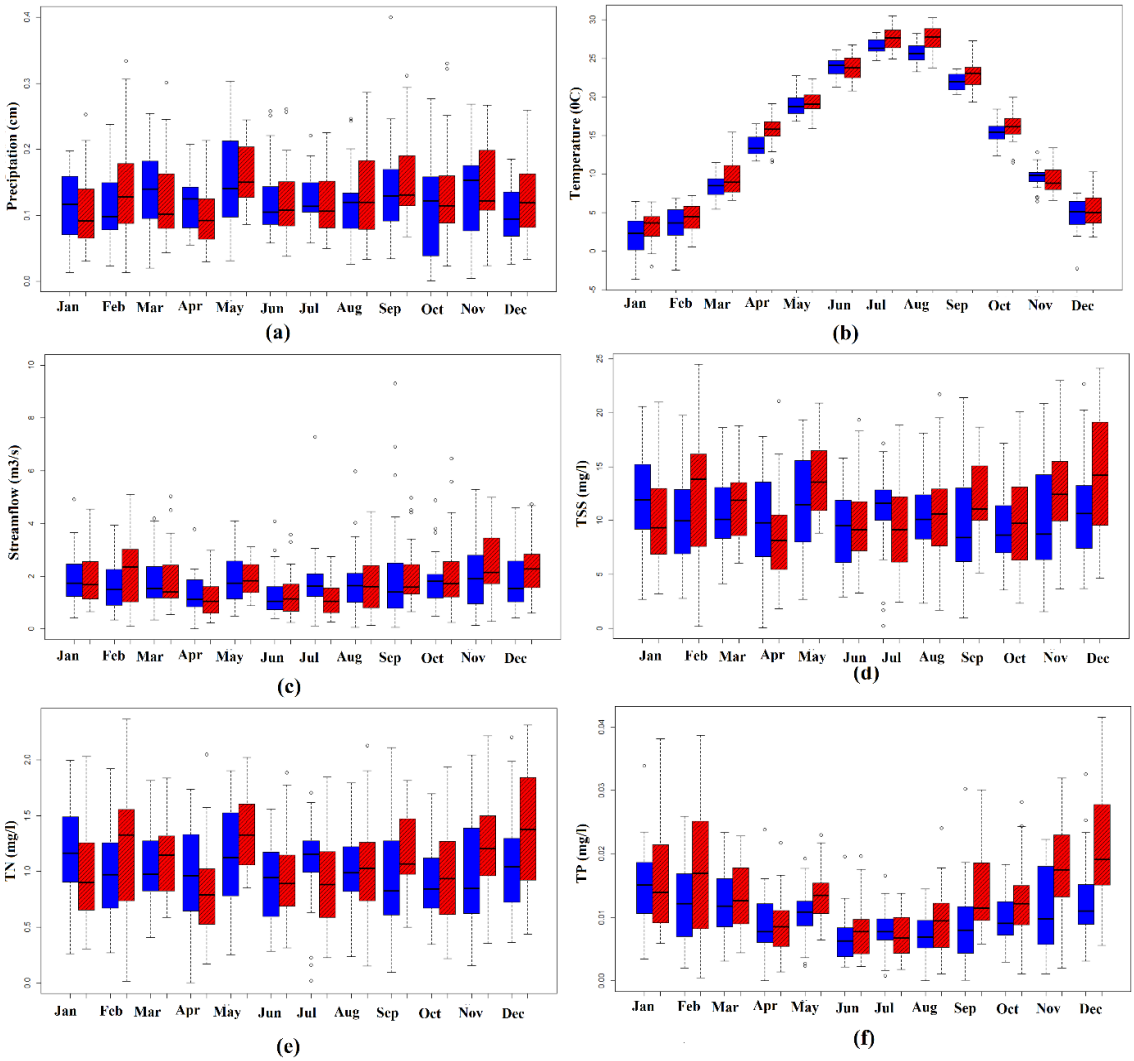

Figure 3.9. Interannual variability of: (a) precipitation, (b) temperature, (c) flow, (d) TSS, (e) TN, and (f) TP. Historical is shown in blue and projected in red cross hatching.

Table 3-11. Statistics during events for the historical and projected periods.

Simulation Results	**Statistical Parameters**		
	Q10	**Q50**	**Q95**
	Historical Period		
Runoff Volume (m^3)	28.92	0.8	0.0012
TSS (mg/l)	529.36	154.2	15.4
TN (mg/l)	50.8	14.9	1.1
TP (mg/l)	1.61	0.0008	$1.8x10^{-7}$
	Projected period		
Runoff Volume (m^3)	55.95	1.32	0.0031
TSS (mg/l)	583.12	167.1	20.1
TN (mg/l)	55.9	15.89	1.9
TP (mg/l)	1.91	0.06	$6.5x10^{-5}$

Figure 3.10 shows a significant difference between the historical and projected runoff volume during larger storm events occurring at the 10% probability. Historical and projected exceedance curves for TSS and TN track very closely, except for small differences apparent in mid-range events (**Figure 3.10**). Of the water quality constituents, TP shows the most difference, and there are more frequent events (**Figure 3.10**). Results in **Table 3-11** show that all the flow statistics (Q95, Q50, and Q10) increase with CC. The results also indicate a 30% to 158% increase in Q10.

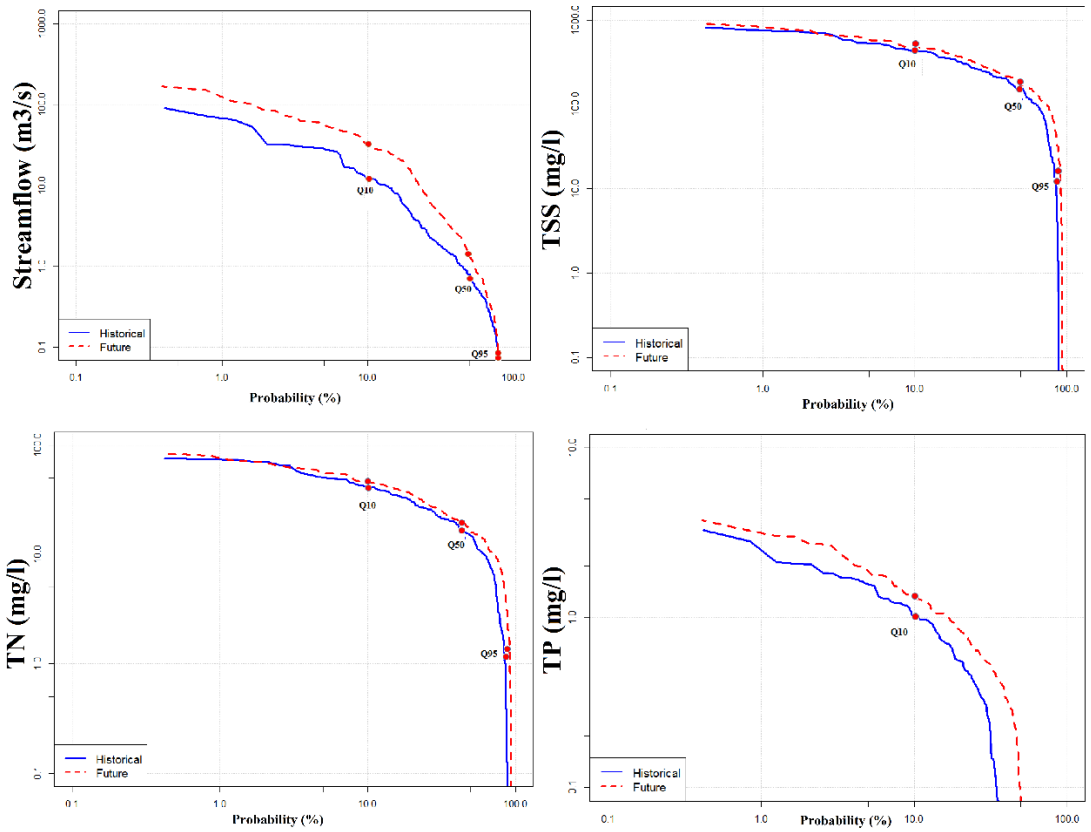

Figure 3.10. Exceedance probability curves for (a) runoff volume, (b) TSS, (c) TN, and (d) TP.

The results of this study provide a guidance to better understand which pollutants are most critical and pose the greatest variability for CC projections. Therefore, it helps managers and decision makers develop better mitigation actions and select the most appropriate SCMs. It may enable a more reliable and rational CC decision-making process for this specific case study watershed. Overlooking the impact of CC on water quantity and quality could result in failing to achieve water quality goals, may result in unanticipated flooding, and likely will result in damages and waste.

3.4 Summary and Conclusion

A hydrologic/hydraulic/water quality model (SWMM) was used to simulate a continuous rainfall-runoff response in an urban watershed, Difficult Run, Fairfax, VA. The model was then calibrated to observed conditions for peak flows, runoff volume, and water quality using two gauging stations in the watershed. The calibrated model was verified by assessing its performance against historical data. After calibration and verification, the impact of CC on the runoff volume and water quality in the watershed was assessed using downscaled precipitation and temperature data. Recent simulations from the NARCCAP were adapted for this purpose, using dynamic downscaling. The hydrology of the Difficult Run watershed was then simulated using SWMM, with the assistance of RSWMM for calibration, event processing and exceedance curve plotting for historical and projected conditions. The following conclusions can be drawn from the study:

1. Three SWMM parameters, including hydraulic width, imperviousness, and depression storage, were altered during calibration. Hydraulic width and imperviousness were the most sensitive parameters affecting peak flows.
2. NARCCAP and other dynamically downscaled model datasets are particularly useful for hydrological modeling because they provide downscaled data for all of the necessary variables from multiple global and regional models and are openly available online. Dynamical downscaling of the CMIP5 models is being performed by the North American Coordinated Regional Climate Downscaling Experiment (NA-CORDEX), but this project is not yet complete. Temperature and precipitation data from NA-CORDEX have been recently published, but other data that are needed for hydrological simulations, such as wind speed and radiation, are not yet available. Thus, the NARCCAP dataset is still the most current set of complete downscaled model data for our study area.
3. The hydrological impact of the CC projection indicates that the mean annual runoff is predicted to increase by 6.5%, and TSS, TN, and TP are predicted to increase by 7.66%, 6.99%, and 8.1%, respectively. Statistically, only projected TP loads were significantly different than historical TP loads.

4. The simulation results demonstrate that the mean, median, maximum, and the range between the 10th and 95th percentiles were projected to increase in the projected with CC conditions. The interannual variability in the projected is also projected to increase.
5. Q10, Q50, and Q95 were compared using exceedance probability curves. Results show that these flow statistics are projected to increase in the future with CC; the greatest difference occurred at the 10th percentile for runoff volume.

The limitations of this analysis stem from the sources of uncertainty, which include: uncertainty in GCMs, including their inherent assumptions regarding future emission of greenhouse gases, uncertainty in the representation of climatology at regional and local scales, and uncertainty of parameters required for input in development of hydrological models. Analysis of uncertainty propagating through the multiple models and processes covered in this study was beyond the scope of this case study, but is a research recommendation. A key limitation of the case study analysis is the use of a single greenhouse emission scenario. However, the contribution of this paper is its development of methods for water quality modeling of an urban watershed subjected to CC. Methods used in this paper can be extended to incorporate a wide range of CC models.

Understanding CC effects on water quantity and quality in urban watersheds will help water resource managers and planners make better decisions in managing water resources issues. Studies such as these can assist them as they evaluate the complex physical, social and economic impacts of CC on urban communities. In addition, making predictions of the impact of CC will help improve the management of stormwater systems to reduce flooding and to produce better water quality through appropriate selection of SCMs.

References for Chapter 3:

Ahmadisharaf, E., Kalyanapu, A.J., 2015. Investigation of the Impact of Streamflow Temporal Variation on Dam Overtopping Risk: Case Study of a High-Hazard Dam, World Environmental and Water Resources Congress 2015@ Sfloods, Droughts, and Ecosystems. ASCE, pp. 1050-1057.

Ahmadisharaf, E., Tajrishy, M., Alamdari, N., 2016. Integrating flood hazard into site selection of detention basins using spatial multi-criteria decision-making. Journal of Environmental Planning and Management 59(8), 1397-1417.

Barco, J., Wong, K.M., Stenstrom, M.K., 2008. Automatic Calibration of the U.S. Epa Swmm Model for a Large Urban Catchment. Journal of Hydraulic Engineering 134(4), 466-474.

Bhaduri, Minner, 2001. Long-Term Hydrologic Impact of Urbanization: A Tale of Two Models. Journal of Water Resources Planning and Management 127(1), 13-19.

Campbell, C.W., Sullivan, S.M., 2002. Simulating time-varying cave flow and water levels using the Storm Water Management Model. Engineering Geology 65(2), 133-139.
CDM Smith Inc., 2015. Netstorm Version 2015.2. http://www.dynsystem.com/netstorm/.
Chen, J., Brissette, F.P., Chaumont, D., Braun, M., 2013. Finding Appropriate Bias Correction Methods in Downscaling Precipitation for Hydrologic Impact Studies over North America. Water Resources Research 49(7), 4187-4205.
Danish Hydrauic Institute, 2016. Mike Urban.
Dicken, C., Nicholson, S., Horton, J., Labay, K., Foose, M., Mueller, J., 2007. Preliminary integrated geologic map databases for the United States.
Drake, A.A., 1986. Geologic Map of the Fairfax Quadrangle, Fairfax County, Virginia.
Elliott, A., Trowsdale, S., 2007. A Review of Models for Low Impact Urban Stormwater Drainage. Environmental Modelling & Software 22(3), 394-405.
Fairfax County, 2007. Difficult Run Watershed Management Plan.
Fowler, H.J., Wilby, R.L., 2007. Beyond the Downscaling Comparison Study. International Journal of Climatology 27(12), 1543-1545.
Fuka, D.R., Walter, M.T., MacAlister, C., Steenhuis, T.S., Easton, Z.M., 2014. Swatmodel: A Multi-Operating System, Multi-Platform Swat Model Package in R. Jawra Journal of the American Water Resources Association 50(5), 1349-1353.
Gao, H., Tang, Q., Shi, X., Zhu, C., Bohn, T., Su, F., Sheffield, J., Pan, M., Lettenmaier, D., Wood, E.F., 2010. Water Budget Record from Variable Infiltration Capacity (Vic) Model. Algorithm Theoretical Basis Document for Terrestrial Water Cycle Data Records.
Gudmundsson, L., Bremnes, J., Haugen, J., Engen-Skaugen, T., 2012. Technical Note: Downscaling Rcm Precipitation to the Station Scale Using Statistical Transformations–a Comparison of Methods. Hydrology and Earth System Sciences 16(9), 3383-3390.
Gupta, H.V., Sorooshian, S., Yapo, P.O., 1999. Status of Automatic Calibration for Hydrologic Models: Comparison with Multilevel Expert Calibration. Journal of Hydrologic Engineering 4(2), 135-143.
Hathaway, J.M., Brown, R.A., Fu, J.S., Hunt, W.F., 2014. Bioretention function under climate change scenarios in North Carolina, USA. Journal of Hydrology 519, Part A(0), 503-511.
Hatt, B.E., Fletcher, T.D., Walsh, C.J., Taylor, S.L., 2004. The Influence of Urban Density and Drainage Infrastructure on the Concentrations and Loads of Pollutants in Small Streams. Environmental Management 34(1), 112-124.
Hayhoe, K., Wake, C., Anderson, B., Liang, X.-Z., Maurer, E., Zhu, J., Bradbury, J., DeGaetano, A., Stoner, A., Wuebbles, D., 2008. Regional Climate Change Projections for the Northeast USA. Mitig Adapt Strateg Glob Change 13(5-6), 425-436.
Hirschman, D., Collins, K., Schueler, T., 2008. Technical Memorandum: The Runoff Reduction Method. Center for Watershed Protection & Chesapeake Stormwater Network.
Huber, W.C., Dickinson, R.E., Rosener, L.A., Aldrich, J.A., 1988. Stormwater Management Model User's Manual, Version 4. U.S. Environmental Protection Agency, Athens, GA.
James, W., Rossman, L.A., James, W.R.C., 2010. User's Guide to Swmm 5 Computational Hydraulics International, Guelph, Ontario, Canada.
Jastram, J.D., 2014. Streamflow, Water Quality, and Aquatic Macroinvertebrates of Selected Streams in Fairfax County, Virginia, 2007 – 12. U.S. Geological Survey will, Reston, VA, p. 82.
Kaushal, S.S., Belt, K.T., 2012. The Urban Watershed Continuum: Evolving Spatial and Temporal Dimensions. Urban Ecosystems 15(2), 409-435.

Lafon, T., Dadson, S., Buys, G., Prudhomme, C., 2013. Bias Correction of Daily Precipitation Simulated by a Regional Climate Model: A Comparison of Methods. International Journal of Climatology 33(6), 1367-1381.
Lee, Y.J., Boynton, W.R., Li, M., Li, Y., 2013. Role of Late Winter–Spring Wind Influencing Summer Hypoxia in Chesapeake Bay. Estuaries and Coasts 36(4), 683-696.
Liu, J., Sample, D., Bell, C., Guan, Y., 2014. Review and Research Needs of Bioretention Used for the Treatment of Urban Stormwater. Water 6(4), 1069-1099.
Madsen, T., Figdor, E., 2007. When it rains, it pours: global warming and the rising frequency of extreme precipitation in the United States. Environment Texas Research & Policy Center, p. 47.
Mearns, L.O., Gutowski, W., Jones, R., Leung, R., McGinnis, S., Qian, Y., 2009. A Regional Climate Change Assessment Program for North America. Eos, Transactions, American Geophysical Union 90(36), 311-311.
Mishra, V., Lettenmaier, D.P., 2011. Climatic Trends in Major U.S. Urban Areas, 1950–2009. Geophysical Research Letters 38(16), L16401.
Moglen, G., Rios Vidal, G., 2014. Climate Change and Storm Water Infrastructure in the Mid-Atlantic Region: Design Mismatch Coming? Journal of Hydrologic Engineering 0(0), 04014026.
Moriasi, D.N., Arnold, J.G., Van Liew, M.W., Bingner, R.L., Harmel, R.D., Veith, T.L., 2007. Model Evaluation Guidelines for Systematic Quantification of Accuracy in Watershed Simulations. Transactions of the Asae 50(3), 885-900.
Najjar, R.G., Pyke, C.R., Adams, M.B., Breitburg, D., Hershner, C., Kemp, M., Howarth, R., Mulholland, M.R., Paolisso, M., Secor, D., Sellner, K., Wardrop, D., Wood, R., 2010. Potential Climate-Change Impacts on the Chesapeake Bay. Estuarine, Coastal and Shelf Science 86(1), 1-20.
Nakićenović, N., Swart, R., 2000. Special Report on Emission Scenarios. Intergovernmental Panel on Climate Change.
Nash, J.E., Sutcliffe, J.V., 1970. River Flow Forecasting through Conceptual Models Part I — a Discussion of Principles. Journal of Hydrology 10(3), 282-290.
National Research Council, 2000. Clean Coastal Waters: Understanding and Reducing the Effects of Nutrient Pollution. National Academies Press.
Natural Resources Conservation Service, 2015. Web Soil Survey. http://websoilsurvey.nrcs.usda.gov/.
Natural Resources Conservation Service, 2016. Win Tr-55. USDA Natural Resource Conservation Service, Washington, DC.
Natural Resources Conservation Service (NRCS), 2015, http://websoilsurvey.nrcs.usda.gov/ Web Soil Survey.
Nelson, E.J., Booth, D.B., 2002. Sediment Sources in an Urbanizing, Mixed Land-Use Watershed. Journal of Hydrology 264(1–4), 51-68.
Park, D., Roesner, L.A., 2012. Evaluation of Pollutant Loads from Stormwater Bmps to Receiving Water Using Load Frequency Curves with Uncertainty Analysis. Water Research 46(20), 6881-6890.
Pavlovic, S., Perica, S., Martin, D., Roy, I., StLaurent, M., Trypaluk, C., Unruh, D., Yekta, M., Bonnin, G., NOAA Atlas 14: Updated Precipitation Frequency Estimates for the United States.
Peck, A., Prodanovic, P., Simonovic, S.P., 2012. Rainfall intensity duration frequency curves under climate change: City of London, Ontario, Canada. Canadian Water Resources Journal 37(3), 177-189.

Rosenberg, E.A., Keys, P.W., Booth, D.B., Hartley, D., Burkey, J., Steinemann, A.C., Lettenmaier, D.P., 2010. Precipitation Extremes and the Impacts of Climate Change on Stormwater Infrastructure in Washington State. Climatic Change 102(1), 319-349.
Rossman, L., 2015. Storm Water Management Model Reference Manual: Volume I–Hydrology. Us Envrionmental Protection Agency, Office of Research and Developement, National Risk Management Laboratory, Cincinnati, Oh 45268.
Rossman, L.A., 2004. Storm Water Management Model User's Manual, Version 5.0, in: U.S. Environmental Protection Agency (Ed.). Cincinatti, OH.
Santhi, C., Arnold, J.G., Williams, J.R., Dugas, W.A., Srinivasan, R., Hauck, L.M., 2001. Validation of the Swat Model on a Large River Basin with Point and Nonpoint Sources. Jawra Journal of the American Water Resources Association 37(5), 1169-1188.
Schaefer, S.C., Alber, M., 2007. Temperature controls a latitudinal gradient in the proportion of watershed nitrogen exported to coastal ecosystems. Biogeochemistry 85(3), 333-346.
Schoof, J.T., 2012. Scale Issues in the Development of Future Precipitation Scenarios. Journal of Contemporary Water Research & Education 147(1), 8-16.
Scully, M.E., 2010. The Importance of Climate Variability to Wind-Driven Modulation of Hypoxia in Chesapeake Bay. Journal of Physical Oceanography 40(6), 1435-1440.
Selvalingam, S., Liong, S.Y., Manoharan, P.C., 1987. Use of RORB and SWMM models to an urban catchment in Singapore. Advances in Water Resources 10(2), 78-86.
Semadeni-Davies, A., Hernebring, C., Svensson, G., Gustafsson, L.-G., 2008. The Impacts of Climate Change and Urbanisation on Drainage in Helsingborg, Sweden: Combined Sewer System. Journal of Hydrology 350(1), 100-113.
Shapiro, S.S., Wilk, M.B., 1965. An Analysis of Variance Test for Normality (Complete Samples). Biometrika 52(3-4), 591-611.
Steinberg, P., 2014. Https://Www.Openswmm.Org/Topic/4390/Rswmm-Autocalibration-of-Swmm-in-R.
Temprano, J., Arango, O., Cagiao, J., Suarez, J., Tejero, I., 2006. Stormwater Quality Calibration by Swmm: A Case Study in Northern Spain. Water Sa 32(1), 55-63.
Teutschbein, C., Seibert, J., 2012. Bias Correction of Regional Climate Model Simulations for Hydrological Climate-Change Impact Studies: Review and Evaluation of Different Methods. Journal of Hydrology 456, 12-29.
U.S. Army Corps of Engineers, 2016. Hydrologic Modeling System, Version 4.1.
USEPA, 2010a. Chesapeake Bay Total Maximum Daily Load for Nitrogen, Phosphorus and Sediment. Us Epa, Washington, D.C.
USEPA, 2010b. Stormwater Best Management Practices (Bmp) Performance Analysis, in: U.S. EPA Region 1 (Ed.). Tetra Tech, Inc., Fairfax, VA, p. 232.
Van Liew, M.W., Arnold, J.G., Garbrecht, J.D., 2003. Hydrologic Simulation on Agricultural Watersheds: Choosing between Two Models. Transactions of the Asae 46(6), 1539-1551.
Wang, L., Chen, W., 2014. Equiratio Cumulative Distribution Function Matching as an Improvement to the Equidistant Approach in Bias Correction of Precipitation. Atmospheric Science Letters 15(1), 1-6.
Warwick, J., Tadepalli, P., 1991. Efficacy of Swmm Application. Journal of Water Resources Planning and Management 117(3), 352-366.
Wood, A.W., Leung, L.R., Sridhar, V., Lettenmaier, D.P., 2004. Hydrologic Implications of Dynamical and Statistical Approaches to Downscaling Climate Model Outputs. Climatic Change 62(1-3), 189-216.

Wright, L., Chinowsky, P., Strzepek, K., Jones, R., Streeter, R., Smith, J., Mayotte, J.-M., Powell, A., Jantarasami, L., Perkins, W., 2012. Estimated Effects of Climate Change on Flood Vulnerability of U.S. Bridges. Mitig Adapt Strateg Glob Change 17(8), 939-955.
Xia, Y.L., Mitchell, K., Ek, M., Sheffield, J., Cosgrove, B., Wood, E., Luo, L.F., Alonge, C., Wei, H.L., Meng, J., Livneh, B., Lettenmaier, D., Koren, V., Duan, Q.Y., Mo, K., Fan, Y., Mocko, D., 2012. Continental-Scale Water and Energy Flux Analysis and Validation for the North American Land Data Assimilation System Project Phase 2 (Nldas-2): 1. Intercomparison and Application of Model Products. Journal of Geophysical Research-Atmospheres 117(D3).
Zahmatkesh, Z., Burian, S., Karamouz, M., Tavakol-Davani, H., Goharian, E., 2014a. Low-Impact Development Practices to Mitigate Climate Change Effects on Urban Stormwater Runoff: Case Study of New York City. Journal of Irrigation and Drainage Engineering 141(1), 04014043.
Zahmatkesh, Z., Karamouz, M., Goharian, E., Burian, S., 2014b. Analysis of the Effects of Climate Change on Urban Storm Water Runoff Using Statistically Downscaled Precipitation Data and a Change Factor Approach. Journal of Hydrologic Engineering 20(7), 05014022.
Zoppou, C., 2001. Review of Urban Storm Water Models. Environmental Modelling & Software 16(3), 195-231.

Chapter 4. Evaluating the treatment performance of retention ponds in an urban watershed with projected climate conditions.

Taken from:
Alamdari N, Sample DJ, Ross A, Easton Z (*In review*) Evaluating treatment performance of retention ponds in an urban watershed under a changing climate. *Landscape and Urban Planning.*

Abstract

Considerable efforts are underway to restore hydrologic function and water quality of watersheds impacted by urban development, however, climate change (CC) may undermine them. Understanding the effect of CC on the efficiency of stormwater control measures (SCMs) such as retention ponds is required if water quality goals are to be met. We simulated an urban watershed using the Storm Water Management Model (SWMM). Downscaled Global Climate Models (GCMs) from the Coupled Model Intercomparison Project Phase 5 (CMIP5) were used to project precipitation and temperature; these were then used to force the SWMM model. Five GCMs, a historical and two Representative Concentration Pathways (RCP 4.5 and 8.5) scenarios were used in an ensemble approach to better assess variability of the results. The results indicated that all the GCMs resulted in increases in annual precipitation and temperature for both RCPs scenarios in comparison with historical conditions. Both RCPs exhibited their largest increases in precipitation, streamflow, and Total Suspended Solids (TSS), Total Nitrogen (TN), and Total Phosphorous (TP) loads in the winter, and summer was associated with the largest increase in temperature. Median reductions in TSS, TN, and TP treatment efficiency for RCP 4.5 were projected to be 6%, 7%, and 11%, respectively; and 11%, 12%, and 17% for RCP 8.5, respectively. Thus, the effectiveness of retention ponds for pollutant removal may be reduced under projected climate conditions. Evaluations such as these can help guide the formation of climate resilient watershed improvement strategies.

Keywords. climate change; hydrologic model; global climate models; regional climate models; representative concentration pathways, retention ponds, removal efficiency.

4.1 Introduction

Future greenhouse gas emission scenarios have been developed based on the expected changes in the global economy, environment, and population (Moss et al., 2010; Pachauri et al.,

2014) and are used as critical assumptions in global climate models (GCMs). As reported by the Intergovernmental Panel on Climate Change (IPCC), mean temperatures are expected to increase by 1.1 to 6.4 °C by 2100 (IPCC, 2014). In the U.S., average air temperatures have already increased by 1°C Heating degree days for nearly 50% of U.S. urban areas declined by a median of -1.7% per decade between 1950-2009 (Mishra and Lettenmaier, 2011). In addition, the number of nights above freezing increased by 6.5% per decade for all urban areas in the U.S. over the same period (Mishra and Lettenmaier, 2011). In the Northeast U.S., Hayhoe et al. (2008) predicted precipitation increases during winter and spring for both higher (A1F1) and lower (B1) greenhouse gas emission scenarios (Nakićenović and Swart, 2000) by 2100. Likewise, Najjar et al. (2010) found that in the mid-Atlantic region of the U.S., CO_2 concentrations are projected to increase by 50-160% by 2100. In addition, sea level is predicted to rise about 0.7-1.6 m and water temperatures are predicted to rise by 2 to 6 °C, respectively. Climate change (CC) may also lead to longer periods between storms resulting in lower groundwater levels and base flows to streams (Power et al., 2005; Saft et al., 2015; van Dijk et al., 2013).

Urban development increases imperviousness, resulting in large increases in the volume of runoff during wet weather conditions (Jennings and Jarnagin, 2002; Pyke et al., 2011; Walsh et al., 2012), decreased groundwater recharge and baseflow in streams, decreasing streamflow in dry weather (Fletcher et al., 2013; Jacobson, 2011), and increasing pollutant washoff to surface waters (Hatt et al., 2004). This leads to streambank and stream channel erosion and degrades aquatic habitats, through a well-known phenomenon known as “urban stream syndrome” (Alberti et al., 2007; Kaushal and Belt, 2012; Nelson and Booth, 2002; Schueler et al., 2009; Walsh et al., 2005). CC may increase these impacts (Imteaz et al., 2011; Lee and Jetz, 2008) as increases in precipitation directly leads to increases in runoff, increasing transport of sediment, nutrients, and other contaminants. Floods may increase the frequency and magnitudes as drainage infrastructure designed for smaller storm events are overwhelmed (Semadeni-Davies et al., 2008). These effects may accelerate stream and aquatic habitat degradation; increasing temperatures may also affect biogeochemical processes across the landscape (Lee et al., 2013; Scully, 2010). As nutrients accumulate in water bodies, eutrophication ensues; perhaps the most well-known example of this phenomenon (and most relevant to this paper) is the Chesapeake Bay estuary (National Research Council, 2000). The U.S. Environmental Protection Agency

(USEPA) recently established a Total Maximum Daily Load (TMDL) for the Chesapeake Bay, limiting nitrogen (N), phosphorus (P), and sediment discharges into its tributaries from municipal wastewater, urban stormwater, and agricultural sources (USEPA, 2010a) in an effort to halt eutrophication of the Bay and restore associates habitats.

Reductions in N, P, and sediment loadings from urban runoff can be achieved by implementing best management practices (BMPs) also called stormwater control measures (SCMs). These practices range from educational programs intended to persuade residents to reduce fertilizer use to physical structures which typically have some water quality treatment capability, however, performance is highly variable (Aguilar and Dymond, 2016; Johnson and Sample, 2017). Some SCMs have infiltrative properties (e.g., bioretention, infiltration basins, swales) that reduce runoff volume and thus may reduce mass loading of nutrients and sediment downstream (Sample et al., 2014). Other SCMs have storage-treatment capabilities. These include retention ponds, which are ubiquitous in urban watersheds (Balascio and Lucas, 2009; Semadeni-Davies, 2006). The ponds may be designed based on the steady-state, continuous, irregular/intermittent release of pollutant loadings (Imteaz et al., 2016). Removal of TSS, TN, and TP in retention ponds depends primarily on the hydraulic retention time (HRT) (Sharma et al., 2016; Vollertsen et al., 2007). Increased rainfall intensities and longer dry weather periods predicted with CC in some regions may affect the efficiency of retention ponds by increasing buildup and wash off of pollutants from land surfaces, increasing pollutant loading (Sharma et al., 2016). Increased runoff induced by CC may shorten the HRTs of retention ponds during extreme events. These effects should be considered to achieve resilient SCMs and urban drainage systems for projected CC conditions. Hathaway et al. (2014) assessed the function of several bioretention systems sized for current conditions during several projected CC scenarios, and found that CC may cause a significant increase in the frequency and magnitude of untreated overflows. Advances in downscaling methods coupled with continuous simulation hydrologic and water quality models make it feasible to assess the treatment performance of retention ponds impacted by CC at appropriate spatial and temporal scales.

Due to the focus on watershed implementation efforts in the Chesapeake Bay watershed, evaluating water quality of CC-impacted watersheds must be done jointly with an assessment of SCM treatment performance in order to select the best strategy for meeting current and future water quality goals. Improving the ability to predict CC impacts on water quality in urban

watersheds is needed to evaluate conditions and select the best treatment strategies .There have been a few studies that assessed the effects of CC on water quality in urban watersheds, and only a handful that assessed CC impacts on the resiliency of SCMs to CC. Assessing performance of SCMs such as retention ponds in the face of CC have not been thoroughly performed, resulting in a lack of understanding how resiliency can be assessed for these systems. Thus, the objectives of this study are: 1) to bracket the long-term changes in water quantity and quality, including streamflow, TSS, TN, and TP loads from a selected urban watershed subject to CC, and; 2) and to characterize the pollutant removal efficiency of retention ponds within that watershed for existing and projected CC conditions. We will accomplish this using statistical downscaling of GCMs coupled with a previously developed, calibrated SWMM model of the Difficult Run watershed in Fairfax, VA.

4.2 Materials and Methods

4.2.1 Study Area

The Difficult Run watershed, at 150 km^2, is the largest watershed in Fairfax County, Virginia USA. Difficult Run lies in the north-central portion of Fairfax County and drains directly to the Potomac River, a tributary of the Chesapeake Bay. The watershed is within the Piedmont physiographic province of Virginia, and consists of 18 sub-watersheds (**Figure 4.1**). The length of the mainstem and tributaries are approximately 63 km and 233 km, respectively. Slope is low to moderate with an average slope of 7.15 %. Soils in the watershed range from sandy loam to clay loams with silt loams being the most dominant soil type, with moderate infiltration capacity. Land use/land cover (LULC) within the watershed is dominated by residential including estate, low, medium and high density (approximately 57%) (Fairfax County, 2007). Distribution of the LULC within the watershed is presented in **Table 4-1**. An estimated total of 18.4 % of the total watershed covered by impervious surfaces (Fairfax County, 2007). This relatively high imperviousness from urban development has caused significant increases in runoff volume and peak, increased transport of pollutants, increased stream instability and erosion, and impairment of stream water quality and stream habitat in the watershed (Schwartz et al., 2017).

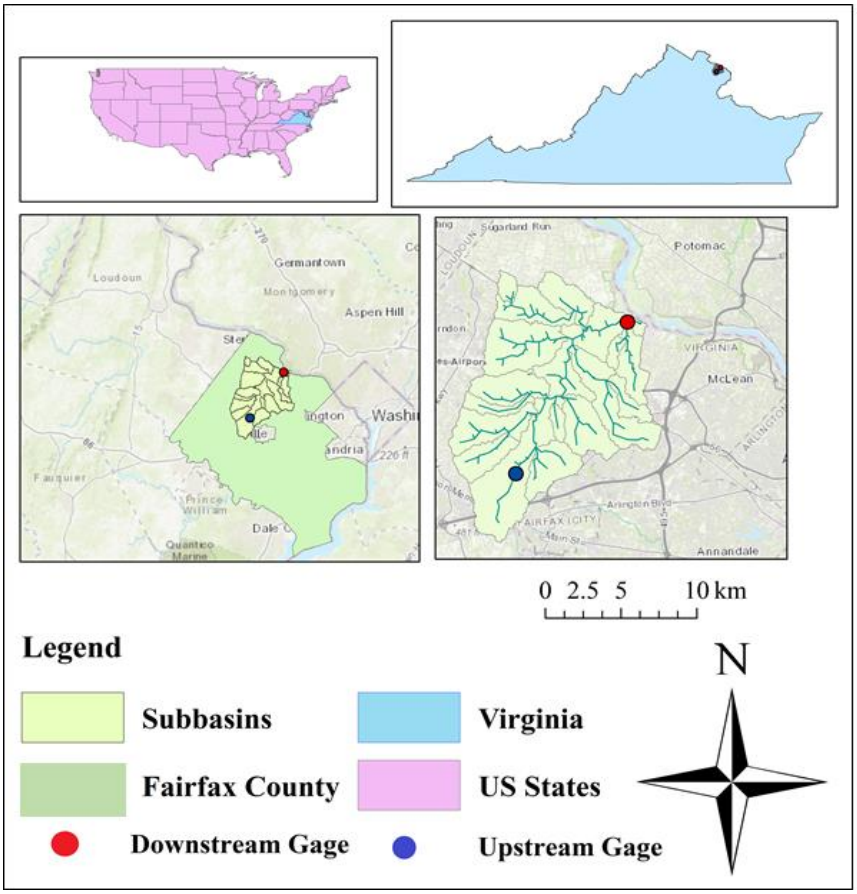

Figure 4.1. Subwatershed location map.

Table 4-1. Existing Land use/Land cover (LULC) in Difficult Run Watershed.

LULC Type	Existing (%)
Open Water	0.4
Developed, Open Space	32.2
Developed, Low Intensity	12.5
Developed, Medium Intensity	6.6
Developed, High Intensity	1.47
Barren Land (Rock/Sand/Clay)	0.02
Deciduous Forest	35.9
Evergreen Forest	2.11
Mixed Forest	1.39
Shrub/Scrub	0.9
Grassland/Herbaceous	0.06
Pasture/Hay	1
Cultivated Crops	0.8
Woody Wetlands	4.3
Emergent Herbaceous Wetlands	0.01

Detailed information of the watershed conditions are presented in (Alamdari et al., 2017).

4.2.2 Hydrologic and Water Quality Modeling

In this study, SWMM version 5.1.012 was employed for hydrologic and water quality modeling. SWMM is a lumped model that can be run for both single event and continuous simulation (Huber et al., 1988; James et al., 2010; Rossman, 2004). SWMM predicts runoff, water surface elevations at each node, and water quality concentrations and loadings, which included TSS, TN and TP. More detailed information on the methodology used for the hydrologic and water quality simulations in this study is presented in Alamdari et al. (2017). SWMM simulates groundwater flow for each subcatchment through a single aquifer, which is defined by the depth of its unsaturated upper zone and lower saturated zone, bottom of aquifer, groundwater flow parameters, porosity, wilting point, field capacity and saturated hydraulic conductivity. This data was obtained from the Fairfax county geologic map (Drake Jr and Lee, 1989) and SSURGO database (Natural Resources Conservation Service (NRCS), 2015, http://websoilsurvey.nrcs.usda.gov/). These parameters were developed from raster grids or attributes associated with a specific area. GIS spatial operations were conducted to create a weighted area average for each subcatchment.

The groundwater coefficients (A1, A2, B1, B2, A3) in the SWMM compute groundwater flow as a function of groundwater and surface water heads (Rossman, 2015). A1 and B1 are groundwater glow coefficient and groundwater flow exponent, respectively. A2 and B2 are surface water flow coefficient and surface water flow exponent, respectively. A3 is surface-groundwater interaction coefficient. The coefficient's upper and lower boundaries for calibration were set based on (Dent et al., 2004; James and James, 1998) which defined the ranges as A1 (0.001-1), B1 (0.1-9.9), A2 (0-1), B2 (0-9.99). A3 was set to zero. A1 must be larger than A2 and B1 must be larger than B2. SWMM allows treatment functions which express the removal of pollutants to be applied to any water quality constituent at any node of the conveyance system (Rossman, 2015); retention ponds are storage nodes. In this study, water quality was modeled using an estimated event mean concentration (EMC) washoff during runoff events and user-defined treatment functions for storage SCMs such as retention ponds, as detailed in a previous related study (Alamdari et al., 2017). EMC is a method used to estimate washoff load (Sansalone and Buchberger, 1997) and is the flow proportional concentration of a given pollutant during the storm event.

EMC is an effective method for estimation of pollutant concentrations as shown by Charbeneau and Barrett (1998) . The authors investigated several methods for generating constituent concentrations for use in stormwater modeling and found that a single EMC for all urban land uses was shown to provide a reasonable estimate of solids loads. Sage et al. (2015) used the conceptual and empirical models to estimate the process of buildup and washoff and demonstrated that the model accurately replicates load estimates. Authors also found that even simple EMC methods confirmed the good predictive power for estimation of washoff loads. Even though the concentration of a pollutant may vary during a rainfall event, a single EMC can be used to characterize runoff constituents (Butcher, 2003).

The National Urban Runoff Database under the USEPA's National Pollutant Discharge Elimination System (NPDES) Stormwater MS4 Phase I Program is created to identify the range of EMC values for different pollutants (Pitt et al., 2004). A summary of P concentrations from urban runoff is illustrated in the study by Sample et al. (2012). These data represent concentrations of TP in urban stormwater from the 29 prototype National Urban Runoff Program (NURP) projects found in USEPA (1983). EMCs for TSS, TN, and TP were chosen from mean values from the National Urban Runoff Program (NURP) (USEPA, 1983) which were in line with other water quality data from Virginia and Chesapeake Bay (Hirschman et al., 2008; Schueler, 2011; USEPA, 2010b). EMCs for TSS, TN, and TP were set at 40 mg/L, 2.9 mg/L, and 0.27 mg/L, respectively (Hirschman et al., 2008; Schueler, 2011; USEPA, 2010b).

4.2.3 Climate Data

To evaluate future CC impacts on runoff quantity and quality, projections were needed for precipitation, temperature, humidity, evaporation, etc. In this study, simulations from the Coupled Model Intercomparison Project Phase 5 (CMIP5) (Taylor et al., 2012) were used. Two time periods, 1971-1998 and 2041-2068 using two Representative Concentration Pathways (RCP 4.5 and 8.5) (Moss et al., 2010) of medium and intensive greenhouse gas emissions were used for historical and projected CC conditions. The two RCPs use radiative forcing values of 4.5 and 8.5 W/m^2, respectively.

Data were obtained from five GCM-RCM combinations: Max Planck Institute Earth System Model, low resolution (MPI-ESM-LR); Goddard Institute for Space Studies Model E, coupled with the Russell ocean model (GISS-E2-R); Community Climate System Model, version 4 (CCSM4); Commonwealth Scientific and Industrial Research Organization Mark, version 3.6.0

(CSIRO Mk3.6.0); and Beijing Climate Center, Climate System Model, version 1.1 (BCC-CSM1.1). These combinations were selected based on performance metrics such as bias, root mean square error (RMSE) and spatial correlation to quantify the errors relative to observed seasonal precipitation, seasonal near-surface air temperature, seasonal sea surface temperature, seasonal atmosphere–land water budgets, hydro climate extremes and etc. in the Northeast and Mid-Atlantic US. (Sheffield et al., 2013). Model performance was calculated based on a normalized metric which ranges between 0 and 1 with 0 indicates the lowest bias and a 1 indicates the highest bias. Then models were ranked according to normalized metric, with 1 indicating the model with the lowest bias and 17 indicating the model with the highest bias. The bias metrics from Sheffield et al. (2013) for regional precipitation from December-February and June-August; regional temperature from December-February and June-August; annual runoff ratios; the annual number of summer days, frost days, growing season length; east–west gradient in the number of persistent precipitation; and soil moisture were compared. Using multiple GCMs and scenarios which will produce a corresponding range of outputs, is known as the ensemble approach. Employing an ensemble approach provides robust estimates of CC impacts and their uncertainty by providing upper and lower bounds based upon a range of anticipated conditions or scenarios (Krysanova et al., 2017) .

The GCM data were bias-corrected using the equidistant cumulative distribution function matching method (Li et al., 2010) for temperature and the “PresRat” method for precipitation which is an extension to equidistant cumulative distribution function matching (EDCDFm) bias correction (Pierce et al., 2015), along with a frequency-dependent bias correction method (Pierce et al., 2015) . The data were statistically downscaled to daily, 1/16° resolution using the Localized Constructed Analog (LCA) algorithm (Pierce et al., 2014).

Daily precipitation data were converted to hourly frequency using a temporal disaggregation method developed to create input data for the Variable Infiltration Capacity model. (Gao et al., 2010). More detailed information on the methodology used for temporal disaggregation is presented in Alamdari et al. (2017).

Data from most recent scenarios including, RCP 4.5 and RCP 8.5 were utilized in this study, allowing an analysis of CC impacts for two scenarios, with the main goal of determining differences in SCM performance between the historical and both CC scenarios using five climate

models. Due to the uncertainty of climate projections, employing two CC scenarios and multiple GCMs provides a robust assessment of potential CC impacts.

4.2.4 Statistical Analysis

Statistical analysis was performed to investigate the significance of the changes in precipitation, runoff, TSS, TN, and TP loads in the watershed. Student's t-test was used to do such analysis and determine whether there was a significant difference between the historical and projected water quality and quality. The two-sample t-test was used to test the similarity of the population means of two groups. The normality of the datasets was checked using the Shapiro-Wilk test (Shapiro and Wilk, 1965). In addition, the effects of CC on water quality and quantity were evaluated using flow statistics of Q95, Q50, and Q10 which represent the exceedance of flow values 95%, 50%, and 10% of the time, respectively. Flow duration curves were developed for different scenarios and GCMs and compared before and after CC. Q95, Q50, and Q10 were computed for characterizing low, median, and high flows.

4.2.5 Methods for assessing performance of retention ponds SCMs for projected CC scenarios

The SWMM model of the Difficult Run watershed in Fairfax, VA, described by Alamdari et al. (2017), was selected for use in this study. The three climate scenarios (Historical, RCP 4.5, and RCP 8.5) were input into each simulation for comparison purposes. The temporal resolution of the projected climate scenarios was 1 hr. Hourly rainfall data were disaggregated to 15-min time step for the proposed H/H simulations using NETSTORM as stated by Alamdari et al. (2017)). The approximately 900 retention ponds in the Difficult Run watershed were aggregated previously in the development of the Difficult Run WMP (Fairfax County, 2007) for simplicity of analysis. These composite retention ponds were modeled in this study to evaluate their effectiveness in removing TSS, TN, and TP loads for projected CC conditions. As stated in the section 4.1.2, pollutant loads in the inlet and outlet of the ponds were determined using estimated event mean concentration (EMC) washoff loading during runoff events and treatment functions for retention ponds. Performance of retention ponds was evaluated based upon mass loading into and out of each pond.

4.3 Results and Discussions

4.3.1 Calibration and Verification

More detailed information on the methodology used for the SWMM model development, calibration, and verification is presented in Alamdari et al. (2017). To summarize the model's efficacy from Alamdari et al. (2017), the calibration and verification results showed good agreement between simulated and observed data with respect to peak flow. Coefficient of determination (R^2), Nash Sutcliffe Efficiency (NSE) (Nash and Sutcliffe, 1970), and Percent Bias (PBIAS) (Gupta et al., 1999) of 0.77, 0.72, and 14.9%, respectively for calibration, and 0.83, 0.79, and 13.8%, respectively for validation were obtained. SWMM calibration results for TSS, TN, and TP indicated R^2 of 0.65, 0.59, and 0.61, respectively.

4.3.2 Climate Change Impacts on Runoff Quantity and Quality

The average annual precipitation and temperature during the historical and projected periods were compared for five selected GCM-RCMs for two RCPs scenarios. Results indicate that the annual mean temperature for RCP 4.5 is predicted to increase by 1.4 °C to 3.2 °C, with a median increase of 2 °C, while the change in the annual precipitation ranges from 1.9% to 12.3% with the median increase of 7.3%. The annual mean temperature for RCP 8.5 is predicted to increase from 2 °C to 4.5 °C, with a median increase of 2.7 °C, while the change in the annual precipitation ranges from 7.6% to 15.4% with a median increase of 11.7%. Model results indicate that the change in annual streamflow for RCP 4.5 is predicted to increase by 4.2% to 38.1% with a median increase of 11.9%; while for RCP 8.5, streamflow is predicted to increase by 6.9% to 26.4% with a median increase of 15.5%.

Annual TSS loads for RCP 4.5 range from -2.8% to 9.2% with a median increase of 3.1%. TSS loads for RCP 8.5 ranged from -4.5% to 13.4%, with a median increase of 3.8%. TN loads for RCP 4.5 range from -3.4% to 8.8%, with a median increase of 2.5%; while for RCP 8.5, TN loads range from -5% to 12.7%, with a median increase of 3.1%. Results for TP loads for RCP 4.5 range from -0.7% to 15.6%, with a median increase of 9.9%; while for RCP 8.5, TP loads range from 0.6% to 18.7%, with a median increase of 10.4%. Changes in seasonal and annual mean precipitation and temperature, streamflow, and pollutant loads for the projected period for both RCPs are shown in **Figure 4.2** and **Figure 4.3**, respectively.

<THIS SPACE LEFT INTENTIONALLY BLANK>

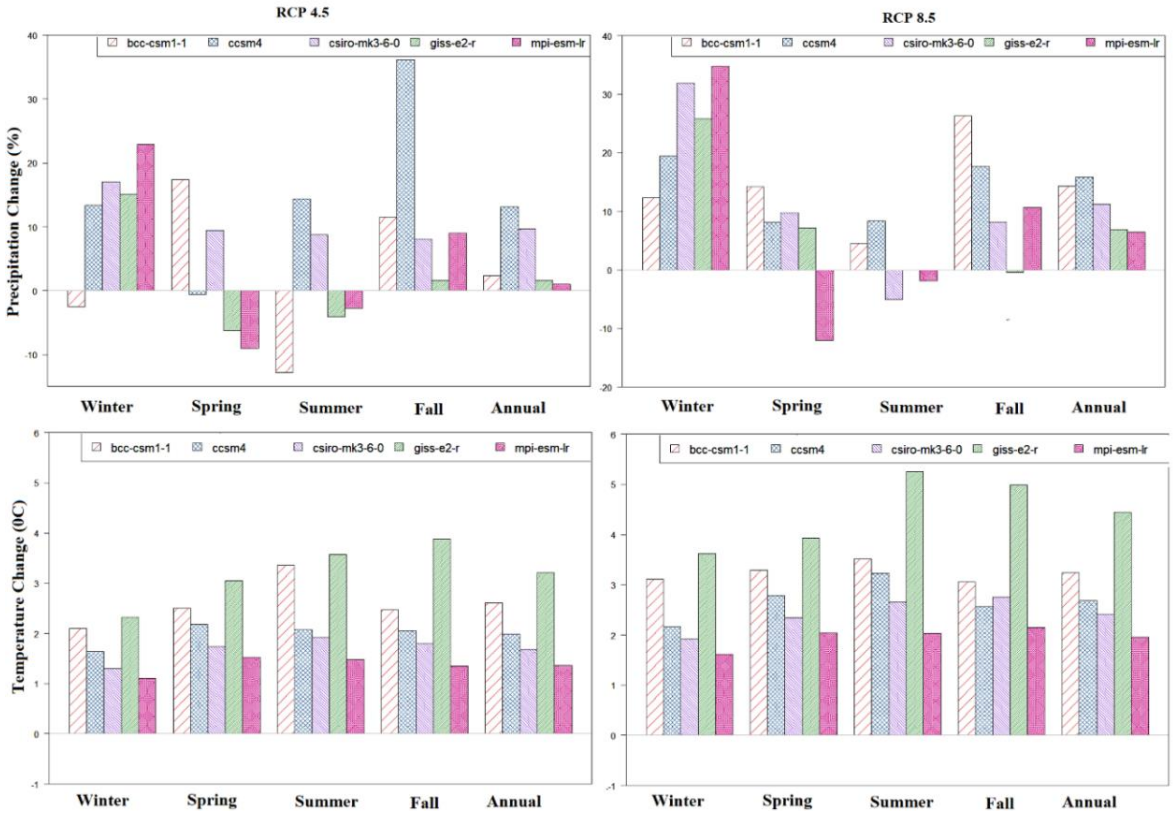

Figure 4.2. Seasonal changes in precipitation (top) and temperature (bottom) between 1971-1998 and 2041-2068.

<THIS SPACE LEFT INTENTIONALLY BLANK>

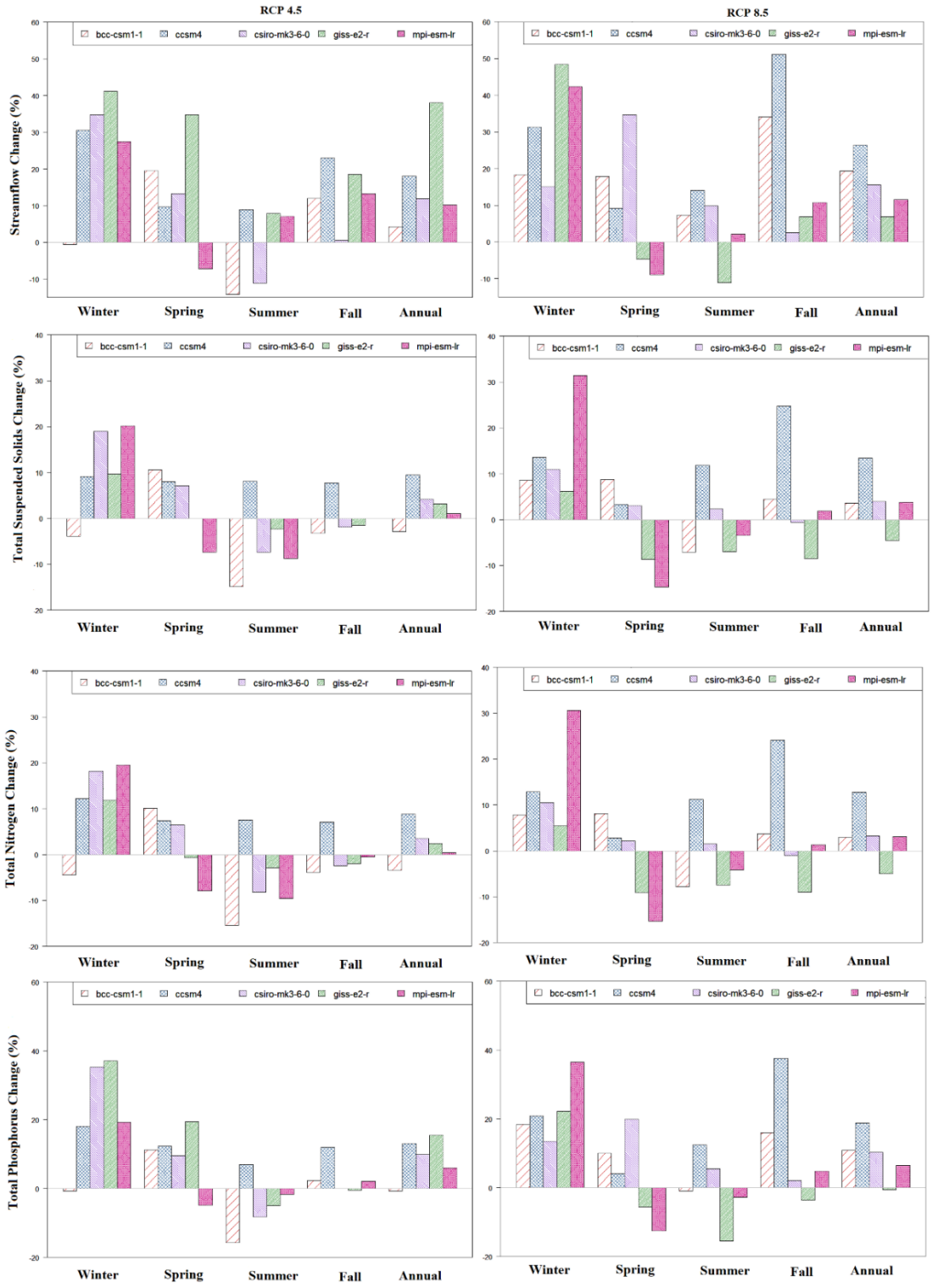

Figure 4.3. Seasonal changes in (a) streamflow, (b) TSS, (c) TN, (d) TP between 1971-1998 and 2041-2068.

Results from projected CC simulations as shown in **Figure 4.2** and **Figure 4.3** indicated that for both RCPs, the largest increase in precipitation, streamflow, and pollutant loads would occur in winter, on average, and the largest temperature increase, on average, would be observed in summer. Higher temperatures may lead to greater evapotranspiration rates and lower soil moisture, which may lead to increased soil storage capacity that can assimilate more precipitation. Higher precipitation in the winter leads to increased streamflow and pollutant loads. Smaller increases in streamflow and pollutant loads were predicted during the summer which could be due to increased evapotranspiration, and lower precipitation during the summer compared to other seasons. RCP 8.5 always predicted a greater median increase in precipitation, temperature, streamflow, and pollutant loads when compared with RCP 4.5.

The predicted increase in mean annual precipitation in the Difficult Run watershed are consistent with work of Najjar et al. (2009) and Howarth et al. (2006), who predicted increases in precipitation over the Chesapeake Bay watershed. These increases in precipitation and temperature affect processes such as sediment and nutrient yields and soil moisture. (Bosch et al., 2014). A shift in seasonal precipitation is also evident in **Figure 4.2** and **Figure 4.3**, which implies drier late summers and wetter winters with CC. The results of this study are also consistent with Hayhoe et al. (2007) that predicted greater winter streamflow due to higher precipitation; and decreased summer streamflow due to increased evapotranspiration and less groundwater recharge during the spring in the Northeast U.S. Groisman et al. (2004) also found an increase in streamflow, especially in wet events in the Northeast U.S. Previous studies in the Mid-Atlantic region found varying streamflow projections from -40% to +30% (Najjar et al., 2010).

The increase in TSS, TN, and TP is mainly driven by increases in runoff predicted by most climate models which could have major impacts on Chesapeake Bay function (Zhang et al., 2013) and urban stormwater systems. Pollutant loads such as TSS and TP also increased during the winter which may result in an increase the rate of erosion where the soils are saturated during major precipitation (Najjar et al., 2010). It should be noted that there is a non-linear function between TSS and streamflow indicating an increase in TSS as streamflow increases (Najjar et al., 2010). As noted by Najjar et al. (2010), more intense precipitation in fewer events will probably increase sediment loading in Chesapeake Bay, but the sensitivity is unknown. TN is also controlled by precipitation and temperature due to CC and an increase in TN may have negative

effects on aquatic ecosystems (Suddick et al., 2013). Although the relative increases in TN and TSS loads were less than TP in the watershed, TN and TSS loads increased in winter (January-March) which is consistent with the increases in winter streamflow. However, TSS, TN, and TP loads decreased in late spring and summer as a result of the reduction in precipitation and streamflow during this period. These results agree with the findings of Chang et al. (2001); (Moore et al., 1997; Najjar et al., 2010; Neff et al., 2000) in Mid-Atlantic region which suggest a possible reduction in eutrophication and pollution levels during spring and late summer for projected climate conditions.

The projected precipitation, temperature variability mainly depends on the selected climate models and scenarios. Moreover, increases in the projected streamflow relative to the historic period result in substantial increases to TSS, TN, and TP, although the magnitude of the change differs among the climate models. The variability between GCMs stems from the difference in their assumptions, model configurations, and model parameterizations (Eghdamirad et al., 2017). The difference in future projections is most likely due to different modeled evapotranspiration, the uncertainty of the models and the difference in the pattern of monthly rainfall between the model and the study area (Najjar et al., 2010). While projected streamflow and pollutant loads vary between an increase and a decrease, the overall trend was an increase.

In general, the study area will may be warmer and wetter, particularly in winter for projected CC conditions. These two key factors probably account for variations in runoff quantity and quality.

4.3.3 Statistical Analysis

4.3.3.1 Student's t-test

A Shapiro-Wilk test was performed for historical and projected data, and the results indicated that, at *p*-values > 0.05, each dataset followed a normal distribution. A pair-wise comparison using the Student's t test was then conducted to determine if there was a significant difference between the mean annual historical and CC projections for all GCM models and scenarios

Analysis of t-test results indicated that differences between the mean annual values of historical and predicted TSS, and TN were not significant at the 95% confidence level for most of the GCMs and for both RCPs. Exceptions to this included the CCSM4 model for both RCPs

for streamflow, TSS, TN, and TP. Differences for most of the GCMs (except MPI-ESM-LR) were found to be significantly different for RCP 8.5 for streamflow. Most GCMs (except MPI-ESM-LR) were found to be significantly different for RCP 8.5 for TP. This implies that streamflow and TP may be more sensitive to CC for higher emission scenarios. TP loads are composed of soluble phosphorus (SP) and particulate phosphorus (PP), and is strongly correlated with peak runoff; PP is strongly correlated with TSS. As a result, increases in precipitation will lead to higher peak runoff, and higher TSS, which may lead to higher TP in the watershed for projected conditions. The results of this study agree with Najjar et al. (2010). The authors found an increase in TSS concentration as flow increases, which stems from enhanced erosion in the streambed. Najjar et al. (2010) also found that the fluxes of sediments and nutrients from the landscape have been significantly affected by climate variability in the Chesapeake Bay.

4.3.3.2 **Streamflow Analysis**

To further study the effect of CC on streamflow and pollutant loads, streamflow were analyzed to determine Q95, Q50, and Q10 were calculated. Exceedance probability curves were developed, as shown in **Figure 4.4**, **Figure 4.5**, **Figure 4.6**, and **Figure 4.7**, for streamflow, TSS, TN, and TP loads, respectively. To further study the effect of CC on streamflow and pollutant loads, exceedance probability curves were analyzed to determine Q95, Q50, and Q10 as shown in Figs. 4-7, for streamflow, TSS, TN, and TP loads, respectively. Flow duration curves were produced based on the simulated streamflow and nutrient loads for the historical period and the two RCP scenarios.

<THIS SPACE LEFT INTENTIONALLY BLANK>

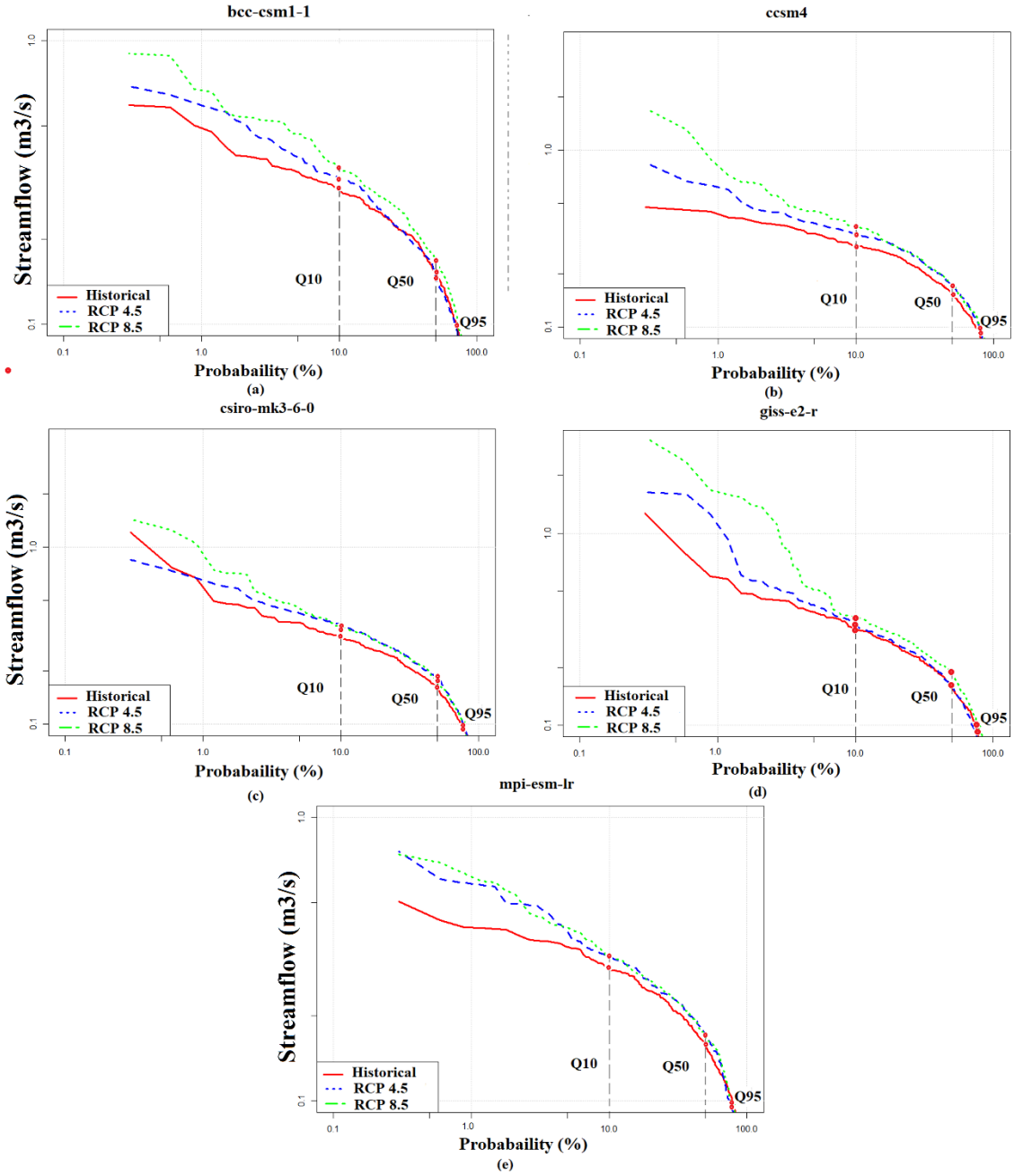

Figure 4.4. Exceedance probability curves for streamflow for all scenarios for GCMs (a) bcc-csm1, (b) ccsm4, (c) csiro-mk3-6-0, (d) giss-e2r, and (e) mpi-esm-lr.

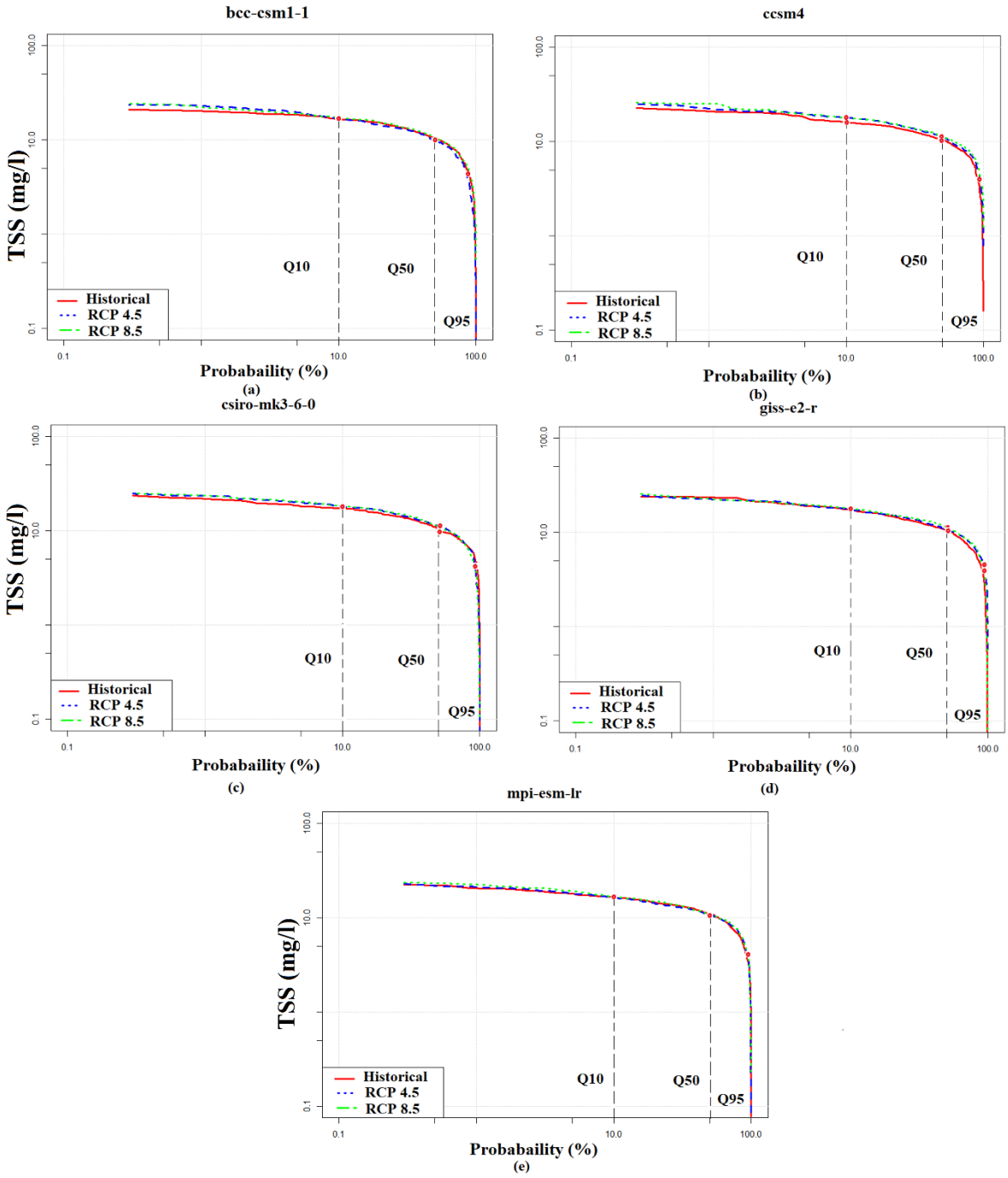

Figure 4.5. Exceedance probability curves for TSS for all scenarios for GCMs (a) bcc-csm1, (b) ccsm4, (c) csiro-mk3-6-0, (d) giss-e2r, and (e) mpi-esm-lr.

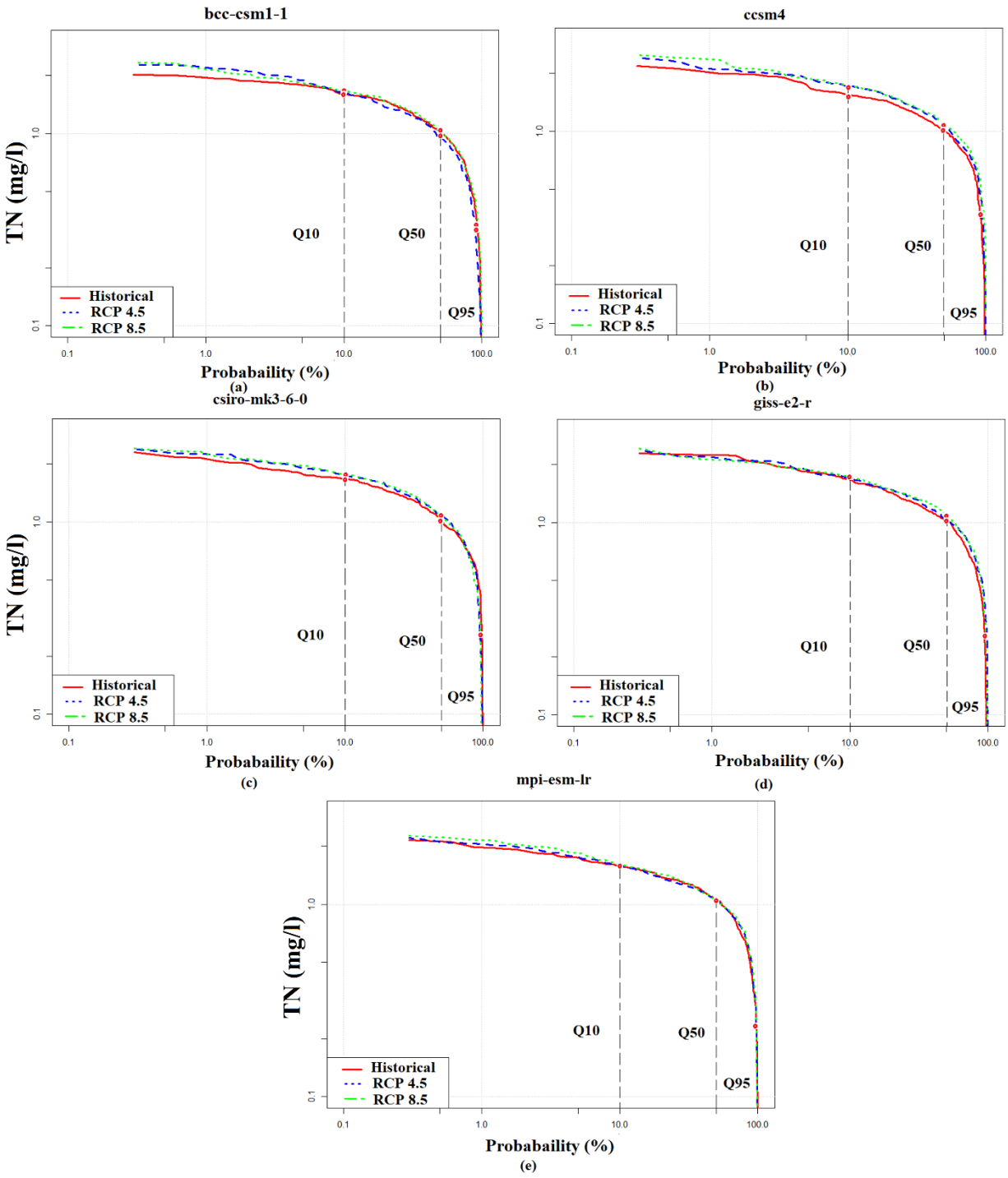

Figure 4.6. Exceedance probability curves for TN for all scenarios for GCMs (a) bcc-csm1, (b) ccsm4, (c) csiro-mk3-6-0, (d) giss-e2r, and (e) mpi-esm-lr.

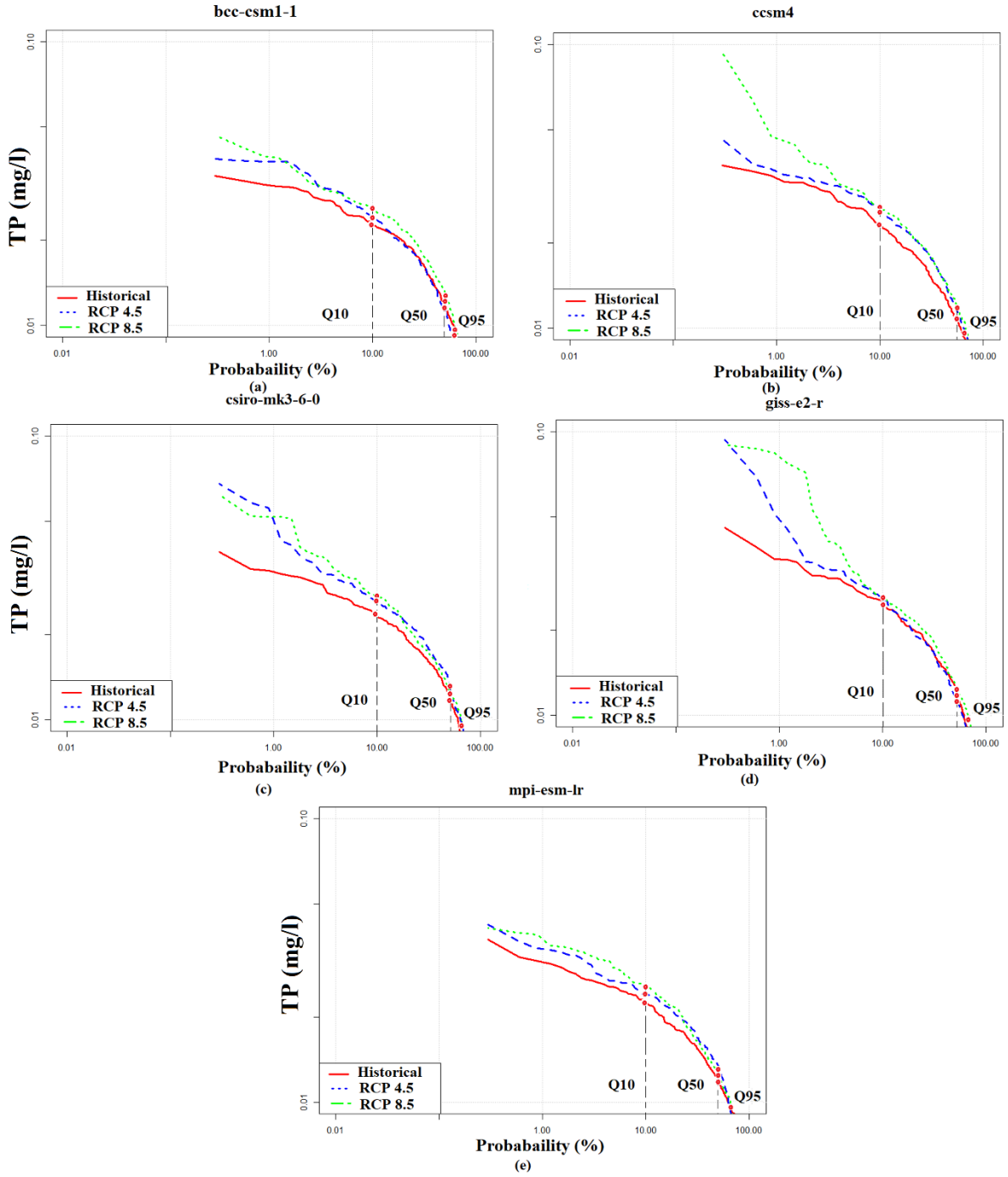

Figure 4.7. Exceedance probability curves for TP for all scenarios for GCMs (a) bcc-csm1, (b) ccsm4, (c) csiro-mk3-6-0, (d) giss-e2r, and (e) mpi-esm-lr.

Considering the high and low flow values, for both historical and projected CC conditions, it can be concluded that the watershed is responding to extreme precipitation events

with relatively high flows due to increased winter precipitation and earlier snowmelt same as shown by (2007) and Najjar et al. (2010) in Mid-Atlantic region. There is also a difference between the historical and projected streamflow (**Figure 4.4**) during larger storm events occurring at the 10% exceedance probability, especially for RCP 8.5. Historical and projected CC exceedance curves for TSS and TN (**Figure 4.5** and **Figure 4.6**, respectively) track very closely, except for small differences in mid-range events for both scenarios. In contrast, TP exhibits the largest difference between historical and projected (**Figure 4.7**). Results agree with our findings that TP and streamflow are more sensitive to CC than TN and TSS based on the larger difference between historical and projected streamflow and TP. Moreover, these results support the contention that CC be considered in designing and protecting urban stormwater systems to best address water quantity and quality impacts. Since Q10 is an indicator of high flows and nutrient loads, and there is larger difference between the historical and projected results at the 10% exceedance probability, the effects of CC should be considered for both flood risk analysis and water quality management.

4.3.4 Performance of retention ponds SCMs for projected CC scenarios

To better understand the differences in effectiveness of retention ponds in removing pollutants for two RCPs by employing five climate models, boxplots for removal efficiency were presented in the **Figure 4.8** for TSS, TN, and TP, respectively.

<THIS SPACE LEFT INTENTIONALLY BLANK>

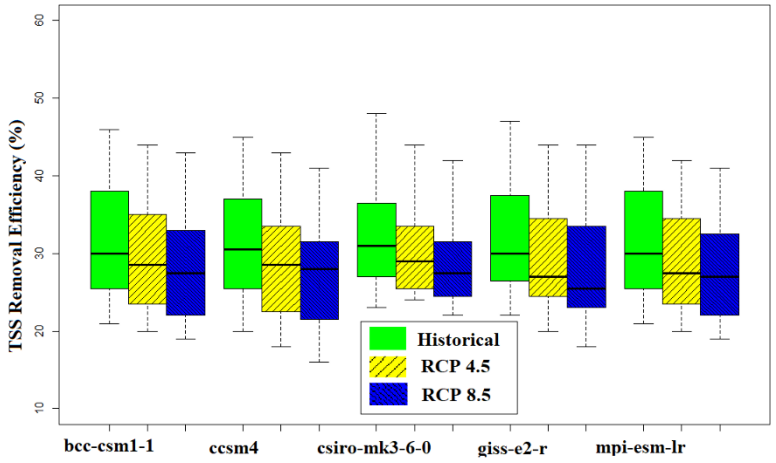

(a)

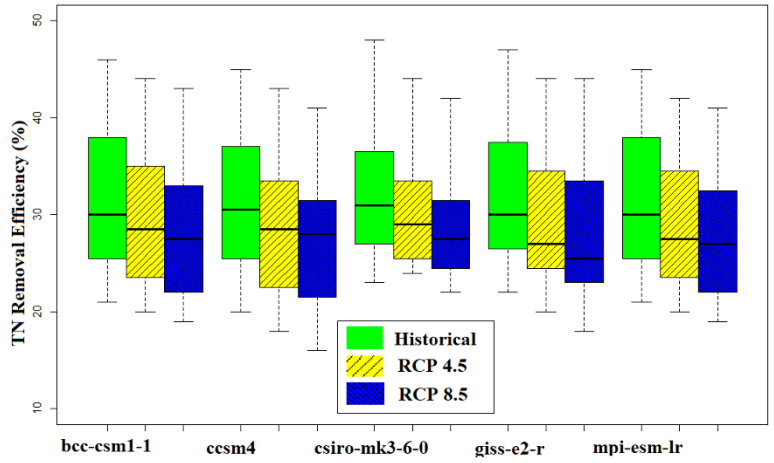

(b)

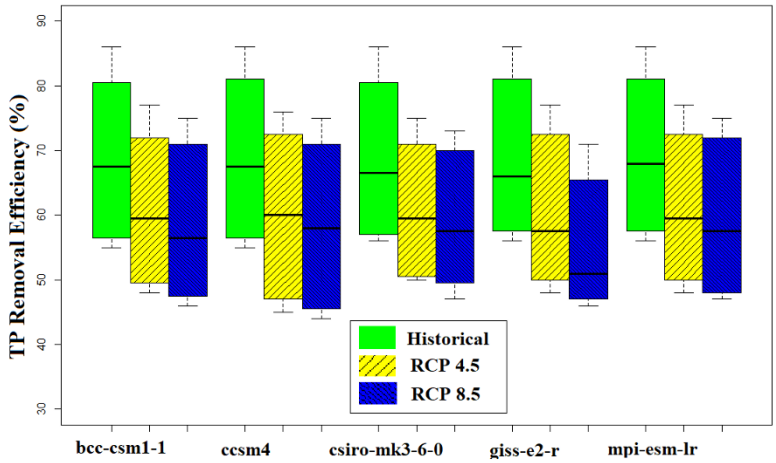

(c)

Figure 4.8. Removal efficiency of retention ponds for (a) TSS, (b) TN, (c) TP.

The approximately 900 retention ponds in the Difficult Run watershed were aggregated to 9 virtual ponds for simplicity of analysis. These composite retention ponds were modeled as storage nodes in the SWMM to evaluate their effectiveness in removing TSS, TN, and TP loads for projected CC conditions. As stated previously, pollutant loads in the inlet and outlet of the ponds were determined using EMC washoff loading and treatment functions for retention ponds. Treatment functions were developed based upon the assumption of irreducible concentration. For the RCP 4.5 scenario, the changes in removal efficiency of the retention ponds between the historical and projected CC conditions was relatively moderate for TSS and TN loads, i.e. removal efficiency decreases were less than 10%, however, the efficiency of retention ponds for TP was reduced by more than 10%. Projections for RCP 4.5 indicated that the changes to TSS, TN, and TP loads removal efficiency range from -5% to -8% with the median of -6%, -6% to -8% with the median of -7%, and -10% to -12% with the median of -11%, respectively. For RCP 8.5 scenario, the reduction in treatment efficiency of retention ponds was higher than that for RCP 4.5 for all models and pollutants. Simulation results for RCP 8.5 indicated that the changes to TSS, TN, and TP loads treatment efficiency ranged from -10% to -13% with the median of -11%, -11% to -13% with the median of -12%, and -14% to -19% with the median of -17%, respectively. The median TSS load removal efficiency of 9 ponds for historical, RCP 4.5, and RCP 8.5 were 29.6%, 27.8%, 26.3%, respectively. The median TN load removal efficiency of the pond for historical, RCP 4.5, and RCP 8.5 were 30.1%, 28%, 26.5%, respectively. The median TP load removal efficiency of the pond for historical, RCP 4.5, and RCP 8.5 were 68.7%, 61.1%, 57.1%, respectively.

As CC caused an increase in TSS, TN, and TP loadings into the retention ponds, their treatment effectiveness may be reduced in comparison with current conditions. Removal of TSS, TN and TP depends mainly on the depth of water and HRT, with longer HRT leading to higher removal rates. High flows may disrupt the settling velocity and HRT during extreme conditions. Given the increase in overall precipitation for all scenarios, especially RCP 8.5, it is logical that larger amount of precipitation would overwhelm the design storage capacities of retention ponds in the watershed, leading to untreated overflows, consistent with Sharma et al. (2016). In the face of non-stationarity, the impacts of CC on urban infrastructure, such as retention ponds, are a concern.

Analysis of seasonal variations as shown in **Figure 4.2** and **Figure 4.3** indicated that the seasonal change should be considered for analysis of relevant changes in the efficiency of these SCMs on the time span that such changes occur. The negative impacts may be observed during the winter where precipitation and flow are high and may significantly contribute to the export of nutrients, sediment and, potentially other pollutants. Several studies have found the lower performance of the retention ponds during winter and spring as a result of ice cover and snowmelt which may lead to reduce retention time and settling velocity, strong stratification, and reduced vertical mixing (Anderson et al., 2002; Marsalek et al., 2003; Oberts, 2003; Roseen et al., 2009). These conditions may reduce the effective storage capacity, and biological activity of the retention pond (Semadeni-Davies, 2006) which means the need for additional storage to meet the minimum performance expectations for projected CC scenarios, costing significantly more.

The reduction in pollutant removal efficiency of retention ponds in the Difficult Run watershed due to CC is of particular concern (Semadeni-Davies, 2012) when considered in the context of regional water quality management strategies. The case study watershed is part of the greater Chesapeake Bay watershed, where significant efforts are underway to reduced pollutant loads, protecting the estuary from eutrophication. Projections indicate that due to CC, discharge loadings will increase; P loading is even more sensitive than sediment and nitrogen. Additional storage and other design improvements will be needed to compensate for the reduced treatment efficiency if water quality objectives of the TMDL are to be met.

4.4 Summary and Conclusions

SWMM was used to simulate rainfall-runoff and streamflow for an urban watershed. The impacts of CC on streamflow and pollutant loads in the watershed were assessed using downscaled precipitation and temperature data from five CMIP5 GCMs. The downscaled GCMs were then used to force the SWMM model. Treatment efficiency of retention ponds within the watershed for TSS, TN, and TP was evaluated. Two CC scenarios, RCP 4.5 and RCP 8.5, and a historical scenario were utilized in this study, allowing an analysis of retention pond treatment performance for two scenarios. Median annual and seasonal precipitation, temperature, streamflow, TSS, TN, and TP are predicted to increase for both RCP scenarios. Analysis of seasonal variability indicated that for both RCP scenarios, winter was associated with the largest increase in precipitation, streamflow, and pollutant loads; and summer was associated with the largest increase in temperature. Statistically, only projected TP loads and streamflow were

significantly different than historical trends; indicating that streamflow and TP may be more sensitive to CC than TSS and TN. Increased TSS, TN, and TP influent loadings and higher inflows may result in reduced treatment effectiveness of retention ponds, especially for TP loads. These results should be considered as an estimate of the minimum reduction due to the necessity of using EMCs for runoff quality, limiting within storm variability. Given the increase in overall precipitation for all scenarios, especially RCP 8.5, it follows that the resulting increased runoff may overwhelm the storage capacities of retention ponds in the watershed, as these systems were designed for historical conditions with no consideration of CC. Additional storage and routing structures may be needed to compensate for these reductions in treatment efficiencies, albeit at additional cost.

The case study watershed is part of the Chesapeake Bay watershed, within which significant efforts are being made to reduce sediment and nutrient loads to restore water quality in the estuary. CC appears to work in tandem with urbanization, increasing runoff and pollutant loads, causing a reduction in treatment efficiency of SCMs such as retention ponds. Since SCMs are one of the main tools used in urban areas to achieve Chesapeake Bay restoration goals, reductions in their effectiveness will need to be addressed, diverting resources from other problem areas. Robust methods for predicting the effects of CC on water quantity, quality and SCM treatment performance at the watershed scale are needed to develop climate resilient strategies that meet water quality goals. The methodology presented in this paper are an initial step in the development of a general method to achieve this.

Limitation of this study stems from the uncertainty associated with the assumptions in the future emission of greenhouse gases, climate models, and calibrated parameters within the hydrologic model. Use of the EMC approach captured annual mass loading, however, it may underestimate within storm variability in concentrations due to its inherent limitations. Future research can address some of these issues by collection of additional within-storm monitoring data in the CB watershed for various land uses. A full assessment of analysis of uncertainty is also recommended.

References from Chapter 4:

Aguilar, M.F., Dymond, R.L., 2016. Evaluation of Variability in Response to the NPDES Phase II Stormwater Program in Virginia. Journal of Sustainable Water in the Built Environment 2(1), 04015006.

Alamdari, N., Sample, D.J., Steinberg, P., Ross, A.C., Easton, Z.M., 2017. Assessing the Effects of Climate Change on Water Quantity and Quality in an Urban Watershed Using a Calibrated Stormwater Model. Water 9(7), 464.
Alberti, M., Booth, D., Hill, K., Coburn, B., Avolio, C., Coe, S., Spirandelli, D., 2007. The Impact of Urban Patterns on Aquatic Ecosystems: An Empirical Analysis in Puget Lowland Sub-Basins. Landscape and Urban Planning 80(4), 345-361.
Anderson, B., Watt, W., Marsalek, J., 2002. Critical issues for stormwater ponds: learning from a decade of research. Water Science and Technology 45(9), 277-283.
Balascio, C.C., Lucas, W.C., 2009. A Survey of Storm-Water Management Water Quality Regulations in Four Mid-Atlantic States. Journal of Environmental Management 90(1), 1-7.
Bosch, N.S., Evans, M.A., Scavia, D., Allan, J.D., 2014. Interacting Effects of Climate Change and Agricultural Bmps on Nutrient Runoff Entering Lake Erie. Journal of Great Lakes Research 40(3), 581-589.
Butcher, J.B., 2003. Buildup, Washoff, and Event Mean Concentrations. JAWRA Journal of the American Water Resources Association 39(6), 1521-1528.
Chang, H., Evans, B.M., Easterling, D.R., 2001. The effects of climate change on stream flow and nutrient loading. JAWRA Journal of the American Water Resources Association 37(4), 973-985.
Charbeneau, R.J., Barrett, M.E., 1998. Evaluation of methods for estimating stormwater pollutant loads. Water Environment Research 70(7), 1295-1302.
Dent, S., Hanna, R.B., Wright, L., 2004. Automated Calibration Using Optimization Techniques with Swmmrunoff. Journal of Water Management Modeling 220, 385-408.
Drake Jr, A., Lee, K., 1989. Geologic Map of the Vienna Quadrangle, Fairfax County, Virginia, and Montgomery County, Maryland.
Eghdamirad, S., Johnson, F., Sharma, A., 2017. How reliable are GCM simulations for different atmospheric variables? Climatic Change.
Fairfax County, 2007. Difficult Run Watershed Management Plan.
Fletcher, T.D., Andrieu, H., Hamel, P., 2013. Understanding, management and modelling of urban hydrology and its consequences for receiving waters: A state of the art. Advances in Water Resources 51(0), 261-279.
Gao, H., Tang, Q., Shi, X., Zhu, C., Bohn, T., Su, F., Sheffield, J., Pan, M., Lettenmaier, D., Wood, E.F., 2010. Water Budget Record from Variable Infiltration Capacity (Vic) Model. Algorithm Theoretical Basis Document for Terrestrial Water Cycle Data Records.
Groisman, P.Y., Knight, R.W., Karl, T.R., Easterling, D.R., Sun, B., Lawrimore, J.H., 2004. Contemporary changes of the hydrological cycle over the contiguous United States: Trends derived from in situ observations. Journal of hydrometeorology 5(1), 64-85.
Gupta, H.V., Sorooshian, S., Yapo, P.O., 1999. Status of Automatic Calibration for Hydrologic Models: Comparison with Multilevel Expert Calibration. Journal of Hydrologic Engineering 4(2), 135-143.
Hathaway, J., Brown, R., Fu, J., Hunt, W., 2014. Bioretention Function under Climate Change Scenarios in North Carolina, USA. Journal of Hydrology 519, 503-511.
Hatt, B.E., Fletcher, T.D., Walsh, C.J., Taylor, S.L., 2004. The Influence of Urban Density and Drainage Infrastructure on the Concentrations and Loads of Pollutants in Small Streams. Environmental Management 34(1), 112-124.

Hayhoe, K., Wake, C., Anderson, B., Liang, X.-Z., Maurer, E., Zhu, J., Bradbury, J., DeGaetano, A., Stoner, A., Wuebbles, D., 2008. Regional Climate Change Projections for the Northeast USA. Mitig Adapt Strateg Glob Change 13(5-6), 425-436.
Hayhoe, K., Wake, C.P., Huntington, T.G., Luo, L., Schwartz, M.D., Sheffield, J., Wood, E., Anderson, B., Bradbury, J., DeGaetano, A., 2007. Past and future changes in climate and hydrological indicators in the US Northeast. Climate Dynamics 28(4), 381-407.
Hirschman, D., Collins, K., Schueler, T., 2008. Technical Memorandum: The Runoff Reduction Method. Center for Watershed Protection & Chesapeake Stormwater Network.
Howarth, R., Swaney, D., Boyer, E., Marino, R., Jaworski, N., Goodale, C., 2006. The Influence of Climate on Average Nitrogen Export from Large Watersheds in the Northeastern United States, Nitrogen Cycling in the Americas: Natural and Anthropogenic Influences and Controls. Springer, pp. 163-186.
Huber, W.C., Dickinson, R.E., Rosener, L.A., Aldrich, J.A., 1988. Stormwater Management Model User's Manual, Version 4. U.S. Environmental Protection Agency, Athens, GA.
Imteaz, M.A., Shanableh, A., Rahman, A., Ahsan, A., 2011. Optimisation of rainwater tank design from large roofs: A case study in Melbourne, Australia. Resources, Conservation and Recycling 55(11), 1022-1029.
Imteaz, M.A., Uddameri, V., Ahsan, A., 2016. Numerical Model for the Transport and Degradation of Pollutants through Wetlands. International Journal of Water 10(1), 1-12.
IPCC, 2014. Climate Change 2014–Impacts, Adaptation and Vulnerability: Regional Aspects. Cambridge University Press.
Jacobson, C.R., 2011. Identification and quantification of the hydrological impacts of imperviousness in urban catchments: A review. Journal of Environmental Management 92(6), 1438-1448.
James, W., James, R., 1998. Users Guide to Swmm4 Runoff and Supporting Modules-Hydrology. Computational Hydraulics International, Guelph, Ontario.
James, W., Rossman, L.A., James, W.R.C., 2010. User's Guide to Swmm 5 Computational Hydraulics International, Guelph, Ontario, Canada.
Jennings, D.B., Jarnagin, S.T., 2002. Changes in Anthropogenic Impervious Surfaces, Precipitation and Daily Streamflow Discharge: A Historical Perspective in a Mid-Atlantic Subwatershed. Landscape Ecology 17(5), 471.
Johnson, R., Sample, D., 2017. A Semi-Distributed Model for Locating Stormwater Best Management Practices in Coastal Environments. Environmental Modelling & Software 91, 70-86.
Kaushal, S.S., Belt, K.T., 2012. The Urban Watershed Continuum: Evolving Spatial and Temporal Dimensions. Urban Ecosystems 15(2), 409-435.
Krysanova, V., Vetter, T., Eisner, S., Huang, S., Pechlivanidis, I., Strauch, M., Gelfan, A., Kumar, R., Aich, V., Arheimer, B., 2017. Intercomparison of regional-scale hydrological models and climate change impacts projected for 12 large river basins worldwide—a synthesis. Environmental Research Letters 12(10), 105002.
Lee, T.M., Jetz, W., 2008. Future battlegrounds for conservation under global change. Proceedings of the Royal Society of London B: Biological Sciences 275(1640), 1261-1270.
Lee, Y.J., Boynton, W.R., Li, M., Li, Y., 2013. Role of Late Winter–Spring Wind Influencing Summer Hypoxia in Chesapeake Bay. Estuaries and Coasts 36(4), 683-696.

Li, H., Sheffield, J., Wood, E.F., 2010. Bias Correction of Monthly Precipitation and Temperature Fields from Intergovernmental Panel on Climate Change Ar4 Models Using Equidistant Quantile Matching. Journal of Geophysical Research: Atmospheres 115(D10).
Marsalek, P., Watt, W., Marsalek, J., Anderson, B., 2003. Winter operation of an on-stream stormwater management pond. Water science and technology 48(9), 133-143.
Mishra, V., Lettenmaier, D.P., 2011. Climatic Trends in Major U.S. Urban Areas, 1950–2009. Geophysical Research Letters 38(16), L16401.
Moore, M.V., Pace, M.L., Mather, J.R., Murdoch, P.S., Howarth, R.W., Folt, C.L., Chen, C.Y., Hemond, H.F., Flebbe, P.A., Driscoll, C.T., 1997. Potential effects of climate change on freshwater ecosystems of the New England/Mid-Atlantic Region. Hydrological processes 11(8), 925-947.
Moss, R.H., Edmonds, J.A., Hibbard, K.A., Manning, M.R., Rose, S.K., Van Vuuren, D.P., Carter, T.R., Emori, S., Kainuma, M., Kram, T., 2010. The Next Generation of Scenarios for Climate Change Research and Assessment. Nature 463(7282), 747.
Najjar, R., Patterson, L., Graham, S., 2009. Climate Simulations of Major Estuarine Watersheds in the Mid-Atlantic Region of the Us. Climatic Change 95(1-2), 139-168.
Najjar, R.G., Pyke, C.R., Adams, M.B., Breitburg, D., Hershner, C., Kemp, M., Howarth, R., Mulholland, M.R., Paolisso, M., Secor, D., Sellner, K., Wardrop, D., Wood, R., 2010. Potential Climate-Change Impacts on the Chesapeake Bay. Estuarine, Coastal and Shelf Science 86(1), 1-20.
Nakićenović, N., Swart, R., 2000. Special Report on Emission Scenarios. Intergovernmental Panel on Climate Change.
Nash, J.E., Sutcliffe, J.V., 1970. River Flow Forecasting through Conceptual Models Part I — a Discussion of Principles. Journal of Hydrology 10(3), 282-290.
National Research Council, 2000. Clean Coastal Waters: Understanding and Reducing the Effects of Nutrient Pollution. National Academies Press.
Natural Resources Conservation Service (NRCS), 2015, http://websoilsurvey.nrcs.usda.gov/ Web Soil Survey.
Neff, R., Chang, H., Knight, C.G., Najjar, R.G., Yarnal, B., Walker, H.A., 2000. Impact of climate variation and change on Mid-Atlantic Region hydrology and water resources. Climate Research 14(3), 207-218.
Nelson, E.J., Booth, D.B., 2002. Sediment Sources in an Urbanizing, Mixed Land-Use Watershed. Journal of Hydrology 264(1–4), 51-68.
Oberts, G., 2003. Cold climate BMPs: Solving the management puzzle. Water Science and Technology 48(9), 21-32.
Pachauri, R.K., Allen, M.R., Barros, V.R., Broome, J., Cramer, W., Christ, R., Church, J.A., Clarke, L., Dahe, Q., Dasgupta, P., 2014. Climate Change 2014: Synthesis Report. Contribution of Working Groups I, Ii and Iii to the Fifth Assessment Report of the Intergovernmental Panel on Climate Change. IPCC.
Pierce, D.W., Cayan, D.R., Maurer, E.P., Abatzoglou, J.T., Hegewisch, K.C., 2015. Improved Bias Correction Techniques for Hydrological Simulations of Climate Change. Journal of Hydrometeorology 16(6), 2421-2442.
Pierce, D.W., Cayan, D.R., Thrasher, B.L., 2014. Statistical Downscaling Using Localized Constructed Analogs (Loca). Journal of Hydrometeorology 15(6), 2558-2585.
Pitt, R., Maestre, A., Morquecho, R., 2004. The National Stormwater Quality Database (Nsqd, Version 1.1), 1st Annual Stormwater Management Research Symposium Proceedings. pp. 13-51.

Power, S., Sadler, B., Nicholls, N., 2005. The Influence of Climate Science on Water Management in Western Australia: Lessons for Climate Scientists. Bulletin of the American Meteorological Society 86(6), 839-844.
Pyke, C., Warren, M.P., Johnson, T., LaGro, J., Scharfenberg, J., Groth, P., Freed, R., Schroeer, W., Main, E., 2011. Assessment of Low Impact Development for Managing Stormwater with Changing Precipitation Due to Climate Change. Landscape and Urban Planning 103(2), 166-173.
Roseen, R.M., Ballestero, T.P., Houle, J.J., Avellaneda, P., Briggs, J., Fowler, G., Wildey, R., 2009. Seasonal performance variations for storm-water management systems in cold climate conditions. Journal of Environmental Engineering 135(3), 128-137.
Rossman, L., 2015. Storm Water Management Model Reference Manual: Volume I–Hydrology. Us Envrionmental Protection Agency, Office of Research and Developement, National Risk Management Laboratory, Cincinnati, Oh 45268.
Rossman, L.A., 2004. Storm Water Management Model User's Manual, Version 5.0, in: U.S. Environmental Protection Agency (Ed.). Cincinatti, OH.
Saft, M., Western, A.W., Zhang, L., Peel, M.C., Potter, N.J., 2015. The influence of multiyear drought on the annual rainfall-runoff relationship: An Australian perspective. Water Resources Research 51(4), 2444-2463.
Sage, J., Bonhomme, C., Al Ali, S., Gromaire, M.-C., 2015. Performance Assessment of a Commonly Used "Accumulation and Wash-Off" Model from Long-Term Continuous Road Runoff Turbidity Measurements. Water Research 78, 47-59.
Sample, D., Lucas, W.L., Janeski, T., Roseen, R.M., Powers, D., Freeborn, J., Fox, L.J., 2014. Greening Richmond, USA: a sustainable urban drainage demonstration project. Proceedings of the Institution of Civil Engineers, Civil Engineering 167(CE2), 88-95.
Sample, D.J., Grizzard, T.J., Sansalone, J., Davis, A.P., Roseen, R.M., Walker, J., 2012. Assessing Performance of Manufactured Treatment Devices for the Removal of Phosphorus from Urban Stormwater. Journal of Environmental Management 113, 279-291.
Sansalone, J.J., Buchberger, S.G., 1997. Partitioning and First Flush of Metals in Urban Roadway Storm Water. Journal of Environmental Engineering 123(2), 134-143.
Schueler, T., 2011. Nutrient Accounting Methods to Document Local Stormwater Load Reductions in the Chesapeake Bay Watershed. Technical Bulletin 9.
Schueler, T., Fraley-McNeal, L., Cappiella, K., 2009. Is Impervious Cover Still Important? Review of Recent Research. Journal of Hydrologic Engineering 14(4), 309-315.
Schwartz, D., Sample, D.J., Grizzard, T.J., 2017. Evaluating the performance of a retrofitted stormwater wet pond for treatment of urban runoff. Environmental Monitoring and Assessment 189(6), 256.
Scully, M.E., 2010. The Importance of Climate Variability to Wind-Driven Modulation of Hypoxia in Chesapeake Bay. Journal of Physical Oceanography 40(6), 1435-1440.
Semadeni-Davies, A., 2012. Implications of climate and urban development on the design of sustainable urban drainage systems (SUDS). Journal of Water and Climate Change 3(4), 239-256.
Semadeni-Davies, A., Hernebring, C., Svensson, G., Gustafsson, L.-G., 2008. The Impacts of Climate Change and Urbanisation on Drainage in Helsingborg, Sweden: Combined Sewer System. Journal of Hydrology 350(1), 100-113.
Semadeni-Davies, A., 2006. Winter Performance of an Urban Stormwater Pond in Southern Sweden. Hydrological Processes 20(1), 165-182.

Shapiro, S.S., Wilk, M.B., 1965. An Analysis of Variance Test for Normality (Complete Samples). Biometrika 52(3-4), 591-611.
Sharma, A.K., Vezzaro, L., Birch, H., Arnbjerg-Nielsen, K., Mikkelsen, P.S., 2016. Effect of Climate Change on Stormwater Runoff Characteristics and Treatment Efficiencies of Stormwater Retention Ponds: A Case Study from Denmark Using Tss and Cu as Indicator Pollutants. Springerplus 5(1), 1984.
Sheffield, J., Barrett, A.P., Colle, B., Nelun Fernando, D., Fu, R., Geil, K.L., Hu, Q., Kinter, J., Kumar, S., Langenbrunner, B., 2013. North American Climate in Cmip5 Experiments. Part I: Evaluation of Historical Simulations of Continental and Regional Climatology. Journal of Climate 26(23), 9209-9245.
Suddick, E.C., Whitney, P., Townsend, A.R., Davidson, E.A., 2013. The role of nitrogen in climate change and the impacts of nitrogen–climate interactions in the United States: foreword to thematic issue. Biogeochemistry 114(1-3), 1-10.
Taylor, K.E., Stouffer, R.J., Meehl, G.A., 2012. An overview of CMIP5 and the experiment design. Bulletin of the American Meteorological Society 93(4), 485-498.
USEPA, 1983. Results of the Nationwide Urban Runoff Program. Water Planning Division Washington, DC.
USEPA, 2010a. Chesapeake Bay Total Maximum Daily Load for Nitrogen, Phosphorus, and Sediment. Annapolis, MD: US Environmental Protection Agency, Chesapeake Bay Program Office. Also Available at http://www. epa. gov/reg3wapd/tmdl/ChesapeakeBay/tmdlexec. html.
USEPA, 2010b. Guidance for Federal Land Management in the Chesapeake Bay Watershed. Chapter 3. Urban and Suburban
van Dijk, A.I.J.M., Beck, H.E., Crosbie, R.S., de Jeu, R.A.M., Liu, Y.Y., Podger, G.M., Timbal, B., Viney, N.R., 2013. The Millennium Drought in southeast Australia (2001–2009): Natural and human causes and implications for water resources, ecosystems, economy, and society. Water Resources Research 49(2), 1040-1057.
Vollertsen, J., Åstebøl, S.O., Coward, J.E., Fageraas, T., Madsen, H.I., Hvitved-Jacobsen, T., Nielsen, A., 2007. Monitoring and Modelling the Performance of a Wet Pond for Treatment of Highway Runoff in Cold Climates, Highway and Urban Environment. Springer, pp. 499-509.
Walsh, C.J., Allison, H.R., Feminella, J.W., Cottingham, P.D., Groffman, P.M., Ii, R.P.M., 2005. The urban stream syndrome: current knowledge and the search for a cure. Journal of the North American Benthological Society 24(3), 706-723.
Walsh, C.J., Fletcher, T.D., Burns, M.J., 2012. Urban Stormwater Runoff: A New Class of Environmental Flow Problem. Plos One 7(9), e45814.
Zhang, Q., Brady, D.C., Ball, W.P., 2013. Long-Term Seasonal Trends of Nitrogen, Phosphorus, and Suspended Sediment Load from the Non-Tidal Susquehanna River Basin to Chesapeake Bay. Science of the Total Environment 452, 208-221.

Chapter 5. Assessing Climate Change Impacts on the Reliability of Rainwater Harvesting Systems.

Taken from:
Alamdari N, Sample DJ, Liu J, Ross A (2018) Assessing climate change impacts on the reliability of rainwater harvesting systems. *Resources, Conservation and Recycling* 132, 178-189.
Alamdari N, Sample DJ, Liu J, Ross A (2018) Water supply and runoff capture reliability curves for hypothetical rainwater harvesting systems for locations across the U.S. For historical and projected climate conditions. *Data in Brief.*

Abstract

Rainwater harvesting (RWH) systems recycle runoff, increasing the sustainability of water supplies; they may also reduce runoff discharges, and thus help meet water quality objectives. RWH systems receive runoff and thus will likely be impacted by changes in rainfall induced by climate change (CC). In this paper, we assess CC impacts on RWH with respect to the reliability of water supply, defined as the proportion of demands that are met; and the reliability of runoff capture, defined as the amount stored and reused, but not spilled. Hypothetical RWH systems with varying storage, rooftop catchments, irrigated areas, and indoor water demand for 17 locations across the U.S. were simulated for historical (1971-1998) and projected (2041-2068) periods using downscaled climate model data assuming future medium-high greenhouse gas emissions. The largest changes in runoff capture reliability would occur in Chicago (-12.4%) and Los Angeles (+12.3%), respectively. The largest change in water supply reliability would occur in Miami (+22.0%) and Los Angeles (-17.9%), respectively. The effectiveness of RWH systems for runoff capture is likely to be reduced in the eastern, northwestern, and southeastern U.S. Conversely, for most locations in the western, southern, and central U.S., RWH systems are expected to become less effective for water supply purposes. The additional storage needed to compensate for these reductions in water supply and/or runoff capture benefits was estimated. The results of this study can be used to design more resilient RWH systems with respect to CC, and thus maximize the dual objectives of RWH.

Keywords: rainwater harvesting, climate change (CC), resiliency, modeling water supply reliability, runoff capture reliability.

5.1 Introduction

The impacts of CO_2 and other greenhouse gas (GHG) production and their effects on the magnitude and variability of the world's climate are well established. GHG emissions increase longwave radiation, resulting in an expected mean surface temperature increase between 1.1 to 6.4 °C. by 2100 (IPCC, 2014). Historical evaluation of the U.S. climate (1950-2009) indicates that significant temperature increases for nearly all U.S. cities are likely, and extreme precipitation increases may occur in one third of them due to climate change (CC) (Mishra and Lettenmaier (2011). Various regional assessments of CC are available, e.g., the Northeast (Hayhoe et al., 2008), the Central U.S. (Hayhoe et al., 2010), and the mid-Atlantic (Najjar et al., 2010). The uncertainty introduced by CC undermines stationarity, the fundamental principle upon which most place-based hydrologic assessments are conducted for infrastructure design (Milly et al., 2008). Milly et al. (2008) and Yang (2010) suggests that, while there are many downsides to the demise of stationarity, perhaps the only upside may be the opportunity to improve the resiliency of urban infrastructure.

Virtually all infrastructure, because it is downgradient and must accommodate runoff impacted by CC, is potentially at risk (Ahmadisharaf and Kalyanapu, 2015; Berggren et al., 2012; Mishra and Lettenmaier, 2011; Nilsen et al., 2011; Rosenberg et al., 2010). Increases in rainfall magnitude and intensity for anticipated CC are likely to cause infrastructure failures (Asadabadi and Miller-Hooks, 2017a, b; Semadeni-Davies et al., 2008; Zahmatkesh et al., 2014). Increased flooding of urban areas may result from CC and its impact on urban infrastructure, which will require significant financial resources to address (Giuffria Jonathon et al., 2017; Wright et al., 2012). Urban development increases imperviousness, resulting in large increases in the rate and volume of runoff, thus increasing the washoff of pollutants from the land into surface waters, resulting in streambank and stream channel erosion and degrading aquatic habitats. Urban development and CC are expected to work in tandem, increasing runoff, degrading streams, and increasing pollutant transport (Alamdari et al., 2017; Alberti et al., 2007; Hatt et al., 2004; Lee et al., 2013; Nelson and Booth, 2002; Schueler et al., 2009; Scully, 2010). There are ways to mitigate the impacts from urban development, and potentially CC, using stormwater control measures (SCMs), also known as best management practices (BMPs). Currently, SCM design focuses upon runoff capture and treatment, some are now able to mitigate CC impacts (Gill et al., 2007; Pyke et al., 2011).

Rainwater harvesting (RWH) has been used for millennia to meet water supply needs and has recently been repurposed as an SCM for managing runoff as a water quality protection measure (Alam et al., 2012; Kahinda et al., 2010; Lassaux et al., 2007; Steffen et al., 2013; Tam et al., 2010). RWH systems store runoff from rooftops or other impervious areas for later use for outdoor irrigation or indoor nonpotable uses such as flushing toilets (Silva et al., 2015). A recent, comprehensive review of RWH is available in Campisano et al. (2017). By reusing stored rainfall instead of discharging it, RWH systems reduce runoff in addition to providing an alternative nonpotable water supply. Young et al. (2009) found that RWH systems could be designed to mimic the function of other SCMs such as sand filters, vegetated roofs, and porous pavement. In many older urban areas, drainage and sewage share a common conveyance, known as a combined sewer. Depending upon capacity, the combined sewer will overflow during moderate to heavy rainfall events, causing significant water quality degradation downstream (Even et al., 2007; Tavakol-Davani et al., 2016). Gold et al. (2010) found that RWH could reduce combined sewer overflows (CSOs) by reducing runoff and decreasing water withdrawals. Tavakol-Davani et al. (2015) found RWH was a cost-effective strategy for CSO control.

A variety of models have been used to simulate RWH and thus potentially help in assessing its benefits. Basinger et al. (2010) developed the Storage and Reliability Estimation Tool (SARET) and used it to simulate RWH reliability and yield. The model was used to size RWH systems to supply flush low flow toilets within a Bronx, New York, U.S. Reductions in runoff volume and nonpotable water demand were predicted to be 28% and 53%, respectively. Ghisi (2010) developed a RWH model and applied it to three cities in Sao Paulo State, Brazil. The authors found that site-specific studies must be performed to consider local rainfall patterns, roof area, and indoor and outdoor water demand to design a RWH system and quantify its benefits. Kim and Yoo (2009) assessed flood control and water supply with and without RWH using a hydrologic model, and found that, for a given urban area, if runoff from 10% of rooftops were diverted to RWH systems, floods would be reduced by 1%. Jensen et al. (2010) developed RWHTools, a daily mass balance model, and applied it to 20 cities in the U.S. to evaluate RWH with respect to the amount of runoff captured and water demand met. The authors found that these two objectives were complementary rather than competitive; however, for the same benefit that met both objectives, a significantly larger tank was often required for some locations and climates. Burian and Jones (2010) evaluated several installed RWH systems within North

Carolina, and found that they are often underutilized. The authors found that nonpotable uses such as toilet flushing may be essential to providing stormwater retention volume as this demand must be met irrespective of hydrologic conditions. Campisano and Modica (2012) determined the optimal size of domestic RWH tanks using the ratio of storage to rainfall multiplied by effective roof area. The authors found that this parameter, termed "storage fraction", generalized rainfall patterns and RWH system performance. The performance of rainwater tanks in Melbourne, Australia was evaluated and optimized using a spreadsheet based daily water balance model by Imteaz et al. (2013); Imteaz et al. (2012). A dry year, an average year, and a wet year was selected. Results indicated that 100% water supply reliability was not achieved for small roof sizes (less than or equal to 100 m^2), even with tanks as large as 10 m^3. Karim et al. (2015) evaluated the reliability and feasibility of the RWH systems in Dhaka City, Bangladesh by employing a daily water balance model and three climate scenarios including wet, average, and dry. The authors found an insignificant increase in the reliability of the RWH system beyond the tank volume of 30 m^3 for three scenarios. Sample et al. (2012) developed the Rainwater Analysis and Simulation Program (RASP) and applied it to assess the dual benefits of water supply and runoff capture reliability of RWH implementation in Richmond, Virginia using tradeoff curves. A key finding of this study was that some input variables were interchangeable if reliability was held constant.

RWH was found to be an effective water supply adaptation strategy for mitigating CC effects, particularly in areas with high water demand (Aladenola and Adeboye, 2010; Boelee et al., 2013; Kahinda et al., 2010; Mukheibir, 2008; Pandey et al., 2003; Rozos et al., 2009). Youn et al. (2012) found that, due to CC, the effective storage capacity of RWH systems in Korea would likely be reduced. Similar results were found by Lash et al. (2014) for the U.K. who used a statistical analysis of projected rainfall for an assessment of CC. Lo and Koralegedara (2015) evaluated the effects of CC on urban RWH in Colombo City, Sri Lanka, and found that residential RWH systems would likely be more affected by CC than non-residential systems. Palla et al. (2012) assessed the performance of domestic RWH systems across Europe with respect to optimal design for CC. Results indicated that the duration of antecedent dry conditions was strongly correlated with RWH system behavior, while event rainfall depth, intensity and duration were weakly correlated. Haque et al. (2016) evaluated the impact of CC on the performance of a residential RWH using a daily water balance model at five locations in the

Greater Sydney region, Australia. As a result of CC, precipitation is anticipated to be reduced, and duration between events increased. The authors found that, for a 3 kL tank, water savings would be reduced between 2-14%. Water supply reliability was found to be reduced between 3-16%, and the number of days the tank would be completely empty is projected to be increased from 8% to 12%. CC impacts on RWH are likely to be greater in the dry season than wet. In contrast, Almazroui et al. (2017) found that in Wadi Al-Lith, Saudi Arabia, CC would likely result in increased precipitation and duration, increasing the feasibility of RWH. The effects of both CC and El Niño on rainfall patterns on the capacity of RWH in Jamaica were evaluated by Aladenola et al. (2016). Results indicated that the higher variability is projected to occur due to CC, however extremely dry years resulting from El Niño (such as occurred in years 1997 and 2009) appear to be more influential; with the caveat that the impact of CC on El Niño patterns is unknown. RWH effectiveness is projected to be reduced, resulting in an increase in the recommended tank size to 4.0 m^3. These studies demonstrate the need for analysis of CC conditions to improve the resilience of RWH systems. The Storm Water Management Model (SWMM) was used in combination with downscaled Coupled Model Intercomparison Project Phase 5 (CMIP5) projections by Tavakol-Davani et al. (2016). SWMM is a commonly used hydrologic and water quality model that can perform both single event and continuous simulations of urban watersheds (Ahmadisharaf et al., 2015; Alamdari, 2016; Huber et al., 1988; James et al., 2010; Rossman, 2004). CMIP5 which is the most current of the CMIPs, is a framework for studying global coupled ocean-atmosphere general circulation models (Brekke et al., 2013). The authors found that RWH increased resilience of urban stormwater infrastructure to CC by limiting CSOs. Downscaling bridges the mismatch between the spatial and temporal resolution of GCMs and RCMs, and the resolution needed for urban hydrologic models which is a spatial resolution of at least 50-100 km^2 and a temporal resolution of at most an hour, respectively (Fowler and Wilby, 2007). RWH systems typically need a subdaily temporal scale to accurately address water supply and runoff capture benefits (Burian and Jones, 2010; Coombes and Barry, 2007; Coombes et al., 2002; Fewkes and Butler, 2000; Herrmann and Schmida, 2000; Sample and Heaney, 2006). The two primary downscaling methods include dynamical and statistical downscaling. Systematic errors due to simplified thermodynamic processes and numerical schemes are inevitable in RCM outputs and such errors can bias the results and should be corrected (Chen et al., 2013). Thus, bias correction is often a required step

after downscaling a dataset to a higher resolution. A variety of bias correction methods were assessed by Chen et al. (2013); (Gudmundsson et al., 2012; Lafon et al., 2013; Li et al., 2010; Rosenberg et al., 2010; Teutschbein and Seibert, 2012), which were found to be plausible by Wood et al. (2004). Recently, Wang and Chen (2014) developed a bias correction method using a modified version of an equiratio cumulative distribution function matching method, which corrects model data using multiplicative scaling factors and improves the equidistant approach in bias correction of precipitation. A modified version of this bias correction method was used for downscaling RCMs in this study.

In summary, while there have been a few studies that assessed the effects of CC on RWH systems, nearly all of these focused upon RWH as a water supply practice. Few studies exist that assessed CC impacts on runoff reduction. We found no studies that assessed the effects of CC on RWH systems with respect to water supply and runoff reduction as dual objectives, which is how RWH is currently being applied in the U.S. The objective of this paper is to address this research gap by comparing the water supply and runoff reduction performance of RWH systems with and without CC for multiple sites across the U.S. using the aforementioned RWH simulation model, RASP. Since current methods for incorporating CC are lacking; in this paper, we will focus upon developing a pilot methodology and applying it to assess RWH systems from selected locations across the U.S. using dynamically downscaled precipitation from a regional climate model, NARCCAP. Results of the simulations will be compared to evaluate the potential impacts of CC and the degree of resilience RWH systems may provide.

5.2 Materials and Methods

5.2.1 Study Area

To characterize a wide variety of RWH system operations with different climate characteristics, 17 locations across the U.S. were selected (**Figure 5.1**). Projections for rainfall across the U.S. from the North American Regional CC assessment program (NARCCAP) (Mearns et al., 2009) were used as inputs to the Rainwater Analysis and Simulation Program (RASP model), after downscaling for historical and projected conditions. Köppen-Geiger climate classifications (Kottek et al., 2006) for each site are listed in the **Table 5-1** for comparability with other studies. Sites were selected primarily for geographic diversity, not by climate class. Eight sites are located within the Cfa (Humid Subtropical) zone; three are located in the Dfa

(Humid Continental) zone, two are located in the Csa (Mediterranean) zone; two are located in the Bsl (Semiarid Steppe) zone; and one is located in Aw (Tropical wet/dry season) zone and another in the Cfb (Marine West Coast) zone.

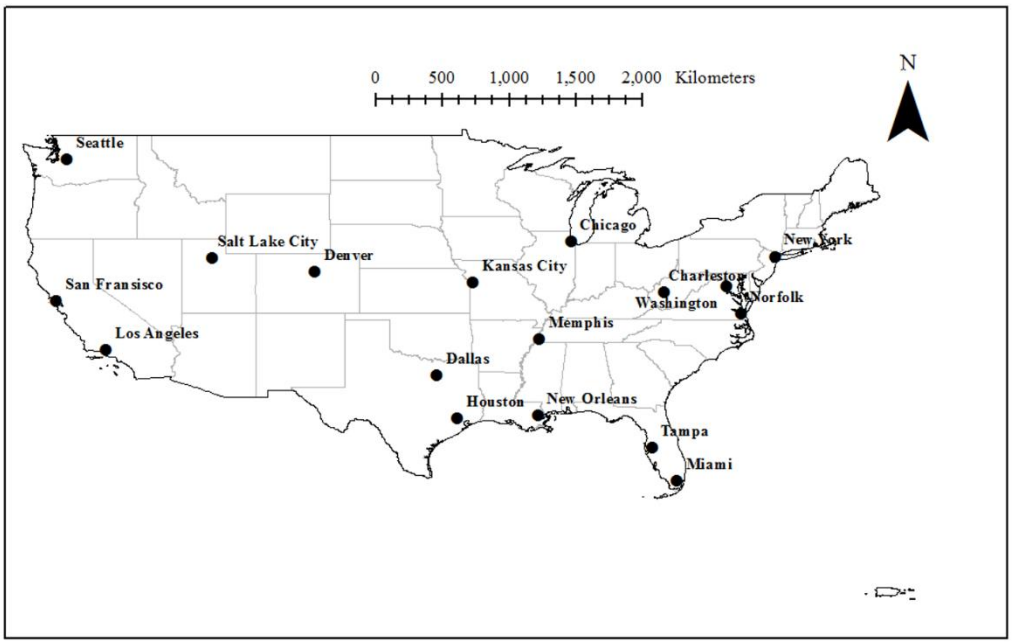

Figure 5.1. Selected sites across the U.S.

Table 5-1. Selected Weather Stations across the U.S.

City	Station	COOPID	Latitude/Longitude
Charleston	Charleston Airport, SC	381544	32.89 N/ 80.04W
Chicago	Chicago O'Hare Airport, IL	111549	41.98 N/ 87.84 W
Dallas	Fort Worth WSFO, TX	413285	32.77 N/ 97.31 W
Denver	Denver Airport, CO	052211	39.85 N/ 104.67 W
Houston	Houston Airport, TX	414300	29.99 N/ 95.34 W
Kansas City	Kansas City Airport, MO	234358	39.30 N/ 94.71 W
Los Angeles	Los Angeles Airport, CA	045114	33.94 N/ 118.41 W
Miami	Miami Airport, FL	085663	25.79 N/ 80.28 W
Memphis	Memphis Airport, TN	405954	35.04 N/ 89.98 W
New Orleans	New Orleans Airport, LA	166660	29.99 N/ 90.26 W
New York	JFK International Airport, NY	305803	40.64 N/ 73.78 W
Norfolk	Norfolk Airport, VA	446139	36.90 N/ 76.19 W
Salt Lake City	Salt Lake City Airport, UT	427598	40.79 N/ 111.98 W
San Francisco	San Francisco Airport, CA	047769	37.62 N/ 122.39 W
Seattle	Seattle Tacoma Airport, WA	457473	47.44 N/ 122.30 W
Tampa	Tampa Airport, FL	088788	27.98 N/ 82.54 W
Washington	Washington Reagan Airport, VA	448906	38.85 N/ 77.04 W

5.2.2 Frequency Analysis

Frequency analysis was used to characterize the long-term behavior of rainfall and dry duration at each site. Frequency analysis is often used as the first step in the design of stormwater SCMs to help understand local hydrological conditions and assess potential CC impacts on design. Frequency analysis was conducted on rainfall events and dry periods, or dry duration.

Historical and projected hourly precipitation data were processed into events using a 6-hr inter-event time. Frequency analysis of rainfall events was conducted by calculating the probability of exceedance by sorting the long-term rainfall depths from the largest to the smallest, then assigning a rank, *m*, to each value, calculating exceedance probability, *P* using the following equation:

$$P = \frac{M}{n+1} \times 100 \qquad (5\text{-}1)$$

Where *n* is the number of rainfall data values. Exceedance probability curves were plotted to compare the probability of storm events for historical and projected periods at each site. Frequency analysis of dry duration was performed in a similar manner. First, very small (≤2.54 mm) rainfall events were screened out. The time between consecutive rainfall events was calculated, and sorted into ranks, and a probability assigned (similar to the previous analysis for rainfall). The probability of dry duration for historical and projected periods at each site for each gap between storms was then compared. A MATLAB program was developed to assist in calculation and plotting results. More information on this method can be found in Liu et al. (2013).

5.2.3 Model Description

The main components of a RWH system include a storage tank, a roof catchment area, a filtration device and pumping. The RASP model code (Sample and Liu, 2014) was used to simulate performance of various RWH systems at the locations listed in **Table 5-1**. The RASP code is written in MATLAB and is available at no cost at https://github.com/RainwaterHarvesting/Rainwater-Analysis-and-Simulation-Program.

RASP uses rainfall data and user-selected design variables, which include tank storage volume, or *TankV*, roof area, or *RoofA*, irrigated area, or *IrArea*, and indoor demand or *POP*. RASP uses the yield before storage (YBS) algorithm adapted from Liaw et al. (2004), which is described in Equations 1 and 2.

$$Y_i = Min(D_i, S_{i-1}) \quad (5\text{-}2)$$

$$S_i = Min(S_{i-1} + Q_i - Y_i, TankV) \quad (5\text{-}3)$$

Where Y_i = Yield at time T $[m^3]$; D_i = Demand at time i $[m^3]$; S_i = Storage at time T $[m^3]$; and Q_i = Runoff inflow during time period T $[m^3]$, T is the time period of interest $[hr]$.

Water supply reliability, which is a dimensionless number ranging from 0 to 1 that reflects the ability of the RWH system to meet system demands is calculated in Equation 3:

$$\lambda_{WS} = \frac{\sum_{i=1}^{T} Y_i}{\sum_{i=1}^{T} D_i} \quad (5\text{-}4)$$

Where λ_{WS} = Volumetric reliability of water supply, dimensionless; Y_i = the sum of yield for entire record to time $T[m^3]$; and D_i = the sum of total demand for entire record to time $T[m^3]$. Runoff capture reliability is a dimensionless number ranging from 0 to 1 that reflects the ability of an RWH system to capture runoff, and is calculated in Equation 4:

$$\lambda_{RC} = 1 - \frac{\sum_{i=1}^{T} U_i}{\sum_{i=1}^{T} Q_i} \quad (5\text{-}5)$$

Where λ_{RC} = Volumetric reliability of runoff capture, dimensionless; and U_i = Spill during time period i $[m^3]$. The sum is the total spill to time $T[m^3]$.

In order to meet the nonpotable use and minimum tank reservation, a potential deficit volume is calculated using Equation 5:

$$De_i = D_i - S_i + R_e \quad (5\text{-}6)$$

Where De_i= Deficit volume at the hour of i $[m^3]$; and R_e = Reserve tank volume$[m^3]$. Reserve tank volume for this study is set to 10% to keep the pump primed and operational. Capacity of the storage to find if spill occurs, is calculated using Equation 6:

$$V_{i+1} = V_i + Q_i - U_j - D_{i+1} \quad (5\text{-}7)$$

Where U_j= Spilled volume at the hour of j ($j = i$, when spill is from dewater, $j = i + 1$, when spill is from overflow) $[m^3]$. When the capacity of the storage is full, a spill occurs. Outdoor irrigation demand was set at an amount of 25.4 mm/week for the months of April–September, and zero otherwise to maximize irrigation use. The reader is referred to Sample et al. (2013) for details on the equations, variable definitions, and limitations of the RASP model. RASP simulations were conducted for each of the 17 locations listed in **Table 5-1**. To evaluate

the behavior of a RWH system, the RASP program was designed to produce λ_{WS} and λ_{RC} for any combination of the four main input variables. Output from each simulation included a listing of the variables and the performance metrics, λ_{WS} and λ_{RC}. A series of tradeoff curves using four main design variables and the reliability metrics were then plotted for historical and projected conditions using contour plots.

5.2.4 Climate Modeling

A CC projection was developed using output from the North American Regional CC Assessment Program (NARCCAP). NARCCAP projections use dynamical downscaling with regional climate models (RCMs) with about 50 km^2 spatial resolution embedded into global climate models (GCMs). The period 1971-1998 was used for simulating historical conditions, and 2041-2068 for simulating projected conditions; it is expected that this latter period will be impacted by CC to a greater degree than the historical period. NARCCAP modeled precipitation was used as a source for the 1971-1998 period instead of direct measurements for comparability of results. The GCM uses historical greenhouse gas concentrations for the historical simulation and the medium-high greenhouse gas emissions scenario, A2 (Nakićenović and Swart, 2000), for the projected CC simulation. While the NARCCAP model performs reasonably well in the mid-Atlantic region and other regions, it may not be universal. The reader is cautioned that these results represent those of our pilot study only, and, while they may incorporate some anticipated trends, they are thus not absolute predictors of RWH performance with CC.

The NARCCAP model MM5I-CCSM was selected as the pilot scenario from the NARCCAP dataset. Biases in the model precipitation data that could affect the hydrological model simulations were corrected using quantile mapping with empirical quantiles (Boé et al., 2007; Gudmundsson et al., 2012). The historical (1971-1998) data were used to calibrate the correction algorithm to adjust for biases relative to observed precipitation data from the National Climatic Data Center, and the correction was applied to the historical and the projected periods. The bias correction algorithm included a step to set precipitation values below a small threshold to zero such that during the calibration period, the corrected model data has the same frequency of days with zero precipitation. NARCCAP provides model output at three-hourly intervals, and the output was resampled to daily intervals for the bias correction algorithm. A temporal disaggregation was then applied to convert the daily rainfall data to hourly frequency using a

method originally developed to create input data for the Variable Infiltration Capacity model (Gao et al., 2010).

5.3 Results and Discussions

5.3.1 Frequency Analysis

Average rainfall for the 17 sites in **Table 5-1** for historical and projected conditions was estimated and is provided in **Table 5-2**, and is shown as a percent change between historical and projected conditions in **Figure 5.2.** Annual precipitation changes comparing historical with projected conditions for selected locations across the U.S.. The regional climate model projects annual rainfall for Charleston, Chicago, Kansas City, Memphis, Miami, New York, Norfolk, Seattle, Tampa, and Washington to increase; the highest and lowest increases were in Chicago (18.6%) and Memphis (2.7%), respectively. In addition, annual rainfall was projected to decrease in Los Angeles, Houston, Denver, Dallas, New Orleans, Salt Lake City, and San Francisco; the highest and lowest decreases were projected in Los Angeles (15.3%) and Salt Lake City (3.0%), respectively.

<THIS SPACE LEFT INTENTIONALLY BLANK>

Table 5-2. Average Annual rainfall for selected locations across the U.S. for historical and projected conditions.

City	Average Annual Rainfall (Historical) (mm)	Average Annual Rainfall (Projected) (mm)
Charleston	1236	1314
Chicago	913	1083
Dallas	849	813
Denver	381	332
Houston	1220	1050
Kansas City	954	1004
Los Angeles	342	290
Memphis	1375	1412
Miami	1571	1816
New Orleans	1682	1557
New York	1078	1147
Norfolk	1122	1154
Salt Lake City	418	405
San Francisco	512	476
Seattle	936	1026
Tampa	1001	1151
Washington	1070	1137

<THIS SPACE LEFT INTENTIONALLY BLANK>

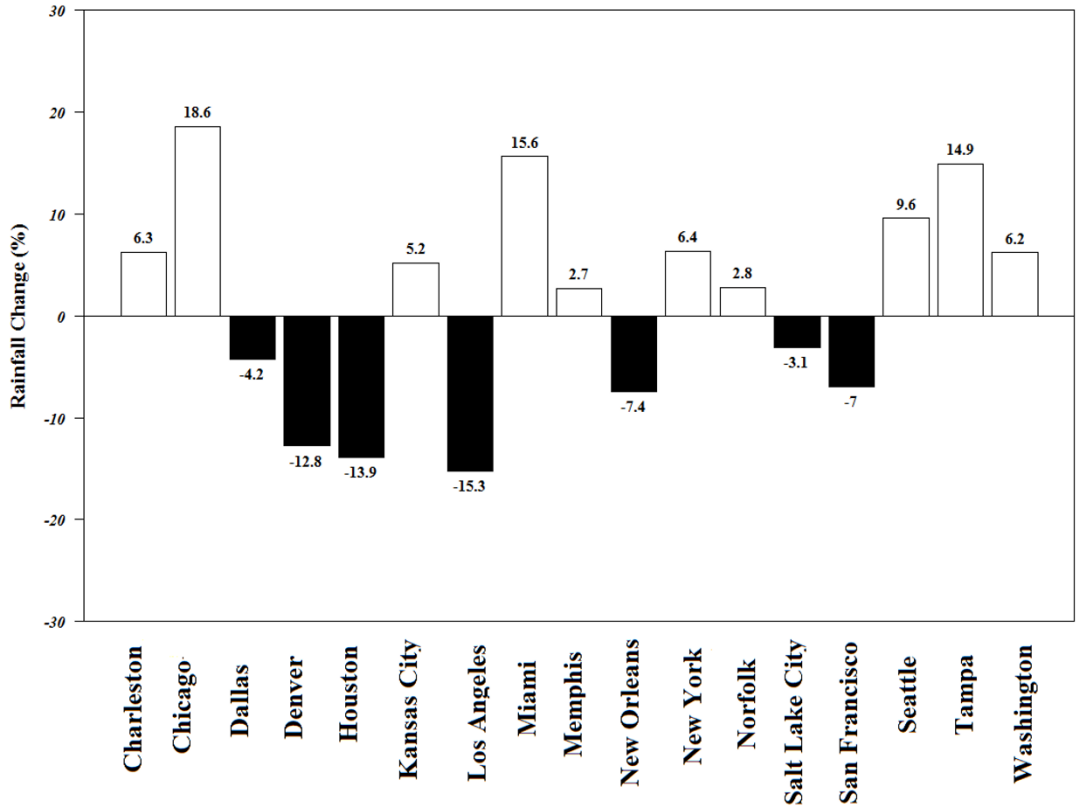

Figure 5.2. Annual precipitation changes comparing historical with projected conditions for selected locations across the U.S.

5.3.1.1 **Frequency Analysis of Rainfall Events**

Since the main input for RWH systems is rainfall, frequency analysis of rainfall was conducted for historical and projected rainfall for the 17 U.S. locations listed in **Table 5-1.** Selected Weather Stations across the U.S.. Duration or probability of exceedance curves were developed for each location. The rainfall frequency of Washington for historical and projected conditions is provided in **Figure 5.3**. as an example; for brevity, curves for the other sites have been placed in Appendix A, Figures A1-A16. The rainfall duration curve for Washington indicates that rainfall was projected to increase due to CC, as shown by the shift of the projected duration curve to the right in **Figure 5.3**. The rainfall corresponding to the 10^{th}, 50^{th}, and 90^{th} exceedance probabilities are provided in **Table 5-3**. The results indicate that in Washington, the

10^{th}, 50^{th}, and 90^{th} percentile exceedance probability rainfall was projected to increase from 16.3 to 16.8 (3.1%), from 2 to 2.5 (25%), and from 0.08 to 0.10 (25%), respectively. Conversely, in Los Angeles, where the rainfall was projected to decrease, the 10^{th}, 50^{th}, and 90^{th} percentile exceedance probability were projected to decrease from 7.1 to 6 (15.6%), from 1.3 to 1 (23.1%), and 0.12 to 0.11 (8.3%), respectively. The 50^{th} percentile exceedance probability of rainfall for historical conditions ranged from 0.5 mm for Denver to 2.2 mm for Norfolk; for projected conditions, rainfall ranged from 0.45 mm for Denver to 2.5 mm for Washington.

The probability of exceedance increased for locations in the eastern, northwestern and southeastern U.S. because rainfall was projected to increase for these locations. Probabilities of exceedance decrease for locations in the western, central and southern U.S. because rainfall was projected to decrease for these locations.

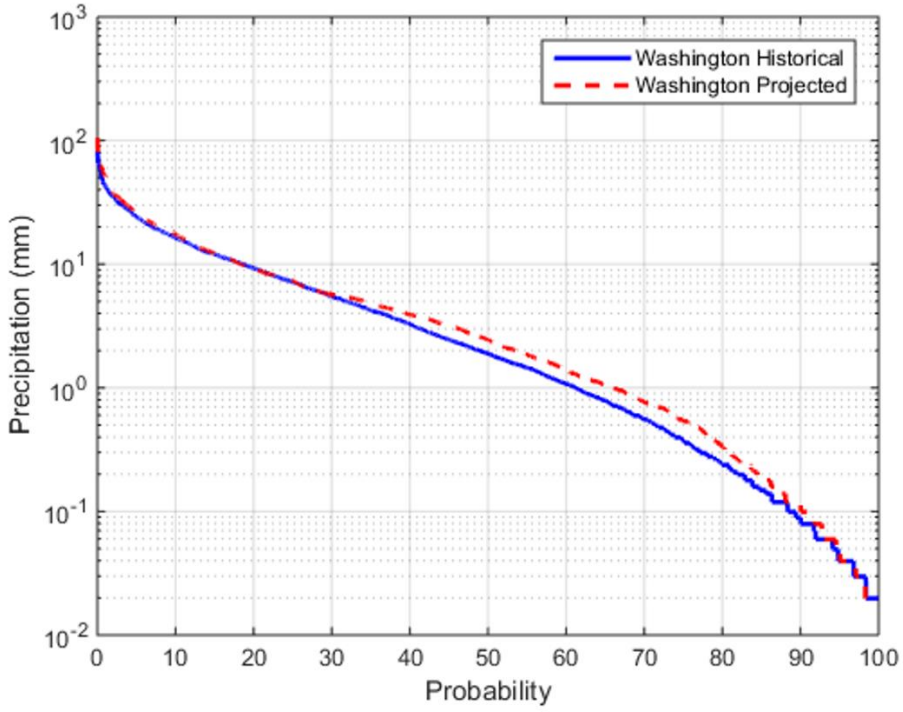

Figure 5.3. Frequency analysis curves of rainfall events for Washington for historical and projected conditions.

5.3.1.2 **Frequency Analysis of Dry Durations**

Frequency analysis of dry duration illustrates the distribution of dry periods at each location. Dry duration is defined as the inter-event periods between two consecutive events of at least 2.54 mm. The frequency of dry duration for Washington with and without CC is provided

in **Figure 5.4** as an example; for brevity, the remaining curves have been placed in Appendix B, Figures B1-B16. The dry duration curve of Washington indicates that the dry durations, or time between rainfall events, were projected to decrease. Eleven sites (excepting Denver, Houston, Los Angeles Miami, and Tampa) exhibited nearly overlapping curves for historical and projected conditions, indicating changes were too small to detect which is due to a small difference in inter-event periods between two consecutive events for historical and projected conditions indicating that the number of dry duration days in these cities may not change significantly with CC. The 10th, 50th, and 90th percentile exceedance values for dry duration for each location are presented in **Table 5-3** and **Table 5-5**. The results indicate that in Washington, the 10th, 50th, and 90th percentile exceedance probability for dry duration were projected to decrease from 6.2 days to 3.8 days (38.7%), from 1 days to 0.9 days (10%), and from 0.53 days to 0.51 days (3.8%), respectively. Conversely, in Los Angeles, where dry duration was projected to increase, the 10th, 50th, and 90th percentile exceedance probability were projected to increase from 28.5 days to 40.2 days (41%), from 1.8 days to 2.8 days (57%), and 0.52 days to 0.55 days (5.8%), respectively. Sites located in the eastern, northwestern, and southeastern part of the U.S. exhibited decreased probabilities of exceedance for dry duration because the number of dry days between storm events decreased for these locations in projected CC conditions. Probabilities increased for locations in the western, central and southern parts of the U.S. for projected CC conditions because the number of dry days between events for projected conditions increased. The largest number of dry duration days was Los Angeles, which indicates that Los Angeles may experience longer dry durations for projected CC conditions. The 50th percentile exceedance probability of dry duration for historical conditions ranged from 1.0 day for Washington and Seattle to 2.2 days for Dallas; for projected conditions, dry duration ranged from 0.9 days for Washington to 2.8 days for Los Angeles.

<THIS SPACE LEFT INTENTIONALLY BLANK>

Table 5-3. Exceedance probabilities of dry duration and rainfall for selected locations across the U.S. for historical conditions.

City	Rain depth (mm)	Rain depth (mm)	Rain depth (mm)	Dry duration (d)	Dry duration (d)	Dry duration (d)
	Exceedance Probability					
	10%	50%	90%	10%	50%	90%
			Historical Period			
Charleston	8.1	1.7	0.12	8.1	1.6	0.66
Chicago	6.2	0.8	0.06	6.5	1.7	0.65
Dallas	9.1	2.0	0.60	16.2	2.2	0.72
Denver	3.0	0.5	0.06	11.1	1.8	0.53
Houston	8.5	1.2	0.08	9.0	1.6	0.42
Kansas City	6.2	1.0	0.09	8.1	1.8	0.46
Los Angeles	7.1	1.3	0.12	28.5	1.8	0.52
Memphis	9.2	1.8	0.12	8.0	1.6	0.51
Miami	5.3	0.8	0.12	8.2	1.4	0.61
New Orleans	10.1	1.8	0.12	7.8	1.4	0.63
New York	7.2	1.2	0.11	6.8	2.0	0.62
Norfolk	16.2	2.2	0.13	3.0	1.1	0.56
Salt Lake City	2.1	0.65	0.07	10.0	1.5	0.53
San Francisco	6.1	0.93	0.08	15.1	1.4	0.60
Seattle	4.2	0.9	0.12	6.1	1.0	0.34
Tampa	8.1	1.2	0.11	10.2	1.5	0.67
Washington	16.3	2.0	0.08	6.2	1.0	0.53

<THIS SPACE LEFT INTENTIONALLY BLANK>

Table 5-4. Exceedance probabilities of dry duration and rainfall for selected locations across the U.S. for projected conditions.

City	Rain depth (mm)	Rain depth (mm)	Rain depth (mm)	Dry duration (d)	Dry duration (d)	Dry duration (d)
	Exceedance Probability					
	10%	50%	90%	10%	50%	90%
	Projected Period					
Charleston	8.1	1.8	0.12	7.8	1.6	0.65
Chicago	7.1	0.9	0.07	6.5	1.7	0.63
Dallas	8.9	1.9	0.60	18.1	2.3	0.74
Denver	2.8	0.45	0.06	12.1	2.1	0.55
Houston	8.1	0.95	0.06	10.2	1.9	0.45
Kansas City	7.1	1.3	0.11	8.1	1.8	0.45
Los Angeles	6.0	1.0	0.11	40.2	2.8	0.55
Memphis	9.2	1.9	0.12	8.0	1.6	0.51
Miami	7.1	1.2	0.12	6.1	1.25	0.60
New Orleans	9.8	1.6	0.12	8.8	1.46	0.64
New York	8.2	1.4	0.11	6.8	2.0	0.62
Norfolk	16.3	2.35	0.13	3.1	1.1	0.55
Salt Lake City	2.1	0.60	0.07	11.4	1.7	0.54
San Francisco	6.0	0.90	0.08	16.4	1.5	0.60
Seattle	4.3	1.1	0.12	6.1	1.0	0.34
Tampa	8.1	1.4	0.13	8.5	1.4	0.65
Washington	16.8	2.5	0.10	3.8	0.9	0.51

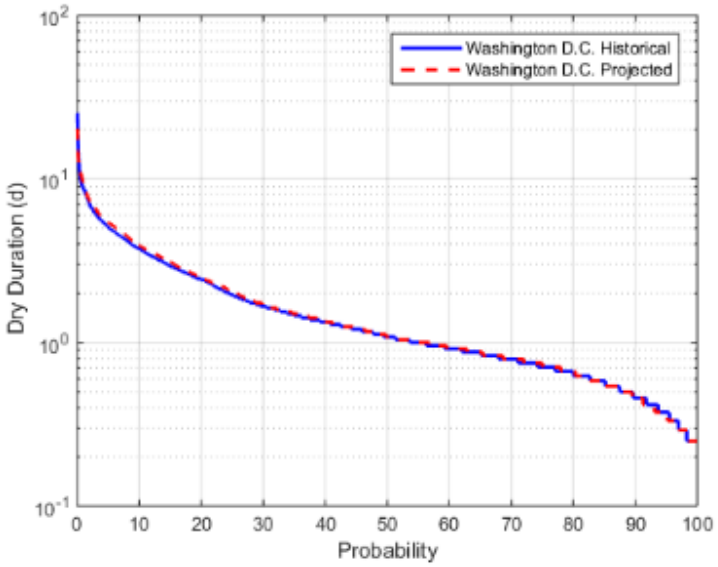

Figure 5.4. Frequency analysis curves of dry duration for Washington historical and projected conditions.

5.3.2 Model Results and Performance Evaluation

Each RWH was simulated using RASP for the 28-year historical and projected CC periods to compare the two performance metrics, λ_{WS} and λ_{RC} for each site. Average λ_{WS} changes at each location for historical and projected conditions are shown in **Table 5-5** and **Figure 5.5**, respectively; λ_{RC} changes are shown in **Table 5-5** and **Figure 5.6**, respectively. Results demonstrated that multiple sites indicated significant changes in λ_{WS} and λ_{RC}. The impact of CC increases λ_{RC} and decreases λ_{WS} for locations in western, central, and southwestern part of the U.S.

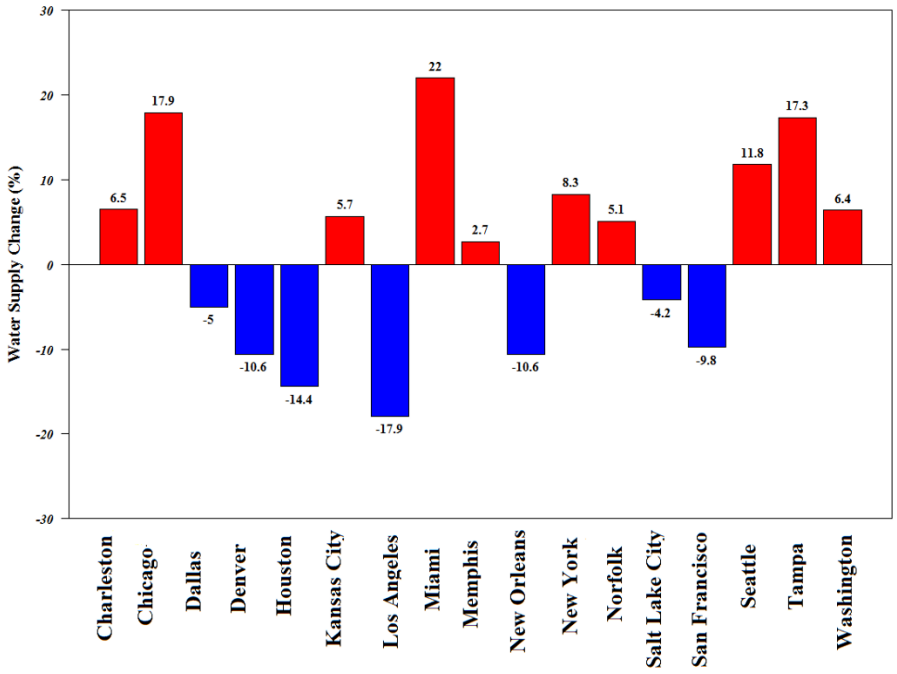

Figure 5.5. Water supply reliability changes at locations across the U.S.

<THIS SPACE LEFT INTENTIONALLY BLANK>

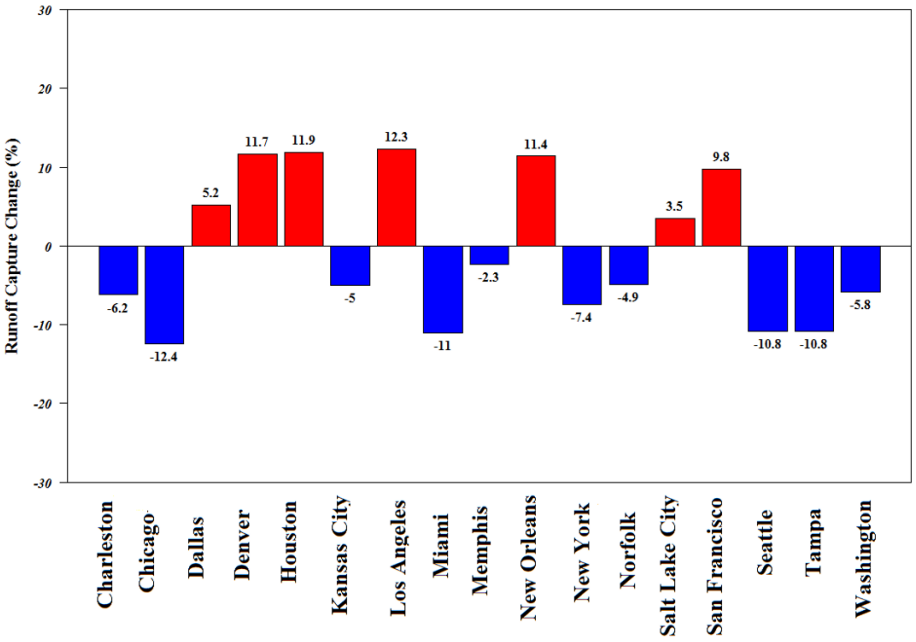

Figure 5.6. Runoff capture reliability changes at locations across the U.S.

Next, a series of tradeoff curves were developed for historical and projected conditions to evaluate λ_{WS} and λ_{RC} for each of the 17 selected locations; these are provided in Figure C1 through Figure C32 in Appendix C and Figure D1 through Figure D32 in Appendix D, respectively. As an example, λ_{WS} and λ_{RC} for Washington for a *RoofA* = 1000 m^2 and *Pop= 0* are presented in **Figure 5.7** and **Figure 5.8**, respectively. It is important at this point to note a key characteristic of the tradeoff curves. The relationship between two inputs with respect to a performance measure is expected to be convex, similar to that of an indifference curve; and conversely, the relationship between two outputs is expected to be concave, similar to a product transformation curve (James and Lee, 1971). This implies a degree of interchangeability between some design variables if the performance, in this case, reliability is held constant (Sample et al., 2013). Care must be taken to distinguish between inputs and outputs, which are different for λ_{WS} and λ_{RC}; this classification illustrates two similar yet different functions of RWH. For λ_{WS}, inputs are *TankV* and *RoofA*, and outputs are *Pop* and *IrArea*. For λ_{RC}, inputs are *TankV*, *Pop*, *IrArea*, and the only output is *RoofA*.

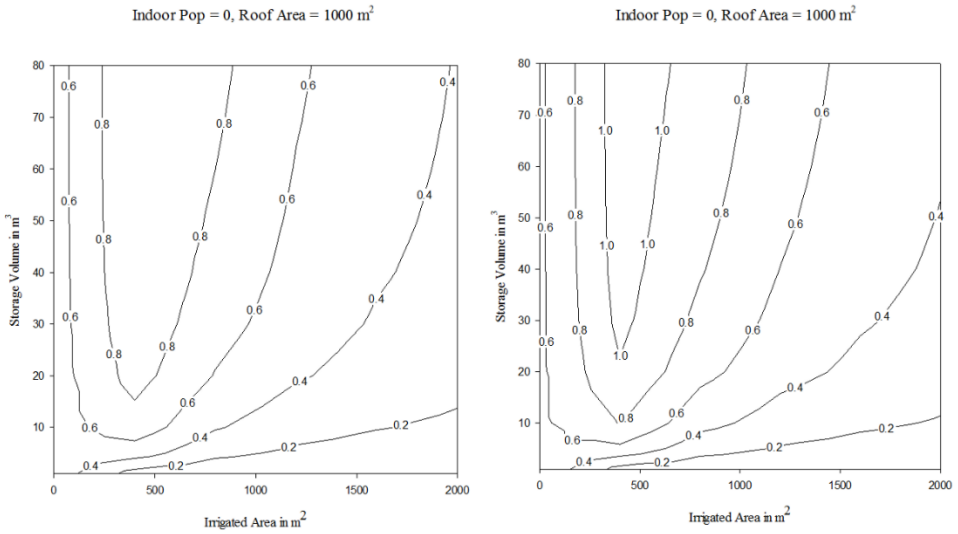

Figure 5.7. Water supply reliability curves for Washington for a) historical and b) projected conditions, for *RoofA* = 1000 m^2 and *Pop*= 0.

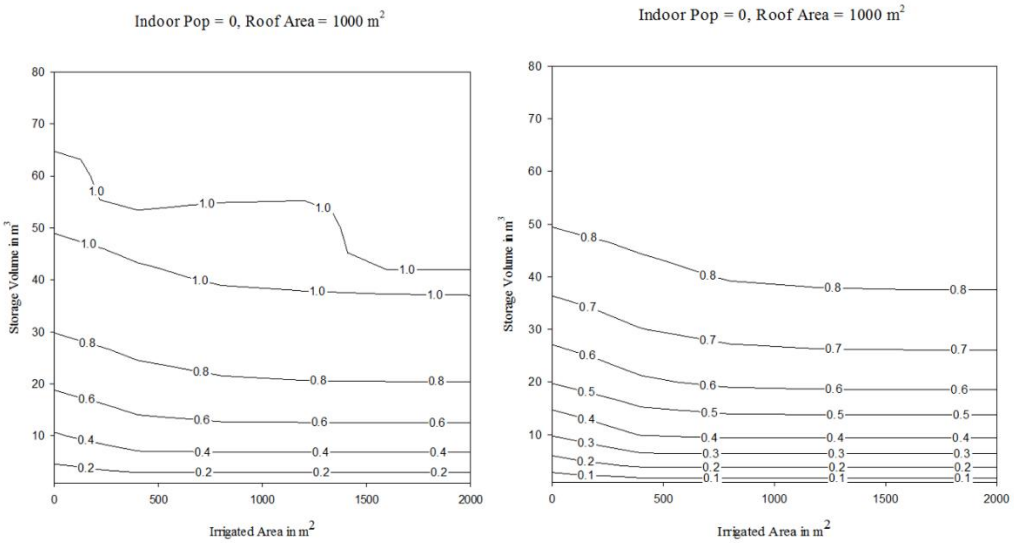

Figure 5.8. Runoff capture reliability curves for Washington a) historical and b) projected conditions, for *RoofA* = 1000 m^2 and *Pop*= 0.

To assess the relationship between *TankV* versus *IrArea* inputs, the λ_{WS} and λ_{RC} for *RoofA* = 1000 m^2 and *Pop= 0* are shown for each location in Appendix C. To assess the relationship between *TankV* versus *Pop*, the λ_{WS} and λ_{RC} for *RoofA* = 1000 m^2 and *IrArea* = 1000 m^2 are shown for each location in Appendix D. λ_{WS} and λ_{RC} for historical and projected conditions for a *RoofA* = 1000 m^2, *IrArea* = 1000 m^2, *TankV* = 10 m^3, *Pop*= 0 and *RoofA* = 1000 m^2 and *IrArea* = 1000 m^2, *TankV* = 20 m^3, *Pop*= 80 are provided in **Table 5-5** and **Table 5-6**, respectively. λ_{WS}

and λ_{RC} for Washington for *RoofA* = 1000 m^2 and *Pop= 0* are presented for *TankV* as a function of *IrArea* in **Figure 5.7** and **Figure 5.8** and for *RoofA* = 1000 m^2 and *IrArea* = 1000 m^2 are presented for *TankV* as a function of *Pop* in **Figure 5.9** and **Figure 5.10**, respectively.

Table 5-5. Water supply and runoff capture reliability for selected locations across the U.S. for historical and projected conditions in the case of *RoofA* = 1000 m^2, *IrArea* = 1000 m^2, *TankV* = 10 m^3, and *Pop*= 0.

City	λ_{WS} **(Historical)**	λ_{WS} **(Projected)**	λ_{RC} **(Historical)**	λ_{RC} **(Projected)**
Charleston	0.247	0.263	0.723	0.678
Chicago	0.200	0.236	0.768	0.673
Dallas	0.168	0.160	0.698	0.734
Denver	0.122	0.109	0.725	0.810
Houston	0.208	0.178	0.628	0.703
Kansas City	0.141	0.149	0.743	0.706
Los Angeles	0.24	0.197	0.626	0.703
Memphis	0.221	0.227	0.701	0.685
Miami	0.218	0.266	0.743	0.661
New Orleans	0.263	0.235	0.616	0.686
New York	0.217	0.235	0.761	0.705
Norfolk	0.322	0.338	0.388	0.369
Salt Lake City	0.095	0.091	0.770	0.797
San Francisco	0.051	0.046	0.653	0.717
Seattle	0.144	0.161	0.729	0.650
Tampa	0.226	0.265	0.734	0.655
Washington	0.311	0.329	0.453	0.425

<THIS SPACE LEFT INTENTIONALLY BLANK>

Table 5-6. Water supply and runoff capture reliability for selected locations across the U.S. for historical and projected conditions in the case of RoofA = 1000 m^2 and IrArea = 1000 m^2, TankV = 20 m3, and Pop= 80.

City	λ_{WS} (Historical)	λ_{WS} (Projected)	λ_{RC} (Historical)	λ_{RC} (Projected)
Charleston	0.227	0.246	0.794	0.729
Chicago	0.187	0.215	0.843	0.743
Dallas	0.148	0.132	0.801	0.833
Denver	0.110	0.08	0.890	0.967
Houston	0.201	0.159	0.774	0.864
Kansas City	0.182	0.193	0.831	0.772
Los Angeles	0.225	0.176	0.762	0.855
Memphis	0.222	0.231	0.761	0.721
Miami	0.262	0.301	0.790	0.702
New Orleans	0.264	0.224	0.741	0.803
New York	0.191	0.210	0.821	0.751
Norfolk	0.181	0.191	0.771	0.720
Salt Lake City	0.081	0.076	0.872	0.891
San Francisco	0.082	0.070	0.776	0.825
Seattle	0.170	0.189	0.786	0.710
Tampa	0.202	0.231	0.814	0.726
Washington	0.175	0.188	0.823	0.758

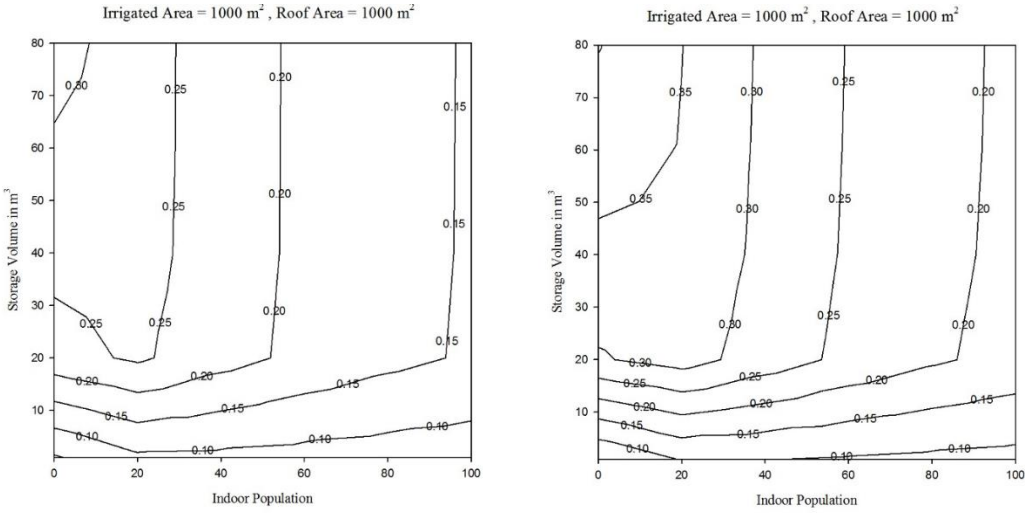

Figure 5.9. Water supply reliability curves for Washington for a) historical and b) projected conditions, RoofA = 1000 m^2 and IrArea = 1000 m^2.

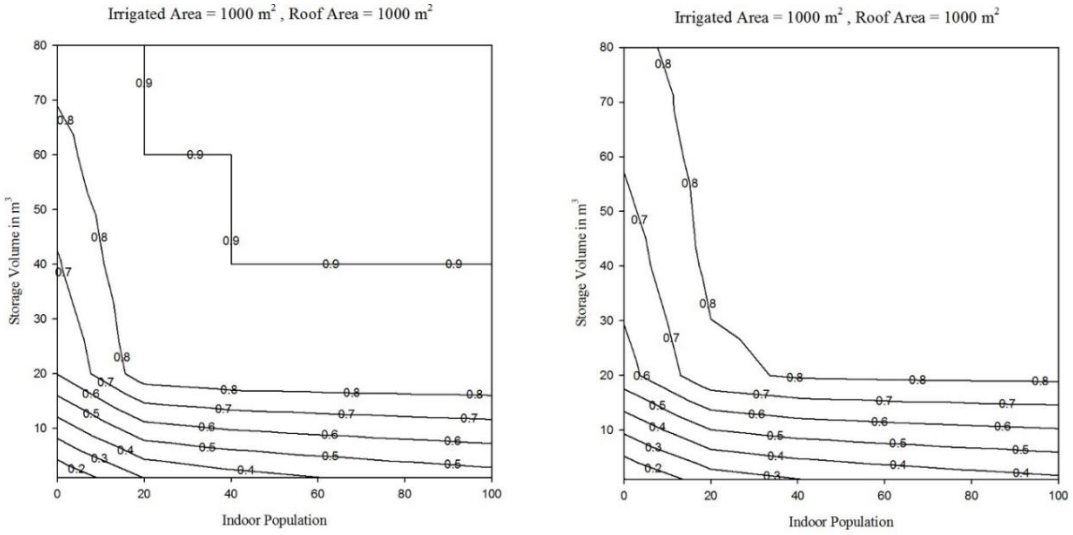

Figure 5.10. Runoff capture reliability curves for Washington for a) historical and b) projected conditions, RoofA = 1000 m^2 and IrArea = 1000 m^2.

The results indicate that λ_{WS} is increasing and λ_{RC} is decreasing, respectively, with CC. It is apparent from the curves that the impact of CC decreases λ_{RC} and increases λ_{WS} in eastern, northwestern, and southeastern part of the U.S. by shifting the curves to the right, away from the origin. Assessing **Figure 5.2**, **Figure 5.5**, and **Figure 5.6** indicates a positive relationship between rainfall and λ_{WS}, and negative relationship between rainfall and λ_{RC}. The results indicate that increasing rainfall can greatly enhance λ_{WS} and reduce λ_{RC}. Conversely, decreasing rainfall may reduce λ_{WS} and increase λ_{RC}. Comparing **Figure 5.7** and **Figure 5.9**, the effect of moving from outdoor demand to indoor demand eliminates the right hand, upward tick of the curve (as in **Figure 5.7**), which negatively impacts performance due to the seasonality of outdoor irrigation. Comparing **Figure 5.8** and **Figure 5.10**, in the latter λ_{RC} is flat and nearly linear. This effect is also due to the seasonality of irrigation demand (**Figure 5.8**) as opposed to indoor demand (**Figure 5.10**).

As CC caused changes in rainfall and the duration of dry periods, those RWH systems in eastern, northwestern, and southeastern U.S. showed an increase in λ_{WS} and a decrease in λ_{RC}; RWH systems in western, southwestern, and central showed a decrease in λ_{WS} and an increase in λ_{RC}. Given the increase in overall rainfall and shorter dry durations, it is logical that a larger number of storms might overwhelm the capability of the available RWH storage at these locations. The change in λ_{WS} and λ_{RC} from the RWH due to CC is of particular interest. The percent difference of λ_{WS} between historical conditions and projected conditions ranged from -

17.9% (Los Angeles) to +22% (Miami). The percent difference in λ_{RC} between historical conditions and projected conditions ranged from -12.4% (Chicago) to +12.3% (Los Angeles). Although the results showed a decrease in λ_{RC} and increase in λ_{WS} for RWH systems at several locations, such as Charleston, Kansas City, Memphis, Norfolk, and Washington had modest reductions in λ_{RC} and modest increases in λ_{WS}, i.e., projected changes were less than ±10%. The RWH systems at Chicago, Miami, and Tampa showed reduction in λ_{RC} and increases in λ_{WS}. Dallas, Salt Lake City, and San Francisco had small increases in λ_{RC} and small decreases in λ_{WS}, less than ±10% between historical conditions and projected conditions. Los Angeles, Houston, and Denver showed significant increases in λ_{RC} and decreases in λ_{WS} between historical conditions and projected conditions. Thus, for Memphis, Los Angeles, and Salt Lake City, RWH remains a good choice for runoff capture, and perhaps for Chicago, as while λ_{RC} is reduced, it is still relatively high (>0.60).

Due to the effect of substitution, it is possible to compensate for changes in performance by increasing storage tank size. This was accomplished by increasing *TankV* until either a λ_{WS} and/or λ_{RC} of 80% (alternatively) was met, first for the case of *RoofA* = 1000 m^2, *IrArea* = 1000 m^2, and *Pop*= 0 and then for the case of *RoofA* = 1000 m^2 and *IrArea* = 1000 m^2, and *Pop*= 80for historical and projected conditions. Results for the 17 selected locations across the U.S. are presented in **Table 5-7** and **Table 5-8** for the first and second cases, respectively. The results presented in **Table 5-7** and **Table 5-8** indicated that as CC caused change in rainfall and length of dry duration, larger tanks are required in eastern, northwestern, and southeastern U.S. and smaller tanks in western, southwestern, and central to meet a goal of 80% λ_{RC}. Conversely, smaller tanks are required in eastern, northwestern, and southeastern U.S. and larger tanks in western, southwestern, and central to meet a goal of 80% λ_{WS}. λ_{WS} results for the case of *RoofA* = 1000 m^2, *IrArea* = 1000 m^2, and *Pop*= 0 show that the tank size needed to achieve an 80% λ_{WS} for historical conditions ranged from Washington and Norfolk at 100 m^3 to Los Angeles at 165 m^3; and for projected conditions, tank size ranged from Washington at 92 m^3 to Los Angeles at 186 m^3 (**Table 5-7**). Assuming a *RoofA* = 1000 m^2 and *IrArea* = 1000 m^2, and *Pop*= 80, for historical conditions, tank size ranged from Charleston at 146 m^3 to Los Angeles at 196 m^3; and for projected conditions from Charleston at 133 m^3 to Los Angeles at 219 m^3, respectively (**Table 5-8**). λ_{RC} results for the case of *RoofA* = 1000 m^2, *IrArea* = 1000 m^2, and *Pop*= 0 show that the tank size needed to achieve an 80% λ_{WS} for historical conditions ranged from Chicago at

7.1 m^3 to Norfolk at 35.2 m^3; and for projected conditions, tank size ranged from Denver and Salt Lake City (tied) at 5.1 m^3 to Washington at 40.3 m^3 (**Table 5-7**). Assuming a *RoofA* = 1000 m^2 and *IrArea* = 1000 m^2, and *Pop*= 80, for historical conditions, tank size ranged from ranged from Salt Lake City at 11.3 m^3 to New Orleans at 20.4 m^3; and for projected conditions, tank size ranged from Salt Lake City at 9.9 m^3 to Norfolk at 23.4 m^3, respectively (**Table 5-8**). It should be noted that in all cases RWH tanks sized to meet water supply purposes alone are always much larger than RWH tanks sized to meet runoff reduction goals alone. The results of this study agree in general with Aladenola et al. (2016); Almazroui et al. (2017); Haque et al. (2016); Lo and Koralegedara (2015); Youn et al. (2012). Regions expecting a decrease in annual precipitation and/or increase in dry duration, water supply reliability of RWH for projected CC is expected to decrease. Conversely, where precipitation is increasing and/or dry duration decreasing, water supply reliability of RWH is expected to increase. As a result of these reliability changes, several studies have proposed larger storage tanks for projected CC to compensate for the performance reduction of RWHs and to meet water demand during dry periods This is consistent with the sites in the eastern, northwestern, and southeastern U.S. where precipitation amount is increasing but the dry durations, or time between rainfall events, were projected to decrease.

<THIS SPACE LEFT INTENTIONALLY BLANK>

Table 5-7. Tank size needed to achieve water supply and runoff capture reliability of 80% for selected locations across the U.S. for historical and projected conditions for *RoofA* = 1000 m^2, *IrArea* = 1000 m^2, and *Pop*= 0.

City	**Tank Size (Historical) (m^3)**	**Tank Size (Projected) (m^3)**	**Tank Size (Historical) (m^3)**	**Tank Size (Projected) (m^3)**
	λ_{WS} = 80%		λ_{RC} = 80%	
Charleston	130	120	10.1	18.2
Chicago	135	127	7.1	15.1
Dallas	140	150	17.2	9.1
Denver	150	161	9.1	5.1
Houston	125	132	20.1	14.2
Kansas City	141	133	10.1	17.3
Los Angeles	165	186	28.2	16.1
Memphis	134	129	11.1	19.1
Miami	143	125	10.0	20.1
New Orleans	121	126	28.3	20.3
New York	130	120	9.1	13.1
Norfolk	100	95	35.2	39.6
Salt Lake City	148	153	8.0	5.1
San Francisco	147	155	18.1	10.0
Seattle	154	146	11.2	19.2
Tampa	140	122	8.0	19.1
Washington	100	92	26.3	40.3

<THIS SPACE LEFT INTENTIONALLY BLANK>

Table 5-8. Tank size needed to achieve water supply and runoff capture reliability of 80% for selected locations across the U.S. for historical and projected conditions for *RoofA* = 1000 m^2 and *IrArea* = 1000 m^2, and *Pop*= 80.

City	Tank Size (Historical) (m^3)	Tank Size (Projected) (m^3)	Tank Size (Historical) (m^3)	Tank Size (Projected) (m^3)
	λ_{WS} = 80%		λ_{RC} = 80%	
Charleston	146	133	19.1	20.2
Chicago	175	165	16.2	18.1
Dallas	157	167	19.1	16.2
Denver	173	185	14.8	12.8
Houston	148	155	19.1	17.2
Kansas City	179	170	18.1	19.7
Los Angeles	196	219	19.8	17.2
Memphis	154	150	20.1	21.2
Miami	193	172	19.8	22.8
New Orleans	149	153	20.4	19.1
New York	175	162	17.8	19.4
Norfolk	155	140	19.2	23.4
Salt Lake City	179	184	11.3	9.9
San Francisco	185	193	18.2	15.7
Seattle	179	171	16.3	19.2
Tampa	174	154	17.3	19.2
Washington	168	151	19.3	22.2

A reduction in reliability of RWH due to CC presents a challenge for water resources managers, designers and planners, as implemented designs built to current standards and specifications may be difficult to adapt. Our study provides stakeholders with a methodology that anticipates changes in RWH due to CC, so simple modifications, i.e., tank sizes, can be made, thus increasing the resiliency of the practice. Evaluating the effects of CC on the resiliency of other SCMs such as bioretention cells, swales, ponds, and etc. is suggested for the future. Thus, the additional storage required in the future can be calculated for better water resources management.

5.4 Summary and Conclusions

CC is anticipated to alter temperature and rainfall magnitudes and timing across the U.S. CC-induced changes in precipitation will likely affect the resilience of urban stormwater infrastructure, particularly SCMs. RWH is emerging as a popular SCM in the U.S. This study

evaluated the performance of RWH systems at 17 selected locations across the U.S. using a simulation program for historical and projected rainfall data. RASP simulated a range of design variables including tank size, roof area, outdoor irrigation and indoor nonpotable water demand. Performance of each hypothetical RWH system installed at 17 selected locations across the U.S. was assessed with respect to the reliability of water supply, which is the proportion of demands that were met; and the reliability of runoff capture, which was the amount stored but not spilled. Simulations were conducted for historical (1971-1998) and projected climate change conditions (2041-2068) developed from recent simulations by NARCCAP. Anticipated CC conditions, including changes in rainfall and duration between rainfall events, were found to result in decreasing runoff capture reliability and increasing water supply reliability for hypothetical RWH systems located in eastern, northwestern, and southeastern U.S. sites. Conversely, for anticipated CC conditions, runoff capture reliability increased and water supply reliability decreased for RWH systems located in western, central, and southern U.S. Although water supply and runoff capture reliability changed at all sites, multiple sites did not indicate significant changes in the aforementioned metrics because rainfall was only moderately altered. Examples of this behavior are Charleston, Dallas, Kansas City, Memphis, Norfolk, Salt Lake City, and Washington. RWH systems located in Chicago, Houston, Los Angeles, Miami, and Tampa demonstrated significant changes in either water supply or runoff capture reliability or both. The shape of tradeoff curves changed significantly for these locations due to the fact that projected rainfall is anticipated to change substantially. RWH tanks sized for water supply reliability alone were much greater than those sized for runoff capture reliability alone.

The results of this study suggest that some RWH systems designed for current conditions may be less effective in the future due to CC at some U.S locations. This paper presents a methodology for assessing CC impacts on the water supply and runoff reduction benefits of RWH systems. These results, while not absolute, can help guide managers and decision makers identify locations in which RWH systems can provide the best runoff capture and water supply benefits. The limitations of this analysis stem from the sources of uncertainty, which include: uncertainty in GCMs, including their inherent assumptions regarding future emission of greenhouse gases; uncertainty in the representation of climatology at regional and local scales; and uncertainty of parameters required for input into the RASP model.

References for Chapter 5:

Ahmadisharaf, E., Kalyanapu, A.J., 2015. Investigation of the Impact of Streamflow Temporal Variation on Dam Overtopping Risk: Case Study of a High-Hazard Dam, World Environmental and Water Resources Congress 2015@ Sfloods, Droughts, and Ecosystems. ASCE, pp. 1050-1057.
Ahmadisharaf, E., Tajrishy, M., Alamdari, N., 2015. Integrating Flood Hazard into Site Selection of Detention Basins Using Spatial Multi-Criteria Decision-Making. Journal of Environmental Planning and Management, 1-21.
Aladenola, O., Cashman, A., Brown, D., 2016. Impact of El Niño and Climate Change on Rainwater Harvesting in a Caribbean State. Water Resources Management 30(10), 3459-3473.
Aladenola, O.O., Adeboye, O.B., 2010. Assessing the Potential for Rainwater Harvesting. Water Resources Management 24(10), 2129-2137.
Alam, R., Munna, G., Chowdhury, M., Sarkar, M., Ahmed, M., Rahman, M., Jesmin, F., Toimoor, M., 2012. Feasibility Study of Rainwater Harvesting System in Sylhet City. Environmental Monitoring and Assessment 184(1), 573-580.
Alamdari, N., 2016. Development of a Robust Automated Tool for Calibrating a Swmm Watershed Model, World Environmental and Water Resources Congress 2016. pp. 221-228.
Alamdari, N., Sample, D.J., Steinberg, P., Ross, A.C., Easton, Z.M., 2017. Assessing the Effects of Climate Change on Water Quantity and Quality in an Urban Watershed Using a Calibrated Stormwater Model. Water 9(7), 464.
Alberti, M., Booth, D., Hill, K., Coburn, B., Avolio, C., Coe, S., Spirandelli, D., 2007. The Impact of Urban Patterns on Aquatic Ecosystems: An Empirical Analysis in Puget Lowland Sub-Basins. Landscape and Urban Planning 80(4), 345-361.
Almazroui, M., Islam, M.N., Balkhair, K.S., Şen, Z., Masood, A., 2017. Rainwater Harvesting Possibility under Climate Change: A Basin-Scale Case Study over Western Province of Saudi Arabia. Atmospheric Research 189, 11-23.
Asadabadi, A., Miller-Hooks, E., 2017a. Assessing Strategies for Protecting Transportation Infrastructure from an Uncertain Climate Future. Transportation Research Part A: Policy and Practice 105, 27-41.
Asadabadi, A., Miller-Hooks, E., 2017b. Optimal Transportation and Shoreline Infrastructure Investment Planning under a Stochastic Climate Future. Transportation Research Part B: Methodological 100, 156-174.
Basinger, M., Montalto, F., Lall, U., 2010. A Rainwater Harvesting System Reliability Model Based on Nonparametric Stochastic Rainfall Generator. Journal of Hydrology 392(3), 105-118.
Berggren, K., Olofsson, M., Viklander, M., Svensson, G., Gustafsson, A.M., Luleå University of, T., Sanitary, E., Architecture, Water, Department of Civil, E., Natural Resources, E., 2012. Hydraulic Impacts on Urban Drainage Systems Due to Changes in Rainfall Caused by Climatic Change. Journal of Hydrologic Engineering 17(1), 92-98.
Boé, J., Terray, L., Habets, F., Martin, E., 2007. Statistical and Dynamical Downscaling of the Seine Basin Climate for Hydro-Meteorological Studies. International Journal of Climatology 27(12), 1643-1655.
Boelee, E., Yohannes, M., Poda, J.-N., McCartney, M., Cecchi, P., Kibret, S., Hagos, F., Laamrani, H., 2013. Options for Water Storage and Rainwater Harvesting to Improve Health and Resilience against Climate Change in Africa. Regional Environmental Change 13(3), 509-519.
Brekke, L., Thrasher, B., Maurer, E., Pruitt, T., 2013. Downscaled Cmip3 and Cmip5 Climate and Hydrology Projections: Release of Downscaled Cmip5 Climate Projections, Comparison

with Preceding Information, and Summary of User Needs. Us Dept. Of the Interior, Bureau of Reclamation, Technical Services Center, Denver.
Burian, S.J., Jones, D., 2010. National Assessment of Rainwater Harvesting as a Stormwater Best Management Practice: Challenges, Needs, and Recommendations, Low Impact Development 2010: Redefining Water in the City. pp. 842-852.
Campisano, A., Butler, D., Ward, S., Burns, M.J., Friedler, E., DeBusk, K., Fisher-Jeffes, L.N., Ghisi, E., Rahman, A., Furumai, H., Han, M., 2017. Urban Rainwater Harvesting Systems: Research, Implementation and Future Perspectives. Water Research 115, 195-209.
Campisano, A., Modica, C., 2012. Optimal Sizing of Storage Tanks for Domestic Rainwater Harvesting in Sicily. Resources, Conservation and Recycling 63, 9-16.
Chen, J., Brissette, F.P., Chaumont, D., Braun, M., 2013. Finding Appropriate Bias Correction Methods in Downscaling Precipitation for Hydrologic Impact Studies over North America. Water Resources Research 49(7), 4187-4205.
Coombes, P.J., Barry, M.E., 2007. The Effect of Selection of Time Steps and Average Assumptions on the Continuous Simulation of Rainwater Harvesting Strategies. Water Science & Technology 55(4), 125-133.
Coombes, P.J., Kuczera, G., Kalma, J.D., Argue, J.R., 2002. An Evaluation of the Benefits of Source Control Measures at the Regional Scale. Urban Water 4(4), 307-320.
Even, S., Mouchel, J.-M., Servais, P., Flipo, N., Poulin, M., Blanc, S., Chabanel, M., Paffoni, C., 2007. Modelling the Impacts of Combined Sewer Overflows on the River Seine Water Quality. Science of the Total Environment 375(1), 140-151.
Fewkes, A., Butler, D., 2000. Simulating the Performance of Rainwater Collection and Reuse Systems Using Behavioural Models. Building Services Engineering Research and Technology 21(2), 99-106.
Fowler, H.J., Wilby, R.L., 2007. Beyond the Downscaling Comparison Study. International Journal of Climatology 27(12), 1543-1545.
Gao, H., Tang, Q., Shi, X., Zhu, C., Bohn, T., Su, F., Sheffield, J., Pan, M., Lettenmaier, D., Wood, E.F., 2010. Water Budget Record from Variable Infiltration Capacity (Vic) Model. Algorithm Theoretical Basis Document for Terrestrial Water Cycle Data Records.
Ghisi, E., 2010. Parameters Influencing the Sizing of Rainwater Tanks for Use in Houses. Water Resources Management 24(10), 2381-2403.
Gill, S.E., Handley, J.F., Ennos, A.R., Pauleit, S., 2007. Adapting Cities for Climate Change: The Role of the Green Infrastructure. Built Environment 33(1), 115-133.
Giuffria Jonathon, M., Bosch Darrell, J., Taylor Daniel, B., Alamdari, N., 2017. Costs of Water Quality Goals under Climate Change in Urbanizing Watersheds: Difficult Run, Virginia. Journal of Water Resources Planning and Management 143(9), 04017055.
Gold, A., Goo, R., Hair, L., Arazan, N., 2010. Rainwater Harvesting: Policies, Programs, and Practices for Water Supply Sustainability, 2010 International Low Impact Development Conference. Asce, San Francisco, Ca. p. 86.
Gudmundsson, L., Bremnes, J., Haugen, J., Engen-Skaugen, T., 2012. Technical Note: Downscaling Rcm Precipitation to the Station Scale Using Statistical Transformations–a Comparison of Methods. Hydrology and Earth System Sciences 16(9), 3383-3390.
Haque, M.M., Rahman, A., Samali, B., 2016. Evaluation of Climate Change Impacts on Rainwater Harvesting. Journal of Cleaner Production 137, 60-69.

Hatt, B.E., Fletcher, T.D., Walsh, C.J., Taylor, S.L., 2004. The Influence of Urban Density and Drainage Infrastructure on the Concentrations and Loads of Pollutants in Small Streams. Environmental Management 34(1), 112-124.
Hayhoe, K., VanDorn, J., Croley, T., Schlegal, N., Wuebbles, D., 2010. Regional Climate Change Projections for Chicago and the Us Great Lakes. Journal of Great Lakes Research 36(sp2), 7-21.
Hayhoe, K., Wake, C., Anderson, B., Liang, X.-Z., Maurer, E., Zhu, J., Bradbury, J., DeGaetano, A., Stoner, A., Wuebbles, D., 2008. Regional Climate Change Projections for the Northeast USA. Mitig Adapt Strateg Glob Change 13(5-6), 425-436.
Herrmann, T., Schmida, U., 2000. Rainwater Utilisation in Germany: Efficiency, Dimensioning, Hydraulic and Environmental Aspects. Urban Water 1(4), 307-316.
Huber, W.C., Dickinson, R.E., Rosener, L.A., Aldrich, J.A., 1988. Stormwater Management Model User's Manual, Version 4. U.S. Environmental Protection Agency, Athens, GA.
Imteaz, M.A., Ahsan, A., Shanableh, A., 2013. Reliability Analysis of Rainwater Tanks Using Daily Water Balance Model: Variations within a Large City. Resources, Conservation and Recycling 77, 37-43.
Imteaz, M.A., Rahman, A., Ahsan, A., 2012. Reliability Analysis of Rainwater Tanks: A Comparison between South-East and Central Melbourne. Resources, Conservation and Recycling 66, 1-7.
IPCC, 2014. Climate Change 2014–Impacts, Adaptation and Vulnerability: Regional Aspects. Cambridge University Press.
James, L.D., Lee, R.R., 1971. Economics of Water Resources Planning. McGraw-Hill, Inc., New York, NY.
James, W., Rossman, L.A., James, W.R.C., 2010. User's Guide to Swmm 5 Computational Hydraulics International, Guelph, Ontario, Canada.
Jensen, M.A., Steffen, J., Burian, S.J., Pomeroy, C., 2010. Do Rainwater Harvesting Objectives of Water Supply and Stormwater Management Conflict, Proceedings of the 2010 International Low Impact Development Conference.
Kahinda, J.M., Taigbenu, A., Boroto, R., 2010. Domestic Rainwater Harvesting as an Adaptation Measure to Climate Change in South Africa. Physics and Chemistry of the Earth, Parts a/B/C 35(13), 742-751.
Karim, M.R., Bashar, M.Z.I., Imteaz, M.A., 2015. Reliability and Economic Analysis of Urban Rainwater Harvesting in a Megacity in Bangladesh. Resources, Conservation and Recycling 104, 61-67.
Kim, K., Yoo, C., 2009. Hydrological Modeling and Evaluation of Rainwater Harvesting Facilities: Case Study on Several Rainwater Harvesting Facilities in Korea. Journal of Hydrologic Engineering 14(6), 545-561.
Kottek, M., Grieser, J., Beck, C., Rudolf, B., Rubel, F., 2006. World Map of the Köppen-Geiger Climate Classification Updated. Meteorologische Zeitschrift 15(3), 259-263.
Lafon, T., Dadson, S., Buys, G., Prudhomme, C., 2013. Bias Correction of Daily Precipitation Simulated by a Regional Climate Model: A Comparison of Methods. International Journal of Climatology 33(6), 1367-1381.
Lash, D., Ward, S., Kershaw, T., Butler, D., Eames, M., 2014. Robust Rainwater Harvesting: Probabilistic Tank Sizing for Climate Change Adaptation. Journal of Water and Climate Change 5(4), 526.

Lassaux, S., Renzoni, R., Germain, A., 2007. Life Cycle Assessment of Water from the Pumping Station to the Wastewater Treatment Plant. International Journal of Life Cycle Assessment 12(2), 118.
Lee, Y.J., Boynton, W.R., Li, M., Li, Y., 2013. Role of Late Winter–Spring Wind Influencing Summer Hypoxia in Chesapeake Bay. Estuaries and Coasts 36(4), 683-696.
Li, H., Sheffield, J., Wood, E.F., 2010. Bias Correction of Monthly Precipitation and Temperature Fields from Intergovernmental Panel on Climate Change Ar4 Models Using Equidistant Quantile Matching. Journal of Geophysical Research: Atmospheres 115(D10).
Liaw, C.-H., Liaw, C., Hsien, Tsai, Y., Lung, 2004. Optimum Storage Volume of Rooftop Rain Water Harvesting Systems for Domestic Use. Journal of the American Water Resources Association 40(4), 901-912.
Liu, J., Sample, D., Zhang, H., 2013. Frequency Analysis for Precipitation Events and Dry Durations of Virginia. Environ Model Assess, 1-12.
Lo, K.F.A., Koralegedara, S.B., 2015. Effects of Climate Change on Urban Rainwater Harvesting in Colombo City, Sri Lanka. Environments 2(1), 105-124.
Mearns, L.O., Gutowski, W., Jones, R., Leung, R., McGinnis, S., Qian, Y., 2009. A Regional Climate Change Assessment Program for North America. Eos, Transactions, American Geophysical Union 90(36), 311-311.
Milly, P.C.D., Betancourt, J., Falkenmark, M., Hirsch, R.M., Kundzewicz, Z.W., Lettenmaier, D.P., Stouffer, R.J., 2008. Stationarity Is Dead: Whither Water Management? Science 319(5863), 573-574.
Mishra, V., Lettenmaier, D.P., 2011. Climatic Trends in Major U.S. Urban Areas, 1950–2009. Geophysical Research Letters 38(16), L16401.
Mukheibir, P., 2008. Water Resources Management Strategies for Adaptation to Climate-Induced Impacts in South Africa. Water Resources Management 22(9), 1259-1276.
Najjar, R.G., Pyke, C.R., Adams, M.B., Breitburg, D., Hershner, C., Kemp, M., Howarth, R., Mulholland, M.R., Paolisso, M., Secor, D., Sellner, K., Wardrop, D., Wood, R., 2010. Potential Climate-Change Impacts on the Chesapeake Bay. Estuarine, Coastal and Shelf Science 86(1), 1-20.
Nakićenović, N., Swart, R., 2000. Special Report on Emission Scenarios. Intergovernmental Panel on Climate Change.
Nelson, E.J., Booth, D.B., 2002. Sediment Sources in an Urbanizing, Mixed Land-Use Watershed. Journal of Hydrology 264(1–4), 51-68.
Nilsen, V., Lier, J.A., Bjerkholt, J.T., Lindholm, O.G., 2011. Analysing Urban Floods and Combined Sewer Overflows in a Changing Climate. Journal of Water and Climate Change 2(4), 260-271.
Palla, A., Gnecco, I., Lanza, L., La Barbera, P., 2012. Performance Analysis of Domestic Rainwater Harvesting Systems under Various European Climate Zones. Resources, Conservation and Recycling 62, 71-80.
Pandey, D.N., Gupta, A.K., Anderson, D.M., 2003. Rainwater Harvesting as an Adaptation to Climate Change. Current Science 85(1), 46-59.
Pyke, C., Warren, M.P., Johnson, T., LaGro, J., Scharfenberg, J., Groth, P., Freed, R., Schroeer, W., Main, E., 2011. Assessment of Low Impact Development for Managing Stormwater with Changing Precipitation Due to Climate Change. Landscape and Urban Planning 103(2), 166-173.

Rosenberg, E.A., Keys, P.W., Booth, D.B., Hartley, D., Burkey, J., Steinemann, A.C., Lettenmaier, D.P., 2010. Precipitation Extremes and the Impacts of Climate Change on Stormwater Infrastructure in Washington State. Climatic Change 102(1), 319-349.
Rossman, L.A., 2004. Storm Water Management Model User's Manual, Version 5.0, in: U.S. Environmental Protection Agency (Ed.). Cincinatti, OH.
Rozos, E., Makropoulos, C., Butler, D., 2009. Design Robustness of Local Water-Recycling Schemes. Journal of Water Resources Planning and Management 136(5), 531-538.
Sample, D., Liu, J., Wang, S., 2013. Evaluating the Dual Benefits of Rainwater Harvesting Systems Using Reliability Analysis. Journal of Hydrologic Engineering 18(10), 1310-1321.
Sample, D.J., Heaney, J.P., 2006. Integrated Management of Irrigation and Urban Storm-Water Infiltration. Journal of Water Resources Planning and Management 132(5), 362-373.
Sample, D.J., Liu, J., 2014. Optimizing Rainwater Harvesting Systems for the Dual Purposes of Water Supply and Runoff Capture. Journal of Cleaner Production 75(0), 174-194.
Sample, D.J., Liu, J., Wang, S., 2012. Evaluating the Dual Benefits of Rainwater Harvesting Systems Using Reliability Analysis. Journal of Hydrologic Engineering 18(10), 1310-1321.
Schueler, T., Fraley-McNeal, L., Cappiella, K., 2009. Is Impervious Cover Still Important? Review of Recent Research. Journal of Hydrologic Engineering 14(4), 309-315.
Scully, M.E., 2010. The Importance of Climate Variability to Wind-Driven Modulation of Hypoxia in Chesapeake Bay. Journal of Physical Oceanography 40(6), 1435-1440.
Semadeni-Davies, A., Hernebring, C., Svensson, G., Gustafsson, L.-G., 2008. The Impacts of Climate Change and Urbanisation on Drainage in Helsingborg, Sweden: Combined Sewer System. Journal of Hydrology 350(1), 100-113.
Silva, C.M., Sousa, V., Carvalho, N.V., 2015. Evaluation of Rainwater Harvesting in Portugal: Application to Single-Family Residences. Resources, Conservation and Recycling 94, 21-34.
Steffen, J., Jensen, M., Pomeroy, C.A., Burian, S.J., 2013. Water Supply and Stormwater Management Benefits of Residential Rainwater Harvesting in Us Cities. Jawra Journal of the American Water Resources Association 49(4), 810-824.
Tam, V.W., Tam, L., Zeng, S., 2010. Cost Effectiveness and Tradeoff on the Use of Rainwater Tank: An Empirical Study in Australian Residential Decision-Making. Resources, Conservation and Recycling 54(3), 178-186.
Tavakol-Davani, H., Burian, S.J., Devkota, J., Apul, D., 2015. Performance and Cost-Based Comparison of Green and Gray Infrastructure to Control Combined Sewer Overflows. Journal of Sustainable Water in the Built Environment 2(2), 04015009.
Tavakol-Davani, H., Goharian, E., Hansen, C.H., Tavakol-Davani, H., Apul, D., Burian, S.J., 2016. How Does Climate Change Affect Combined Sewer Overflow in a System Benefiting from Rainwater Harvesting Systems? Sustainable Cities and Society 27, 430-438.
Teutschbein, C., Seibert, J., 2012. Bias Correction of Regional Climate Model Simulations for Hydrological Climate-Change Impact Studies: Review and Evaluation of Different Methods. Journal of Hydrology 456, 12-29.
Wang, L., Chen, W., 2014. Equiratio Cumulative Distribution Function Matching as an Improvement to the Equidistant Approach in Bias Correction of Precipitation. Atmospheric Science Letters 15(1), 1-6.
Wood, A.W., Leung, L.R., Sridhar, V., Lettenmaier, D.P., 2004. Hydrologic Implications of Dynamical and Statistical Approaches to Downscaling Climate Model Outputs. Climatic Change 62(1-3), 189-216.

Wright, L., Chinowsky, P., Strzepek, K., Jones, R., Streeter, R., Smith, J., Mayotte, J.-M., Powell, A., Jantarasami, L., Perkins, W., 2012. Estimated Effects of Climate Change on Flood Vulnerability of U.S. Bridges. Mitig Adapt Strateg Glob Change 17(8), 939-955.
Yang, Y.J., 2010. Redefine Water Infrastructure Adaptation to a Nonstationary Climate. Journal of Water Resources Planning and Management 136(3), 297-298.
Youn, S.-g., Chung, E.-S., Kang, W.G., Sung, J.H., 2012. Probabilistic Estimation of the Storage Capacity of a Rainwater Harvesting System Considering Climate Change. Resources, Conservation and Recycling 65, 136-144.
Young, K.D., Younos, T., Dymond, R.L., Kibler, D.F., 2009. Virginia's Stormwater Impact Evaluation: Developing an Optimization Tool for Improved Site Development, Selection and Placement of Stormwater Runoff Bmps. Vwrrc Sr44–2009, Virginia Tech, Blacksburg, USA.
Zahmatkesh, Z., Karamouz, M., Goharian, E., Burian, S., 2014. Analysis of the Effects of Climate Change on Urban Storm Water Runoff Using Statistically Downscaled Precipitation Data and a Change Factor Approach. Journal of Hydrologic Engineering 20(7), 05014022.

Chapter 6. An External Control Program for SWMM: Calibration, Sensitivity, and Optimization of Stormwater Control Measure Selection in Urban Watersheds.

Taken from:
Alamdari N, Sample DJ, Steinberg P (*In review*). An External Control Program for SWMM: Calibration, Sensitivity, and Optimization of Stormwater Control Measure Selection in Urban Watersheds. *Environmental Modelling & Software.*

Abstract

Significant efforts are being made to restore urban watersheds, using stormwater control measures (SCMs). Evaluation of SCM implementation often requires a hydrologic model. We enhanced an external control program for the Storm Water Management Model (SWMM) to assist this evaluation by providing automated calibration, sensitivity analysis, and cost-optimization functions. This program, RSWMM-Cost, was demonstrated using a SWMM model of the Difficult Run watershed of Fairfax County, Virginia. Calibration was conducted for the entire 150 km^2 watershed. Sensitivity analysis was performed by varying single SCM characteristics as a function of performance. Cost-optimization was applied to a 123.4 ha headwater subcatchment using a nonlinear evolutionary solver. A cost-effectiveness curve was generated, consisting of sets of SCMs that are on or near optimal. An example was provided which uses this curve to identify the best set of SCM implementation strategies for meeting required load reductions.

Keywords: cost optimization, autocalibration, sensitivity, SWMM, load reductions.

6.1 Introduction

Remediating the degradation of surface waters resulting from urban development is often accomplished through implementation of watershed-based management strategies. Stormwater control measures (SCMs) (also known as best management practices or BMPs) are some of the methods used to restore urban watersheds and achieve downstream water quality goals. Implementing SCMs can have large upfront and recurring costs. Funding for water quality programs is limited and often must compete with other urban priorities. Thus, it is essential to select the most appropriate SCM for a given watershed considering site constraints, limitation of particular SCMs, size, and cost-effectiveness. Tools that combine simulation with cost estimation

and optimization to form a simulation-optimization framework could greatly assist in the evaluation of watershed management strategies.

New methods for mitigating urban impacts have emerged in the U.S. these are known collectively as low impact development (LID). The objective of LID is to restore the hydrology and water quality of an urban site to pre-developed, natural conditions (Prince George's County, 2000). Examples of SCMs that implement principles of LID include green roofs, bioretention systems, permeable pavements, dry swales, and infiltration trenches. Each of these practices has been demonstrated to be effective in reducing runoff and pollutant loadings (Bedan and Clausen, 2009; Davis et al., 2009; Elliott and Trowsdale, 2007; Hathaway et al., 2008; Hunt et al., 2006; Myers et al., 2011).

Several computational models have been used to assess effectiveness of LID practices, these were reviewed by Eckart et al. (2017). The Storm Water Management Model (SWMM) (Huber, W.C. et al., 1988; Rossman, 2004) is a publically available model that can be used to simulate water quantity and quality in urban watersheds for event-based and continuous simulation of runoff (Elliott and Trowsdale, 2007; Zoppou, 2001). SWMM can simulate the hydrologic performance of LID practices (Lucas and Sample, 2015), based on fundamental hydrologic processes that are characterized by a series of vertical layers (Gironás et al., 2009). Hydrologic models such as SWMM are characterized by complex relationships and a relatively large number of variables and parameters. Calibration is often performed to assist in assigning appropriate values to some inputs, and assures the model is accurately representing the actual system being simulated (Eckhardt and Arnold, 2001; Gupta et al., 1998; Yapo et al., 1998). Proper calibration of hydrologic models for urban watersheds is necessary to ensure reliable prediction of water quantity and quality, and to assist in the assessment of SCMs. Manual calibration and verification can be tedious and time consuming, creating the need and motivation for more efficient methods for calibrating hydrologic models. A calibration procedure of SWMM was initially suggested by Maalel and Huber (1984). Applications of calibration methods to SWMM include expert systems (Delleur and Baffaut, 1990), knowledge-based systems (Liong et al., 1991), and genetic algorithms (GAs) by Mancipe-Munoz et al. (2014). Single-objective optimization methods have inherent limitations as they tend to lump multiple objectives into one. They may not account for various objectives of calibration such as minimizing model prediction errors and maximizing correlation between model predictions and observations (Yapo et al.,

1998). Multi-objective optimization can address these shortcomings (Gupta et al., 1998; Madsen, 2000; Reed et al., 2013; Yapo et al., 1998). While the advantages of multi-objective optimization for calibration are well documented, to date, there have been few applications of it with SWMM.

Sensitivity analysis is a simple way to find the relative influence of each input parameters on watershed model results. Research suggests that use of sensitivity analysis reduces variance in model results (Hameed, 2015). Sensitivity analysis can identify the parameters that provide the most effect on selected results during calibration (Song et al., 2015). The hydrologic performance of SCMs varies with design configurations (Ahiablame et al., 2012; Li and Babcock, 2014). Sensitivity analysis was conducted using System for Urban Stormwater Treatment and Analysis Integration (SUSTAIN) by Lee et al. (2012). The authors found that flow volume was reduced and pollutant removal efficiency increased when the SCM footprint, vertical storage, and intercepting drainage area increased. Jia et al. (2015) varied 12 key parameters of two impervious land covers (roof and pavement) within SUSTAIN. Results indicated that the washoff coefficient, and exponent to the peak flow reduction rate, was very sensitive, and the maximum buildup and washoff exponent to different pollutant loadings was also fairly sensitive. Chui et al. (2016) assessed the sensitivity of the hydrological performance of green roofs, bioretention and permeable pavements to different design parameters, including initial saturation, hydraulic conductivity, and berm height. Results indicated that green roofs were sensitive to initial saturation and hydraulic conductivity, while bioretention was sensitive to hydraulic conductivity and berm height. Permeable pavement was sensitive only to hydraulic conductivity. These limited studies indicate that more research focused upon the sensitivity of SCM performance to design parameters is needed as few tools exist for facilitating this task, which, in effect, is optimizing the parameters of a single SCM for a single performance metric and variable.

A key challenge in urban watershed management is identifying cost-effective stormwater management strategies that will meet water quality objectives. Liu et al. (2016) applied nonlinear spatial optimization techniques for selection and placement of GI SCMs using the Long-Term Hydrologic Impact Assessment-Low Impact Development (L-THIA-LID) model to reduce the impacts of urban development and climate change on runoff and water quality. Chang et al. (2011) determined optimal design strategies for green roofs and cisterns for a residential home using a cost-benefit-risk trade-off method. Jia et al. (2015); Lee et al. (2012); Sun et al. (2016)

applied SUSTAIN to urban watersheds to determine the optimal location, type, and cost of SCMs and generated a cost-effectiveness curve for meeting water quality and quantity goals. SUSTAIN is a simulation-optimization tool for optimizing the selection and sizing of SCMs in a watershed, using computation algorithms similar to SWMM but within an ArcGIS 9.3.1 interface. SUSTAIN is able to analyze SCMs applications using an optimization algorithm to find sets of cost-effective solutions and generate a cost-effectiveness curve. SUSTAIN, like SWMM, incorporates LID simulation. While SUSTAIN is similar to SWMM, it is a completely separate model that must be developed independently, within ArcGIS 9.3.1. The use of ArcGIS 9.3.1 and the Spatial Analyst extension limits the utility of SUSTAIN, because this version of ArcGIS is dated (ArcGIS 10.6 is now available). In the authors' opinion, this effort might be better spent refining and/or calibrating existing urban watershed models. Model software such as SWMM that is relatively easy to use and has a wide user base may be a better platform for an optimization tool. Several studies have coupled existing hydrological models, including the Soil and Water Assessment Tool (SWAT) and the Model for Urban Stormwater Improvement Conceptualization (MUSIC) with GA to achieve water quantity goals (e.g., peak flow reduction) (Kaini et al., 2008; Montaseri et al., 2015). Tools such as the BMP Decision Support System (BMPDSS) and the Multi-Objective, Socio-Economic, Boundary-Emanating, Nearest Distance (MOSEBEND), have been developed to optimize location, and selection of SCMs to meet runoff reduction goals (Cano and Barkdoll, 2016; Jia et al., 2012). BMPDSS is unable to simulate SCMs such as permeable pavement, and no automated calibration capability is available. MOSEBEND focuses solely on runoff reduction goals and does not consider pollutant removal efficiency, which is important for effective stormwater pollution mitigation strategies.

Zhang and Chui (2018) commented that coupling SWMM with optimization is straightforward because SWMM has a simple structure, open source features, and an LID module. Optimization tools such as SWMM-GA, SWMM-TOPSIS, SWMM-PSO, and GreenPlan-IT were built upon SWMM (Sebti et al., 2016; Song and Chung, 2017) and were demonstrated to be effective for urban drainage planning and design. Baek et al. (2015); Duan et al. (2016); Jung et al. (2016); Li et al. (2015) coupled optimization methods with SWMM to find the optimized size of SCMs, including detention ponds and permeable pavement to minimize local flooding. Each of these studies focuses upon a single rather than multiple objectives, such as maximizing runoff reduction, and/or maximizing reduction in multiple pollutant loadings (i.e.

TSS, total nitrogen (TN), and total phosphorous (TP)). The ability to optimize selection and size of individual SCM using an existing SWMM model of a realistic, medium-sized catchment (200-400 ha) remains a research need. This scale is large enough to be realistic, but not so large that the range of potential SCM implementation sites becomes overly large and impractical for a simple demonstration. The change in focus from controlling peak runoff to reducing runoff volume tends to favor decentralized SCMs such as bioretention. This results in a large increase in the numbers of SCMs that must be evaluated compared with traditional practices such as retention ponds, which tend to be fewer in number. A balance between upstream GI practices and downstream ponds should be assessed. Developing an easy to use tool that performs these tasks and can wrap around the current version of SWMM, which is arguably the most widely used urban watershed model, without altering its source code would be novel, and would be beneficial as previously developed models could be reused.

The goal of this research was to meet this challenge by adapting an existing tool, RSWMM, and enhancing it with respect to three specific objectives. First, a module was developed for calibrating SWMM to observed data using multi-objective optimization. Second, a structured means of performing sensitivity analysis was developed, so that water quality performance of single SCMs could be assessed as a function of various design characteristics. Third, cost-optimization was incorporated using a nonlinear evolutionary solver, so that the most cost-effective sets of SCMs for a specific location in the watershed based upon SCM design characteristics and physical constraints could be identified. Cost-optimization was based on a multi-objective consideration, i.e., runoff volume, and multiple pollutants (TSS, TN, and TP). The modified program, RSWMM-Cost was applied to the Difficult Run watershed of Fairfax County as an example.

6.2 Materials and Methods

6.2.1 Study Area

In previous research, the authors refined, extended, and calibrated a SWMM model of Difficult Run, a 150 km^2 watershed, the largest watershed in Fairfax County, a suburb of Washington, DC (Alamdari et al., 2017). Difficult Run flows to the Potomac River, which then drains to the Chesapeake Bay. The watershed is within the Piedmont physiographic province of Virginia (**Figure 6.1**). The watershed was selected for this study because: 1) an existing SWMM

model was available for the watershed, and 2) it is part of the greater Chesapeake Bay watershed, and is thus subject to reduction of sediment and nutrients (TN and TP) as part of the total maximum daily load (TMDL) to prevent eutrophication of the estuary (USEPA, 2010). Land use/land cover (LULC) within the greater Difficult Run watershed is dominated by residential development, including estate, low, medium, and high densities (approximately 57%) (Fairfax County, 2007). Approximately 18.4 % of the total watershed covered by impervious surfaces (Fairfax County, 2007). The watershed consists of 18 named tributary sub-watersheds. Watershed slope is low to moderate with an average slope of 7.2%. Soils in the watershed range from sandy loam to clay loams with silt loams being the most dominant soil group, with moderate infiltration properties. Water quality and streamflow monitoring have been conducted in this watershed by the U.S. Geological Survey in partnership with Fairfax County for the past seven years (Jastram, 2014). Results have indicated increased streamflow and pollutant loadings as the result of urban development and its impact of runoff, and the associated streambank erosion and channel erosion. We selected a 123.4 ha headwater watershed as an application test case for the sensitivity analysis and cost-optimization modules (**Figure 6.1**). The details of headwater subcatchment, including parking lots, buildings, conduits, and nodes are shown in **Figure 6.2**. Approximately 33.2% of the headwater subcatchment is currently covered by impervious surfaces. Subcatchment slope is low to moderate with an average slope of 6%. Soils in the subcatchment range from sandy loam to clay loams with silt loams being the most dominant soil group, with moderate infiltration properties.

<THIS SPACE LEFT INTENTIONALLY BLANK>

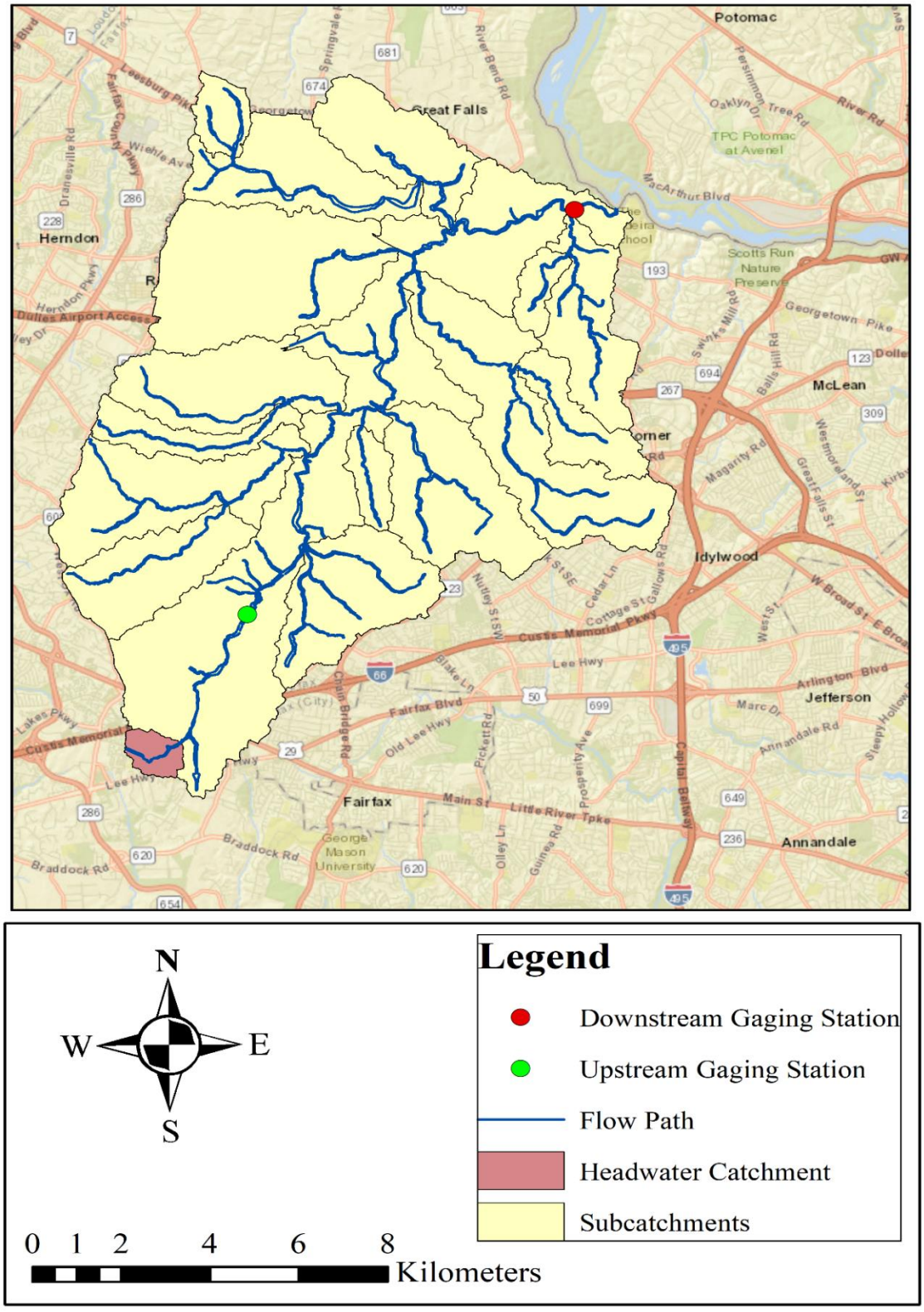

Figure 6.1. Difficult Run Watershed and subcatchment locations.

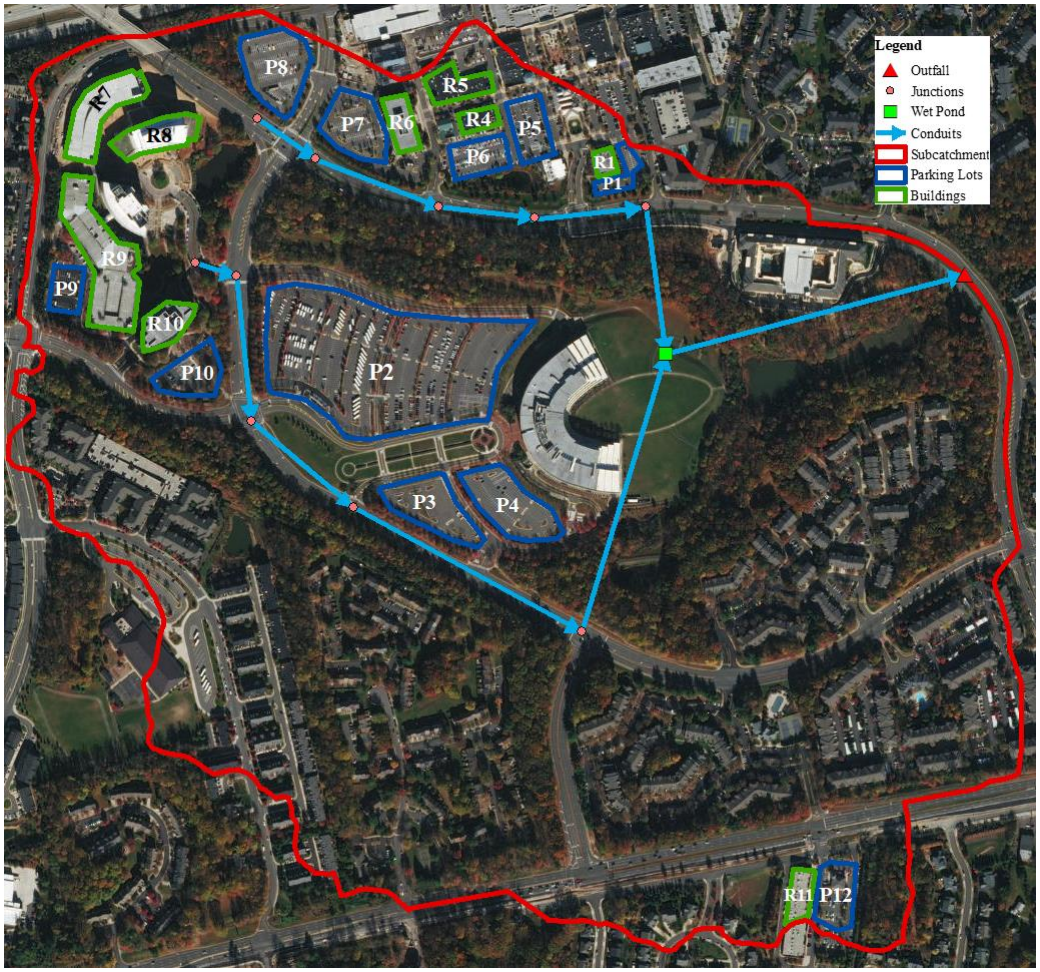

Figure 6.2. Difficult Run Watershed and subcatchment locations.

6.2.2 Hydraulic/Hydrologic (H/H) and Water Quality Modeling

SWMM version 5.1.012 was used for hydrologic and water quality modeling. SWMM is a lumped model that can be run for both single event and continuous simulation (Huber, W. C. et al., 1988; James et al., 2010; Rossman, 2004). SWMM predicts runoff, water surface elevations, and water quality concentrations and loadings, which in the case of our example include TSS, TN and TP. Water quality in SWMM was modeled using an estimated event mean concentration (EMC), or $C_{x,i+1}^{*}$ washoff during runoff events and user-defined treatment equations of the form $C_{\mathrm{x},i+1} = C_{x,i+1}^{*} + \left(C_{\mathrm{x},i} - C_{x,i+1}^{*}\right)e^{-10^{-4}\left(\frac{\mathrm{DT}}{D}\right)}$ for storage SCMs such as retention ponds as described in Alamdari et al. (2017) where: C_X is the concentration of constituent x in mg·L^{-1}, D is water depth in m, DT is time step in seconds, i and i+1 represent the previous and current time, and $C_{x,}^{*}$is minimum residual concentration of constituent x in mg·L^{-1}. This relation follows the

irreducible concentration principle, i.e., reduction of a pollutant follows an exponential rate, reaching an asymptote as concentrations get smaller. EMCs for TSS, TN, and TP were set at 40 mg/L, 2.9 $mg \cdot L^{-1}$, and 0.27 $mg \cdot L^{-1}$, respectively, based on Virginia monitoring data (Hirschman et al., 2008).

6.2.3 RSWMM-Cost Development

To efficiently perform calibration, sensitivity analysis and cost-optimization without altering the SWMM source code, an external, freely available control program is needed. R is an open source, freely available system that can be used for statistical analysis and programming and has been successfully used in hydrological modeling and its capabilities are well recognized (Fuka et al., 2014). R is compatible with most operating systems. Because of these capabilities, R was chosen for use in this study for development of a control module that could execute SWMM simulations repetitively, change key parameters according to user direction; and assess results by a post processor.

An existing R code known as RSWMM (Steinberg, 2014) was identified. As outlined in the objectives, several enhancements were added as modules to this program to create RSWMM-Cost. These included multi-objective optimization for automatic calibration, incorporating sensitivity analysis, and multiple objective cost-optimization. In addition, event separation, and a graphical post-processor was added to view exceedance and cost-effectiveness curves of the output.

6.2.3.1 Frequency Calibration Procedure

Calibration of the Difficult Run watershed model was conducted by varying identified sensitive parameters, as described in the following section. Hourly rainfall data were disaggregated into 15-min time steps using NetSTORM (CDM Smith Inc., 2015). Then, the simulation results were aggregated to an hourly time series and SWMM was calibrated with respect to runoff quantity and quality in upstream and downstream sub-catchments. Two gaging stations located in upstream and downstream subcatchments (location shown in **Figure 6.1**) were used for calibration and verification.

The autocalibration tool embedded within this RSWMM-Cost module utilizes a multi-objective optimization package, Non-dominated Sorting Genetic Algorithm II (NSGA-II). NSGA-II provides functions for box-constrained multi-objective optimization. Three objective

functions—coefficient of determination (R^2), Nash Sutcliffe Efficiency (NSE), and Percent Bias (PBIAS)—were used. Calibration and verification were performed on the 2010 and 2013 data, respectively, with a maximum number of iterations set at 500. The reader is referred to Alamdari et al. (2017) for more description of these methods.

6.2.4 Sensitivity Analysis

SA was conducted in two separate stages. First, sensitivity analysis was performed to identify which parameters would be most effective in minimizing differences between observed and predicted results during calibration and validation. Second, SA was performed to assess the hydrologic and water quality performance of SCMs with respect to design and watershed characteristics (i.e., underdrain system capacity, soil media depth, and contributing area). Monte Carlo simulation was used to produce simulation results with SCM design variables. Then the relationship between the changing parameters (SCM design configurations), and the four constituents (TSS, TN, TP and runoff volume) was explored by using the Breiman's Random Forest (Breiman, 2001) algorithm Breiman's Random Forest can be used to identify the most influential parameters in the model. Random Forest is a non-parametric ensemble decision tree technique which identifies the most important parameters in terms of each constituent and runoff. This method develops a large number of regression trees, with each tree based on a bootstrapped sample of the dataset. Random Forest models are well suited to datasets with non-linear relationships and are insensitive to outliers and noise (Breiman, 2001). No studies, to date, exist to use random forest to find the most influential SCM design characteristics in SWMM.

Each of these processes was automated in RSWMM-Cost. A sensitivity analysis was then conducted to assess the changes in runoff volume and load reduction by varying the most influential SCM design characteristics, and a plot produced of the subsequent relationship. Relative sensitivity was computed from Equation 1:

$$\text{Relative Sensitivity} = \left(\frac{\partial R}{\partial P}\right)\left(\frac{P}{R}\right) \quad (6\text{-}1)$$

Where ∂R is the difference between the original and the new model output, ∂P is the difference between original and adjusted parameter value, R is the original model output, and P is the original value of parameter of interest (James and Burges, 1982).

6.2.5 Cost Optimization

The costs of SCM implementation were estimated using an spreadsheet-based cost estimation procedure developed by Johnson and Sample (2017) based upon work by King and Hagan (2011) and Weiss et al. (2007), after updating the cost base to January, 2018 (Engineering News Record Construction Cost Index of 10,878). The total present cost (TPC) equation general form is presented as Equation 2:

$$TPC = \beta_0(WQV)^{\beta_1} \quad (6\text{-}2)$$

Where TPC is in U.S. dollars and represents the total cost over 20 years of operation, WQV is the water quality volume in m^3, and β_0 and β_1 are constants. WQV in the SCMs is calculated by multiplying the treatment area and storage depth. Storage depth was calculated for GI by summing the individual layer depths multiplied by their void ratios.

The same cost database used by Johnson and Sample (2017) (adjusted for 2018) was employed to drive SCM cost estimates. **Table 6-1** presents the constant values (β_0, β_1) used to estimate the costs associated with each SCM. Costs for green roofs are estimated to be 215.3 per m^2 (Scholz-Barth, 2001).

Table 6-1. Constants in equations, based on King and Hagan (2011), updated to January 2018.

SCMs	2005 β0	2018 β0	β1
Wet Pond	4398	6025	0.512
Bioretention	1542	2112	0.776
Dry Swale	1542	2112	0.776
Permeable Pavement	2237	3084	0.817

The spreadsheet costing procedure is callable by RSWMM-Cost; and provides flexibility for the user to modify this procedure as more information and more detailed costing models become available.

Next, an optimization module was developed as part of RSWMM-Cost to identify the groups of the most cost-effective SCMs in the modeled watershed. NSGA-II was employed as the optimization algorithm. The optimization problem formulation can be mathematically expressed as:

$$\text{Minimize } \sum_{i=1}^{n} cost(SCM)_i$$

$$\text{Maximize } \sum_{j=1}^{n} (Runoff\ Reduction)_j$$

$$\text{Maximize } \sum_{j=1}^{n} (TSS\ Reduction)_j \tag{6-3}$$

$$\text{Maximize } \sum_{j=1}^{n} (TN\ Reduction)_j$$

$$\text{Maximize } \sum_{j=1}^{n} (TP\ Reduction)_j$$

Subject to:

$$x_{1,j}, x_{2,j} \leq .05 \cdot PA_j \text{[1]} \tag{6-4}$$

$$x_{3,j} \leq .5 \cdot PA_j \text{[2]} \tag{6-5}$$

$$x_{4,k} \leq RA_k \text{[3]} \tag{6-6}$$

$$x_5 \leq 8{,}096 \text{[4]} \tag{6-7}$$

$$x_{1,j}, x_{2,j}, x_{3,j} \geq \begin{Bmatrix} 0, if\ not\ chosen, (\alpha_{i,j} = 0) \\ 101, if\ chosen\ (\alpha_{i,j} = 1) \end{Bmatrix} \text{[5]} \tag{6-8}$$

$$x_{4,k} \geq \begin{Bmatrix} 0, if\ not\ chosen, (\alpha_{i,j} = 0) \\ 101, if\ chosen\ (\alpha_{i,j} = 1) \end{Bmatrix} \text{[6]} \tag{6-9}$$

$$d_5 x_5 \geq WQ_V \text{[7]} \tag{6-10}$$

$$\sum_{j=1}^{n} \alpha_{i,j} = 1 \text{[8]} \tag{6-11}$$

$$x_{i,j}, x_{4,k}, x_5 \geq 0 \text{[9]} \tag{6-12}$$

[1] Maximum area of bioretention and dry swales, m^2.
[2] Maximum area of permeable pavement, m^2.
[3] Maximum area of green roof, m^2.
[4] Maximum area of retention pond, m^2.
[5] Minimum area of bioretention, dry swales, and permeable pavement, m^2.
[6] Minimum area of green roof, m^2.
[7] Minimum volume of retention pond, m^3.
[8] Restriction on bioretention, dry swale, permeable pavement; a given parking lot (j) can only have one SCM.
[9] Nonnegativity constraint.

Where:

$x_{i,j}$=Area of SCM i for parking area j.
$x_{4,k}$=Area of Green Roof i for building roof k.
$\alpha_{i,j}$=Binary variable, 0 or 1.
i=1, 2 ….m, where m is the m^{th} SCM type (i.e., bioretention, dry swale, permeable pavement), m=4.
j=1, 2……n, where n is the n^{th} source area (parking area).
k=1, 2……o, where o is the o^{th} source area (building).
WQ_V= Water quality volume, m^3.
PA_j=Parking lot j area in m^2.
RA_k=building roof j area in m^2.
d_5=depth of pond (SCM_5), fixed, 3.1 m.

Where $(SCM)_i$ represents the SCMs within the watershed, $(Runoff\ Reduction)_j$ *(%)*, is the runoff reduction at the watershed outlet, $(TSS\ Reduction)_j$ *(%)* , $(TN\ Reduction)_j$ *(%)*, $(TP\ Reduction)_j$ *(%)*, are the TSS, TN, and TP reduction at the watershed outlet, respectively. The SCM size, type, and numbers, runoff reduction, pollutant loads reduction, and SCM costs are saved sequentially in a spreadsheet after each model run. For potential locations in the watershed, user defined the feasible range of SCMs and configuration parameters. Then, RSWMM-Cost was run; which, once completed plotted the SCM cost-effectiveness curve.

Finding suitable locations for SCMs in the watershed is a complex process influenced by physical measures, such as slope of the contributing drainage area, soil and land use characteristics. In addition, it is helpful to consider minimum and maximum areas of each SCM that bear on the feasibility of using such a device at a given location. The list of constraints and rules for potential locations and feasible range of SCMs and configuration parameters is provided in **Table 6-3**. Potential areas for SCM implementation were estimated for the selected catchment using available data and spatial analysis. We assessed implementation of decentralized SCMs—bioretention, permeable pavement, dry swale, and green roof—in coordination with a single retention pond at the subcatchment outlet. The width and the depth of each SCM specification were fixed, but the areas of the SCMs were set as design variables exclusively for the entire watershed. Permeable pavement, bioretention and dry swale were considered for each parking lot, and green roofs were considered for each flat roofed commercial building. Most of the property and buildings in the headwater subcatchment are currently owned

by Fairfax County. The number and area (or length) of each SCM in the catchment was optimized as a design variable while the width, depth, and other SCM parameters were pre-specified. The SCM constraint table used by Johnson and Sample (2017) was used. Iterative searches were performed using the optimization engine to identify sets of cost-effective solutions. The search process depended on the cost and SCM treatment effectiveness of each SCM or combination evaluated. The cost-effective curve of the best solutions was then plotted.

Table 6-2. Rules used for determining SCMs used to retrofit impervious areas in the selected headwater watershed.

SCM siting rules	
1.	All commercial, flat-roof buildings were considered for potential green roof retrofits.
2.	All green roof installations were either 1) discharged to nearby parking lot bioretention or dry swale installations, in series; or 2) conveyed directly to main storm drainage conveyance and the pond.
3.	All parking areas were considered for permeable pavement, bioretention, and dry swales. In each parking lot, bioretention and dry swales were not mixed, i.e., only one practice was used.
4.	The maximum size of a permeable pavement used to retrofit a parking lot was set at 50% of the parking lot area.
5.	For parking lots being considered for retrofit by bioretention or dry swales, the maximum area set aside for bioretention and/or dry swale used to retrofit a parking lot was set at 5% of the parking lot area.
6.	The minimum size of a permeable pavement, dry swale, and/or bioretention used to retrofit a parking lot was set at 101 m^2. There is an option of having no SCM in any given parking lot.
7.	The minimum size of a green roof used to retrofit a building was set at 101 m^2.
8.	The resulting net runoff from the treated areas and untreated streets and pervious areas was piped directly to a wet pond.
9.	The minimum size of the wet pond was set at what was needed to effectively treat a water quality event (25.4 mm).

6.3 Results and Discussions

6.3.1 Calibration and Verification

Calibration and verification were performed using the data from upstream and downstream gauging stations. Hydraulic width, imperviousness, and depression storage for impervious and previous areas were the most sensitive parameters for calibration; each parameter was adjusted to improve agreement between observed and predicted runoff. Adjusting the

hydraulic width of some of the smaller catchments in the watershed did not have much impact on runoff. Unsurprisingly, simulations using SWMM have found that runoff is most sensitive to imperviousness (Barco et al., 2008; Delleur and Baffaut, 1990; Liong et al., 1991; Tan et al., 2008). Depression storage for impervious and pervious did not have significant effects on the results. Calibration and verification results based on runoff for downstream gaging station are shown in **Figure 6.3**.

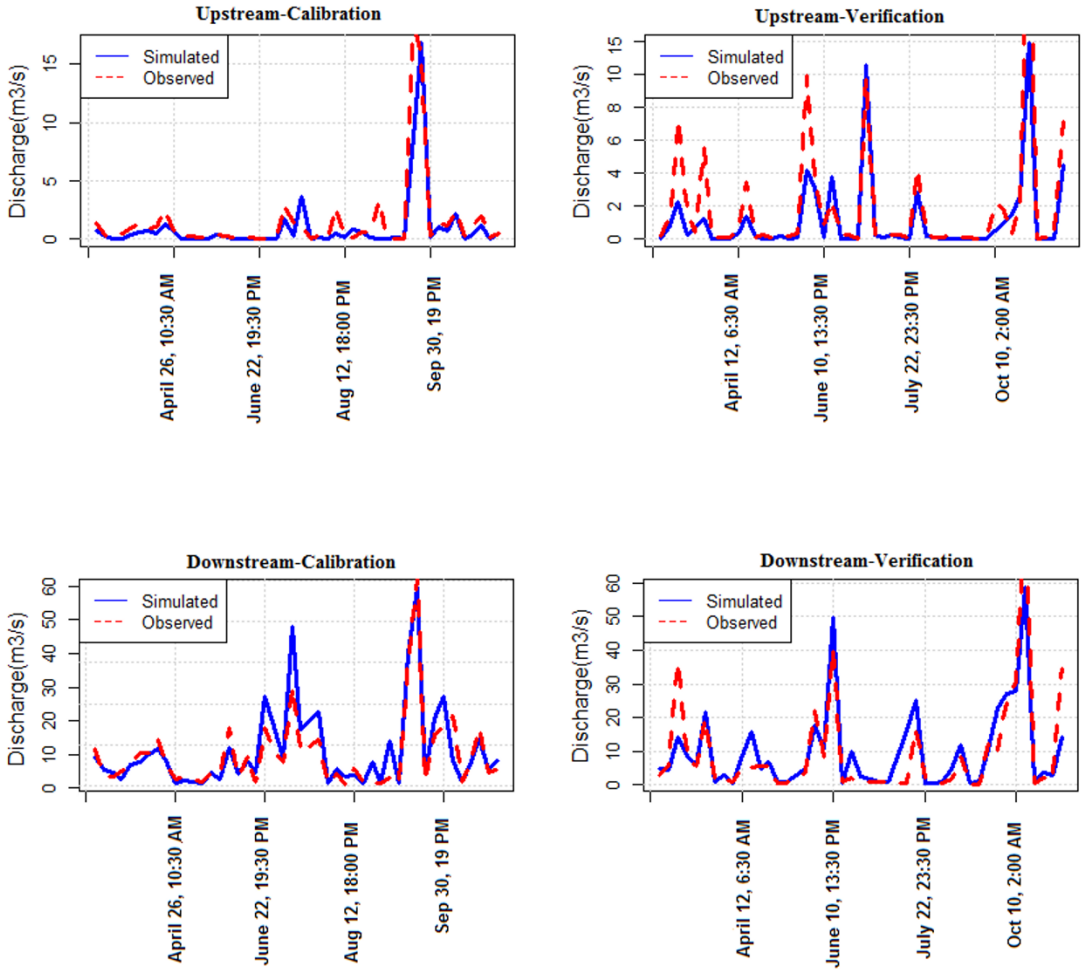

Figure 6.3. Calibration and validation results at the Difficult Run upstream and downstream gauging stations.

The results indicate an underestimation of runoff in the verification period especially in wet events that might be due to possible weaknesses of some processes in the SWMM model such as groundwater recharge. Since SWMM primarily focuses on surface runoff simulation, flows that are produced via infiltration loss and routed through subsurface might not be fully

captured and simulated by the model. Calibration and verification comparisons of predicted and observed runoff were presented in **Table 6-3**. According to the criteria of Santhi et al. (2001); Van Liew et al. (2003); and Moriasi et al. (2007), the simulated and observed runoff show a good level of agreement on an event basis.

Table 6-3. Results of hydrologic calibration and verification for Difficult Run upstream and downstream gauging stations.

Gage Location	Period	Model Performance		
		R^2	NSE	PBIAS
Upstream	Calibration	0.74	0.71	−17.8%
	Verification	0.71	0.65	6.1%
Downstream	Calibration	0.78	0.73	13.3%
	Verification	0.72	0.69	15.4%

* R^2: Coefficient of Determination.
* NSE: Nash-Sutcliffe Efficiency Coefficient.
* PBIAS: Percent Bias.

A simplified assessment of performance was also conducted using R^2 by comparing predicted values with station annual loads in the absence of sufficient observed water quality data. Model results for TSS, TN, and TP showed an R^2 of 0.61, 0.57, and 0.58, during calibration at the upstream gauging station; and an R^2 of 0.65, 0.59, and 0.61, during calibration at the downstream gauging station. Prediction of water quality seems less accurate than runoff (based on R^2 during the calibration), primarily due to limited water quality data available, yet the calibration results indicated that observed and predicted data are in fair agreement and the model can be used for water quality simulation. Performance of the model through calibration for TSS, TN, and TP is illustrated in **Figure 6.4 a** and **Figure 6.4 b** for upstream and downstream gage locations, respectively.

<THIS SPACE LEFT INTENTIONALLY BLANK>

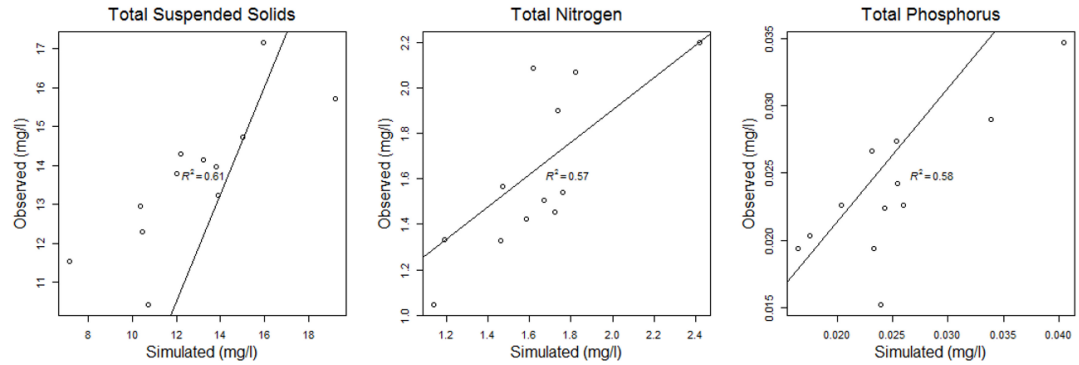

(a)

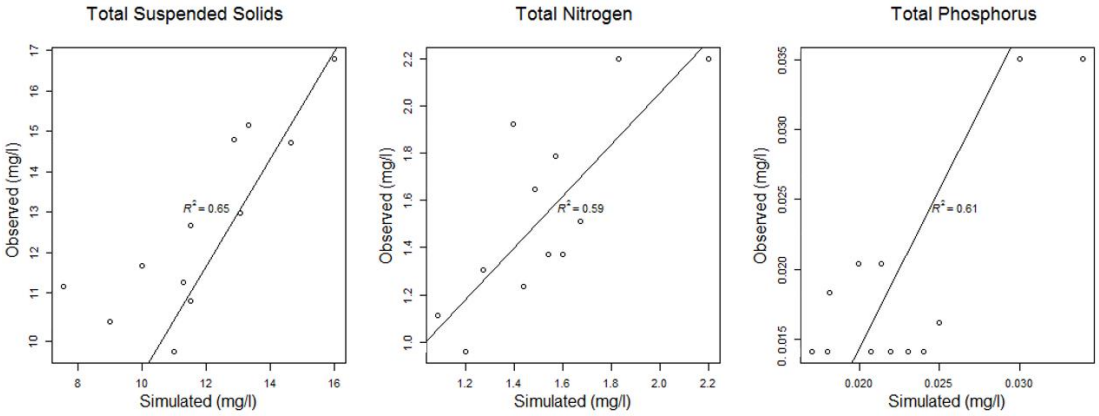

(b)

Figure 6.4. (a) Water quality calibration results at the Difficult Run upstream gauging station; (b) Water quality calibration results at the Difficult Run downstream gauging station.

6.3.2 Sensitivity Analysis

The sensitivity of the hydrologic performance to SCM design configurations (underdrain system capacity, soil media depth and contributing area) was analyzed using 1000 Monte Carlo simulations to produce randomized SCM design variables for bioretention. Then, the relationship between the SCM design configurations, and the four constituents (TN, TP, TSS and runoff volume) was explored by using the Random Forest algorithm described earlier. A Monte Carlo simulation was then run on each sensitive parameter to find the relationship between percent load and runoff reduction and the changed parameters. The results for runoff, TSS, TN, and TP are presented in the **Figure 6.5** and **Figure 6.6**.

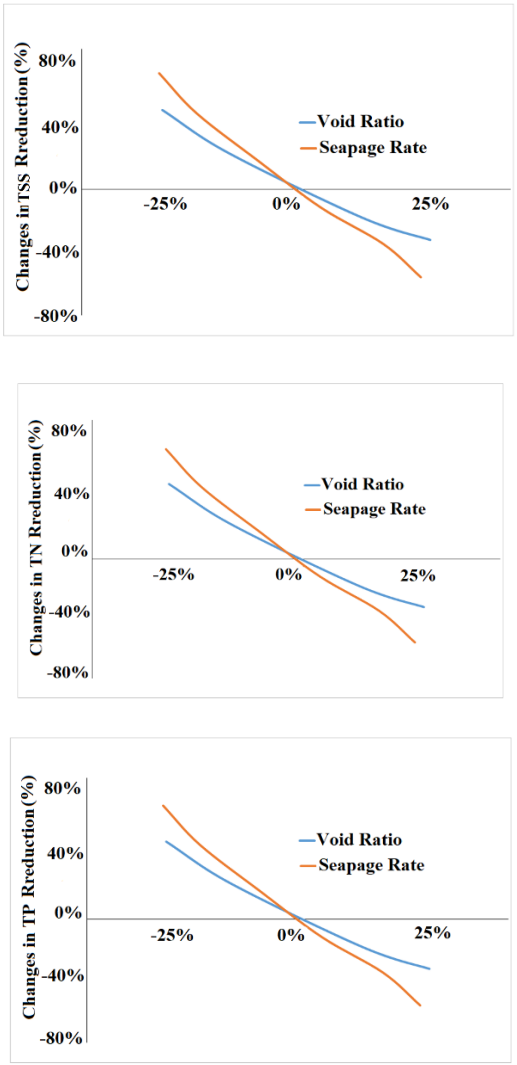

Figure 6.5. Sensitivity analysis for pollutants in Bioretention.

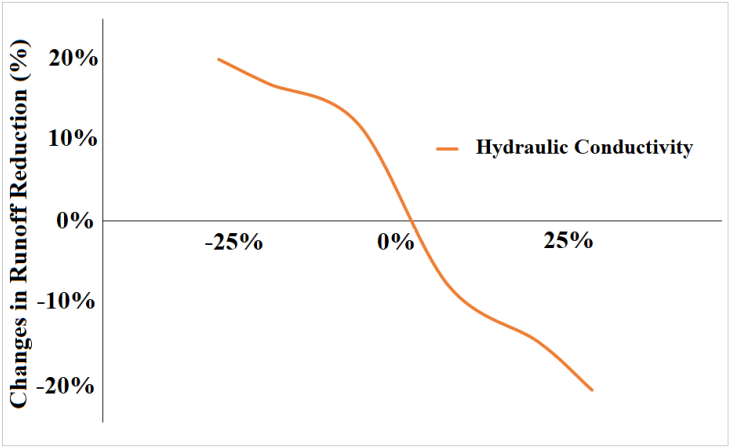

Figure 6.6. Sensitivity analysis for pollutants in Bioretention.

The results indicated that the most important parameters in terms of each constituent for bioretention include void ratio, and seepage rate in soil media. In terms of runoff, the most important parameter was hydraulic conductivity. Seepage rate is the rate at which water seeps into the native soil below the layer ($mm \cdot hr^{-1}$). The results showed that the higher hydraulic conductivity, the higher runoff reduction. This is because a high hydraulic conductivity allows more rainfall to infiltrate into the bioretention, which is then further infiltrated into the surrounding soil, increasing the overall water retention. Seepage rate also exerts a similar influence for pollutant loads as pollutant loads seep into the soil at higher rate.

6.3.3 Cost-optimization

Next, SCMs were selected and sized, considering their cost and modeled effectiveness. We optimized the selection, placement, and size of our selected group of SCMs for a specific small watershed. Site-specific hydrologic modeling parameters were derived from the existing calibrated hydrologic model developed by Alamdari et al. (2017). The derived modeling parameters were surface depression storage, roughness coefficient, and Green Ampt infiltration parameters (i.e., hydraulic conductivity, suction head, and initial moisture deficit). It is important to note that optimization should only proceed after the model is adequately calibrated and verified but models used for planning purposes are not often calibrated. To quickly assess a wide range of SCM implementation scenarios, cost-effectiveness curves based on runoff and load reductions were developed (**Figure 6.7** and **Figure 6.8**).

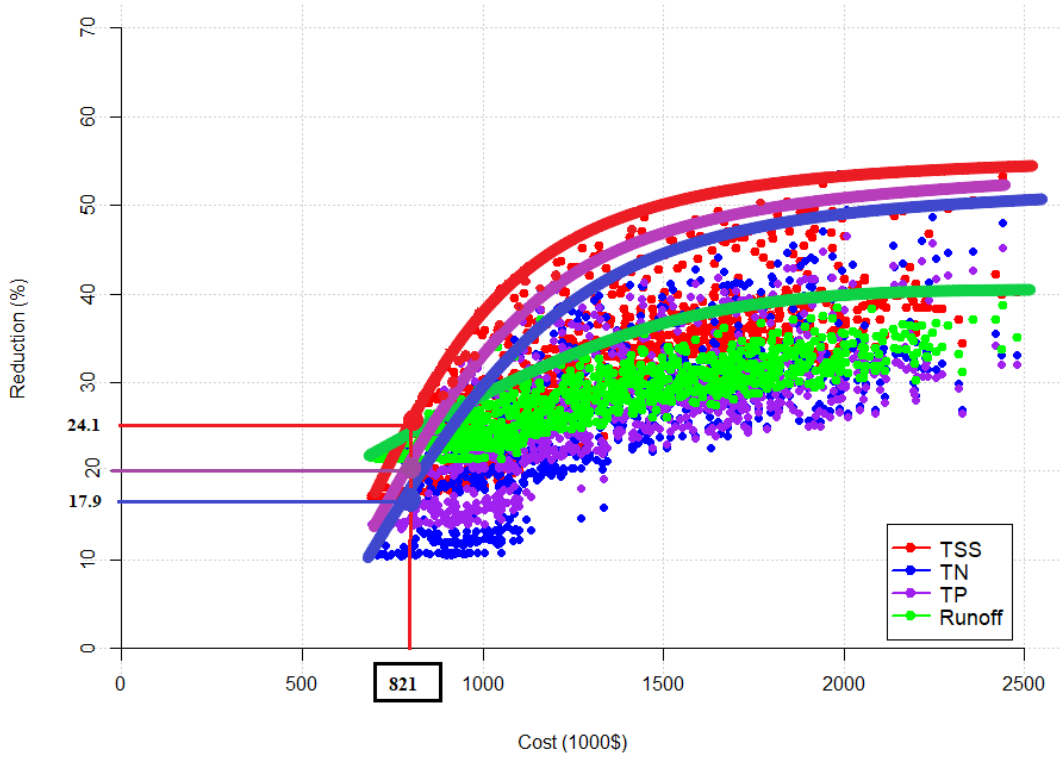

Figure 6.7. Cost-effective curve for a wide variety range of SCMs, with a single retention pond.

<THIS SPACE LEFT INTENTIONALLY BLANK>

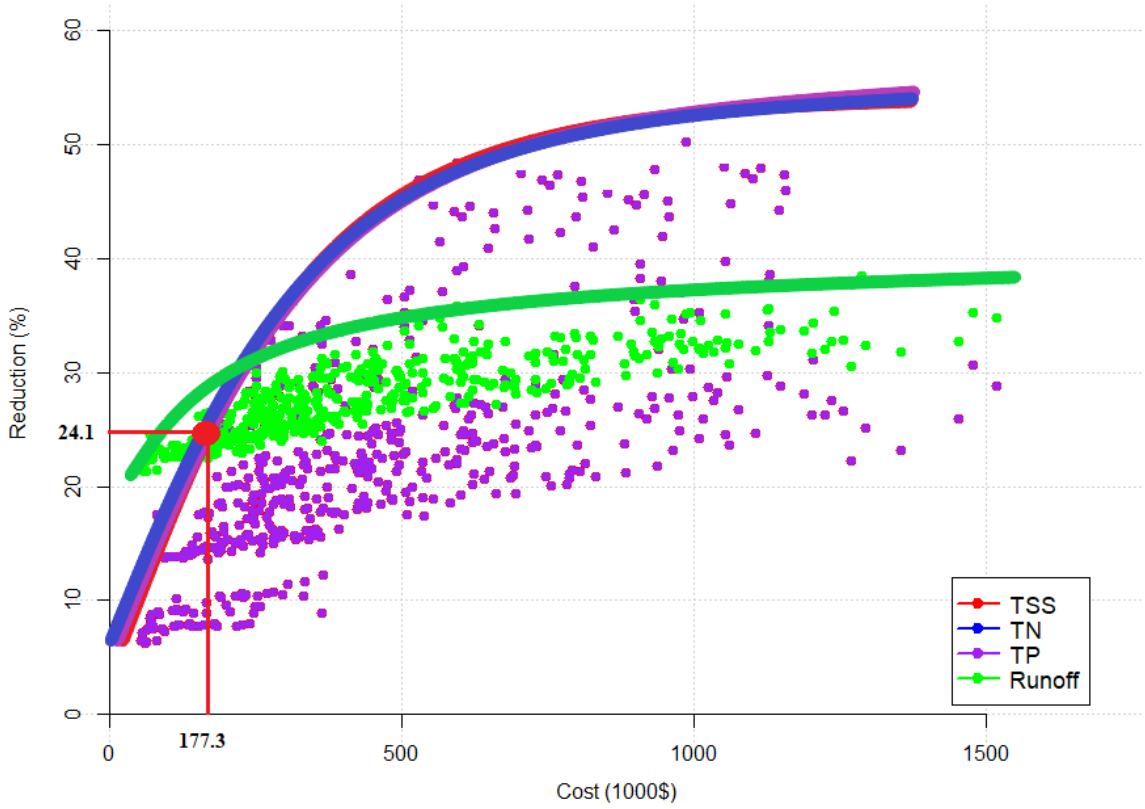

Figure 6.8. Cost-effective curve for a wide variety range of SCMs without a retention pond.

Each data point in **Figure 6.7** and **Figure 6.8** represents the percent load/runoff reduction developed from the output of a single SWMM run, and the associated cost of a SCM implementation scenario. The cost-effectiveness curve provides a relationship between the SCM cost and reduction effectiveness which aims at identifying the cost-effective solutions within the specified target range. The curves were fit into the points that are associated with the minimum costs for runoff, TSS, TN, and TP. The detailed modeling results of each scenario from RSWMM-Cost, including the size, type and number of individual SCMs are provided as an MS Excel database in the Appendix B. Solutions on or near the curves in **Figure 6.7** and **Figure 6.8** represent optimal (i.e., least-cost) or near-optimal solutions for a wide range of removal effectiveness on the basis of load (TSS, TN, or TP) and/or runoff reductions. The reader may note there are many different GI and retention pond configurations; selection of which depends upon available funding and water quality goals.

A modest but specific and practical example using these curves is provided next. Stormwater is regulated by the National Pollutant Discharge Elimination System (NPDES) Municipally

separate storm sewer system (MS4) permitting program, in this case, the MS4 program is operated by Fairfax County under the Virginia Stormwater Management Program (VSMP) permit #VA0088587 (Virginia DEQ, 2015). Chesapeake Bay requirements have been added to the permit at its last renewal. This permit requires a reduction in existing loading for TSS, TN, and TP for the current permit cycle ending in 2020, and the next permit cycle ending in 2025; the latter cycle incurs a sevenfold increase in required reductions; we chose this latter period for this example. One reason the 123.4 ha watershed was selected was that much of the land is owned by the County, making it potentially easier to implement solutions and maintain the retrofitted SCMs. For our hypothetical example, we assumed that this watershed would offset required load reductions in other Difficult Run watersheds by a ratio of 4:1, enabling Fairfax County to leverage its investment if it so chooses. This results in a required reduction of the 123.5 subcatchment of 174 kg of TN, 14.2 kg of TP, and 15,569 kg of TSS or a reduction of 23.9%, 10.4%, and 13.4%, respectively. The optimal combination of SCMs were saved in spreadsheet and are presented as Table A-1. Those solutions near the respective TSS, TN, and TP curves (**Figure 6.7**) represent configurations that are likely at or near the minimum costs needed to achieve these TSS, TN, and TP reductions. While runoff reduction is not an explicit goal required by the permit, since it is a goal of the VSMP, it is thus provided in **Figure 6.7**. The results indicate that for obtaining the solution to meet all the criteria are shown in circles, a 167.2 m^2 dry swale followed by a 4,108.6 m^2 retention pond will need to be installed at a cost of $820,981 to meet required reductions in TSS, TN, and TP (**Table 6-4**). The reader should note that achieving a single purpose objective, i.e., meeting the % reduction in either TSS, TN, or TP is less expensive than meeting all three simultaneously (these solutions are also provided in **Table 6-4**. If no retention pond is included, and reductions are met completely with GI practices, optimal or near-optimal solutions can be found in **Figure 6.8**. Achieving the same reductions in TSS, TN, and TP as in the previous example will require a 186.6 m^2 dry swale and a 207.2 m^2 bioretention cell at a cost of $177,227 (**Table 6-5**).

Table 6-4. Best Solutions to meet TSS, TN, and TP requirements[1].

Solutions	SCMs	P3 (m^2)	P4 (m^2)	Pond (m^2)	Cost ($)
1	Bioretention Permeable Pavements Dry Swales	209.2			

	Green Roofs Retention		3612.3	788,425
2	Bioretention Permeable Pavements Dry Swales			
	Green Roofs Retention		3718.9	705,957
3	Bioretention Permeable Pavements Dry Swales			
	Green Roofs Retention		3718.9	705,957
ALL	Bioretention Permeable Pavements Dry Swales	167.2		
	Green Roofs Retention		4108.6	820,981

[1]P1, P2, P5, P6, P7, P8, P9, P10, P12, R1, R4, R5, R6, R7, R8, R9, R10, and R11 had no SCMs installed for the best solution.

<THIS SPACE LEFT INTENTIONALLY BLANK>

Table 6-5. Best Solutions to meet TSS, TN, and TP requirements[1].

Solutions	SCMs	P2 (m^2)	P3 (m^2)	P4 (m^2)	P12 (m^2)	Pond (m^2)	Cost ($)
1	Bioretention				145.9		
	Permeable Pavements						
	Dry Swales			210.1			
	Green Roofs						
	Retention						163,435
2	Bioretention	103.0					
	Permeable Pavements						
	Dry Swales						
	Green Roofs						
	Retention						53,615
3	Bioretention		149.2				
	Permeable Pavements						
	Dry Swales						
	Green Roofs						
	Retention						71,479
ALL	Bioretention		207.2				
	Permeable Pavements						
	Dry Swales				186.6		
	Green Roofs						
	Retention						177,227

[1]P1, P5, P6, P7, P8, P9, P10, R1, R4, R5, R6, R7, R8, R9, R10, and R11 had no SCMs installed for the best solution.

Comparing these suggested mix of SCMs, it is apparent that green roof solutions are not close to either cost effectiveness curve compared to other SCM combinations. The reason for this is that green roofs do not treat runoff from the surrounding impervious areas, only treats what falls on it. Also, while green roofs reduce runoff through evapotranspiration, this is much less than the infiltration from a comparably sized bioretention or dry swale (Chui et al., 2016). Green roofs are also much more expensive than other SCMs. Thus, implementing dry swale and bioretention are typically more cost-effective for runoff volume and load reduction. Permeable pavements are not as cost-effective as bioretention cells, dry swales and retention ponds because the cost of permeable pavement is much higher. Permeable pavements do not also provide as many benefits in energy savings, urban heat island effect mitigation and carbon dioxide

reduction, etc. (Chui et al., 2016). The large difference in cost between solutions with and without a retention pond indicate that GI practices may be a more economical means of achieving TSS, TN, and TP reduction goals. However, it should be pointed out that the retention pond provides significant storage in a single SCM and can have a large effect on hydrology immediately downstream, thus providing significant flood control benefits which are not considered in this simple analysis.

The study watershed is part of the greater Chesapeake Bay watershed, where significant efforts have been and are being made to reduced pollutant loads to protect the estuary from eutrophication. Those strategies that meet the water quality and quantity goals are identified for a small headwater subcatchment. This simple example was chosen to illustrate the use of the RSWMM-Cost software. There are many directions that could be chosen for future improvements, including providing more robust life cycle cost analysis including the cost of installing, operating, maintaining, and replacing a SCM throughout its expected lifetime. A major revision of SWMM (6.0) has been underway; one potential improvement could include the ability to model treatment performance of GI. The results of this study illustrate the potential usefulness of RSWMM-Cost in guiding selection of alternative SCM implementation strategies with a limited budget.

6.4 Summary and Conclusions

A hydrologic/hydraulic/water quality model (SWMM) was used to simulate a continuous rainfall-runoff response in an urban watershed, Difficult Run, Fairfax, Virginia. The model was then calibrated to observed conditions for peak flows, runoff volume, and water quality (TSS, TN, and TP) using two gauging stations in the watershed. To evaluate potential variations in the effectiveness by adjusting SCM design specifications, a sensitivity analysis was conducted. The goal of this research was to develop a method for selecting combinations of SCMs that are the most cost-effective at improving runoff water quality. The Difficult Run watershed is part of the Chesapeake Bay estuary which is experiencing eutrophication due to excessive loading of nutrients and sediment. The USEPA has established a TMDL for the Chesapeake Bay, limiting N, P, and sediment discharges to its tributaries. Significant efforts are now being made by local governments to comply with the Chesapeake Bay and other TMDLs. RSWMM-Cost was developed and used to facilitate calibration and sensitivity analysis. Using the RSWMM-Cost, cost-effectiveness curves were developed for runoff and pollutant load reductions by applying

four distributed SCMs: bioretention cells, permeable pavement, dry swales, and green roofs; and a single retention pond to a headwater subcatchment of the Difficult Run watershed. Comparing these suggested mix of SCMs, it is apparent that green roof solutions are not close to either cost effectiveness curve compared to other SCM combinations, likely due to their higher costs and low runoff reduction. Optimization can be powerful when combined with a process simulation model and cost analysis. RSWMM-Cost can be used to evaluate the effectiveness of wide ranges of SCMs. This model can be used to analyze a variety of SCMs for developing TMDL implementation plans, identifying management practices to achieve pollutant reductions in an area regulated by a stormwater permit, and determining optimal SCM implementation strategies for reducing volume to combined sewer overflow systems. The results of this study illustrate the potential usefulness of RSWMM-Cost in guiding selection of alternative SCM implementation strategies with a limited budget.

Determining the most cost-effective combination of SCMs is a challenge because of differences in spatial location, the need to incorporate hydrologic model results, and complexities associated with nonlinearities in costs. Developing tools to combine watershed simulation with cost estimation and optimization algorithms could assist greatly in the evaluation of management strategies. By identifying the most cost-effective watershed improvement strategies, funding for watershed restoration can be stretched, i.e., more load reductions can be achieved for the same amount of resources. This could lower the costs of watershed restoration, speeding up the restoration process, and allow more load reduction for the same investment.

References for Chapter 6:

Ahiablame, L.M., Engel, B.A., Chaubey, I., 2012. Effectiveness of Low Impact Development Practices: Literature Review and Suggestions for Future Research. Water, Air, & Soil Pollution 223(7), 4253-4273.

Alamdari, N., Sample, D.J., Steinberg, P., Ross, A.C., Easton, Z.M., 2017. Assessing the Effects of Climate Change on Water Quantity and Quality in an Urban Watershed Using a Calibrated Stormwater Model. Water 9(7), 464.

Baek, S.-S., Choi, D.-H., Jung, J.-W., Lee, H.-J., Lee, H., Yoon, K.-S., Cho, K.H., 2015. Optimizing low impact development (LID) for stormwater runoff treatment in urban area, Korea: Experimental and modeling approach. Water research 86, 122-131.

Barco, J., Wong, K.M., Stenstrom, M.K., 2008. Automatic Calibration of the U.S. Epa Swmm Model for a Large Urban Catchment. Journal of Hydraulic Engineering 134(4), 466-474.

Bedan, E.S., Clausen, J.C., 2009. Stormwater Runoff Quality and Quantity from Traditional and Low Impact Development Watersheds1. Wiley Online Library.

Breiman, L., 2001. Random Forests. Machine Learning 45(1), 5-32.

Cano, O.M., Barkdoll, B.D., 2016. Multiobjective, Socioeconomic, Boundary-Emanating, Nearest Distance Algorithm for Stormwater Low-Impact Bmp Selection and Placement. Journal of Water Resources Planning and Management 143(1), 05016013.
CDM Smith Inc., 2015. Netstorm Version 2015.2. http://www.dynsystem.com/netstorm/.
Chang, N.-B., Rivera, B.J., Wanielista, M.P., 2011. Optimal Design for Water Conservation and Energy Savings Using Green Roofs in a Green Building under Mixed Uncertainties. Journal of Cleaner Production 19(11), 1180-1188.
Chui, T.F.M., Liu, X., Zhan, W., 2016. Assessing Cost-Effectiveness of Specific Lid Practice Designs in Response to Large Storm Events. Journal of Hydrology 533, 353-364.
Davis, A.P., Hunt, W.F., Traver, R.G., Clar, M., 2009. Bioretention Technology: Overview of Current Practice and Future Needs. Journal of Environmental Engineering 135(3), 109-117.
Delleur, J.W., Baffaut, C., 1990. Calibration of Swmm Runoff Quality Model with Expert System. Journal of Water Resources Planning and Management 116(2), 247-261.
Duan, H.-F., Li, F., Yan, H., 2016. Multi-Objective Optimal Design of Detention Tanks in the Urban Stormwater Drainage System: Lid Implementation and Analysis. Water Resources Management 30(13), 4635-4648.
Eckart, K., McPhee, Z., Bolisetti, T., 2017. Performance and Implementation of Low Impact Development–a Review. Science of the Total Environment 607, 413-432.
Eckhardt, K., Arnold, J., 2001. Automatic Calibration of a Distributed Catchment Model. Journal of Hydrology 251(1), 103-109.
Elliott, A., Trowsdale, S., 2007. A Review of Models for Low Impact Urban Stormwater Drainage. Environmental Modelling & Software 22(3), 394-405.
Fairfax County, 2007. Difficult Run Watershed Management Plan.
Fuka, D.R., Walter, M.T., MacAlister, C., Steenhuis, T.S., Easton, Z.M., 2014. Swatmodel: A Multi-Operating System, Multi-Platform Swat Model Package in R. Jawra Journal of the American Water Resources Association 50(5), 1349-1353.
Gironás, J., Roesner, L.A., Davis, J., Rossman, L.A., Supply, W., 2009. Storm Water Management Model Applications Manual. National Risk Management Research Laboratory, Office of Research and Development, US Environmental Protection Agency Cincinnati, OH.
Gupta, H.V., Sorooshian, S., Yapo, P.O., 1998. Toward Improved Calibration of Hydrologic Models: Multiple and Noncommensurable Measures of Information. Water Resources Research 34(4), 751-763.
Hameed, M.A., 2015. Evaluating Global Sensitivity Analysis Methods for Hydrologic Modeling over the Columbia River Basin. Portland State University.
Hathaway, A.M., Hunt, W.F., Jennings, G.D., 2008. A Field Study of Green Roof Hydrologic and Water Quality Performance. Transactions of the Asabe 51(1), 37-44.
Hirschman, D., Collins, K., Schueler, T., 2008. Technical Memorandum: The Runoff Reduction Method. Center for Watershed Protection & Chesapeake Stormwater Network.
Huber, W.C., Dickinson, R.E., Roesner, L.A., Aldrich, J.A., 1988. Storm Water Management Model User's Manual, Version 4. Project Summary.
Huber, W.C., Dickinson, R.E., Rosener, L.A., Aldrich, J.A., 1988. Stormwater Management Model User's Manual, Version 4. U.S. Environmental Protection Agency, Athens, GA.
Hunt, W.F., Jarrett, A.R., Smith, J.T., Sharkey, L.J., 2006. Evaluating Bioretention Hydrology and Nutrient Removal at Three Field Sites in North Carolina. Journal of Irrigation and Drainage Engineering 132(6), 600-608.

James, L., Burges, S., 1982. Selection, Calibration, and Testing of Hydrologic Models, Hydrologic Modeling of Small Watersheds Ct Haan, Hp Johnson, Dl Brakensiek, 437–472, American Society of Agricultural Engineers, St. Joseph, Mich.
James, W., Rossman, L.A., James, W.R.C., 2010. User's Guide to Swmm 5 Computational Hydraulics International, Guelph, Ontario, Canada.
Jastram, J.D., 2014. Streamflow, Water Quality, and Aquatic Macroinvertebrates of Selected Streams in Fairfax County, Virginia, 2007 – 12. U.S. Geological Survey will, Reston, VA, p. 82.
Jia, H., Lu, Y., Shaw, L.Y., Chen, Y., 2012. Planning of Lid–Bmps for Urban Runoff Control: The Case of Beijing Olympic Village. Separation and Purification Technology 84, 112-119.
Jia, H., Yao, H., Tang, Y., Shaw, L.Y., Field, R., Tafuri, A.N., 2015. Lid-Bmps Planning for Urban Runoff Control and the Case Study in China. Journal of Environmental Management 149, 65-76.
Johnson, R., Sample, D., 2017. A Semi-Distributed Model for Locating Stormwater Best Management Practices in Coastal Environments. Environmental Modelling & Software 91, 70-86.
Jung, Y.-w., Han, S.-i., Jo, D., 2016. Optimal Design of Permeable Pavement Using Harmony Search Algorithm with Swmm, Harmony Search Algorithm. Springer, pp. 385-394.
Kaini, P., Artita, K., Nicklow, J., 2008. Designing Bmps at a Watershed-Scale Using Swat and a Genetic Algorithm, World Environmental and Water Resources Congress 2008: Ahupua'a. pp. 1-10.
King, D., Hagan, P., 2011. Costs of Stormwater Management Practices in Maryland Counties, Technical Report Series. University of Maryland Center for Environmental Science, Solomons, MD.
Lee, J.G., Selvakumar, A., Alvi, K., Riverson, J., Zhen, J.X., Shoemaker, L., Lai, F.-h., 2012. A Watershed-Scale Design Optimization Model for Stormwater Best Management Practices. Environmental Modelling & Software 37, 6-18.
Li, F., Duan, H.-F., Yan, H., Tao, T., 2015. Multi-Objective Optimal Design of Detention Tanks in the Urban Stormwater Drainage System: Framework Development and Case Study. Water Resources Management 29(7), 2125-2137.
Li, Y., Babcock, R.W., 2014. Green Roof Hydrologic Performance and Modeling: A Review. Water Science & Technology 69(4), 727-738.
Liong, S., Chan, W., Lum, L., 1991. Knowledge-Based System for Swmm Runoff Component Calibration. Journal of Water Resources Planning and Management 117(5), 507-524.
Liu, Y., Theller, L.O., Pijanowski, B.C., Engel, B.A., 2016. Optimal Selection and Placement of Green Infrastructure to Reduce Impacts of Land Use Change and Climate Change on Hydrology and Water Quality: An Application to the Trail Creek Watershed, Indiana. Science of the Total Environment 553(Supplement C), 149-163.
Lucas, W.C., Sample, D.J., 2015. Reducing Combined Sewer Overflows by Using Outlet Controls for Green Stormwater Infrastructure: Case Study in Richmond, Virginia. Journal of Hydrology 520, 473-488.
Maalel, K., Huber, W., 1984. Swmm Calibration Using Continuous and Multiple Event Simulation, 3rd International Conference on Urban Storm Drainage. Chalmers University, Goteborg, Sweden, pp. 595-604.
Madsen, H., 2000. Automatic Calibration of a Conceptual Rainfall–Runoff Model Using Multiple Objectives. Journal of Hydrology 235(3), 276-288.

Mancipe-Munoz, N., Buchberger, S., Suidan, M., Lu, T., 2014. Calibration of Rainfall-Runoff Model in Urban Watersheds for Stormwater Management Assessment. Journal of Water Resources Planning and Management 140(6), 05014001.
Montaseri, M., Afshar, M.H., Bozorg-Haddad, O., 2015. Development of Simulation-Optimization Model (Music-Ga) for Urban Stormwater Management. Water Resources Management 29(13), 4649-4665.
Moriasi, D.N., Arnold, J.G., Van Liew, M.W., Bingner, R.L., Harmel, R.D., Veith, T.L., 2007. Model Evaluation Guidelines for Systematic Quantification of Accuracy in Watershed Simulations. Transactions of the Asae 50(3), 885-900.
Myers, B., Beecham, S., van Leeuwen, J.A., 2011. Water Quality with Storage in Permeable Pavement Basecourse. Proceedings of the Institution of Civil Engineers. Water Management 164(7), 361-361.
Prince George's County, 2000. Low-Impact Development Design Strategies, an Integrated Design Approach. Department of Environmental Resources, Programs and Planning Division,, Largo, MD.
Reed, P.M., Hadka, D., Herman, J.D., Kasprzyk, J.R., Kollat, J.B., 2013. Evolutionary Multiobjective Optimization in Water Resources: The Past, Present, and Future. Advances in Water Resources 51, 438-456.
Rossman, L.A., 2004. Storm Water Management Model User's Manual, Version 5.0, in: U.S. Environmental Protection Agency (Ed.). Cincinatti, OH.
Santhi, C., Arnold, J.G., Williams, J.R., Dugas, W.A., Srinivasan, R., Hauck, L.M., 2001. Validation of the Swat Model on a Large River Basin with Point and Nonpoint Sources. Jawra Journal of the American Water Resources Association 37(5), 1169-1188.
Scholz-Barth, K., 2001. Green Roofs: Stormwater Management from the Top Down. Environmental Design & Construction 4(1).
Sebti, A., Carvallo Aceves, M., Bennis, S., Fuamba, M., 2016. Improving Nonlinear Optimization Algorithms for Bmp Implementation in a Combined Sewer System. Journal of Water Resources Planning and Management 142(9), 04016030.
Song, J.Y., Chung, E.-S., 2017. A Multi-Criteria Decision Analysis System for Prioritizing Sites and Types of Low Impact Development Practices: Case of Korea. Water 9(4), 291.
Song, X., Zhang, J., Zhan, C., Xuan, Y., Ye, M., Xu, C., 2015. Global Sensitivity Analysis in Hydrological Modeling: Review of Concepts, Methods, Theoretical Framework, and Applications. Journal of Hydrology 523, 739-757.
Steinberg, P., 2014. Https://Www.Openswmm.Org/Topic/4390/Rswmm-Autocalibration-of-Swmm-in-R.
Sun, Y., Tong, S., Yang, Y.J., 2016. Modeling the Cost-Effectiveness of Stormwater Best Management Practices in an Urban Watershed in Las Vegas Valley. Applied Geography 76, 49-61.
Tan, S.B., Chua, L.H., Shuy, E.B., Lo, E.Y.-M., Lim, L.W., 2008. Performances of Rainfall-Runoff Models Calibrated over Single and Continuous Storm Flow Events. Journal of Hydrologic Engineering 13(7), 597-607.
USEPA, 2010. Chesapeake Bay Total Maximum Daily Load for Nitrogen, Phosphorus, and Sediment. Annapolis, MD: US Environmental Protection Agency, Chesapeake Bay Program Office. Also Available at http://www. epa. gov/reg3wapd/tmdl/ChesapeakeBay/tmdlexec. html.
Van Liew, M.W., Arnold, J.G., Garbrecht, J.D., 2003. Hydrologic Simulation on Agricultural Watersheds: Choosing between Two Models. Transactions of the Asae 46(6), 1539-1551.

Virginia DEQ, 2015. Authorization to Discharge under the Virginia Stormwater Management Program and the Virginia Stormwater Management Act, Permit # Va0088587, Fairfax County.
Weiss, P.T., Gulliver, J.S., Erickson, A.J., 2007. Cost and Pollutant Removal of Storm-Water Treatment Practices. Journal of Water Resources Planning and Management 133(3), 218-229.
Yapo, P.O., Gupta, H.V., Sorooshian, S., 1998. Multi-Objective Global Optimization for Hydrologic Models. Journal of Hydrology 204(1-4), 83-97.
Zhang, K., Chui, T.F.M., 2018. A Comprehensive Review of Spatial Allocation of Lid-Bmp-Gi Practices: Strategies and Optimization Tools. Science of the Total Environment 621, 915-929.
Zoppou, C., 2001. Review of Urban Storm Water Models. Environmental Modelling & Software 16(3), 195-231.

Chapter 7. Conclusions and Future Research

Significant investments are being made in constructing SCMs, yet their performance remains highly variable. Climate is a key factor affecting SCM performance. While SCMs can be evaluated individually, it is also necessary to evaluate their collective performance as part of a watershed. Changes in rainfall magnitude and intensity from CC may cause urban stormwater infrastructure to fail, as documented by several studies. Only a few studies have focused on evaluating the performance of individual SCMs subject to CC; most of these focus on hydraulic function, not water quality. The ability to assess the impact of CC on both hydrologic and water quality treatment could assist in the selection of the most appropriate SCMs to address water management goals and conserve limited financial resources.

While tools are available for simulating urban hydrology and water quality, in general, they are difficult to calibrate, to conduct sensitivity analysis with, and to perform cost optimization. As part of this research, an easy to use tool that performs these tasks and wraps around the current version of the most commonly applied urban simulation model, SWMM, was developed. No modifications to the SWMM source code were needed. Determining the most cost-effective combination of SCMs is a challenge because of differences in spatial location, the need to incorporate hydrologic model results, and complexities associated with nonlinearities in costs. RSWMM-Cost, which combines watershed simulation with cost estimation and optimization, should greatly facilitate the evaluation of management strategies. By identifying the most cost-effective watershed improvement strategies, funding for watershed restoration can be stretched, i.e., more can be done for the same amount of financing. This could lower the costs of watershed restoration, speed up the process, and allowing more to be done for the same investment. RSWMM-Cost can be used to evaluate the effectiveness of wide ranges of SCMs. This program can be used to analyze a variety of SCMs for developing TMDL implementation plans, identifying management practices to achieve pollutant reductions in an area regulated by a stormwater permit, and determining optimal SCM implementation strategies for reducing volume to combined sewer overflow systems.

The Difficult Run watershed is part of the Chesapeake Bay estuary which is experiencing eutrophication due to excessive loading of nutrients and sediment. The USEPA has established a TMDL for the Chesapeake Bay, limiting N, P, and sediment discharges to its tributaries. Significant efforts are now being made by local governments to comply with the Chesapeake Bay

and other TMDLs. For these reasons, and the availability of modeling and monitoring data, Difficult Run was selected as a case study watershed. CC appears to work in tandem with urbanization, increasing runoff and pollutant loads, causing a reduction in treatment efficiency of SCMs such as retention ponds. Since SCMs are one of the main tools used in urban areas to achieve Chesapeake Bay restoration goals, reductions in their effectiveness will need to be addressed, diverting resources from other problem areas. Robust methods for predicting the effects of CC on water quantity, quality and SCM treatment performance at the watershed scale are needed to develop climate resilient strategies that meet water quality goals. The examples presented in these projects are an initial step in the development of general methods to achieve these goals.

Understanding CC effects on hydrologic functions of water systems can help water resources managers and planners to make better decisions. Studies such as these can assist them as they evaluate the complex physical, social and economic impacts of CC on urban communities. In addition, making predictions of the impact of CC on stormwater infrastructure can help improve the management of stormwater systems by helping to reduce flooding and to produce better water quality treatment through implementation of SCMs.

The results of this study may suggest that some SCMs designed for current conditions may be less effective in the future due to CC. Our work presents a methodology for assessing CC impacts on the water supply and runoff reduction benefits of RWH systems and removal efficiency of retention ponds. These results, while not absolute, can help guide managers and decision makers identify locations in which stormwater systems can provide the best results at the lowest cost.

The limitation of this analysis include uncertainty associated with the assumptions in the future emission of greenhouse gases, climate models, calibrated parameters within the hydrologic model, uncertainties in flow for a chosen SCM and incorporating physical processes such as buildup and washoff that may more accurately define runoff water quality. At this time, however, with the level of data that are available, the event mean concentration (EMC) approach is appropriate, particularly when the focus is upon annual loads. Future work based upon this research should incorporate uncertainty analysis of the major processes and variables affecting the hydrologic and water quality processes, treatment effectiveness and economic modeling. Improvements in the computational efficiency of stormwater modeling using parallel processing

would also be beneficial. Snowmelt and ice cover analysis and the effects of them on the efficiency of the SCMs were not performed. Rainfall intensity, duration, and frequency analysis would be recommended in the future since they are important factors affecting washoff loads and transport of sediment and nutrients.

We also can assess the efficiency of SCMs for existing and projected climate scenarios and identify how these measures can be adapted to keep the same level of performance with CC. Those projects that are the most resilient to CC may also provide additional flood risk reduction benefits. Thus, we can identify the most resilient and cost-effectiveness set of SCMs in an urban watershed that achieve our water quantity and quality goals. In addition, cost optimization by consideration of whole life cycle cost and multiple environmental, social and economic benefits can provide communities with a tool that takes into account the costs associated with planning, designing, constructing, operating, maintaining and replacing stormwater infrastructure. This tool would guide planners and decision makers in comparing benefits and costs of stormwater infrastructure alternatives using tools that utilize cost, design, and performance datasets, ultimately seeking to improve the efficiency of stormwater management.

Appendices

The complete version of appendix A, B, C and D are available as supplements to an online article, available at: https://www.sciencedirect.com/science/article/pii/S2352340918302282.

Miami and Los Angeles are presented here as examples:

Appendix A. Frequency Analysis of Rainfall

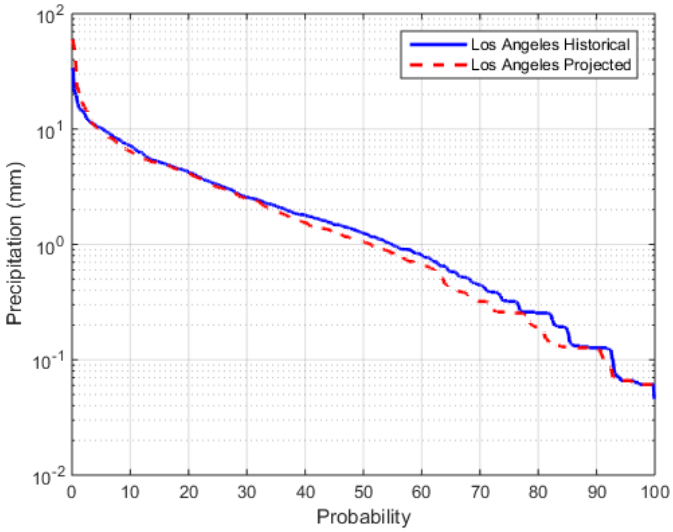

Figure A1. Frequency analysis curves of rainfall events for Los Angeles for historical and projected conditions.

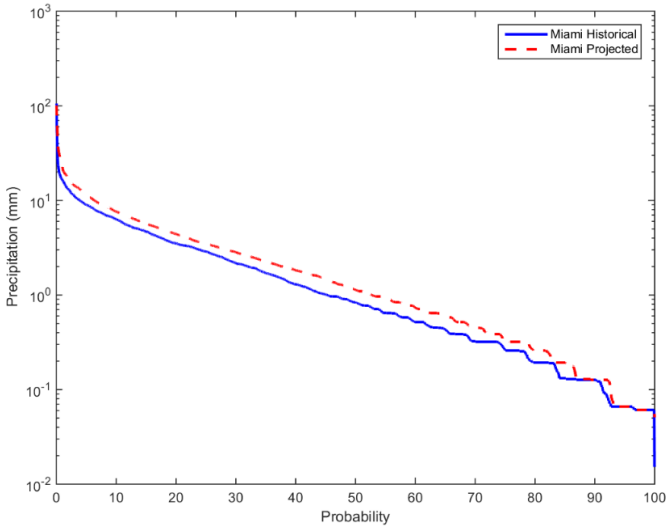

Figure A2. Frequency analysis curves of rainfall events for Miami for historical and projected conditions.

Appendix B. Frequency Analysis of Dry Duration

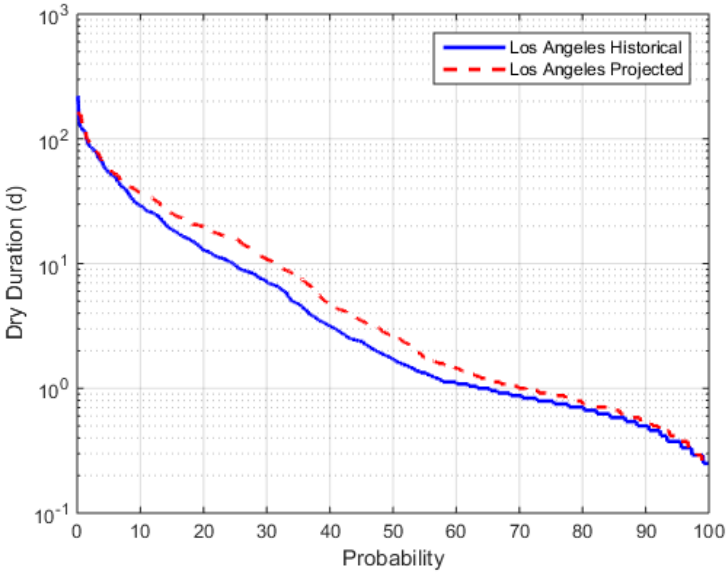

Figure B1. Frequency analysis curves of dry duration for Los Angeles for historical and projected conditions.

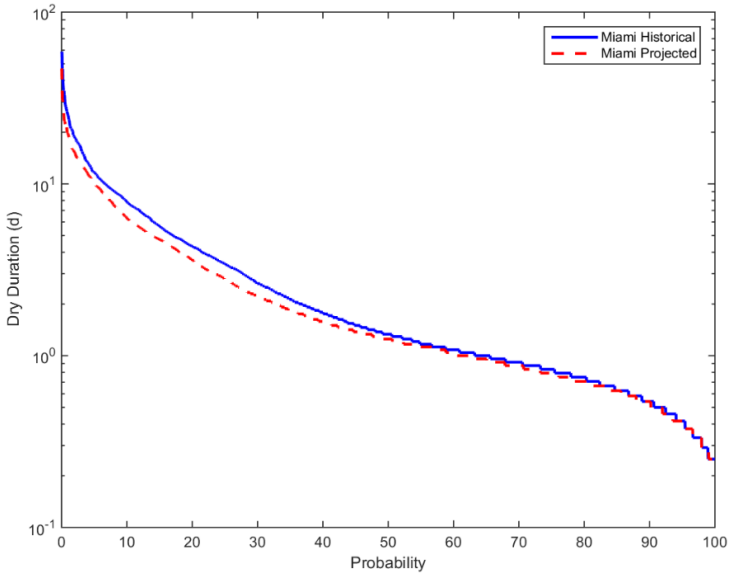

Figure B2. Frequency analysis curves of dry duration for Miami for historical and projected conditions.

Appendix C. Water supply and Runoff Capture Tradeoff Curves for Outdoor Demand

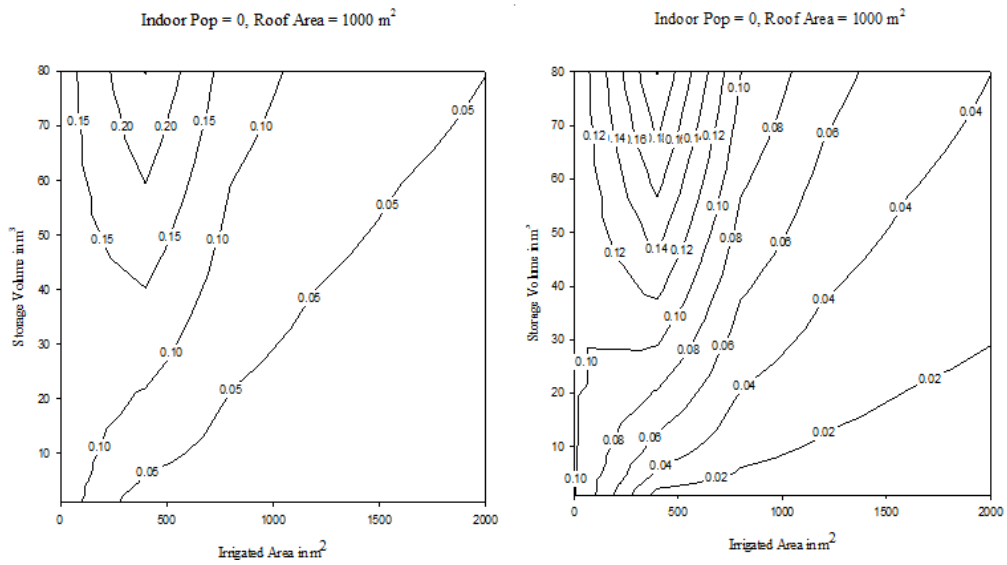

Figure C1. Water supply reliability curves for Los Angeles for historical and projected conditions.

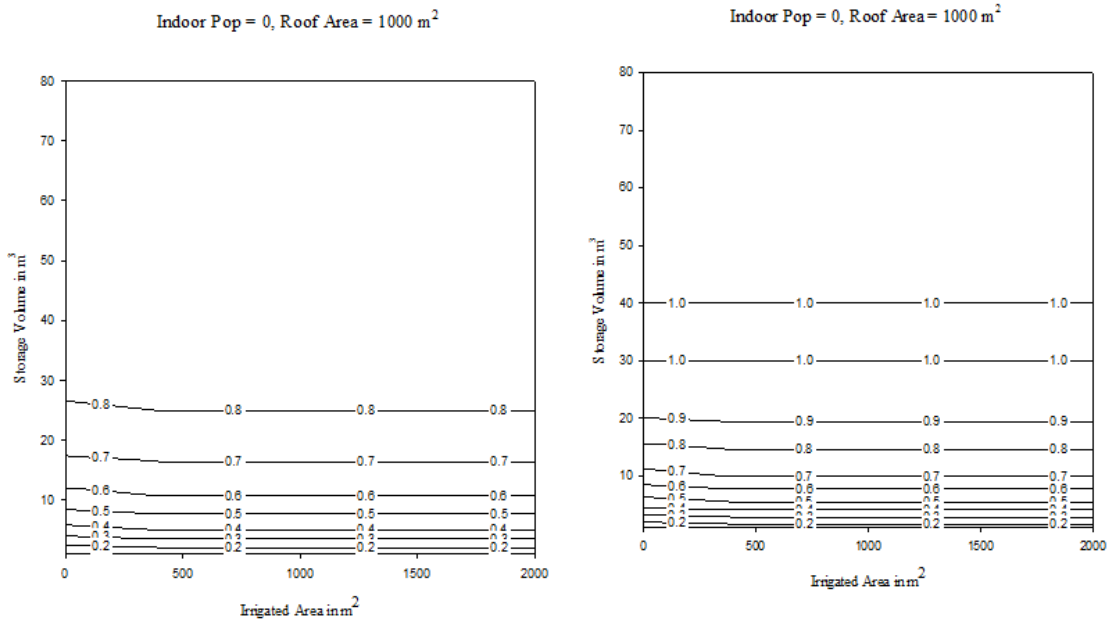

Figure C2. Runoff Capture reliability curves for Los Angeles for historical and projected conditions.

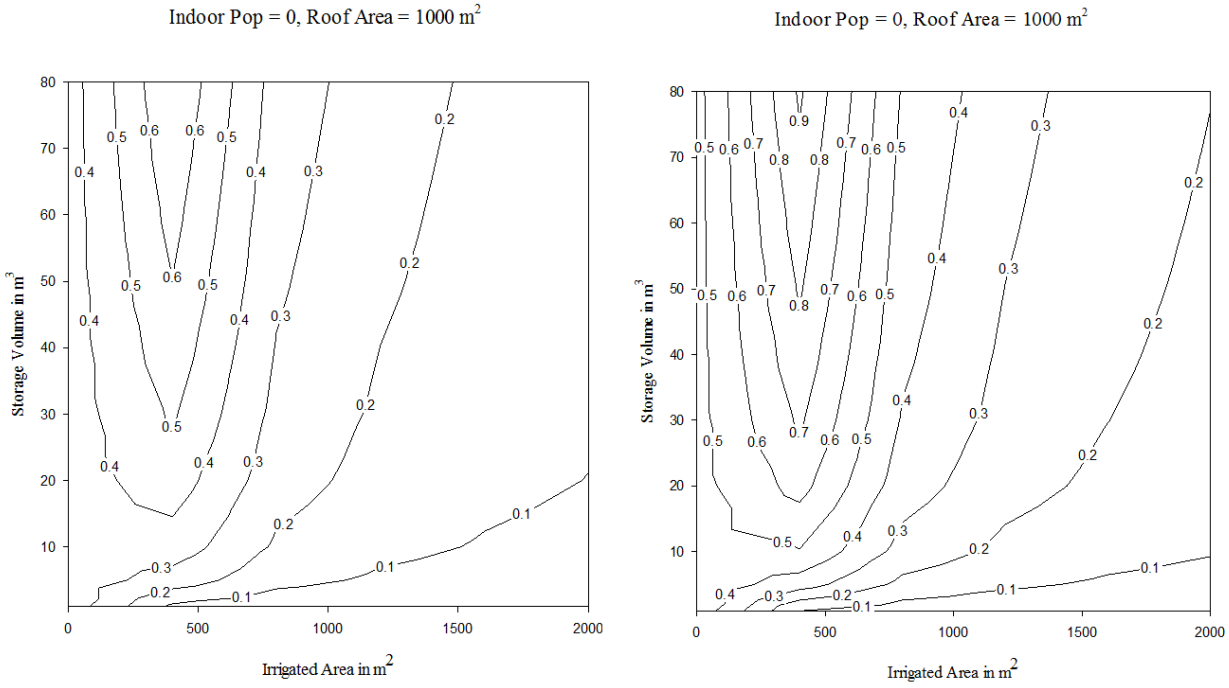

Figure C3. Water supply reliability curves for Miami for historical and projected conditions

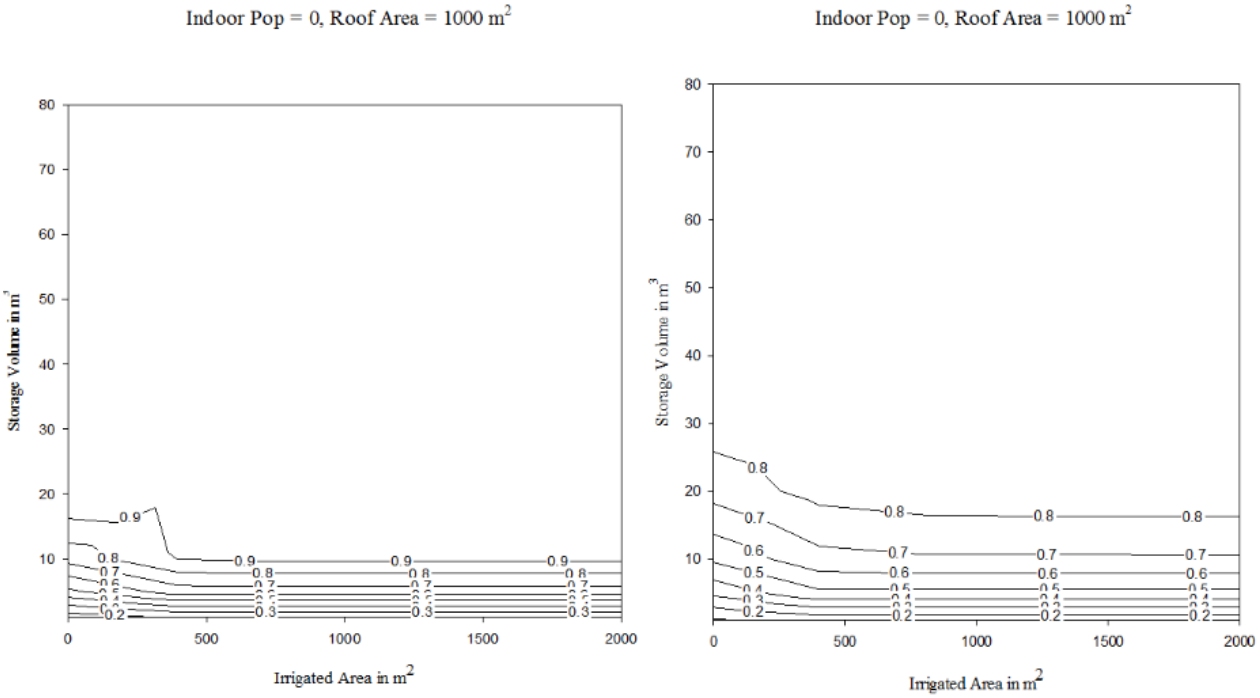

Figure C4. Runoff Capture reliability curves for Miami for historical and projected conditions.

Appendix D. Water Supply and Runoff Capture Tradeoff Curves for Indoor Demand

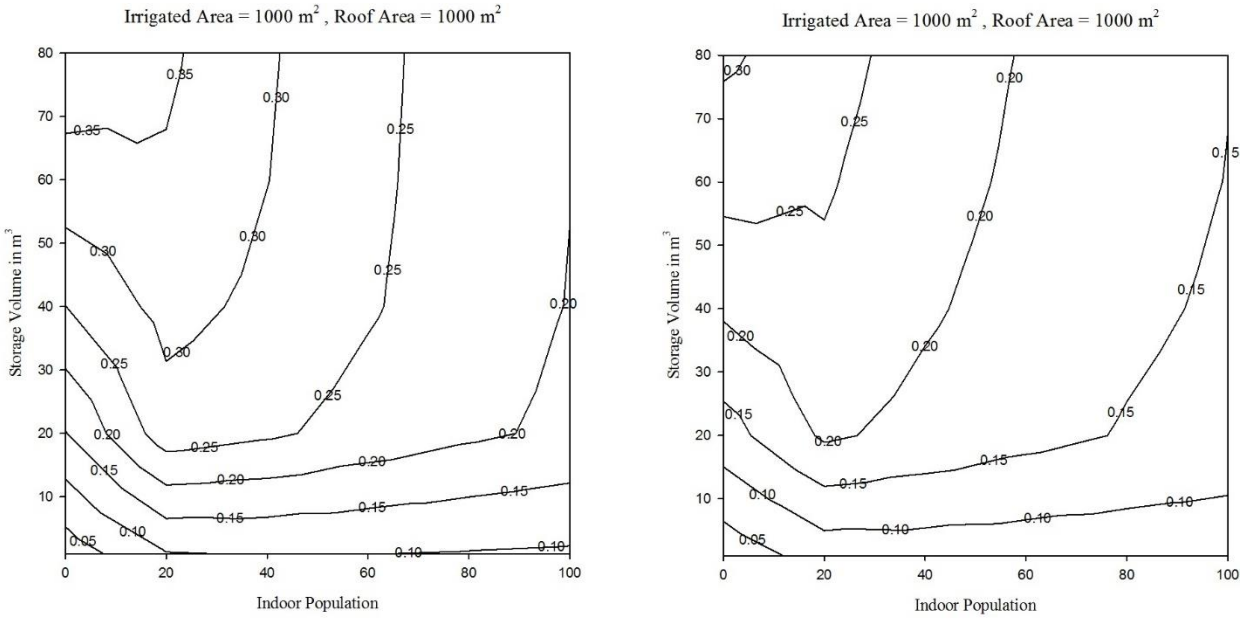

Figure D1. Water supply reliability curves Los Angeles for historical and projected conditions.

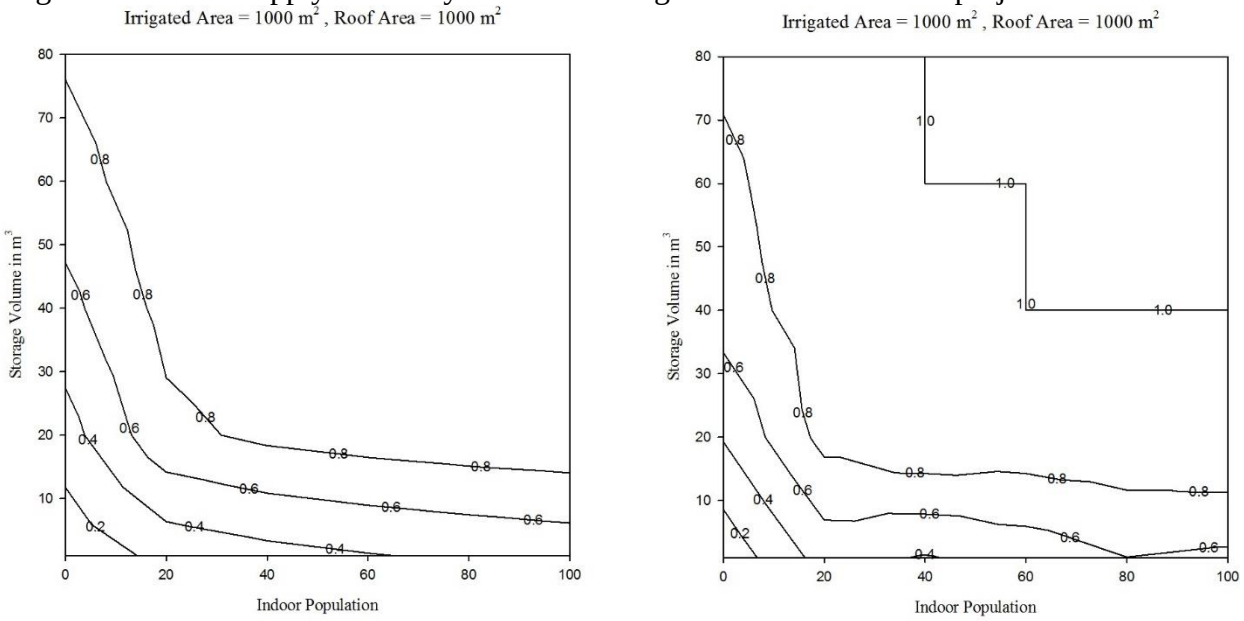

Figure D2. Runoff Capture reliability curves for Los Angeles for historical and projected conditions.

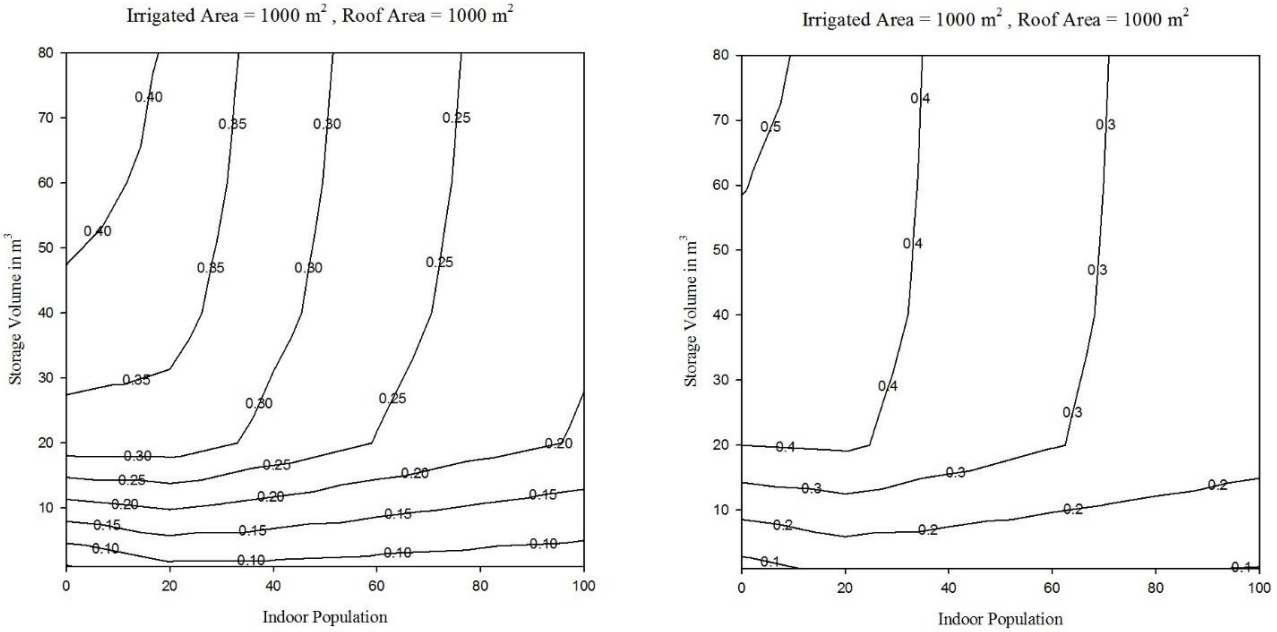

Figure D3. Water supply reliability curves for Miami for historical and projected conditions.

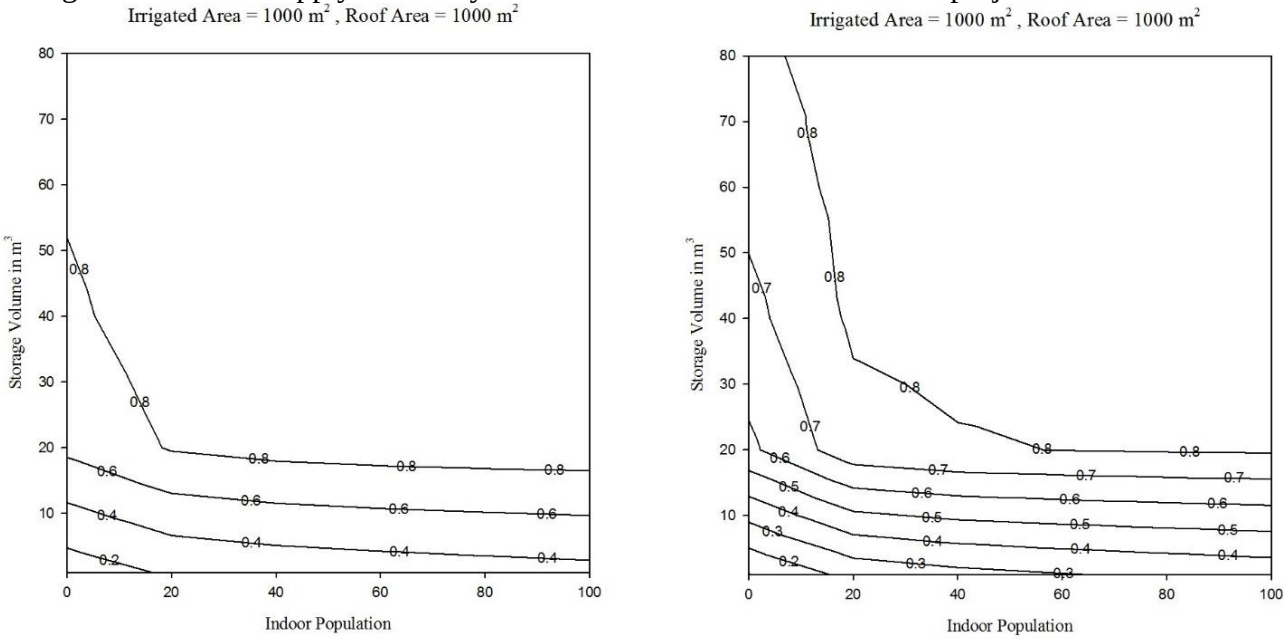

Figure D4. Runoff Capture reliability curves for Miami for historical and projected conditions.

Appendix E. Software/Data Availability

Table E-1. Software/Data Availability.

Software/Data Availability	Information
Name of software or dataset	RSWMM-Cost[i]
Developer and contact	Nasrin Alamdari
Telephone	216-715-4492; 716-239-9288
Fax	(540) 231-3199
Email numbers	alamdari@vt.edu
Year first available	2018
Hardware required	Personal computer, recommended minimum 64 bit machine, i7 or better, 8GB RAM or better, at least 500 GB storage available
Software required	R 3.2.5 for windows available for free download from https://cran.r-project.org/bin/windows/base/
Availability	https://github.com/nasrinalam/RSWMM-CostAutomation
Cost	Free
Program language	R
Program size	76 kb
Data: form of repository	Files
Size of archive	< 1 MB
Access form	FTP

[i] RSWMM was originally developed by Peter Steinberg (psteinberg@continuum.io), available at: https://www.openswmm.org/Topic/4390/rswmm-autocalibration-of-swmm-in-r